



HAL
open science

COUP-TFI is required in the differentiation and migration of granule cells in the developing dentate gyrus

Joséphine Parisot

► **To cite this version:**

Joséphine Parisot. COUP-TFI is required in the differentiation and migration of granule cells in the developing dentate gyrus. Agricultural sciences. Université Nice Sophia Antipolis, 2015. English. NNT : 2015NICE4089 . tel-01646936v1

HAL Id: tel-01646936

<https://theses.hal.science/tel-01646936v1>

Submitted on 24 Nov 2017 (v1), last revised 28 Mar 2018 (v2)

HAL is a multi-disciplinary open access archive for the deposit and dissemination of scientific research documents, whether they are published or not. The documents may come from teaching and research institutions in France or abroad, or from public or private research centers.

L'archive ouverte pluridisciplinaire **HAL**, est destinée au dépôt et à la diffusion de documents scientifiques de niveau recherche, publiés ou non, émanant des établissements d'enseignement et de recherche français ou étrangers, des laboratoires publics ou privés.

Université Nice Sophia Antipolis
Ecole doctorale ED85 Sciences de la Vie et de la Santé

Thèse de doctorat en Biologie
Spécialité « Interaction Moléculaire et Cellulaire »
soutenue le 23 novembre 2015

COUP-TFI est nécessaire dans la différenciation et la migration des granules du gyrus denté

Joséphine PARISOT

Président : Dr. MANTEGAZZA Massimo

Rapporteurs : Dr. NICOLIS Silvia

Dr. ABROUS Nora D.

Directeur : Dr. STUDER Michèle

University Nice Sophia Antipolis
Ecole doctorale ED85 Sciences de la Vie et de la Santé

Ph.D. thesis in Biology
Speciality « Molecular and Cellular Interactions »
presented on 23rd November 2015

COUP-TFI is required in the differentiation and migration of granule cells in the developing dentate gyrus

Joséphine PARISOT

President: Dr. MANTEGAZZA Massimo
Reviewers: Dr. NICOLIS Silvia
Dr. ABROUS Nora D.
Advisor: Dr. STUDER Michèle

Résumé

L'hippocampe est un composant majeur du cerveau des mammifères. Il appartient à l'archicortex, la partie la plus ancienne du télencéphale, et joue d'importants rôles dans la mémoire, l'apprentissage et la navigation spatiale. L'hippocampe comprend deux régions distinctes : les champs ammoniens et le gyrus denté ou DG, composés de trois couches cellulaires. Le DG est la principale zone d'entrée d'informations dans l'hippocampe et son développement commence au jour embryonnaire 14 (E14.5) chez la souris. Pendant ma thèse, je me suis intéressée à un régulateur de transcription important, le récepteur nucléaire COUP-TFI, exprimé dans le neocortex et l'hippocampe, et décrit comme jouant des rôles clefs dans la spécification et la migration neocorticale. Cependant, peu de choses sont connues sur son implication dans l'hippocampe, et plus particulièrement dans le DG. COUP-TFI y est exprimé en gradient à la fois dans les progéniteurs proliférants et dans les neurones différenciés, et est fortement localisé dans le neuroépithélium du DG à E14.5. Le but majeur de ma thèse était ainsi de déchiffrer le rôle de COUP-TFI dans le développement de l'hippocampe, et spécifiquement au cours de la différenciation et migration des cellules granulaires, population principale du DG. À l'aide de deux lignées de souris mutantes, dans lesquelles COUP-TFI est soit inactivé dans les progéniteurs et leur descendance, soit seulement dans les cellules post-mitotiques, j'ai montré que l'absence de COUP-TFI induit différents degrés d'altérations de la croissance de l'hippocampe. En l'absence de COUP-TFI dans les progéniteurs, les précurseurs des cellules granulaires se différencient précocement et présentent une prolifération diminuée. De plus, la migration des granules est altérée conduisant à des localisations aberrantes et à la présence de clusters hétérotopiques dans le DG. Au stades postnataux, les afférences du cortex entorhinale n'innervent pas le DG septal et l'apoptose est accrue dans cette région. En conséquence, le gyrus denté en résulte fortement réduit à l'âge adulte, particulièrement dans la région septale, tandis que le pôle temporal est moins affecté. À l'inverse, la perte de COUP-TFI dans les cellules différenciées n'entraîne que des anomalies mineures et transitoires. Ensemble, mes résultats indiquent que COUP-TFI est impliqué dans la régulation d'aspects particuliers de la différenciation et migration des granules, principalement au niveau des progéniteurs, et propose COUP-TFI comme un nouveau régulateur de transcription requis dans le développement et le fonctionnement de l'hippocampe.

Abstract

The hippocampus is a major component of the mammalian brain. It belongs to the archicortical domain, the most ancient portion of the telencephalon, and plays important roles in memory, learning, and spatial navigation. The hippocampal formation comprises two cytoarchitecturally distinct regions: the hippocampus proper and the dentate gyrus or DG, showing a three-layered appearance. The DG is the primary gateway for input information into the hippocampus and its development begins at Embryonic day 14 (E14.5) in the mouse. During my thesis work, I have challenged the role of a strong transcriptional regulator, the nuclear receptor COUP-TFI, expressed in the neocortex and hippocampus and described to play key roles during neocortical specification and migration. Yet, little is known about its involvement in the hippocampus, and more particularly in the DG. COUP-TFI is expressed in a gradient fashion in both proliferating progenitors and differentiated neurons in the hippocampus, and is highly localized in the DG neuroepithelium at E14.5. The major aim of my thesis work was thus to decipher the role of COUP-TFI in the developing hippocampus, and specifically in cell differentiation and migration of granule cells, the major cell population of the DG. With the help of two conditional knock-out mouse lines, in which COUP-TFI is either ablated in progenitors and their derivatives, or solely in post-mitotic cells, I have shown that absence of COUP-TFI function induces different degrees of hippocampal and DG growth impairments. In the absence of COUP-TFI in progenitors, granule cell precursors tend to differentiate precociously and exhibit diminished proliferative activity along the various migratory routes. In addition, the migratory behavior of granule cells is impaired leading to aberrant final locations and presence of heterotopic clusters within the DG. At postnatal stages, inputs from the entorhinal cortex fail to innervate the septal/dorsal DG and apoptosis is abnormally increased in this region. As a consequence, the dentate gyrus results strongly reduced at adult stages, particularly in the septal/dorsal region, whereas the temporal/ventral DG is less affected. On the contrary, loss of COUP-TFI in differentiated cells leads only to minor and transient abnormalities. Together, my results indicate that COUP-TFI is involved in regulating particular aspects of granule cell differentiation and migration predominantly in progenitor dorsal cells, and propose COUP-TFI as a novel transcriptional regulator required in hippocampal development and functions.

Acknowledgments

First, I would like to thank my supervisor and lab director Michèle Studer for giving me the opportunity to accomplish my Ph.D. in her laboratory. Thank you for your numerous advices and fruitful discussions on the project, for your patience and availability and for always encouraging me. Thank you also to Gemma Flore, for sharing some of her results, and to Elvira De Leonibus' lab for good collaboration. I am also thankful to Silvia Nicolis, Nora D. Abrous and Massimo Mantegazza for accepting to be part of my thesis defense jury.

I would like to thank also all the former and present members of the Studer's lab for the great and multicultural experience they provided. It was a real pleasure to be part of such a strong community. Thank you all for your kindness, your friendship, your laughs in good moments and your support in bad. I would like to particularly thank Maria Anna and Michele for all the great moments we spent together, in and out the lab. Will it be in a microscope room or at an archery lesson, I'm always having fun with you. Thanks again to Maria Anna, and also to Christian for always being available to discuss scientific questions or teach me experimental procedures. Thank you also to Eya for always managing the lab like no-one, and for your incredible and exciting story-telling skills (« They had fences ! »). Thank you Audrey for our many talks about everything and nothing, for your french-teaching-to-a-native-french-speaker ability and for being such a good shoulder to cry in rough times. I am also thankful to Kawssar for her kindness. You have been a great "one-year-older-than-me" mother, in addition to being a great scientist. Many thanks also to Elia, the parallel "robot" Ph.D student. I always admire how many things you know about so many topics. Thank you for the many technical helps you brought me. I am also grateful to the former members of the Studer's lab: Lisa for your kindness and our career talks, but also Nuria, Nadia, Mariel, Salsa and Jessica for your kindness. I would like also to thank all the other members of the institute that brought great and fun moments during my Ph.D.

I would like also to thank my family for their support. My dad first, gone too soon during these years, and which I cruelly miss. My mom and “papa-Paul”, for their advices, support, and for being there for me, as well as all my siblings: Louis, Antoine, Clémence, Grégoire, Justine and Adélaïde. I love you all, no matter how far or busy we get.

Many thanks also to Kernel Panic’s members and friends, and all the people I might forget, for keeping me busy in my spare time and for the many enjoyable moments.

Last but not least, I would like to thank Romain, my boyfriend of now already 10 years. Thanks for being here when I need you, for pushing me when necessary, and for understanding me so well.

Résumé	5
Abstract	7
Acknowledgments	9

CHAPTER 1

Introduction **19**

I / The hippocampus **21**

A) Hippocampal anatomy **21**

- 1) General anatomy 21
- 2) Hippocampus proper (Hp) 24
- 3) Dentate gyrus (DG) 26
- 4) Connectivity: the three synaptic system 27

B) Hippocampal functions **29**

- 1) Memory & Learning 30
- 2) Spatial Navigation 31
- 3) Stress response 32
- 4) Adult Neurogenesis 33
- 5) Septal/Temporal -specific functions 34
- 6) Disruption / Pathology of the hippocampus 35

C) Hippocampal development **37**

- 1) Early cortical patterning events 37
- 2) Hippocampus proper development 38
- 3) Dentate gyrus development 38
 - a - Neuronal differentiation: Transcription Factor cascade* 40
 - b - Migration* 46
 - c - Maturation & connectivity* 50
- 3) Interneurons, glia and hippocampal fissure 51
 - a- Interneurons* 51
 - b- Glia* 52
 - c- Hippocampal fissure (Hf)* 53

II / COUP-TFI **54**

A) COUP-TF classification, sequence, structure and conservation **54**

- 1) COUP-TF classification 54
- 2) COUP-TF DNA sequence and protein structure 55
- 3) COUP-TF conservation 56

B) COUP-TFI expression in the developing mouse brain **57**

C) COUP-TFI gene regulation **58**

Table of Contents

1) Regulation of COUP-TFI expression: upstream regulators	58
2) COUP-TFI transcriptional activity: downstream targets	59
<i>a- Transcriptional repressor activity</i>	60
<i>b- Transcriptional activator activity</i>	61
D) COUP-TFI functions in the developing Central Nervous System	62
1) Neuronal migration	62
<i>a- Glia-guided radial migration</i>	62
<i>b- Tangential migration</i>	63
2) Cytoskeletal machinery	64
3) Interneuron specification	64
4) Neurogenesis, gliogenesis, and neuronal fate specification	65
<i>a- Neuronal fate specification</i>	65
<i>b- Neurogenic-gliogenic switch</i>	66
5) Neocortical area patterning	66
6) Hippocampal development	67
E) Human COUP-TFI dysfunctions	68
III / Aim of the study	69

CHAPTER 2

Materials and Methods 71

I / Animals and genotyping 73

A) Mice models	73
1) <i>COUP-TFI^{fl/fl};Emx1Cre</i> line: « <i>EmxCKO</i> »	74
2) <i>COUP-TFI^{fl/fl};Nex-Cre</i> line: « <i>NexCKO</i> »	74
3) <i>Thy1-eYFP-H</i> line: « <i>Thy1-YFP</i> »	74
B) Genotyping	75
1) <i>DNA extraction</i>	75
2) <i>PCR</i>	75
3) <i>Visualisation</i>	76

II / Tissue Preparation 77

A) Dissection, Fixation and Embedding	77
B) Cryosections	77
C) Vibratome sections	78

III / Histological procedures 78

A) Birth-dating: EdU labelling	78
B) Immunofluorescence	78
C) Immunohistochemistry	80
D) RNA probe synthesis and In Situ Hybridization	81
1) <i>RNA probe synthesis</i>	81
2) <i>In Situ Hybridization</i>	81

E) Nissl Staining	83
F) Axonal tracing by injection of lipophilic DiI	83
G) Imaging	84
H) Three-dimensional reconstruction	84

IV / Quantification and Statistical analysis **84**

CHAPTER 3

Results **87**

I / COUP-TFI is expressed in the developing and adult hippocampus **89**

- 1) COUP-TFI is expressed in the hippocampus in a low septal to high temporal gradient **89**
- 2) COUP-TFI expression is abolished in mitotic or post-mitotic cells in conditional mutants **91**

II / COUP-TFI is required in the growth and morphogenesis of the postnatal hippocampus and dentate gyrus **92**

- 1) Lack of COUP-TFI leads to developmental malformations of the postnatal dentate gyrus **92**
- 2) COUP-TFI loss-of-function induces a more severe hippocampal and dentate gyrus impairment in the septal than the temporal pole **97**
- 3) COUP-TFI is not involved in specifying the septal and temporal identities of the hippocampus **102**

III / COUP-TFI does not act on hem-derived signaling factors **105**

IV / COUP-TFI is required in granule cell differentiation during DG development **106**

- 1) COUP-TFI deficient mice have decreased proliferation in the developing dentate gyrus **106**
- 2) COUP-TFI EmxCKO brains have a diminished number of intermediate progenitors (IPCs) during embryonic phases of granule cell differentiation **109**
- 3) Post-natal mitotic differentiation of granule cells and SGZ establishment are altered in the absence of COUP-TFI **116**
- 4) The reduced DG cell population does not differentiate into granule cells in the absence of COUP-TFI **125**

V / Abnormal granule cell migration in COUP-TFI mutants **128**

- 1) Impaired cell migration leads to the formation of ectopic clusters and altered laminar organization in COUP-TFI-deficient DG **128**

Table of Contents

- 2ry matrix migratory stream	128
- Layer distribution	130
2) Loss of COUP-TFI leads to altered guidance cues signaling	133
3) Loss of COUP-TFI impacts the formation of radial glia scaffolds	135
<u>VI / COUP-TFI inactivation leads to increased apoptosis in the newborn dentate gyrus</u>	<u>138</u>
<u>VII / COUP-TFI is required in the establishment and maturation of granule cell connectivity in the septal pole</u>	<u>141</u>
1) COUP-TFI mitotic inactivation alters the septal but not the temporal perforant path fibers	141
2) COUP-TFI loss does not affect granule cell dendritic growth but induces an impairment of inner molecular layer fibers	143
3) Mossy fibers are present but immature in the absence of COUP-TFI	145
<u>VIII / Behavior</u>	<u>147</u>
CHAPTER 4	
Discussion and Perspectives	149
<u>Discussion</u>	<u>151</u>
<u>Perspectives</u>	<u>164</u>
Annexe	165
References	191
<u>Résumé</u>	<u>220</u>

Figure index

Figure 1. Localization of the hippocampal region in human and mouse brains.	22
Figure 2. Anatomy of the hippocampus.	23
Figure 3. Hippocampal connectivity.	28
Figure 4. Dentate gyrus development.	39
Figure 5. Transcription factor cascade involved in granule cell differentiation.	41
Figure 6. COUP-TFI sequence conservation among vertebrates.	56
Figure 7. Molecular mechanisms of COUP-TF as repressor and activator.	60
Figure 8. COUP-TFI loss-of-function mouse models used in this study.	73
Table 1. List of primary antibodies used in this study.	79
Table 2. List of secondary antibodies used in this study.	80
Figure 9. Counting methodology examples.	85
Figure 10. COUP-TFI is expressed in a gradient in the developing and adult hippocampus.	90
Figure 11. COUP-TFI loss of expression in NexCKO and EmxCKO mutant hippocampi.	93
Figure 12. COUP-TFI loss-of function induces growth impairment.	95
Figure 13. Developmental defects lead to strong hippocampal volume reduction in the adult EmxCKO brain but not in NexCKO.	96
Figure 14. The septal pole of the hippocampus is particularly affected in EmxCKO.	98
Figure 15. The number of coronal sections in the septal hippocampus is reduced in both NexCKO and EmxCKO during post-natal development.	99
Figure 16. COUP-TFI inactivation induces a disorganization of the rostral/septal DG lamination but not its temporal portion, in both NexCKO and EmxCKO.	101
Figure 17. Preserved septo-temporal identity of COUP-TFI-deficient hippocampi.	103
Figure 18. COUP-TFI does not alter hem-derived factors.	105
Figure 19. Decreased proliferation in COUP-TFI deficient DG.	107
Figure 20. Mitotic cell populations during embryonic DG development.	112
Figure 21. Late mitotic and early post-mitotic cell populations during embryonic DG development.	113
Figure 22. Post-mitotic cell populations during embryonic DG development.	114
Figure 23. Mitotic cell populations during post-natal DG development: Mcm2/Tbr2.	118
Figure 24. Mitotic cell populations during post-natal DG development: Pax6/Tbr2.	119
Figure 25. Reduced mitotic cell populations in COUP-TFI-deficient DG at post-natal stages.	120
Figure 26. The proportion of mitotic cell sub-populations are not altered in mutant DG at post-natal stages.	121
Figure 27. Early post-mitotic cell population Tbr2/Prox1+ in post-natal DG.	121

Figure index

Figure 28. Post-mitotic cell population during post-natal DG development: Tbr2/Tbr1.	123
Figure 29. Late post-mitotic cell populations during post-natal DG development: Prox1/NeuN.	123
Figure 30. EmxCKO early born DG neurons are less numerous, but differentiate in granule cells in the same proportion as the Control.	127
Figure 31. Impaired secondary migratory stream and presence of heterotopic clusters of post-mitotic cells during EmxCKO DG post-natal development.	129
Figure 32. COUP-TFI inactivation leads to impairment in layers distribution of mitotic cells during post-natal development.	131
Figure 33. Reelin signal is altered in EmxCKO DG at birth.	133
Figure 34. Increased CXCR4 transcript levels in EmxCKO 2ry matrix at birth.	135
Figure 35. COUP-TFI inactivation leads to glia scaffold disorganization in post-natal DG.	137
Figure 36. COUP-TFI loss-of-function induces a perinatal apoptosis in the developing dentate gyrus.	139
Figure 37. Impaired perforant path fibers in the septal COUP-TFI EmxCKO mutant hippocampus.	142
Figure 38. Granule cell dendritic arborization is not altered in the absence of COUP-TFI.	144
Figure 39. Mossy fibers are present but immature in EmxCKO mutant hippocampi.	146
Table 3. Summary of the phenotypes observed in the two COUP-TFI-deficient models.	151

Abbreviations

Abbreviation	Meaning	Abbreviation	Meaning
1ry / 2ry / 3ry	Primary / Secondary / Tertiary Matrix	Mcm2	Minichromosome maintenance 2
BLBP	Brain-Lipid-Binding Protein	MF	Mossy fibers
CA1/2/3	Cornus Ammonis field 1/2/3	ml	Molecular layer
CKO	Conditional knock-out	ND1 (NeuroD1)	Neurogenic differentiation gene 1
CNS	Central Nervous System	NeuN	Neuronal Nuclei gene
COUP-TFI COUP-TFII	Chicken ovalbumin upstream promoter - transcription factor I or II	Nex	Neurogenic differentiation factor 6/ Math2 gene
CR	Calretinin	NR2F1 NR2F2	Nuclear Receptor subfamily 2, group F 1 or 2
Cre	Cyclization Recombination enzyme	NSC	Neural stem cell
DBD	DNA binding domain	oml	Outer molecular layer
DG	Dentate gyrus	P0	Post-natal day 0
dgn	Dentate gyrus neuroepithelium	Pax6	Paired box-gene 6
E16.5	Embryonic day 16.5	PBS	Phosphate-buffered saline pH7.4
EdU	5-ethynyl-2'-deoxyuridine	pcl	Pyramidal cell layer
Emx 1 Emx2	Empty spiracles homeobox 1/2 gene	PFA	Paraformaldehyde
fi	Fimbria	PP	Perforant path
gcl	Granule cell layer	Prox1	Homeobox prospero-like gene 1
GFAP	Glial fibrillary acidic protein	RGC	Radial glia cell
HF	Hippocampal formation	RT	Room temperature
Hf	Hippocampal fissure	Sb	Subiculum
hi	Hilus	SC	Schaffer Collaterals
CXCR4	C-X-C chemokine receptor type 4	SGZ	Sub-granular zone
Hp	Hippocampus proper	slm	Stratum lacunosum molecular
Hpn	Hippocampus proper neuroepithelium	slu	Stratum lucidum
IF	Immunofluorescence	so	Stratum oriens
IHC	Immunohistochemistry	sr	Stratum radiatum
iml	Inner molecular layer	SVZ	Sub-ventricular zone
IPC	Intermediate progenitor cells	Tbr1 / Tbr2	T-box brain gene 1/2
ISH	<i>In situ</i> hybridization	TF	Transcription Factor
Ki67	Nuclear antigen pKI-67 proliferation marker	UB	Upper blade
LB	Lower blade	vz	Ventricular zone
LBD	Ligand binding domain	Wnt	Wingless/int genes
LV	Lateral Ventricle	YFP	Yellow fluorescent protein
Map2	Microtubules associated protein 2		

CHAPTER 1

Introduction

I / The hippocampus

The hippocampus was first described by the Venetian anatomist Julius Caesar Aranzi in the XVIth century. Its particular shape led him to name it from the Greek word for seahorse (*hippos* = horse and *kampos* = sea monster). The hippocampus has been extensively studied since then, and is now one of the most studied regions of the brain, due to its relative simple structure and connectivity, as well as its major function in memory and spatial navigation.

In this first part of my introduction, I will give a short overview of the main features of hippocampal anatomy and the different cell types and hippocampal fields, as well as the basic circuitry. Then, I will quickly describe its different known physiological functions as well as some of the clinical consequences when things go wrong. Finally, I will describe the sequential steps of hippocampal development in more details, with special emphasis on dentate gyrus development.

A) Hippocampal anatomy

1) General anatomy

In vertebrates, the dorsal telencephalon contains the cerebral cortex, subdivided into many histologically and functionally distinct regions. The main subdivisions, based on radial organization, divide the cerebral cortex into the neocortex and allocortex, which includes the archicortex, the paleocortex, and the transitional periallocortex (Zilles and Wree, 1995). Whereas the neocortex is composed of six layers, the allocortex that is evolutionary older, is formed by three to four layers (Bayer, 1985). The hippocampus belongs to the archicortical domain, the more ancient portion of the telencephalon and is characterized by a 3-layers lamination.

The hippocampal region embeds two different but connected structures (**Figure 1**; Bayer, 1985):

- the parahippocampal region comprising perirhinal, postrhinal and entorhinal cortex, as well as parasubiculum, presubiculum and subiculum;
- and the hippocampal formation (HF), or simply referred as “hippocampus”.

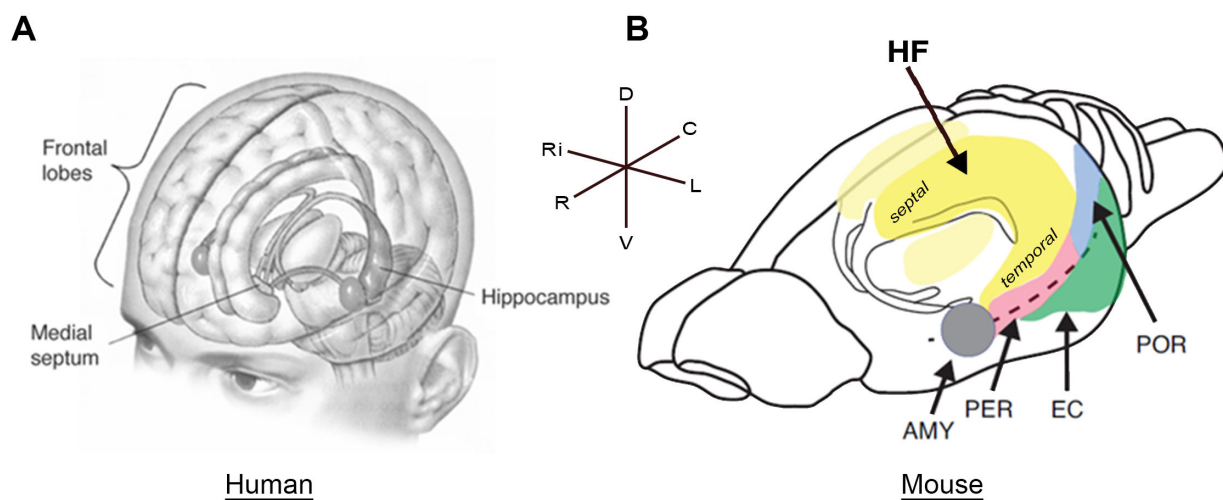


Figure 1. Localization of the hippocampal region in human and mouse brains.

A. Localization of the hippocampus in the human brain. **B.** Localization of the hippocampus in the mouse brain. The hippocampal formation is indicated in yellow, along with the different surrounding structures. The septal and temporal pole of the hippocampus are also indicated. *AMY*: Amygdala; *EC*: entorhinal cortex; *HF*: hippocampal formation; *PER*: perirhinal cortex; *POR*: postrhinal cortex. Adapted from open source image and from Kesner 2013.

The hippocampus is a bilateral structure, located inside the medial temporal lobe, beneath the cortical surface (**Figure 1**). In mouse, the hippocampal formation extends along a longitudinal axis referred to as the septo-temporal axis: the septal pole is located rostro-dorsally and the temporal pole caudo-ventrally (**Figure 1B**; Amaral and Witter, 1989). Notably, the septal and temporal hippocampi are often referred to as dorsal and ventral hippocampi, respectively, but correspond to the same structures. The terms of septal and temporal will be preferred to dorsal and ventral in this study.

The hippocampus appears as a C-shape structure (**Figure 2B**), and the pial membrane invagination at the center forming this particular shape is called the hippocampal *sulcus* or hippocampal fissure (Hf). During evolution, due to the huge expansion of the neocortex in humans and other primates, the hippocampus has been pushed to the deeper part of the brain, and as a consequence, its orientation has been inverted, compared to other mammals.

The hippocampal formation itself is subdivided from proximal to distal into two distinct regions: the hippocampus proper (Hp), and the dentate gyrus (DG) (**Figure 2B**; Bayer, 1985). These two structures are described hereafter.

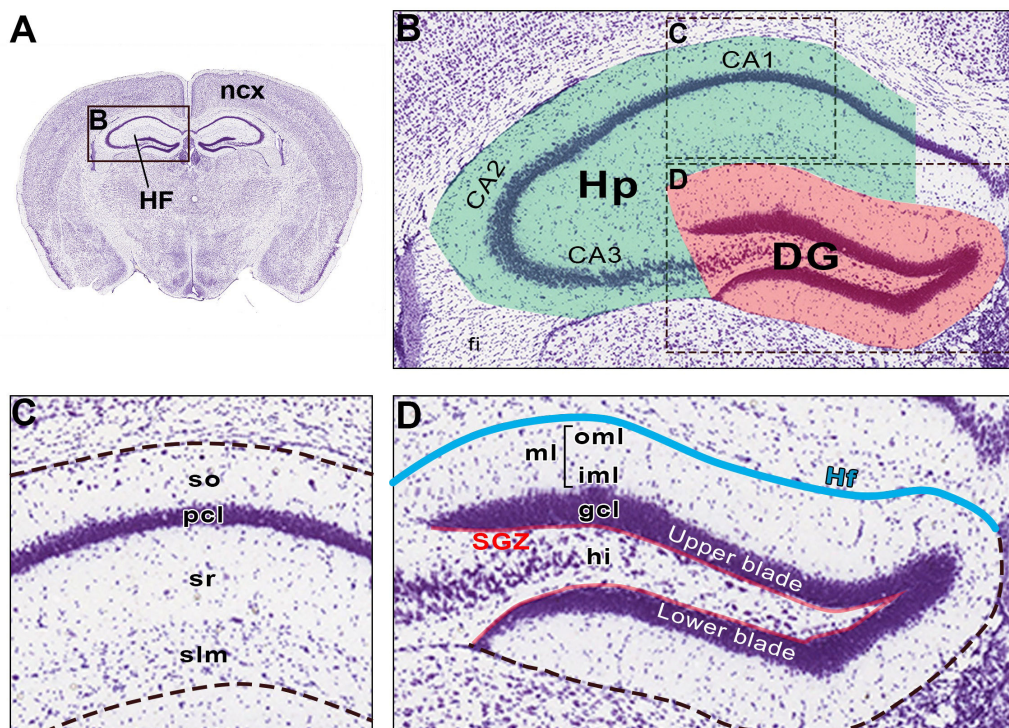


Figure 2. Anatomy of the hippocampus.

A. View of a coronal section of an adult mouse brain, stained with Nissl, at the level of the septal/rostral hippocampus. **B.** Magnification of the box in A showing hippocampal formation anatomy. The two regions hippocampus proper (Hp) and dentate gyrus (DG) are labelled in green and red, respectively. **C.** Magnification of the box C in B showing hippocampus proper layers, at the level of the CA1 field. **D.** Magnification of the box D in B showing dentate gyrus three layers. The upper and lower blades are also indicated. *CA1/2/3*: cornu Ammonis field 1/2/3; *DG*: dentate gyrus; *fi*: fimbria; *gcl*: granule cell layer; *Hf*: hippocampal fissure; *HF*: hippocampal formation; *hi*: hilus; *Hp*: hippocampus proper; *ml*: molecular layer; *ncx*: neocortex; *pcl*: pyramidal cell layer; *slm*: stratum lacunosum moleculare; *so*: stratum oriens; *sr*: stratum radiatum. Adapted from Allen Brain Atlas.

2) Hippocampus proper (Hp)

The hippocampus proper (Hp), often referred to as the fields of Ammon's horn or Cornus Ammonis (CA) fields, can also be divided into three main regions: the CA1, CA2 and CA3, located from proximal (closer to the midline) to distal (closer to the DG), respectively (**Figure 2B**). These fields have been first described by Ramón y Cajal in the XIXth century based on their cell-size characteristics and later described by his student Lorente de Nó. Since then, several studies showed that each CA has specific characteristics, such as distinct function, connectivity and gene expression patterns. However, it is interesting to note that there are no sharp delimitations between these regions. The existence of the CA2 region has been subject to many controversy, due to its resemblance with a CA1-CA3 mixed portion, however recent data have highlighted several unique features of this substructure in terms of gene expression, connectivity patterns and neuronal physiology (Witter and Amaral, 2004; Young *et al.*, 2006; Cui *et al.*, 2013; Kohara *et al.*, 2014).

The Hp, as part of an archicortical domain, is formed by three main cell layers: the *stratum oriens*, the *stratum pyramidale* and the *stratum radiatum*. However, in addition to these layers, there are also layers containing only fibers (axons and/or dendrites). Therefore, taken all together, from the ventricular surface to the pial surface, the layers that compose the Hp are the followings (**Figure 2B,C**; Bayer, 1985):

- The Alveus, the most superficial layer that contains the axons of pyramidal neurons passing toward the fimbria/fornix, one of the major outputs of the Hp.
- The *stratum oriens* (so), which contains the cell bodies of inhibitory cells, as well as basal dendrites of pyramidal neurons.
- The *stratum pyramidale* or pyramidal cell layer (pcl), the most easily distinguishable, contains the cell bodies of the excitatory pyramidal neurons. This stratum also contains the cell bodies of many interneurons.

- The *stratum lucidum* (slu), one of the thinnest layers in the Hp, found in the CA3 only, and containing axons from the DG granule cells, called the Mossy fibers.
- The *stratum radiatum* (sr), as the stratum oriens contains septal and commissural fibers. It also contains projections from CA3 to CA1, called Schaffer collateral fibers, as well as some interneurons.
- The *stratum lacunosum moleculare* (slm), only present in the CA1 field, and containing Schaffer collateral fibers, projections from entorhinal cortex called the perforant path fibers, and distal dendrites of pyramidal cells.

Pyramidal cells are the main projection excitatory neurons of the hippocampus proper. Their cell bodies possess a triangle shape and are localized in the pyramidal cell layer. Their apical dendritic tree is found in the *stratum radiatum*, whereas their basal dendrites and axon extend toward the *stratum oriens*.

The different CA fields express specific genes that can be used as markers. As an example, pyramidal cells express Math2, also called Nex or NeuroD6, (Bartholomä and Nave, 1994; Schwab *et al.*, 2000) and Dkk3 (Diep *et al.*, 2004) that are absent from DG granule cells. More specifically, CA1 pyramidal cells are characterized by the expression of POU domain gene SCIP (Frantz *et al.*, 1994), while CA3 pyramidal cells express factors such as the kainate receptor subunit KA1 (Castillo *et al.*, 1997), the RNA-binding protein HuB (Okano and Darnell, 1997), as well as the post-synaptic scaffolding protein Homer3 in their dendrites (Shiraishi *et al.*, 2004). Moreover, the small CA2 field expresses the voltage-dependent calcium channel gamma subunit 5 CACNG5 (also known as TARP gamma-5) specifically (Fukaya *et al.*, 2005; Kato *et al.*, 2008).

Finally, the hippocampal fissure, as mentioned earlier, separates the CA1 field from the DG (**Figure 2D**). Although the hippocampal fissure could be considered a virtual line in adult brains (Sievers *et al.*, 1992), it certainly represents in the embryonic brain a real pial membrane containing meningeal tissue as well as blood vessels.

3) Dentate gyrus (DG)

The DG has a V-shape structure, composed of 2 blades: an upper blade (or supra-pyramidal blade) located dorsally, and a lower blade (or infra-pyramidal blade) located ventrally (**Figure 2D**). As it is part of the archicortical region, the DG is also composed of 3 layers that form this V-shape structure.

These 3 layers are, from the deepest part to the pial surface (**Figure 2D**; Bayer, 1985):

- The *stratum polymorph* or polymorphic layer, also commonly named the hilus (hi), a complex cellular and plexiform zone containing different cell types not well characterized so far. The hilus is also the place where all axons from the granule cells, called the mossy fibers, converge toward the CA1 region. This layer was in the past incorrectly denominated CA4, as if it was considered a terminal portion of the CA3 field (Lorente de Nó, 1934).
- The *stratum granulosum* or granule cell layer (gcl), a dense and easily distinguishable layer containing cell bodies of granule projection neurons.
- The *stratum moleculare* or molecular layer, a broad plexiform zone that mainly contains the dendritic tree of granule cells and afferent axons with which they form synapses. These axons include the commissural fibers from the contralateral DG and inputs from the medial septum (Matthews *et al.*, 1986), both found in the inner molecular layer (iml); as well as the perforant path fibers from the entorhinal cortex, found in the outer molecular layer (oml).

In addition to these three layers, another specific region can be identified in adult mammals DG: the subgranular zone (SGZ). Positioned between the hilus and the granule cell layer (**Figure 2D**), the SGZ is composed of cells that have retained their proliferative capacity and form a neurogenic pool producing new granule cells throughout adulthood (Altman and Bayer, 1990).

Granule cells are the main projection excitatory neurons of the DG. Their cell bodies are round and are localized in the granule cell layer. Their dendritic trees are found in the molecular layer, whereas their axons extend toward the hilus, in the *stratum lucidum*.

As for pyramidal cells of the Hp, DG granule cell can be specifically labeled with several markers. Among them, the most common is the prospero-related homeobox gene Prox1, which is expressed by granule cells throughout development and into adulthood, but is absent from other cell types of the hippocampus (Oliver *et al.*, 1993; Galeeva *et al.*, 2007). In addition, mature granule cells are specifically distinguished by the expression of the calcium-binding protein Calbindin in the adult brain, (Sloviter, 1989), as well as Dock10 and C1ql2 (Iwano *et al.*, 2012).

4) Connectivity: the three synaptic system

The hippocampus connectivity has been well studied and described in literature, and is, thanks to this and its relative simplicity, a model often used for electrophysiological studies. The main connectivity circuit of the hippocampus is formed by an excitatory glutamatergic loop named the three synaptic system (**Figure 3**; Andersen *et al.*, 1971).

As partially described above, the dentate gyrus is the primary gateway for inputs into the hippocampus. It receives connections from the entorhinal cortex (EC), called the perforant path (**Figure 3**; Ramón y Cajal, 1893; Witter *et al.*, 1989), whose axons form synapses with granule cell dendrites in the molecular layer. Granule cells then send axons to the hilus toward the CA3 region (**Figure 3**). They extend mainly through the *stratum lucidum* of the hippocampus proper, but some fibers are also found within or under the pyramidal cell layer. These axons, called the mossy fibers, form synapses with CA3 pyramidal dendrites within the *stratum lucidum* above the pyramidal cell layer (Blackstad *et al.*, 1970; Gaarskjaer, 1978; Swanson *et al.*, 1978; Claiborne *et al.*, 1986). Next, pyramidal axons project through the *stratum radiatum* and *stratum lacunosum moleculare*, toward the CA1 field (**Figure 3**). These

fibers, called the Schaffer collaterals, form synapse with CA1 pyramidal dendrites (Ishizuka *et al.*, 1990). Finally, axons from the CA1 pyramidal cells innervate, through the *stratum oriens*, the nearby Subiculum and back to the entorhinal cortex, thus forming the main output connections of the hippocampus. Altogether, the perforant path, the mossy fibers and the Schaffer collaterals form the so-called “three synaptic system”.

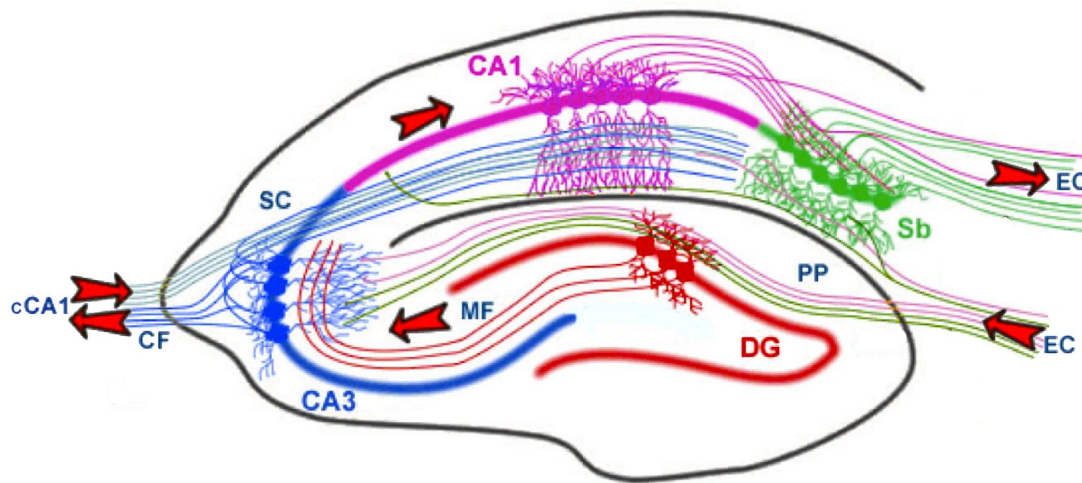


Figure 3. Hippocampal connectivity.

The main components of hippocampal connectivity are represented on this schema, including the tri-synaptic circuit (perforant path PP - mossy fibers MF - Schaffer collaterals SC) and the CA3 to CA1 commissural fibers (CF). DG is represented in red, CA3 in blue, CA1 in purple, and subiculum in green. *cCA1*: contralateral CA1; *CA1/3*: cornus Ammonis field 1/3; *CF*: commissural fibers; *DG*: dentate gyrus; *EC*: entorhinal cortex; *MF*: mossy fibers; *PP*: perforant path; *Sb*: subiculum; *SC*: Schaffer collaterals. Adapted from Kesner 2013.

Moreover, in mammalian brains, the two hemispheres are often inter-connected and the hippocampus does not make exception. Whereas connections within the same hemisphere are grouped under the term of associational fibers, connections between the two hippocampi are called the commissural fibers. Indeed, these axons cross the brain by the dorsal and ventral commissures (Blackstad 1956; Amaral *et al.*, 1984). Thus, the dentate gyrus receives afferences from the contralateral DG, which forms synapses with granule cell dendrites in the molecular layer. Moreover, CA3 pyramidal axons innervate both the ipsi- and the contralateral CA1 (**Figure 3**; Ishizuka *et al.*, 1990; Li *et al.*, 1994). Notably, although the two

hippocampi are highly connected in rodents (Raisman, 1965; Gottlieb and Cowan, 1973), this commissural connection is more dispersed in primates (Amaral *et al.*, 1984).

In addition to the three synaptic associational and commissural systems, many other types of connections have been described. As an example of other intrinsic connections, perforant path fibers from the entorhinal cortex also establish inputs directly with pyramidal neurons of CA3, CA1 and Subiculum (Steward and Scoville, 1976). And in addition to entorhinal cortex efferences, one of the major extrinsic outputs of the hippocampus is the reciprocal connection with the septum.

A complex inhibitory network of interneurons is also present in the hippocampus (reviewed in Freund and Buzsaki, 1996; Kullmann, 2011), but will not be discussed here.

B) Hippocampal functions

The hippocampus is a major component of the brain in humans and other mammals. Initially, until the 1930s, the hippocampal region was considered by neuroanatomists to be part of the olfactory system, but this was proven wrong, notably by the influential review of Alf Brodal (Brodal, 1947). Another influential neuroanatomical hypothesis was proposed by James W. Papez, who suggested that the hippocampus was part of a circuit, the so-called Papez-circuit, which would provide the anatomical substrate of emotion (Papez, 1937). This idea was supported by the contemporary work of Klüver and Bucy that showed that removal of the medial temporal lobe causes profound emotional disturbances in monkeys (Klüver and Bucy, 1937). However, it was subsequently shown that the loss of fear and other behavioral alterations could be attributed to the amygdala and its connections with the visual regions of the inferotemporal cortex (Mishkin, 1954; Schreiner and Kling, 1956; Weiskrantz, 1956) and not to hippocampal damages. Again, Brodal commented this Papez theory as of « historical interest only » (Brodal, 1981). Nevertheless, although only moderate evidence supports the hypothesis that the hippocampus is involved in emotion, it is occasionally brought back to light (Gray and McNaughton, 2000; Gray, 2001).

Nowadays, the scientific community has largely admitted the important role played by the hippocampus in memory and learning, and additional theories of hippocampal functions in spatial navigation and stress response have emerged. These three aspects of hippocampal functions are further described hereafter.

1) Memory & Learning

One of the first evidence that the hippocampus plays a role in memory was the famous report of Scoville and Milner (Scoville and Milner, 1957). In the early 1950s, in the attempt to relieve epileptic seizures, the patient H.M. underwent a surgical ablation of its two hippocampi. The surgery consequently led to severe anterograde amnesia, and a partial retrograde amnesia: H.M. was unable to form new memory and could not remember any events that occurred just before his surgery. Several other studies have since then confirmed the role of hippocampus in forming new memory (Rolls, 1996; Kesner, 2013). Despite this retrograde effect, which extended to a few years before the brain damage, older memories remained following hippocampal damage, suggesting that the consolidation of memories over time involves the transfer from the hippocampus to other parts of the brain (Squire and Schacter, 2002).

The memory can be subdivided into two types of memory. On one hand, the declarative memory corresponds to memories that can be explicitly verbalized, such as memory of facts (semantic memory) and memory about experienced events (episodic memory). On the other hand the non-declarative memory among which the procedural memory, gathers memory and learning of motor or cognitive skills, such as riding a bike or playing an instrument. Damage to the hippocampus affects the declarative episodic memory (Squire, 1992; Squire *et al.*, 2004), but does not affect the non-declarative procedural memory, suggesting that the hippocampus is specifically involved in declarative memory, whereas the non-declarative depends on different brain regions.

2) Spatial Navigation

In the 1970s, O'Keefe and Dostrovsky discovered neurons in the rat hippocampus, later called « place cells », that appeared to show activity related to the rat's location within its environment (O'Keefe and Dostrovsky, 1971). The existence of these place cells have also been reported in human brain (Ekstrom *et al.*, 2003). Interestingly, both pyramidal cells of the hippocampus proper and granule cells of the dentate gyrus show « place cell » responses.

This discovery suggested that the hippocampus might act as a neural representation of the environment, a cognitive map (O'Keefe and Nadel, 1978). Evidences of this theory are numerous (for review, see Good, 2002). First, since this “place cells” discovery, other types of cells playing a role in spatial navigation were discovered, such as head direction cells, grid cells, and border cells. Although they are located in several parts of the rodent brain, these regions are strongly connected to the hippocampus (Moser *et al.*, 2008; Solstad *et al.*, 2008). Moreover, behavioral studies showed that rats with hippocampal lesions are impaired in learning certain spatial memory task, such as the radial arm (Olton *et al.*, 1979; Jarrard 1983), the T- maze (Rawlins and Olton, 1982) and the Morris water maze, in which rats with a lesioned hippocampus fails to find a hidden, but not a visible, platform (Morris *et al.*, 1982; Pearce *et al.*, 1998). In addition to rodents, damage to the anatomical homologue of the hippocampus in birds and the hippocampus in humans are known to disrupt spatial learning. Finally, in human, the « cognitive map » theory is also validated by several data: patients that do not have a fully functional hippocampus often get lost (Chiu *et al.*, 2004); and it was reported that the posterior hippocampus of experienced Londoner taxi drivers (who needed to know all the streets of London by heart) were significantly larger relative to control subjects, showing a positive correlation between hippocampal volume and the navigation skills of taxi drivers (before the use of GPS navigators) (Maguire *et al.*, 2000).

3) Stress response

Anxiety, fear and stress are very different functions from memory, but surprisingly the hippocampus has also been implicated in these processes. Several evidences have validated this theory.

First, the animal and human hippocampus contains a high density of mineralocorticoid and glucocorticoid receptors (MR and GR, respectively) (McEwen 1968, 1980), which are known to mediate stress-related corticosteroid actions. Second, there is an inverted U-shaped function between levels of stress and memory: studies showed that increasing stress has initially synergistic but later deleterious effects on learning capability in mice (Yerkes and Dodson, 1908). Thus, mild stress and low concentrations of steroids can facilitate spatial memory (Akirav *et al.*, 2004), contextual fear conditioning (Cordero *et al.*, 2003), and classic eye-blink conditioning (Shors, 2001); while moderate to high levels of stress or steroid can impair spatial memory (Diamond *et al.*, 1996; Conrad *et al.*, 1999), recognition memory (Baker and Kim, 2002) and contextual fear conditioning (Pugh *et al.*, 1997). In addition, stress modulates the intrinsic hippocampus excitability as well as the activity-dependent synaptic plasticity associated with learning and memory (Foy *et al.*, 1987; Garcia *et al.*, 1997; Diamond and Park, 2000; Kim and Diamond, 2002). Thus, stress or stress hormone elevation can cause deleterious structural changes both in animals (Woolley *et al.*, 1990; Magarinos and McEwen, 1995; Sapolsky *et al.*, 1985; Mizoguchi *et al.*, 1992) and humans (Starkman *et al.*, 1992) and can impair neurogenesis in the post-natal and adult DG (Cameron and Gould, 1994; Gould *et al.*, 1997), through an indirect glucocorticoid mechanism since granule cell progenitors do not express MR and GR (Kim and Diamond, 2002).

Together, these data have demonstrated a role of the hippocampus in the negative feedback regulation of the hypothalamic-pituitary-adrenal axis (reviewed in Jacobson and Sapolsky, 1991; and Herman *et al.*, 2005), the major system involved in orchestrating the body's reactions to stress.

4) Adult Neurogenesis

As mentioned earlier, one striking feature of the dentate gyrus, distinct from the other cortical structures, is that it contains a source of adult neurogenesis in mammals. The first evidence was published more than 50 years ago by Joseph Altman and colleagues (Altman, 1962, 1969; Altman and Das, 1965). The rodent forebrain possesses two regions with active ongoing neurogenesis during adulthood: the subventricular zone (SVZ) lining the lateral ventricles, and the subgranular zone (SGZ) in the DG. This SGZ consists of a niche of precursor cells located at the border between the hilus and the granule cell layer (**Figure 2D**), and the basic steps in the process of forming new neurons in this area are quite well understood (Abrous *et al.*, 2005). In addition to rodent brains, evidences for adult neurogenesis are also found in the human dentate gyrus (Eriksson *et al.*, 1998).

These DG SGZ stem-like cells have the capacity to proliferate but are more restricted in their multipotent function than stem cells. New generated cells migrate short distance to the granule cell layer and differentiate into neurons. These cells have been shown to exhibit granule cells properties: they receive synaptic input (Kaplan and Hinds, 1977), extend axons into the CA3 region (Stanfield and Trice, 1988; Markakis and Gage, 1999), express several biochemical markers of granule cells, including NeuN, calbindin, MAP-2, and Tuj1 (Kuhn *et al.*, 1996; Gould *et al.*, 2001), and depict granule cells electrophysiological properties (Van Praag *et al.*, 2002).

Additionally, multiple molecules that regulate the development of the granule cell layer are thought to have a similar function during adult neurogenesis of the SGZ. Among them, Wnt, BMP, Shh, and Notch regulate neural precursor cell maintenance, proliferation, and differentiation in the adult SGZ (Alvarez-Buylla and Lim, 2004; Fuentealba *et al.*, 2012). Similarly, granule cell differentiation during development and adult stages share common factors in their sequential gene expression, such as the expression of the doublecortin DCX, the basic helix-loop-helix transcription factor NeuroD1 (ND1) and the prospero-related homeobox gene Prox1 (detailed in *Introduction-I-C-3-a*)

Several studies suggest that this continuous generation of DG neurons is required in learning and acquisition of new memories (Van Dijck *et al.*, 2000; Aimone *et al.*, 2006) and in the behavioral effects of neuropathy (Gu *et al.*, 2011; Surget *et al.*, 2011; Zhang and Luo, 2011). Indeed, it has been reported that SGZ neurogenesis is crucial for DG repairing processes: adult neurogenesis is induced following DG damages such as mechanical or excitotoxic lesions (Gould and Tanapat, 1997) or ischemia and seizures resulting in granule cell death (Parent *et al.*, 1997; Kee *et al.*, 2001; Scharfman, 2004). Some evidence even suggests that neurogenesis is upregulated in neurodegenerative conditions such as Alzheimer's disease (Jim *et al.*, 2004).

Furthermore, studies have unraveled that the DG adult neurogenesis can be modulated by several factors. Among them, levels of circulating steroid hormones can act either in promoting or inhibiting adult neurogenesis. Thus, glucocorticoids inhibit the production of new neurons by decreasing the precursor proliferation (Gould *et al.*, 1991; Cameron and Gould, 1994) and conversely, removal of circulating adrenal steroids has the opposite effect (Gould *et al.*, 1992; Cameron and Gould, 1994). On the contrary, the ovarian steroid estradiol has a positive effect on the production of new cells in the adult rats DG (Tanapat *et al.*, 1999). Another known factor modulating DG adult neurogenesis is the environmental experience: stress decreases the rate of cell proliferation in the adult DG (Tanapat *et al.*, 2001; Malberg and Duman, 2003; Westenbroek *et al.*, 2004; Lemaire *et al.*, 2000), while environmental enrichment promotes cell proliferation and neurogenesis (Amrein *et al.*, 2004; Kempermann *et al.*, 1997; Brown *et al.*, 2003).

5) Septal/Temporal -specific functions

In the 1990s, Moser and Moser suggested that the hippocampus does not act as a unitary structure, but the septal and temporal pole might play different roles (reviewed in Fanselow and Dong, 2010). Indeed, anatomical studies indicated that connections of the septal (dorsal/rostral) and temporal (ventral/caudal) hippocampus differ (Swanson and Cowan, 1977). Moreover, spatial memory has been reported to depend on the septal pole but not on the

temporal pole (Moser *et al.*, 1993; Moser *et al.*, 1995). On the contrary, lesions of the temporal, but not of the septal pole, alter stress responses and emotional behavior (Henke, 1990). Therefore, these studies and a substantial number of others support the theory that the septal pole of the hippocampus is specifically involved in memory function, whereas the temporal pole modulates more emotional and affective processes.

Notably, it has also been demonstrated that “place cells” respond to fields that vary in a gradient along the length of the hippocampus: cells at the septal end show the smallest fields and cells at the temporal tip show fields that cover the entire environment (Moser *et al.*, 2008), suggesting that spatial navigation is also regionalized along the hippocampus. Consistent with this idea and as described earlier, the posterior (temporal pole) hippocampus, but not the anterior (septal pole) one of experienced taxi drivers is significantly larger compared to control subjects.

Although no distinct markers have been reported to specifically label the septal and the temporal pole of the hippocampus, few studies have demonstrated by transcriptome analyses that several genes are differentially enriched in the septal or temporal hippocampus (Leonardo *et al.*, 2006; Christensen *et al.*, 2010; O’Reilly *et al.*, 2014). In addition, several genes are expressed in a gradient along the longitudinal axis in the neocortex and in the archicortex, and can therefore be used to distinguish septal versus temporal poles of the hippocampus.

6) Disruption / Pathology of the hippocampus

Functional magnetic resonance imaging (fMRI) analyses of some neuropsychiatric disorders have hinted to the requirement of the hippocampus in various types of mental activities in humans.

As an example, decreased hippocampal volume has been observed in patients with depression or post-traumatic stress disorder (PTSD) (Campbell *et al.*, 2004; Woon *et al.*, 2010). Anatomical abnormalities in the hippocampus are also observed in epilepsy, lissencephaly,

and schizophrenia (Baulac *et al.*, 1998; Harrison, 2004; Donmez *et al.*, 2009). Some of these symptoms are thought to be associated with the migration deficit of hippocampal neurons during development (Barkovich *et al.*, 1991; Dobyns *et al.*, 1996; Montenegro *et al.*, 2006).

More specifically, migration defects of dentate granule cells, called the Granule Cell Dispersion (GCD), have been associated with Temporal Lobe Epilepsy (TLE) (Houser, 1990). The extracellular glycoprotein Reelin, which is known to act as a stop signal for migrating neurons, seems to be involved in this process: humans with GCD exhibit a decreased Reelin expression and treatment of mice with GCD with Reelin rescued granule cell distribution (Haas *et al.*, 2002; Müller *et al.*, 2009). Despite this correlation, it still remains to be elucidated whether epilepsy is caused by these hippocampal abnormalities and/or whether they are consequences of the cumulative seizures. However, unilateral injections of the glutamate agonist kainate into the mouse hippocampus induce epileptic seizures and, with some delay, a characteristic Granule Cell Dispersion (Bouilleret *et al.*, 1999; Heinrich *et al.*, 2006), suggesting that GCD is a result of seizure activity rather than being its source.

In addition, the hippocampus is one of the first regions to suffer damage in Alzheimer's Disease (AD): neuropathological changes are thought to appear initially in the entorhinal cortex and progress from there to the hippocampus, before reaching the neocortex as the disease progresses (Braak *et al.*, 1993). AD is associated with hippocampal atrophy, both in patients with established dementia and in the presymptomatic stage of AD (Bobinski *et al.*, 1999; Convit *et al.*, 1997). Entorhinal and hippocampal damages are present in the disease earliest stages, before AD can be clinically diagnosed, at a time called the mild cognitive impairment (MCI), making of the detection of medial cortex damages in MCI an important tool to achieve earlier diagnosis and treatment of AD. Interestingly, determination of hippocampal atrophy can distinguish AD from normal aging with a high degree of specificity and sensitivity (Jack *et al.*, 1997). Moreover, because the hippocampus plays crucial roles in memory and spatial navigation, its neuropathological changes in AD induces the well-known AD symptoms of memory loss and disorientation. Consistently, deficits of episodic memory have been correlated with atrophy of the hippocampus but not with atrophy of structures outside the medial temporal lobe.

C) Hippocampal development

1) Early cortical patterning events

The hippocampus arises from the caudomedial portion of the dorsal telencephalic neuroepithelium (Stanfield and Cowan, 1979a,b; Bayer, 1980a,b). Cortical progenitors are found along this edge and form the cortical hem (also called hem) that controls hippocampal and dentate development at the earliest stages. Indeed, loss of function mutations inducing hem defects, such as for *Lhx5* (Zhao *et al.*, 1999), lead to secondary hippocampal defects due to the loss of hem-derived patterning signals. The hem expresses many of these inductive signaling factors, such as the Bone Morphogenetic Protein (BMP) and Wnt family members (Furuta *et al.*, 1997; Grove *et al.*, 1998). The Wnt signaling pathway controls the production and migration of granule cell progenitors during Dentate Gyrus formation (Galceran *et al.*, 2000; Lee *et al.*, 2000; Roelink, 2000). BMP signaling, however, is required for cortical hem formation and thus has only a secondary effect on DG formation, since BMPs do not seem to be necessary any longer for specification of hippocampal cell identities once the hem is formed (Hébert *et al.*, 2002).

Wnt signaling plays a crucial role in the development of the dentate gyrus. Loss of several components of the Wnt pathway leads to defective DG development and absence of DG neural stem cells (Galceran *et al.*, 2000; Lee *et al.*, 2000; Zhou *et al.*, 2004; Li and Pleasure, 2005). Among them, *Lef1*, a Wnt-activated transcription factor selectively expressed in the developing dentate, regulates the generation of DG granule cells since its loss leads to an abnormally small dentate gyrus as a result of decreased proliferation of progenitor cells (Galceran *et al.*, 2000). In addition, activation of the Wnt signaling pathway also induces the expression of the homeobox gene *Prox1* selectively in granule neurons and regulates dentate gyrus neurogenesis in the adult (Lie *et al.*, 2005; Machon *et al.*, 2007; Karalay *et al.*, 2011).

Another important factor for the onset of dentate gyrus formation is the homeobox-containing transcription factor *Emx2*. In mice null for *Emx2*, the development of the dentate gyrus is affected at the onset of its formation with defects in the dentate neuroepithelium (Pellegrini *et*

al., 1996; Yoshida *et al.*, 1997). As a consequence, the DG is missing and the hippocampus proper is reduced. The few granule cells produced in the mutant are poorly differentiated (Savaskan *et al.*, 2002). Several evidences suggest that this problem could be a defect in the cortical positional information signaling cascade mediated by Wnt signaling, which regulates *Emx2* (Muzio *et al.*, 2002, 2005; Ligon *et al.*, 2003).

2) Hippocampus proper development

The developmental processes of the hippocampal pyramidal cell layer of the hippocampus proper (CA fields) are roughly similar to those of the neocortical pyramidal cells. In both cases, cells are born in the ventricular zone (VZ), differentiate in the sub-ventricular zone (SVZ) and migrate radially along radial glial fibers to their definitive locations in the pyramidal cell layer, in an inside-out pattern: deep layers are formed first, followed by upper layers (Rakic, 1978; Supèr and Uylings, 2001). As a consequence, the most recent neurons are found in more superficial layers.

Since this study is focusing on Dentate Gyrus development, no further description will be given to the development of the Cornus Ammonis in this introduction.

3) Dentate gyrus development

Compared to hippocampus proper and neocortex, the morphogenesis of the dentate granule cell layer is fundamentally different (Angevine, 1965; Stensaas, 1967; Schlessinger *et al.*, 1975; Bayer, 1980a,b; Eckenhoff and Rakic, 1984; Rickmann *et al.*, 1987; Altman and Bayer, 1990a-c; Sievers *et al.*, 1992; Li and Pleasure, 2005; Li *et al.*, 2009). One of the main difference is that DG development is uniquely characterized by the existence of precursor cells that divide and migrate at the same time, generating post-mitotic, immature neurons that also migrate before reaching their final locations (Altman and Bayer, 1990a).

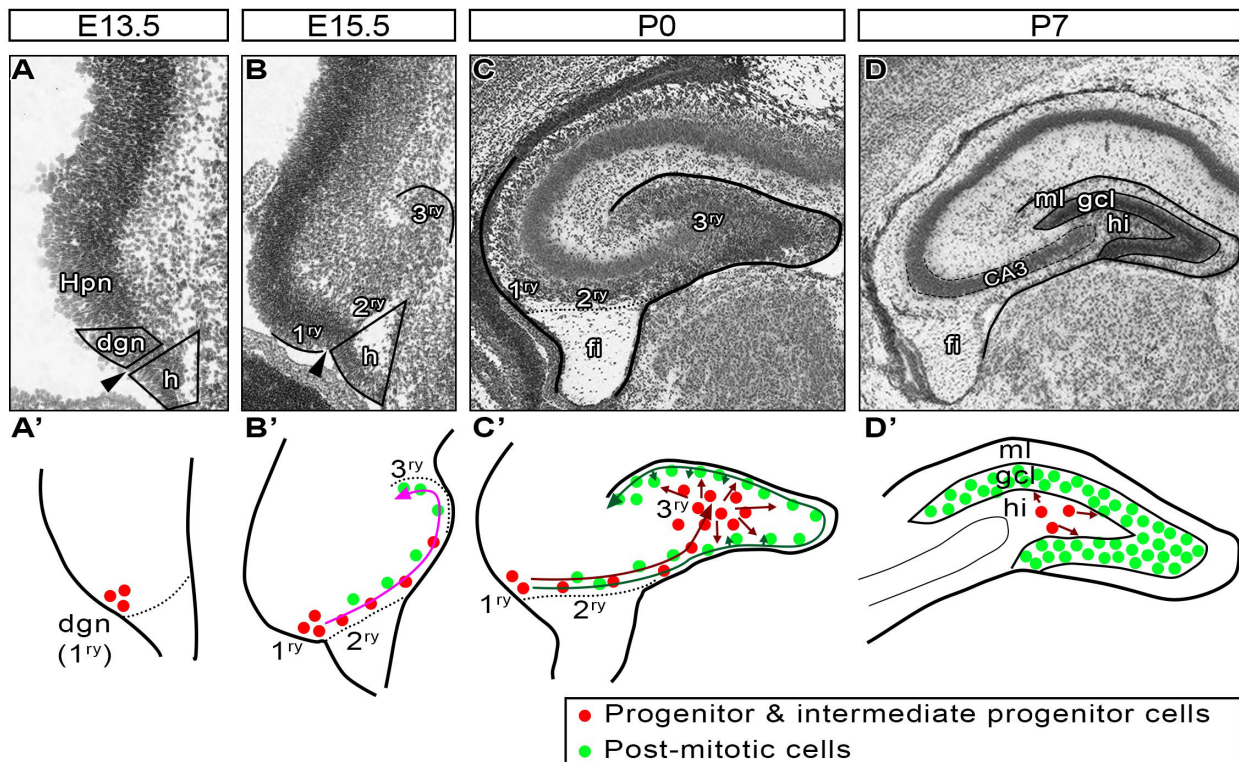


Figure 4. Dentate gyrus development.

Dentate gyrus developmental steps at E13.5, E15.5, P0 and P7 in mouse. The upper panel (A-D) shows DG anatomy on coronal sections labelled with Nissl staining. The lower panel (A'-D') shows representative schemas of the different developmental stages. Progenitors of the granule cells originate from the dentate gyrus neuroepithelium (dgn, or primary matrix 1ry), a restricted neuroepithelial area of the medial pallium, established around E13.5 in mice (A) and located the dorsal edge of the hem (h) around a ventricular indentation called the dentate notch (black arrowhead in A and B). Starting at E15.5 (B-B'), a mix of mitotic (red dots in B') and post-mitotic (green dots in B') cells travel through the secondary (2ry) matrix (purple arrow in B'). At the end of their migration, cells accumulate in the tertiary (3ry) matrix. Two routes of migration occurs: while early-generated post-mitotic cells migrate along the pial surface (green arrow in C'), forming first the DG upper blade, progenitors accumulate in the 3ry matrix (red arrows in C'), where they form a second germinative pool that will generate the vast majority of granule cells within the first postnatal weeks (C'-D'). As time proceeds, hilar proliferative zone becomes restricted to the SGZ, the adult neurogenesis niche of the dentate gyrus. *1ry/2ry/3ry*: primary/secondary/tertiary matrix; *CA3*: cornus Ammonis field 3; *dgn*: dentate gyrus neuroepithelium; *fi*: fimbria; *gcl*: granule cell layer; *h*: hem; *Hpn*: hippocampus proper neuroepithelium; *hi*: hilus; *ml*: molecular layer.

In 1990, Altman and Bayer demonstrated that proliferative stem cells and progenitors of the granule cells initially originate from a restricted area of the neuroepithelium of the medial

pallium. This focal region is located at the dorsal edge of the hem (which will later become the fimbria), next to a ventricular indentation called the dentate notch (black arrowhead in **Figure 4A-B**). This dentate gyrus neuroepithelium (dgn), or primary matrix (1^{ry}) is first established at around E13.5 in mice (**Figure 4A-A'**). It contains progenitor cells that share several characteristics with astroglia (shape, markers) and are called Radial Glia Cells (RGCs). RGCs divide in the ventricular zone and give rise to Intermediate Progenitor Cells (IPCs) that have retained their mitotic activity. Starting at E15.5 (**Figure 4B-B'**), IPCs travel through the dorsal portion of the fimbria (suprafimbrial region). This stream of migratory cells, called the secondary matrix (2^{ry}), is composed of a mix of dividing progenitors and post-mitotic immature neurons. At the end of their migration, these cells accumulate in the tertiary matrix (3^{ry}), or DG anlage, which will become the major proliferative zone of postnatal dentate development. While DG morphogenesis starts early in embryonic development, the vast majority of neurons are generated within the first four postnatal weeks (Muramatsu *et al.*, 2007). As postnatal time proceeds (**Figure 4C-D**), the hilar proliferative zone becomes restricted to the SGZ, the adult neurogenesis niche of the dentate gyrus. Although the adult neurogenesis of the DG is well studied, the mechanisms regulating its establishment during DG development are poorly understood.

The progression from stem/progenitor cell to mature neuron requires several steps, including specific molecular pathways, migration and positioning of newborn cells, and finally maturation and establishment of a proper connectivity. These three processes are described hereafter.

a - Neuronal differentiation: Transcription Factor cascade

Several transcription factors and signaling pathways, most of them commonly used during cellular differentiation in other systems, are required for the development of the DG (Kempermann *et al.*, 2004; Frotscher *et al.*, 2007; Li and Pleasure, 2007). This sequential expression of transcription factors, called the transcription factor cascade, guides the transition from neural stem cells to progenitors and ultimately to post-mitotic mature neurons.

Although many other genes are expressed during granule cell differentiation, I will present here the major steps and the main factors involved. The members of this transcription factor cascade used in this study are summarized in **Figure 5**.

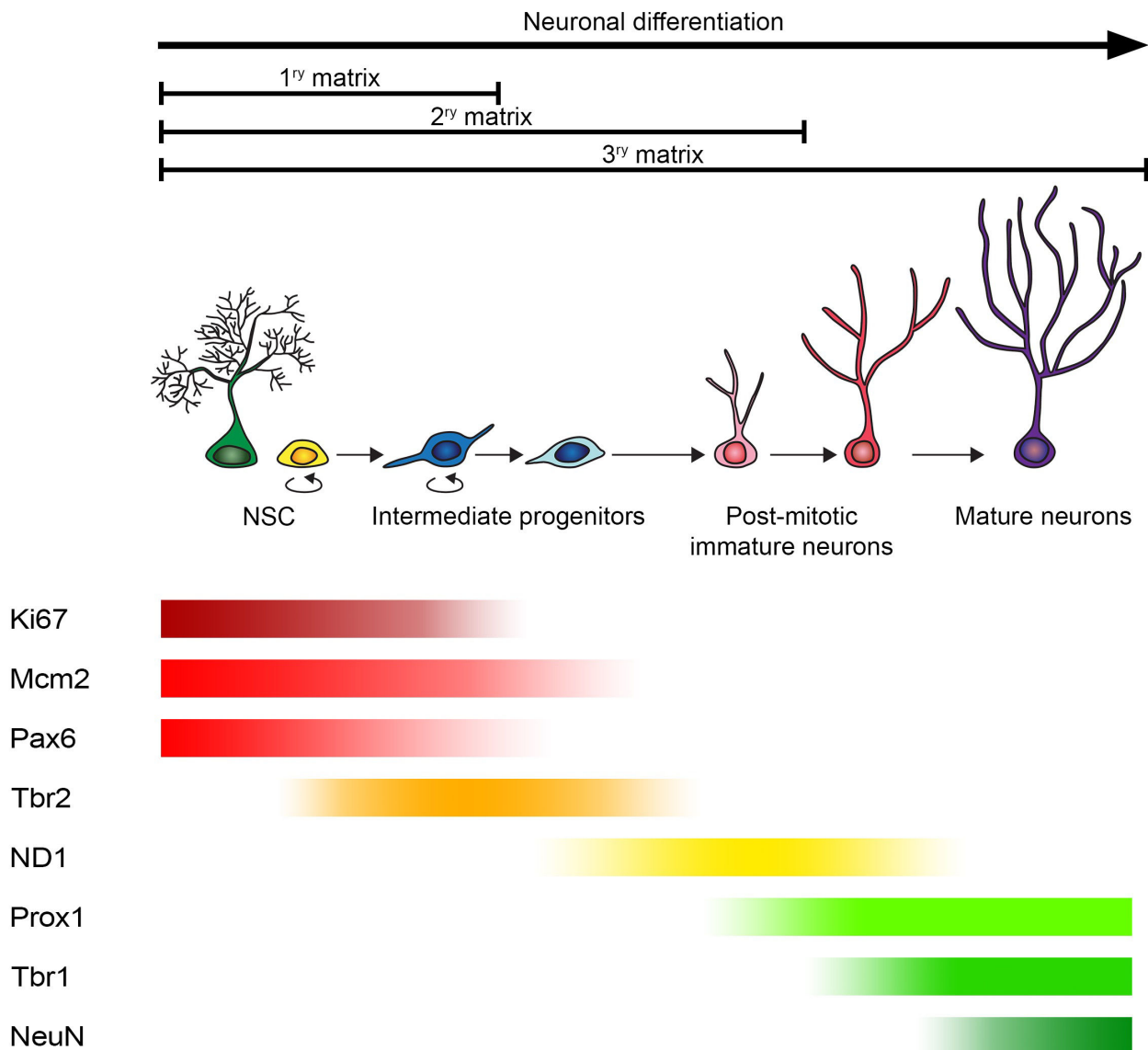


Figure 5. Transcription factor cascade involved in granule cell differentiation.

Schematic representation of granule cell differentiation, with the different sequence of cell types from neural stem cell (NSC) to intermediate progenitors and post-mitotic granule cells. Their localization in the three matrices and the specific transcription factors or markers they express are also indicated.

The primary matrix contains neural stem and progenitor cells, the RGCs, which possess self-renewal capability, and therefore are expressing markers of the cell cycle, such as Ki67 or Mcm2. These progenitors are also characterized by the expression of the transcription factors Sox2 and Pax6. Following several rounds of divisions, IPCs are subsequently generated and start to express the T-box transcription factor Tbr2. IPCs are found in the dentate sub-ventricular zone of the primary matrix, in the stream of migration (secondary matrix) from E15.5, and in the tertiary matrix at later stages. While migrating, IPCs divide, allowing amplification of granule cell numbers. The end of this transient amplifying progenitor phase is marked by the expression of the bHLH transcription factor ND1 in neuronal committed IPCs (Miyata *et al.*, 1999). The latter pushes cells to exit the cell cycle and gives rise to early immature post-mitotic neurons, mostly localized in the tertiary matrix. Post-mitotic neurons gradually mature and express the transcription factors ND1, Prox1, Tbr1, and finally NeuN that mark sequential discrete steps of granule cell maturation. Interestingly, although most of these transcription factors, such as Pax6, Tbr2, Tbr1 and NeuN, are common to the neocortex and hippocampus (Englund *et al.*, 2005; Hevner *et al.*, 2006), Prox1 expression is specific to granule cells of the dentate gyrus and is absent in the adjacent hippocampus proper (Lavado *et al.*, 2010).

Several loss- and gain-of-function studies have unraveled the specific roles of these transcription factors in DG granule cell differentiation. The investigated functions of some of these factors are presented hereafter.

- **Sox2**

The transcription factor Sox2 [SRY (sex determining region Y)-box 2], a member of the SOXB1 family, is expressed by cortical mitotic precursors but absent from IPCs (Zappone *et al.*, 2000; Graham *et al.*, 2003) and is a key determinant of neural stem/progenitor cell maintenance in the cerebral cortex. Sox2 overexpression represses neuronal differentiation (Bani-Yaghoub *et al.*, 2006; Bylund *et al.*, 2003; Graham *et al.*, 2003), whereas Sox2 down-regulation induces cell cycle exit and expression of early differentiation markers (Graham *et al.*, 2003). In humans, rare Sox2 mutations have been reported to cause impaired hippocampal development, among other symptoms (Sisodiya *et al.*, 2006). In the hippocampus, Sox2 was

also shown to be required for neural stem cell maintenance, by regulating soluble factors, including Shh (Favaro *et al.*, 2009). Additionally, Sox2 deficiency causes neurodegeneration and impaired neurogenesis in the adult mouse brain (Ferri *et al.*, 2004) and conditional ablation of Sox2 in adult hippocampal NPCs impairs the activation of proneural and neurogenic genes, resulting in increased neuroblast death and functionally aberrant newborn neurons (Amador-Arjona *et al.*, 2015).

- **Pax6**

The Paired box-gene 6 (Pax6) gene encodes a transcription factor involved in peripheral and CNS development (reviewed in Simpson and Price, 2002). Pax6 is strongly expressed in neural stem/progenitor cells, the RGC (Götz *et al.*, 1998), and plays an important role in brain patterning, neuronal specification, neuronal migration, and axonal projections (Osumi, 2001; Simpson and Price, 2002). In addition, and because it is known that neural progenitors cells and astrocytes share common characteristic (such as GFAP expression), Pax6 expression was also reported in astrocytic precursor and mature astrocytes (Sakurai and Osumi, 2008). In the developing and adult hippocampus, Pax6 is expressed in the neural stem/progenitor cells (**Figure 5**; Duan *et al.*, 2013) and regulates cell proliferation and differentiation in the adult SGZ (Maekawa *et al.*, 2005).

- **Tbr2**

IPCs in the developing and adult DG specifically express the T-box transcription factor Tbr2 (**Figure 5**; Hodge *et al.*, 2008; Roybon *et al.*, 2009). Similar to its known role in embryonic neocortex (Arnold *et al.*, 2008; Sessa *et al.*, 2008), recent reports show that Tbr2 ablation leads to an increased proliferation of neural stem/progenitor cells, as well as an IPC depletion and consequent decrease of granule cell neurogenesis (Hodge *et al.*, 2012). It has also been suggested that Tbr2 may promote progression from multipotent neural stem cell to neuronal-specified IPC by directly repressing Sox2. In an other recent study, Hodge *et al.* showed that Tbr2 has additional functions during DG morphogenesis (Hodge *et al.*, 2013): it is expressed in Cajal-Retzius cells derived from the cortical hem and ablation of Tbr2 in these cells results in ectopic accumulation of Cajal-Retzius cells during their migration to the developing dentate gyrus.

- **NeuroD1 (ND1)**

In the hippocampus, the bHLH transcription factor ND1 is expressed by late IPCs and early post-mitotic neurons (**Figure 5**; Miyata *et al.*, 1999). It has been reported that NeuroD1 (ND1, also named BETA-2) deficient mice have a dramatic defect in the proliferation of progenitor cells that reach the dentate gyrus and a significant delay in the differentiation of granule cells, leading to malformation of the granule cell layer and excess cell death (Liu M. *et al.*, 2000). Interestingly, loss of ND1 does not affect other hippocampal neurons (Miyata *et al.*, 1999; Liu M. *et al.*, 2000), probably due to the expression of Math2 and NeuroD2, two closely related family members, in these other regions (Pleasure *et al.*, 2000b; Schwab *et al.*, 2000). In summary, ND1 essential function is to control terminal neuronal differentiation of granule cells.

- **Prox1**

Prox1, a prospero-related homeobox gene (Oliver *et al.*, 1993), is commonly used as a specific marker for granule cells of the DG, both in adults and during development. Lavado *et al.* have reported that functional inactivation of Prox1 during development results in defective granule cell maturation and consequent absence of this cell population (Lavado *et al.*, 2010). In addition, they also show that ectopic expression of Prox1 in neural stem cells promotes premature differentiation both during DG development and adult neurogenesis in the SGZ (Lavado *et al.*, 2010). Moreover, conditional *Prox1 knock-out* mice show that Prox1 post-mitotically specifies and maintains granule cell identity over CA3 pyramidal cell fate (Iwano *et al.*, 2012). Thus, Prox1 is a crucial factor regulating granule cell fate differentiation and maintenance. Furthermore Galichet *et al.* demonstrated that dentate progenitors also express Prox1, even if at low levels (Galichet *et al.*, 2008)

- **Tbr1**

The T-box brain gene 1 (Tbr1) is expressed in post-mitotic projection neurons (Englund *et al.*, 2005) and regulates their differentiation (Hevner *et al.*, 2001; Bedogni *et al.*, 2010). Tbr1 mutants exhibit impaired differentiation in frontal cortex and neocortical layer VI (Bedogni *et al.*, 2010). Although it is supposed to have similar functions in DG granule cell differentiation, Tbr1 role in hippocampal development is poorly documented.

- **NeuN**

NeuN was originally discovered by the production of a novel anti-NeuN antibody permitting to label a nuclear antigen restricted to neurons (Mullen *et al.*, 1992). Since then, this pan-neuronal marker has been actively used to assess the functional state of neurons, as well as the differential morphological diagnosis of cancer (You *et al.*, 2005). However, the structure of the protein remained unknown until recently, and the function of this protein is still not clear (reviewed in Gusel'nikova and Korzhevskiy, 2015). Several evidences suggest however that the NeuN protein is a product of the Fox-3 gene, which belongs to the Fox-1 gene family (Kim *et al.*, 2009).

- **Calbindin and Calretinin**

Calbindin and Calretinin are calcium-binding protein expressed by several neuronal sub-populations and associated among other roles with calcium homeostasis (Baimbridge *et al.*, 1992; Zheng *et al.*, 2004) and interneuron expression patterns (Freund and Buzsáki, 1996). They are also expressed during DG granule cell differentiation: transient expression of Calretinin defines early post-mitotic step of neuronal differentiation in adult SGZ neurogenesis (Liu *et al.*, 1993; Brandt *et al.*, 2003) and mature granule cells express Calbindin, and this expression is correlated with the appearance of glutamatergic inputs and integration into the synaptic circuit (Sloviter, 1989).

In addition to all these transcription factors, other genes have been involved in regulating granule cell differentiation at different step of the process. Among them, Neurogenin 2 (Ngn2)-expressing progenitors generate most or all dentate granule cells and elimination of Ngn2 function results in the loss of a large fraction of dentate granule cells and in a severe defect in DG morphogenesis (Galichet *et al.*, 2008). Also, Nuclear Factor I A (NFIA) regulates both the repression of the progenitor cell state and the activation of differentiation gene programs regulating neural development (Piper *et al.*, 2010). *MicroRNAs* have as well been reported to regulate granule cell differentiation, since lack of *miRNAs* at early stages causes precocious differentiation, and inactivation of the RNase III enzyme Dicer causes abnormal hippocampal development and morphological impairments (Li *et al.*, 2011).

b - Migration

Neuronal migration in the neocortex is well studied, and the cellular dynamics and molecular mechanisms involved in neuronal migration are also well understood. Because the hippocampus and neocortex belong to the cerebral cortex, their neuronal migration was first thought to be similar, but strong differences have been highlighted in the last few years.

Around E15.5 in mice, progenitors and differentiating granule cells start to migrate away from the 1st matrix through the 2nd matrix. Gradually, this dentate migration divides into two routes (**Figure 4C'**) (Altman and Bayer, 1990c; Hayashi *et al.*, 2015):

- The first dentate migration follows the subpial route. Cells migrate along the pial surface, accumulate in the 3rd matrix and forms the outer part of the granule cell layer. Cells from this dentate migration travel in an outside-in pattern: earliest born cells migrate the furthest while the following cells accumulate behind them. Therefore, oldest granule cells are located at the tip of the upper blade, and younger cells at the tip of the lower blade. As a consequence, the upper blade of the granule cell layer is formed before the lower blade.

- The secondary dentate migration reaches the prospective hilus. Progenitors from the ventricular zone that have retained their proliferative capacity settle in the prospective DG, where they form a second germinative zone. Following further proliferation, these newly born granule cells integrate the inner part of the granule cell layer (Altman and Bayer, 1990c; Martin *et al.*, 2002; Namba *et al.*, 2005, 2007, 2011). Thus, at the opposite of the neocortex and the hippocampus proper, the granule cell layer has an outside-in lamination pattern, where the earliest-born cells settle in the outermost layers.

While the first dentate migration exhaust around birth, the second stream is mostly a post-natal feature, and give rise to almost 80% of the granule cells during the first week (Bayer, 1980a). Adult neural stem cells of the DG (the SGZ) are thought to derive from this second proliferative zone and thus from neural stem cells of the ventricular zone (Altman and Bayer,

1990c; Seri *et al.*, 2004), although a recent study has challenged this view by revealing that adult neural stem cells are induced at peri-natal stages (Li *et al.*, 2013).

Dentate granule migration is regulated by several factors (Hayashi *et al.*, 2015), gathered here in three main features. First, neuronal migration requires proper cytoskeletal machinery, enabling cells to acquire a bipolar and/or multipolar cell shape they need for proper migration. Second, different chemokines are involved in attracting or repulsing migrating granule cells. They form a guidance cue/receptors system required for driving migrating cells toward their targets. Third, dentate migration also depends on the presence of a proper scaffold, formed by radial glia fibers, along which differentiating granule cells travel.

- **Cytoskeletal machinery**

In the last 20 years, many molecules involved in the cytoskeletal machinery have been reported to be required during neuronal migration.

Inactivation of the serine/threonine kinase Cdk5 or its regulatory co-factor p35 display disrupts laminar formation in the neocortex and hippocampus (Ohshima *et al.*, 1996; Wenzel *et al.*, 2001; Ohshima *et al.*, 2005). In the neocortex, Cdk5 regulates multipolar-to-bipolar transition of migratory neurons via RapGEF2 phosphorylation (Ohshima *et al.*, 2007; Ye *et al.*, 2014), and a similar mechanism may also act during hippocampal development.

The microtubule-associated protein Doublecortin (DCX) is a causative gene for X-linked lissencephaly (des Portes *et al.*, 1998). Hemizygous *Dcx* mutant males display abnormal migration of CA3 neurons, while neocortical and DG neurons are quite normal (Corbo *et al.*, 2002). Moreover, *double knock-out* of *Dcx* and the doublecortin-like kinase 1 (*Dclk1*) or 2 (*Dclk2*) show abnormalities also in DG lamination (Deuel *et al.*, 2006; Tanaka *et al.*, 2006; Kerjan *et al.*, 2009). These results suggest that DCX is involved in regulating the cytoskeletal changes necessary for hippocampal neuronal migration.

As another example, Lis1 (PAFAH1B1) regulates microtubule-based transport (Sasaki *et al.*, 2000), and is another causative gene for lissencephaly (Reiner *et al.*, 1993; Lo Nigro *et al.*,

1997). *Lis1 knock-out* mice exhibit discontinuous and multiple Hp pyramidal cell layer and a less concentrated granule cell layer (Fleck *et al.*, 2000), making of Lis1 another factor involved in hippocampal neuronal migration.

In addition, the small Rho GTPase Rnd2 is a key modulator of radial migration in the cortex. It is involved in the regulation of multipolar-to-bipolar shaped cells transition and bipolar-shaped cell migration during mid-late stages of corticogenesis, and is directly activated by the proneural gene Ngn2 (Heng *et al.*, 2008; Nakamura *et al.*, 2006). Notably, our group has reported that Rnd2 expression is directly repressed by the transcription factor COUP-TFI in the neocortex (Alfano *et al.*, 2011). Other factors, such as FlnA and RhoA have also been shown to control multipolar-shaped cell migration and their transition to bipolar-shaped cells in the neocortex (LoTurco and Bai, 2006; Ge *et al.*, 2006), and other molecules, such as Mdgal, N-cofilin, and integrins have been implicated in the maintenance of bipolar cell polarity and interaction of migrating neurons with the radial glia (Takeuchi and O'Leary, 2006; Bellenchi *et al.*, 2007; Dulabon *et al.*, 2000; Marchetti *et al.*, 2010).

- **Guidance cues**

In addition to their widespread expression in the immune system, it is now known that chemokines (chemotactic cytokines) and their receptors are expressed throughout the central nervous system. All of the major cell types in the brain, including neurons and glia, express many of the known receptors for chemokines (Bajetto *et al.*, 2001). Chemokines and their receptors have an important chemotactic function in the migration of developing neurons during embryogenesis (Zou *et al.*, 1998), and some, such as CXCR4 and Reelin, control the migration of granule cell progenitors during dentate gyrus formation (Bagri *et al.*, 2002; Lu *et al.*, 2002; Li *et al.*, 2009; Förster *et al.*, 2002, 2006; Sibbe *et al.*, 2009).

The CXCR4 receptor is one of the most highly expressed chemokine receptors both during development and in the mature brain (Jazin *et al.*, 1997, McGrath *et al.*, 1999, Lavi *et al.*, 1997). Deletion of the gene coding for the CXCR4 receptor, or of its ligand Stromal cell-Derived Factor 1 (SDF1, also named CXCL12) results in embryonic lethality. The brains of

mouse embryos homozygous for the absence of CXCR4 receptors have severe abnormality in the development of cerebellar morphology (Zou *et al.*, 1998, Ma *et al.*, 1998). SDF1 is expressed in the meninges and in Cajal-Retzius cells, around the hippocampal fissure, and migrating granule cells express the receptor CXCR4 (Bagri *et al.*, 2002), supporting an interaction between CXCR4 and SDF1 in granule cell migration. *CXCR4* mutant mice exhibit a severe abnormality in the development of the DG due to defective granule cell positioning (Bagri *et al.*, 2002).

The giant glycoprotein Reelin is synthesized by Cajal-Retzius cells (CR cells) and interneurons and secreted into the extracellular matrix (Haas *et al.*, 2002; Alcantara *et al.*, 1998; Pesold *et al.*, 1998; Ramos-Moreno *et al.*, 2006). After this secretion, Reelin is proteolytically cleaved and activate target cells, expressing the lipoprotein receptors, such as the very-low-density lipoprotein receptor (VLDLR) and apolipoprotein E receptor 2 (ApoER2) (Nakano *et al.*, 2007; Trommsdorff *et al.*, 1999). In the neocortex, the reelin-deficient mice, the so-called *reeler*, display disrupted layer formation, including overall approximate inversion of the birthdate-dependent layering (Caviness, 1973). In the hippocampus, *reeler* mice also exhibit a hippocampal inverted layer formation, as well as a less densely packed DG and a reduced number of granule cells (Caviness, 1973; Stanfield and Cowan, 1979a,b; Boyle *et al.*, 2011). Interestingly, injection of CR-50, a function-blocking antibody against Reelin protein, into the ventricle of mouse embryos resulted in a similar layer pattern to that of *reeler* mice in the Hp (Nakajima *et al.*, 1997), implying that Reelin controls hippocampal neuronal migration in a cell-autonomous manner. Additionally, it has been shown that Reelin and its downstream effector Dab1 guide the detachment of migrating neurons from this radial glia scaffold (Dulabon *et al.*, 2000; Olson *et al.*, 2006; Sanada *et al.*, 2004).

- **Radial Glia scaffold**

During development of the nervous system, RGCs regulate boundary demarcation and act as scaffolds for migrating neurons (Götz and Barde, 2005). Radial Glia plays an important role in hippocampal morphogenesis (Rickmann *et al.*, 1987; Sievers *et al.*, 1992). In these studies,

two distinct glial bundles have been identified: the supragranular bundle, derived from the ammonic neuroepithelium, and the fimbrial bundle, derived from the fimbrial glioepithelium. Both have been postulated to regulate granule cell migration (Altman and Bayer, 1990a,b; Nakahira and Yuasa, 2005). Both of these glial bundles express GFAP, but seem to be regulated by distinct molecular determinants. As an example, the supragranular bundle fails to develop in *Nfib*-deficient mice, resulting in a failure of hippocampal fissure formation, and in the absence of proper DG morphogenesis (Barry *et al.*, 2008), while the fimbrial bundle remains intact.

Moreover, in addition to its cell-autonomous role (see above), Reelin also act in a non-cell-autonomous manner on neuronal migration. Particularly, it was reported that Reelin and its downstream effector *Dab1* affect differentiation, branching and radial alignment of RGCs in the hippocampus (Soriano and Del Rio, 2005), and loss of these genes results in an abnormal radial fiber formation, and a consequent failed neuronal migration (Förster *et al.*, 2002). Interestingly, Zhao *et al.* rescued *reeler* malformation in the orientation of RGCs fibers and dentate cell migration *in vitro* by adjacently co-culturing *reeler* DG and wild-type DG (Zhao *et al.*, 2006)

c - Maturation & connectivity

In addition to the expression of transcription factors required in late neuronal differentiation (such as *Tbr1*, *NeuN*, etc), and to their proper localization within the granule cell layer, granule cells also require a proper cytoarchitecture to mature: a well developed dendritic tree, containing mature synapses with their proper afferents, and correctly elongated axons reaching their targets. Overall, the final maturation of a neuron depends on its connectivity and ultimately its integration into the neuronal network.

Perforant path fibers from the entorhinal cortex are among the first afferents to reach the DG in rodents: they arrive in the outer molecular layer at E18/E19 (Supèr and Soriano, 1994). This early arrival implies that targeted granule cells cannot control their regional specificity

and layer-specific termination, since most of them are generated after birth (*cf. Introduction-I-C-3*). Instead, Cajal-Retzius cells have been shown to serve as transient targets of early arriving entorhinal fibers in the absence of granule cells (Del Rio *et al.*, 1997; Frotscher *et al.*, 2001). However, their secreted molecule Reelin is not required in this process, since *reeler* (Reelin-deficient) mice have correct perforant path lamination (Del Rio *et al.*, 1997; Zhao *et al.*, 2003).

As for mossy fibers, they start to appear at the day of birth and develop within the next 3-5 days in rats (Amaral and Dent, 1981; Blaabjerg and Zimmer 2007). Spines on the proximal CA3 pyramidal cell dendrites start to develop about one week after birth, but a mature mossy fiber terminal develop at 3 postnatal weeks (Amaral and Dent, 1981; Gaarskjaer, 1985; Blaabjerg and Zimmer, 2007). Notably, it has also been reported that mossy fibers development at septal levels seems to be relatively delayed compared to temporal levels (Blaabjerg and Zimmer 2007). In addition, the calcium-binding protein Calbindin is particularly abundant in the granule cell mossy fibers (Baimbridge and Miller, 1982; Celio, 1990). Calbindin can bind free calcium and thus regulate the intracellular calcium homeostasis, which is essential for synaptic transmission and granule cell excitability (Smith and Augustine, 1988).

3) Interneurons, glia and hippocampal fissure

a- Interneurons

In addition to pyramidal cells of the hippocampus proper and granule cells of the dentate gyrus, the third main neuronal population in the hippocampus is represented by interneurons. Interneurons are GABAergic neurons that inhibit the activity either of excitatory neurons or of other interneurons (Helmstaedter *et al.*, 2007). Thus, interneurons influence the response of excitatory neurons to incoming inputs and balance neuronal activity (Lee *et al.*, 2010; McBain and Fisahn, 2001).

The main sources of interneurons of the hippocampus are the Medial and Caudal Ganglionic Eminences (MGE and CGE, respectively) (Nery *et al.*, 2002; Pleasure *et al.*, 2000a; Butt *et al.*, 2005; Lavdas *et al.*, 1999). Of all the different subsets of interneurons, somatostatin- and parvalbumin-expressing ones derive exclusively from the MGE, whereas calretinin- and VIP-positive interneurons derive from the CGE. CGE-derived cells travel within the caudal migratory stream (CMS) (Yozu *et al.*, 2005; Marin and Rubenstein, 2001), while MGE-derived cells migrate dorsally to the cortex (Marin and Rubenstein, 2001). The genesis of GABAergic interneurons occurs in mice between E11 and E17 (Soriano *et al.*, 1986, 1989a,b). Most of the interneurons from CA1 and CA3 fields are generated at E12–E13 and derive from the MGE and CGE, whereas the majority of DG interneurons originate at E13–E14 (Soriano *et al.*, 1989a,b). From their birthplace, interneurons migrate tangentially for long distances through the neocortex, and ultimately reach the hippocampus (Yozu *et al.*, 2005). Hippocampal interneurons have been shown to colonize the hippocampal primordium by E15 (Manent *et al.*, 2006). At this stage, migrating interneurons form two distinct pathways: one superficial in the molecular zone (MZ) in continuity with the cortical superficial stream, and the other one in the SVZ. By E16, the superficial MZ stream reaches CA3, whereas the deep stream reaches CA1 but stops at the border of CA3. Interneurons colonize the DG primordium via the superficial stream by E17 (for review, see Danglot *et al.*, 2006).

b- Glia

Progenitors from the cerebral cortex produce both neurons and glia. A characteristic feature of this process is that, in the developing mammalian nervous system, neurogenesis precedes gliogenesis (Miller and Gauthier, 2007). In the mouse hippocampus, neurogenesis occurs until around E16.5, and is followed by gliogenesis that peaks at E17.5 (Subramanian *et al.*, 2011).

The molecular mechanisms that control this neurogenic-gliogenic switch are not very well understood. Nevertheless, the Notch signaling pathway is known to play a fundamental role in this process. Accumulating evidences indicate that Notch pathway promotes glial

differentiation while it inhibits premature neuronal differentiation (Artavanis-Tsakonas *et al.*, 1999, Lütolf *et al.*, 2002). Similarly, NFIA acts downstream of Notch to initiate gliogenesis via activation of the astrocyte-specific gene GFAP, (Shu *et al.*, 2003; Cebolla and Vallejo, 2006; Namihira *et al.*, 2009). In addition, NFIA downregulates the activity of the Notch signaling pathway by repressing the key Notch effector Hes1 (Piper *et al.*, 2010). Moreover, the LIM-homeodomain transcription factor Lhx2 is also involved in regulating this transition in the developing hippocampus (Subramanian 2011): disrupting Lhx2 function causes the premature production of astrocytes at stages when neurons are normally generated; and at the contrary, Lhx2 overexpression is sufficient to suppress astrogliogenesis by blocking NFIA-mediated activation of GFAP. Therefore, Lhx2 appears to act as a “brake” on Notch/NFIA-mediated astrogliogenesis. Strikingly, this critical role for Lhx2 has been demonstrated to be spatially restricted to the hippocampus (Subramanian *et al.*, 2011).

c- Hippocampal fissure (Hf)

The hippocampal fissure formation remains to be clarified. However, it has been suggested that the hippocampal fissure is formed through the maturation of the supra granular bundle of radial glia and the subsequent migration of neurons, and not through a mechanism such as membrane invagination as its appearance would suggest (Barry *et al.*, 2008). Furthermore, Hf region is known to be populated from its onset with Cajal-Retzius cells, which express factors such as the chemokine SDF1 and the extracellular matrix protein Reelin (see above).

II / COUP-TFI

Chicken Ovalbumin Upstream Promoter Transcriptional Factors (COUP-TF) were originally identified as transcriptional factors regulating the expression of the COUP element (Chicken Ovalbumin Upstream Promoter) in chicken oviducts (Wang *et al.*, 1989). In 1987, the first COUP-TF, the human COUP-TFI (hCOUP-TFI), was purified and characterized from HeLa cells nuclear extract (Wang *et al.*, 1987).

In this second part of my introduction, I will present the classification, structure and species conservation of the COUP-TF factors. Then, I will describe COUP-TFI expression profile during mouse development. Finally, I will review the main known physiological functions during nervous system development as well as its putative involvement in human disorders. Although COUP-TFII functions will be mentioned (reviewed in Lin F-J *et al.*, 2011), a particular attention will be given to COUP-TFI (for review, see Alfano *et al.*, 2014).

A) COUP-TF classification, sequence, structure and conservation

1) COUP-TF classification

The COUP-TF factors belong to the steroid/thyroid hormone receptor superfamily of nuclear receptors (Pereira *et al.*, 2000). According to the nuclear receptor nomenclature of 1999, they are part of the NR2F (Nuclear Receptor Family 2) subgroup.

In mammals, as well as in the majority of higher vertebrates, two COUP-TF members encoded by distinct genes and located on different chromosomes, have been identified:

- COUP-TFI (also called EAR-3 or NR2F1) (Wang *et al.*, 1989, Miyajima *et al.*, 1988)
- COUP-TFII (also called ARP-1 or NR2F2) (Ladias *et al.*, 1991, Wang *et al.*, 1991).

In non-mammalian vertebrates, such as *Zebrafish* and *Xenopus*, a third member has been identified but poorly studied. It is called EAR2, is expressed in the brain and can form heterodimers with COUP-TFII (Miyajima *et al.*, 1988, Avram *et al.*, 1999). Moreover, insects and invertebrates such as *Drosophila*, *Caenorhabditis elegans* and sea urchin possess only one member.

In addition, these Transcription Factors are classified as orphan nuclear receptors, because no physiological ligands for any COUP-TF have been identified so far (Germain *et al.*, 2006).

2) COUP-TF DNA sequence and protein structure

In mice, COUP-TF proteins are encoded by the genes *mCOUP-TFI* and *mCOUP-TFII*, located on the chromosome 13 and 7, respectively (Qiu *et al.*, 1995). Both *mCOUP-TFI* and *mCOUP-TFII* DNA sequence contains 3 exons (Qiu *et al.*, 1995), and their mRNA is about 4.5 kb (Miyajima *et al.*; 1988, Jonk *et al.*, 1994). In human, *COUP-TFI* was mapped to the chromosome 5 (5q14) and *COUP-TFII* to the chromosome 15 (15q26) (Qiu *et al.*, 1995).

COUP-TF members have been shown to possess 4 motifs that are highly conserved between COUP-TFI and COUP-TFII (Qiu *et al.*, 1994a; Tsai and Tsai, 1997):

- A central DNA-binding domain (DBD), for which COUP-TFI and -II possess 80% of homology in humans, suggesting that they both bind to a similar if not identical response element.
- A putative C-terminal ligand-binding domain (LBD), for which the two members share 97% of homology in humans.
- Two activation function domains, AF-1 and AF-2, necessary for co-factor recruitment. The AF-2 motif located in the LBD is highly similar between COUP-TFI and -II. On the contrary, AF-1 is located in the N-terminal domain and has only 45% of homology between the two members (Ladiaz *et al.*, 1991; Wang *et al.*, 1989). This implies that the two COUP-TF homologs might have different molecular interactions and therefore distinct functions.

Similarly to other members of the steroid/thyroid hormone receptor superfamily, the DBD of COUP-TF contains two zinc finger domains (Cooney *et al.*, 1992). It has been reported that COUP-TF form homodimers and bind to a wide range of direct repeat AGGTCA motifs, with a variety of spacing and orientation (Cooney *et al.*, 1992; Kliewer *et al.*, 1992). However, COUP-TF exact cellular localization and dynamics underlying their action are still largely unknown.

3) COUP-TF conservation

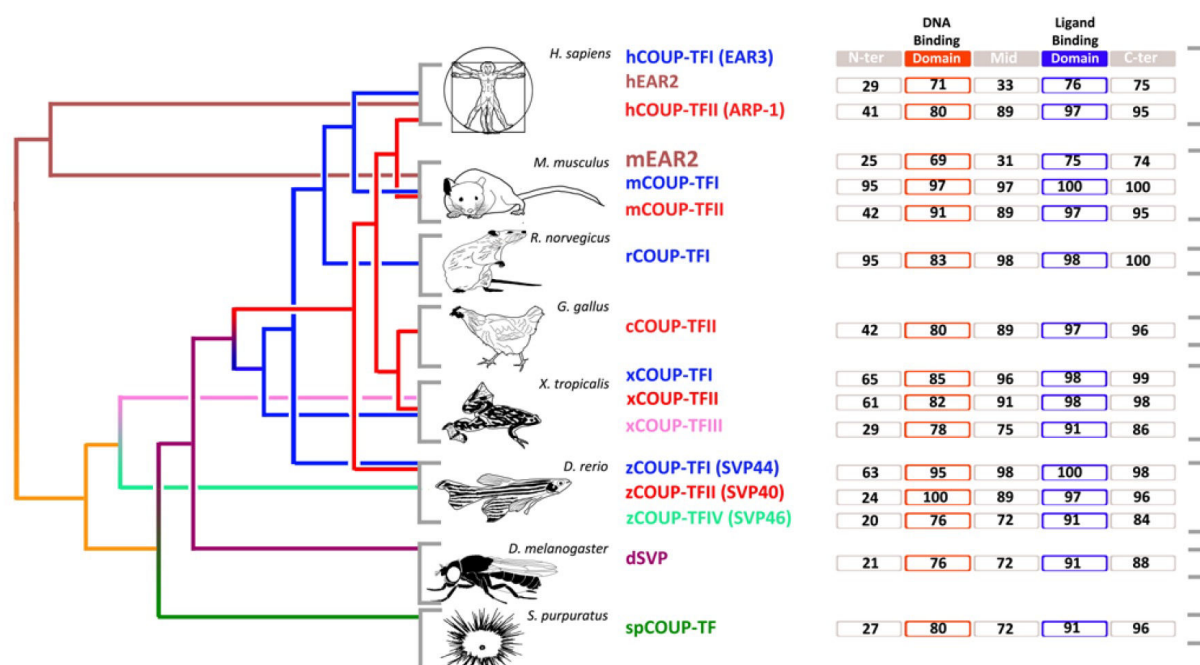


Figure 6. COUP-TFI sequence conservation among vertebrates.

Schematic representation of the homologies of *COUP-TF* genes in different classes of animals. Distinct colors in the phylogenetic tree indicate divergence in different types of proteins within the *COUP-TF* family. Numbers in the protein domains indicate score of sequence homology with respect to the corresponding human *COUP-TFI* (EAR3) domains. The N-terminal, DBD (DNA binding domain), middle, LBD (ligand binding domain) and C-terminal domains of each *COUP-TF* homologous sequence are compared to the human *COUP-TFI* homologue and homology score percentages are reported in the respective rectangle. From Alfano *et al.*, 2014.

The COUP-TF nuclear receptors sequences are remarkably conserved through many distant vertebrate species like human, mouse, rat, hamster, chicken, *Xenopus*, and *zebrafish*, and to invertebrate species such as the sea urchin (**Figure 6**; Alfano *et al.*, 2014). In particular, the DBD and LBD sequences of both COUP-TFI and -II are strikingly conserved among species (Tsai and Tsai, 1997). This high degree of evolutionary conservation strongly suggests that the COUP-TF family plays critical roles in many biological functions, which are similar in different vertebrate species, and probably between vertebrates and invertebrates (Alfano *et al.*, 2014; Tsai and Tsai, 1997).

B) COUP-TFI expression in the developing mouse brain

The expression of COUP-TFI in mouse embryo is first detected at E7.5. It is then up-regulated at E9.5, reaches maximal levels around E13.5, and is gradually down-regulated later on (Qiu *et al.*, 1994b). The two COUP-TF homologs are expressed in almost all of the forebrain structures during embryonic development suggesting that they are strongly involved in forebrain development (Alfano *et al.*, 2014). At E13.5, COUP-TF are both expressed in the cerebral cortex (in the archicortex, paleocortex and neocortex), in the preoptic area, in the lateral and caudal ganglionic eminences (LGE and CGE, respectively), in the most dorsal region of the medial ganglionic eminence (dMGE), and in scattered cells of the ventral telencephalon (Tripodi *et al.*, 2004; Armentano *et al.*, 2006).

In the neocortex, COUP-TFI exhibits a high caudo-lateral to low rostral-medial expression gradient (Qiu *et al.*, 1994b; Liu Q. *et al.*, 2000; Armentano *et al.*, 2006, 2007; Tomassy *et al.*, 2010). This graded pattern is first seen around E9.0 when the rostral neural plate closes, and is maintained after birth (Liu Q. *et al.*, 2000, Zhou *et al.*, 2001). Interestingly, and unlike other gradient-expressed transcription factors, such as Pax6 or Emx2, COUP-TFI is expressed both in mitotic and post-mitotic cells in the cerebral cortex (Alfano *et al.*, 2014) and might therefore be involved at different steps of neuronal differentiation.

C) COUP-TFI gene regulation

1) Regulation of COUP-TFI expression: upstream regulators

It has been reported that *COUP-TF* genes are regulated by several signaling molecules. These upstream regulators include Sonic hedgehog (Shh) (Krishnan *et al.*, 1997), retinoids (Qiu *et al.*, 1994a; Fjose *et al.*, 1995; Zhuang and Gudas, 2008), Mitogen-Activated Protein Kinase (MAPK) and Protein Kinase C (PKC) signaling pathways (Gay *et al.*, 2002), as well as dopamine (Power *et al.*, 1991).

During forebrain development, COUP-TF expression levels are modulated by two important morphogens, Fgf8 and Shh, involved in antero-posterior and dorso-ventral patterning, respectively (O'Leary *et al.*, 2007, Sousa and Fishell, 2010). The Fibroblast Growth Factor Fgf8 has been shown to repress COUP-TFI expression in the rostral regions of the mammalian embryonic neocortex (Garel *et al.*, 2003, Storm *et al.*, 2006). Similarly, the zinc finger transcription factor Sp8, which is a downstream effector of Fgf8 signaling (Storm *et al.*, 2006), is expressed in a complementary pattern to COUP-TFI (Sahara *et al.*, 2007) and is thus known to promote rostral cortical development (Sahara *et al.*, 2007; Zembrzycki *et al.*, 2007). Recently, Sp8 and COUP-TFI have been reported to mutually repress each others cortical neuroepithelial expression along the rostro-caudal and dorso-ventral axes (Borello *et al.*, 2014; Alfano *et al.*, 2014). On the other hand, Shh has been shown to regulate COUP-TFII expression during the differentiation of spinal motoneurons in the developing neural tube (Lutz *et al.*, 1994), but nothing is known on whether COUP-TFI is also under the control of Shh during brain development.

COUP-TF genes are also targeted by retinoids (Neuman *et al.*, 1995; Schuh and Kimelman 1995; Van der Wees *et al.*, 1996) and are up-regulated during retinoid-induced differentiation *in vitro* (Tsai and Tsai, 1997; Pereira *et al.*, 1995; Fjose *et al.*, 1995; Jonk *et al.*, 1994; Pickens *et al.*, 2013). Retinoids induce COUP-TF expression in zebrafish and mouse brains *in vivo* (Fjose *et al.*, 1995, Clotman *et al.*, 1998; Alfano *et al.*, 2014). However, retinoids effects on COUP-TF action and expression remain still unclear.

Furthermore, the sequence of COUP-TFI contains several putative phosphorylation sites recognized and phosphorylated *in vivo* by MAPK and PKC (Gay *et al.*, 2002). Interestingly, these two types of phosphorylation differentially modulate COUP-TFI functions. Whereas PKC-mediated phosphorylation enhances COUP-TFI affinity for DNA, MAPK-mediated phosphorylation positively regulates the transactivating function of COUP-TFI, possibly by recruiting specific co-activators (Gay *et al.*, 2002). As a consequence, multiple extracellular signals acting on these phosphorylation sites might influence COUP-TFI activity (Gay *et al.*, 2002).

Finally, dopamine might be another potential inducer of the transcriptional activity of human COUP-TF (Power *et al.*, 1991). This study shows that dopamine induces the expression of COUP-TF target genes *in vitro*, and that it is specific to COUP-TF modulation, since this activation is abolished when hCOUP-TF terminal domain is deleted (Power *et al.*, 1991). But no direct evidence on whether this effect is reproduced also *in vivo* has been reported so far.

2) COUP-TFI transcriptional activity: downstream targets

Members of the COUP-TF family are prevalently transcriptional repressors (Ladiaz *et al.*, 1992; Paulweber *et al.*, 1991; Rottman *et al.*, 1991; Widom *et al.*, 1992). However, it has been reported that they can also positively regulate a considerable number of genes (Lu *et al.*, 1994; Power and Cereghini, 1996; Hall *et al.*, 1995).

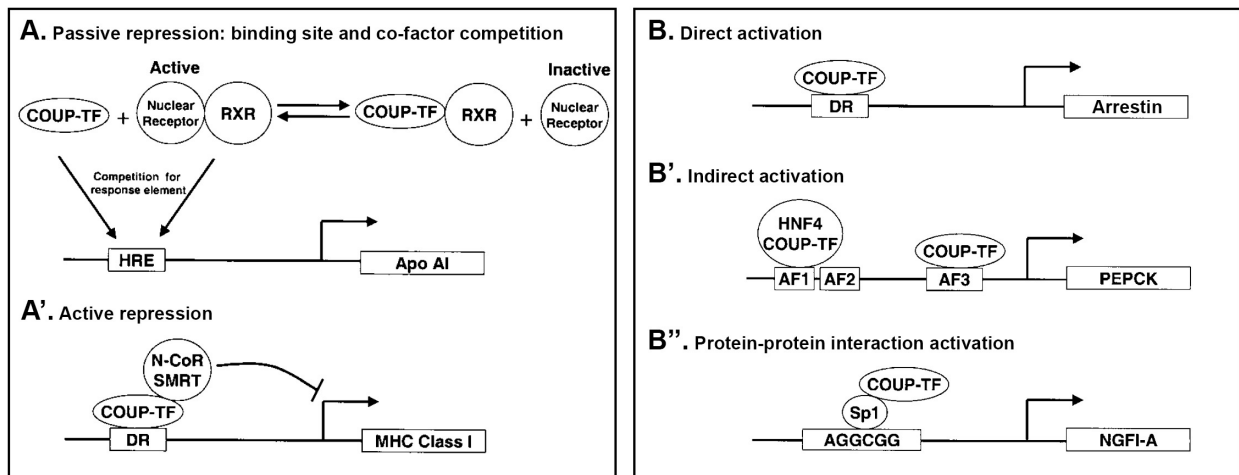


Figure 7. Molecular mechanisms of COUP-TF as repressor and activator.

A-A'. Molecular mechanisms of COUP-TF as repressors: passive repression by competition for binding site or co-factors (**A**) and active repression by interacting with co-repressors (**A'**). **B-B'**. Molecular mechanisms of COUP-TF as activators: direct activation by binding to DNA response element (**B**), indirect activation by acting as accessory factors for transcription activation (**B'**), and activation through protein-protein interaction with a DNA-bound factor (**B''**). *DR*: direct repeats; *AF*: accessory factor elements; *PEPCK*: phosphoenolpyruvate carboxykinase, *HRE*: hormone response element, *MHC*: major histocompatibility complex, *ApoAI*: apolipoprotein AI. From Park *et al.*, 2003.

a- Transcriptional repressor activity

COUP-TF members have been shown to possess a strong transcriptional repressor activity. There are four mechanisms that account for the repressive effects of COUP-TFs:

- COUP-TFs can repress gene expression by outcompeting the binding sites of other hormone receptors (**Figure 7A**), such as the thyroid hormone receptor (TR), the retinoic acid receptors (RAR), and the vitamin D receptor (vDR) (Cooney *et al.*, 1993; Tran *et al.*, 1992).
- COUP-TFs have also been reported to subtract common co-factors from other hormone receptors, such as the retinoid X receptor (RXR) (**Figure 7A**), consequently repressing transcription of their target genes (Cooney *et al.*, 1993; Leng *et al.*, 1996; Berrodin *et al.*, 1992; Kliewer *et al.*, 1992; Casanova *et al.*, 1994).
- In a more active way, COUP-TFI can repress its target genes by interacting with co-repressors, such as the nuclear co-repressor (NCoR) and the silencing mediator of

retinoic acid and thyroid hormone receptor (SMRT) (**Figure 7A'**; Shibata *et al.*, 1997), and as a consequence recruit histone deacetylases to inactivate a given promoter function (Zamir *et al.*, 1996; Perissi *et al.*, 2004).

- Finally, COUP-TFs can also repress transcription by directly binding to the LBD of nuclear hormone receptors, a process called transrepression (Leng *et al.*, 1996).

b- Transcriptional activator activity

In addition to their repressor activity, COUP-TF can also function as transcriptional activators for many different genes (Lu *et al.*, 1994; Power and Cereghini, 1996; Hall *et al.*, 1995). Positive regulation by COUP-TF can be carried out by at least three different molecular mechanisms (**Figure 7B-B''**):

- COUP-TFs can bind to DNA sequences containing a specific motif and directly activate gene expression (**Figure 7B**), as it has been demonstrated for some Apolipoproteins (Ladas and Karathanasis, 1991; Haddad *et al.*, 1986; Reue *et al.*, 1988), and the lactoferrin (Liu and Teng, 1991). Similarly, in the arrestin gene promoter, a DR-7 element mediates the positive transcriptional effect of COUP-TF (Lu *et al.*, 1994).
- Alternatively, COUP-TF can activate transcription by binding to a DNA element and indirectly influencing expression in the context of several other transcription factors (**Figure 7B'**), as in the phosphoenolpyruvate carboxykinase (PEPCK) gene glucocorticoid response unit (GRU) (Hall *et al.*, 1995; Scott *et al.*, 1996).
- Finally, COUP-TFs can activate transcription through protein-protein interaction with a DNA-bound factor (**Figure 7B''**), such as with HNF-4 in the HNF-1a gene promoter (Ktistaki *et al.*, 1997) with Sp1 in the trout estrogen receptor (Lazennec *et al.*, 1997) and the phosphoenolpyruvate carboxykinase (Hall *et al.*, 1995).

D) COUP-TFI functions in the developing Central Nervous System

In 20 years of intensive research since their discovery, COUP-TF transcription factors have been implicated in many vital processes, such as organogenesis, angiogenesis, and metabolic homeostasis, as well as in a variety of developmental programs. These developmental processes include cell fate determination, cell differentiation, cell survival, and cell migration. I will focus here on neural developmental processes and will present the data available so far on COUP-TFI functions in the developing central nervous system.

1) Neuronal migration

During cerebral cortex development, neurons migrate to their proper location using two main migration modes: the glia-guided radial migration, and the tangential migration. COUP-TFI has been involved in the regulation of these two types of neuronal migration, even if its importance in this process and the mechanisms underlying their function are still largely unknown.

a- Glia-guided radial migration

The radial migration concerns cells migrating perpendicular to the ventricular surface, heading toward the pial surface. The principal and well-described type of radial migration is the glia-guided radial migration. In this mode of migration, neurons adopt a bipolar shape, and migrate along the processes of RGC, also called neuronal apical progenitors, using them as a scaffold (LoTurco and Bai, 2006; Tabata and Nakajima, 2003).

Our group recently reported that COUP-TFI plays an important role in this glia-guided migration during development of the neocortex, mainly through transcriptional regulation of *Rnd2*, a small Rho GTPase modulator of radial migration (Alfano *et al.*, 2011). Indeed, COUP-TFI directly represses *Rnd2* expression in migrating post-mitotic cells, and as a consequence favors late (E14.5) newborn neurons to reach their proper position (Alfano *et al.*,

2011). In addition, the group also showed that COUP-TFI mutant neurons fail to be pulled by their leading process toward the pial surface and possess abnormally long apical dendrites (Alfano *et al.*, 2011). Therefore, COUP-TFI might act on the neuronal cytoskeletal machinery, crucial for proper radial migration.

b- Tangential migration

The tangential migration concerns cells migrating parallel to the ventricular surface, traveling in some cases very long distances (reviewed in Chedotal and Rijli, 2009; Corbin *et al.*, 2001; Marin and Rubenstein, 2001).

Cajal-Retzius cells (CR cells), for example, originate in different regions of the brain and constitute a transient population of neurons invading the cortex as early as E10.5 by tangential migration (reviewed in Puelles, 2011; Borello and Pierani, 2010; Marin-Padilla, 1998; Soriano and Del Rio, 2005). COUP-TFII is expressed in the cortical hem, the major source of CR cells, and in a subtype of CR cells in the cerebral cortex (Tripodi *et al.*, 2004, Takiguchi-Hayashi *et al.*, 2004), and might thus be involved in the migration of CR cells invading the neocortical primordium. COUP-TFI, however, is not expressed in this cell population (Tripodi *et al.*, 2004).

The other cell population tangentially migrating long distances are cortical interneurons. They originate from the ganglionic eminences and travel to different regions of the developing cortex, including neocortex and allocortex (Faux *et al.*, 2012; Tanaka and Nakajima, 2012a,b). This cortical interneuron tangential migration has been correlated with COUP-TF expression (Tripodi *et al.*, 2004). Although both genes are expressed at high levels in the caudal ganglionic eminence (CGE), they seem to be expressed in different cortical interneuron populations that follow distinct migratory paths: dorsal and ventral for COUP-TFI (Tripodi *et al.*, 2004), and caudal for COUP-TFII (Miyoshi *et al.*, 2010). Whereas the latter has been shown to promote caudal migration of CGE cells in a cell-autonomous way (Kanatani *et al.*, 2008), the influence of COUP-TFI in interneuron migration is still not clear and requires further study.

2) Cytoskeletal machinery

As mentioned above, COUP-TFI might regulate neuronal cytoskeletal machinery. This is supported by several discoveries.

First, our group showed that COUP-TFI-deficient primary hippocampal neurons have an abnormal distribution of actin- and tubulin-rich structures, leading to defects in axons and neurite formation and elongation (Armentano *et al.*, 2006). In a more recent study, the group showed that COUP-TFI mutant neurons have abnormally long apical dendrites in the neocortex *in vivo* (Alfano *et al.*, 2011) and abnormal axonal morphology leading to severe impairments in cortico-cortical commissures, including corpus callosum, anterior and hippocampal commissures (Armentano *et al.*, 2006). COUP-TFI mutants also have a significant decrease in MAP1B expression, an important cytoskeleton-associated protein involved in microtubule dynamics, as well as an abnormal localization of Rnd2 (Armentano *et al.*, 2006), which has been involved in neurite outgrowth (Uesugi *et al.*, 2009), and axonal branching (Kakimoto *et al.*, 2004). Therefore, in COUP-TFI mutant cells, abnormal Rnd2 levels might alter biochemical interactions amongst cytoskeletal proteins, ultimately leading to the observed axonal growth and morphological abnormalities. Taken together, these data strongly suggest that COUP-TFI might control several cytoskeletal molecules involved in different biological processes, from cell division to cell migration and axonal elongation.

3) Interneuron specification

Any impairment in interneuron migration or specification is associated, among others, with the onset of epileptic seizures (Baraban, 2007; Cossart *et al.*, 2005). Even if it is not clear yet whether COUP-TFI is involved in interneuron migration, our group has demonstrated that COUP-TFI plays a crucial role in the specification of distinct interneuron subpopulations (Lodato *et al.*, 2011). By abolishing COUP-TFI function in intermediate progenitors and early post-mitotic interneurons derived from the medial and caudal ganglionic eminences, the proportion of MGE- versus CGE-derived interneuronal sub-types is altered (Lodato *et al.*,

2011). On the other hand, whether COUP-TFII can play a role in cortical interneuron specification is still unclear.

4) Neurogenesis, gliogenesis, and neuronal fate specification

a- Neuronal fate specification

Seven-up (Svp), the homologue of COUP-TFs in the *Drosophila melanogaster*, was first identified as a crucial factor in cell fate specification of fly eye photoreceptors (Mlodzik *et al.*, 1990). In the ventral nerve cord of *Drosophila*, neuroblasts (neural stem cells) sequentially express Hunchback (Hb), Krüppel (Kr), Pdm1/Pdm2, Castor (Cas), and Grainyhead (Grh) (Isshiki *et al.*, 2001). After each neuroblast division, these transcription factors remain expressed in the founder ganglion mother cell (GMC), and are silenced in the cells that switch to a new cell fate program. *Svp* is able to promote the switch from Hb to Kr expression stage by inhibiting Hb during mitosis (Kanai *et al.*, 2005). *Svp* is expressed both in the neuroblasts and in the GMC and the expression of Prospero (a homeodomain protein) in the GMC suppresses *Svp* function in these cells, which consequently continue to express Hb (Mettler *et al.*, 2006). Interestingly, *Svp* has a second wave of expression at later stages of neurogenesis: in double Cas/Grh-positive neuroblasts, *Svp* has a “sub-temporal” function, contributing to the specification of a subgroup of interneurons via selective inactivation of specific genes (Benito-Sipos *et al.*, 2011). Finally, *Svp* also plays a role in the adult, where it limits neuroblast proliferation to avoid abnormal expansion of proliferating precursors in ectopic territories (Maurange *et al.*, 2008). Altogether, the *COUP-TF* fly homologue *Svp* was shown to act as a strong transcriptional regulator during temporal specification of cell lineage formation at early and late stages of development.

Similarly, COUP-TFI seems to control neuronal cell fate in a temporally controlled manner in mammals. In the absence of COUP-TFI, upper layers (late-born neurons) are thinner and lower layer (early-born neurons) are mis-specified (Armentano *et al.*, 2007; Faedo *et al.*, 2008, Tomassy *et al.*, 2010). COUP-TFI-deficient mice show a reduced number of

progenitors exiting the cell cycle and undergoing the neurogenic program, confirming a role for COUP-TFI in cell cycle control. COUP-TFI-overexpressing mice, on the other hand, have an opposite phenotype where progenitors anticipate their cell cycle exit and deplete the progenitor pool (Faedo *et al.*, 2008), leading again to a reduced production of late-born neurons and a thinning of upper layers. Little is known on how COUP-TFI acts in the production and specification of different progenitor populations.

Together these results demonstrate a crucial role of COUP-TFI in neurogenesis and fate specification.

b- Neurogenic-gliogenic switch

The only study reporting a possible role for COUP-TF genes in the switch between neurogenesis and gliogenesis in the cortex comes after knocking-down both COUP-TFs by *shRNA in vitro* and in the cortex (Naka *et al.*, 2008). *In vitro*, down-regulation of both COUP-TFs prolong neurogenesis and consequently delay the onset of gliogenesis. Similarly, in the cerebral cortex, knocking-down COUP-TF leads to an increase of early-born neurons and to the production of neurons at the expense of glia cells (Naka *et al.*, 2008). In addition, COUP-TFI/II knock-down leads to an altered methylation pattern of GFAP promoter, a crucial factor of glial fate specification (Naka *et al.*, 2008). Together these data indicate that COUP-TFs are necessary but not sufficient to control gliogenesis and that they limit the neurogenic temporal window rather than promoting gliogenesis.

5) Neocortical area patterning

As expected by its graded cortical expression profile, COUP-TFI controls the tangential subdivision of the neocortex into functional areas, called arealization (Zhou *et al.*, 2001; Armentano *et al.*, 2007). Each functional area can be distinguished by its specific cytoarchitecture and connectivity, and is specialized in elaborating motor or sensory inputs (reviewed in O'Leary *et al.*, 2007). Morphogens, produced by organizing centers (hem,

antrum and septum), are responsible for patterning the neocortex, via modulating the expression of areal patterning genes. Refinement in functional areas is then permitted by the arrival of thalamo-cortical afferences (O'Leary *et al.*, 2007). COUP-TFI is one of the four so far reported areal patterning gene, along with Pax6, Emx2 and Sp8. Together with Emx2, it promotes caudal fate specification (Armentano *et al.*, 2007; Zhou *et al.*, 2001; Bishop *et al.*, 2000). Indeed, COUP-TFI inactivation in progenitors leads to an expansion of the rostral/motor region, at the expense of caudal/sensory regions (Armentano *et al.*, 2007). Some evidences suggest that COUP-TFI acts by competing with Fgf8 signaling, which promotes rostral fate specification (Garel *et al.*, 2003; Fukuchi-Shigomori and Grove, 2003; Cholfin and Rubenstein, 2008). However, the molecular mechanisms by which Fgf signalling controls COUP-TFI and/or vice versa are still unclear.

6) Hippocampal development

Studies investigating COUP-TFI functions in the cerebral cortex are numerous, but most of them occur in the neocortex. The role of COUP-TF specifically in the hippocampus, which belongs to the archicortex, is poorly studied. The only evidence of a requirement of COUP-TFI in the hippocampus comes from our group. In 2006, Armentano *et al.* showed a strongly reduced hippocampus in newborn COUP-TFI *null* brains together with failed midline crossing of hippocampal commissural projections in COUP-TFI-deficient mice (Armentano *et al.*, 2006). Moreover, primary cultures of hippocampal neurons lacking COUP-TFI showed a defect in neurites outgrowth and an abnormal axonal morphology (Armentano *et al.*, 2006). However, nothing is known on whether COUP-TFI acts intrinsically in the differentiation and functional connectivity of the hippocampus proper and DG.

Regarding COUP-TFII, the only study dealing with the hippocampus supports its involvement in the caudal migration of interneurons (Kanatani *et al.*, 2008).

E) Human COUP-TFI dysfunctions

Very few studies have been investigating the role of COUP-TFI (NR2F1 or EAR3) in human patients. Mutation within the 5q15 region, including COUP-TFI gene have been reported in several patients. Cardoso *et al.* described three patients that had large deletions (6–17 Mb) in this region and exhibited severe neurocognitive phenotypes, epilepsy, periventricular heterotopia, and some dysmorphic features (Cardoso *et al.*, 2009). The patient described by Brown *et al.* had 360 and 454 kb deletions on both sides of an inversion and presented hearing loss, dysmorphism, and developmental delay (Brown *et al.*, 2009). In addition, Al-Kateb *et al.* reported one patient with a deletion of 582 kb within 5q15, accompanied by optic atrophy, dysmorphism and global developmental delay (Al-Kateb *et al.*, 2013). Taken together, the size of the minimal overlapping deletion in all these five patients is around 230 kb and encompasses two genes: the uncharacterized non-coding RNA FLJ42709 and COUP-TFI, suggesting COUP-TFI gene as the most likely candidate for the overlapping phenotypes (Al-Kateb *et al.*, 2013). A more direct genotype-phenotype study comes from Bosch *et al.* who demonstrated that four individuals with optic atrophy and cerebral visual impairment (CVI) had heterozygote *de novo* point mutations in COUP-TFI, and that conversely, two persons with a similar phenotype had deletions comprising the COUP-TFI gene (Bosch *et al.*, 2014). Overall, these studies strongly indicate that COUP-TFI can play an important role in the development of the visual system and that its haploinsufficiency can lead to optic atrophy with intellectual impairments in humans (Bosch *et al.*, 2014). However, additional patients with precisely characterized mutations are still needed to unravel the full pathogenicity of the loss of a COUP-TFI allele in humans.

Our group is currently working with an international network of clinicians to further link the phenotypes described in the mouse with the cortical abnormalities found in patients with mutations and/or deletion of COUP-TFI. The aim is to use the mutant COUP-TFI mouse line as a research model *in vivo* and as a way to further understand the link between genotype and phenotype during the process of cortical malformations. The data obtained in mice will then be compared with those from the clinical and molecular analysis of patients with mental

retardation, cerebral malformation and early epilepsy associated with a deletion in the 5q14.3-q15 chromosome region and linked to COUP-TFI haploinsufficiency (Cardoso *et al.*, 2009).

III / Aim of the study

As described above, COUP-TFI has been shown to act as a strong transcriptional regulator in the developing neocortex, having, among others, key roles in neuronal migration, neurogenesis and arealization. Yet, little is known to date, about its involvement outside the neocortex, and particularly in the hippocampus. Thus, the main aim of my thesis project is to unravel its function during hippocampal development.

Since the Dentate Gyrus is the primary gateway for input information into the hippocampus, most of my thesis work has focused on dentate gyrus development. I have analyzed different processes required in DG development, such as cell proliferation, differentiation and maturation, as well as migration and lamination.

Since COUP-TFI is expressed in both mitotic and post-mitotic cells in the cortex, I have dissected its role independently in the two cell populations by using two distinct conditional *knock-out* mice, the *EmxCKO* and *NexCKO*.

CHAPTER 2

Materials and Methods

I / Animals and genotyping

All lines were maintained on the C57BL/6 genetic background. The day of the vaginal plug was considered as embryonic day 0.5 (E0.5). For the analyses described here, conditional knock-out mice were compared with *COUP-TFI*^{flx/flx} littermates (referred in this study as « *Controls* ») which have no detectable phenotypes. Experiments involving mice were performed by authorized investigators following national ethical guidelines.

A) Mice models

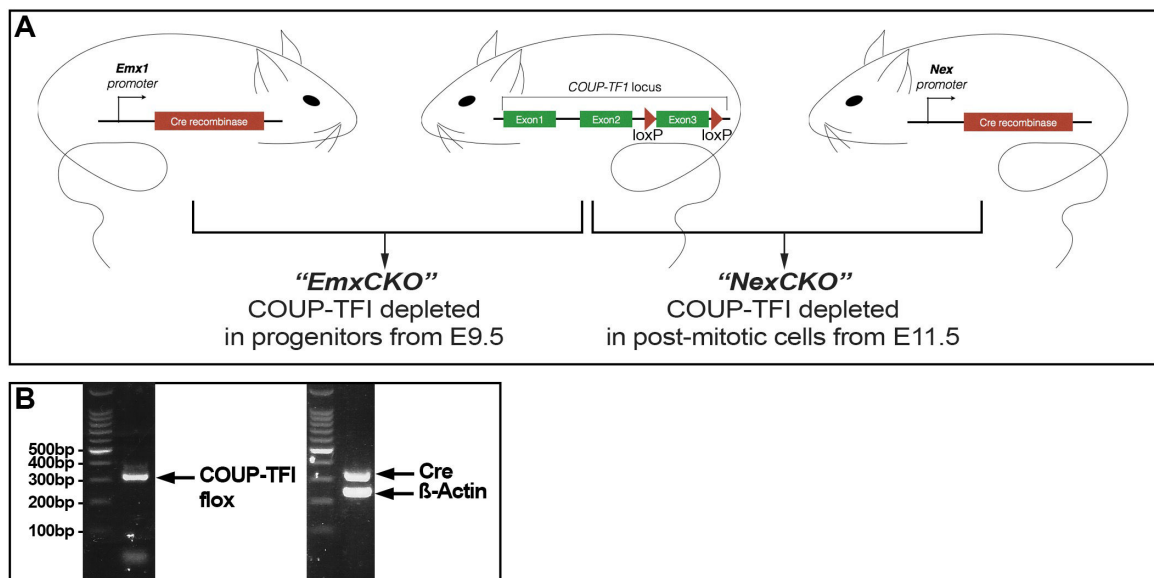


Figure 8. *COUP-TFI* loss-of-function mouse models used in this study.

A. Schematic representation of the three different transgenic mouse line: the *Emx1-IRES-Cre* and *Nex-Cre* mice in which the Cre recombinase is expressed under the promoter of *Emx1* or *Nex*, respectively; and the *COUP-TFI*^{flx/flx} mice, in which the third exon of *COUP-TFI* is flanked with *loxP* sites. Crossing the latter with either of the two former results in *COUP-TFI* conditional knock-out mice, called « *EmxCKO* » and « *NexCKO* ». **B.** Example of genotype visualization on a 2% agarose gel. The band of *COUP-TFI* floxed, of the *Cre-recombinase* and of the β -*Actin* are presented.

1) *COUP-TFI*^{fl/fl};*Emx1Cre* line: « *EmxCKO* »

The *COUP-TFI*^{lox/lox} mice, previously generated in the Studer lab (Armentano *et al.*, 2007), were mated with *Emx1-IRES-Cre* transgenic mice obtained from K.R.Jones (Gorski *et al.*, 2002). A viable and fertile Conditional Knock-Out (CKO) mouse line was obtained: *COUP-TFI*^{fl/fl};*Emx1Cre*. They are referred in this study as « *EmxCKO* ». In the resulting mice, COUP-TFI is inactivated in dorsal cortical progenitors from embryonic day 9 (E9.5) (**Figure 8A**).

2) *COUP-TFI*^{fl/fl};*Nex-Cre* line: « *NexCKO* »

The *COUP-TFI*^{lox/lox} mice, were mated with *Nex-Cre* transgenic mice obtained from K.A. Nave (Goebbels *et al.*, 2006). A viable and fertile CKO mouse line was obtained: *COUP-TFI*^{fl/fl};*Nex-Cre*. They are referred in this study as « *NexCKO* ». In the resulting mice, COUP-TFI is inactivated in post-mitotic cells from E11.5 (**Figure 8A**) (Goebbels *et al.*, 2006).

3) *Thy1-eYFP-H* line: « *Thy1-YFP* »

The transgenic mouse line *Thy1-eYFP-H* (Feng *et al.*, 2000) (referred in this study as « *Thy1-YFP* ») obtained from Josh Sanes (Harvard, USA), were kept in a heterozygous genotype and crossed with the *COUP-TFI*^{fl/fl};*Emx1Cre* mice. The resulting *COUP-TFI*^{fl/fl};*Emx1Cre*;*Thy1-eYFP* were viable and fertile and are referred to « *EmxCKO* » mutant mice, which express the eYFP under the neural-specific promoter of the *Thy1* gene. Thus, many neurons, such as the pyramidal cells of the neocortical layers 5 and 6 and a subset of granule cells of the dentate gyrus, are labelled with YFP from post-natal stages (P14) (Porrero *et al.*, 2010). Since *Thy1* is a cell surface protein, eYFP marks the soma and the processes (axons and dendrites) of the neurons, allowing to visualize their cell morphology.

B) Genotyping

1) DNA extraction

DNA was extracted either from hand tissue at embryonic stage, or from tail or ear tips at post-natal stages. Tissues were incubated in 500µl Lysis Buffer [50mM Tris pH 7.5, 100mM EDTA pH 8, 100mM NaCl, 1% SDS] + Proteinase K [1.0mg/ml] (Roche Applied Science 03115801001) at 58°C until complete dissolution. DNA was then precipitated with 500µl of 2-Propanol and centrifuged at 14000g for 5 minutes. Then, pellets were washed with 1ml of Ethanol 70% and centrifuged at 14000g for 2 minutes. Finally, pellets were dried at room temperature, resuspended in 100µl of H₂O mQ at 37°C under agitation for 1h, and kept at -20°C until genotyping.

2) PCR

Mice were genotyped by Polymerase Chain Reaction (PCR), following standard methods.

- To genotype the COUP-TFI locus, three primers were used in the same reaction, allowing to identify at once both the WT and the mutant (*COUP-TFI floxed* and *COUP-TFI null*) alleles.

The primers used were the following:

forward primer « ARM5'3' » : 5'- CTGCTGTAGGAATCCTGTCTC -3'

reverse primer #1 « Ex351 » : 5'- AATCCTCCTCGGTGAGAGTGG -3'

reverse primer #2 « ARM402 » : 5'- AAGCAATTTGGCTTCCCCTGG -3'

The PCR reaction was performed preparing a mix containing: 1µl of DNA, 2µl of ARM5'3' primer, 1µl of Ex351 primer, 1µl of ARM402 primer and 5µl of GreenTaq (Promega M7423)

• To genotype the *Cre-recombinase* locus, two primers (« Cre fw » and « Cre rev »), internal to the transgene were used. In the same reaction, two other primers (« CCRmL » and « CCRmR »), designed within the ubiquitous expressed gene β -actin, were added as an internal control. The primers used were the following:

« Cre Fw »: 5'- CCCGCAGAACCTGAAGATGT -3'

« Cre Rev »: 5'- TGATCCTGGCAATTTTCGGCT -3'

« CCRmL »: 5'- CAACCGAGACCTTCCTGTTC -3'

« CCRmR »: 5'- ATGTGGATGGAGAGGAGTCG -3'

The PCR reaction was performed preparing a mix containing: 1 μ l of DNA, 1 μ l of each primers and 5 μ l of GreenTaq.

• The PCR program used was the following:

95°C	10'	
95°C	1']
60°C	1'	} 25 cycles
72°C	1']
95°C	1']
60°C	1'	} 25 cycles
72°C	1']
72°C	8'	
4°C	-	

3) Visualisation

PCR results were visualized by electrophoresis using a Agarose 2% gel with BET 1 μ l/ml (Ethidium Bromide, Roth 7870.2) in TBE (45 mM Tris-borate, 1 mM EDTA, in H₂Omq). Molecular weights of the different amplified fragments were analyzed by using a molecular weight ladder (promega G2101). Specific molecular weights obtained are the following:

COUP-TFI WT: 240 bp

COUP-TFI floxed: 310 bp

Cre: 400 bp

β -Actin: 250 bp

An example of a gel with the different genotypes is presented in **Figure 8B**.

II / Tissue Preparation

A) Dissection, Fixation and Embedding

For isolating E16.5 brains, pregnant females were euthanized by cervical dislocation and embryonic brains were rapidly dissected in Phosphate-Buffered Saline 0,1M pH7.4 (PBS 1X). For post-natal stages (from P0 to P14), animals were anesthetized intraperitoneally with Pentobarbital and their brains were fixed with intra-cardiac perfusion of ParaFormAldehyde (PFA) 4% (Sigma Aldrich P6148) in PBS. In both cases, dissected brains were post-fixed in PFA 4% at 4°C, either 2h for immunolabelling experiments, or overnight for *in situ* hybridization experiments, and then washed several times in PBS.

Brains cut with a cryostat were first dehydrated by successive passages in a Sucrose gradient at 4°C: Sucrose 10%, 20% and 30%, in PBS. Brains were then embedded in Optimum Cutting Temperature medium (OCT, Leica Microsystems) and stored at -80°C until cutting. Brains cut with a vibratome were washed after post-fixation and embedded in 4% Agar (Sigma Aldrich A5054) in PBS prior sectioning.

In order to get a good penetration of both PFA and Sucrose in the hippocampus, P14 brains were cut through the midline and split into two hemispheres prior to post-fixation step.

B) Cryosections

OCT-embedded brains were cut coronally or sagittally with a cryostat (Leica CM3050 S), at a thickness of 16µm. Sections were collected on SuperFrost Plus slides (Fisher Scientific 12092702) and left to dry overnight at RT.

For each stage, different numbers of series were cut throughout the brain, allowing a good rostro-caudal representation of the entire hippocampus on each series. For coronal section, 5 series were collected from E16.5 brains, 6 series from P0, and 10 series from P7 and P14 brains; for sagittal P7 sections, 4 series from each hemisphere were collected. After complete drying, of at least one night at room temperature, slides were stored at -80°C.

C) Vibratome sections

Agar-embedded brains were cut with a vibratome (Leica VT1000S), at a thickness of 100 or 200µm, depending of the procedure. Sections were collected with a brush and stored in PBS until further process.

III / Histological procedures

A) Birth-dating: EdU labelling

Pregnant females were injected intraperitoneally at specified timepoints with 200µl of EdU at 2,5µg/µl (Fisher Scientific 11590926) that was diluted according to the manufacturer's instructions. EdU revelation was performed by using the EdU Click-It Alexa Fluor 647 kit (FisherScientific 10063724), and slides were then performed for immunofluorescence (see below).

B) Immunofluorescence

For immunofluorescence (IF) procedures, mouse brain were post-fixed 2h in 4% PFA (*cf. Materials and Methods-II-A*) and immunolabelling were performed on 16µm cryosections. Slides, stored at -80°C, were dried at room temperature for at least 1h before being briefly washed in PBS. Slides were then boiled in an unmasking solution [8,5mM Sodium Citrate, in H₂O, pH6]. This step, also called “antigen retrieval” allows exposing antigens and increasing the binding efficiency of the antibodies to their targets. After 15 seconds of boiling, slides were let to cool down in the solution on ice. After 3 PBS washes of at least 5min each, slides were incubated with 1ml each of blocking solution [10% Serum, 0,3% Triton in PBS] for 1h at RT. Sections were then incubated over-night at 4°C with 250µl/slide of primary

antibodies, diluted in 3% Serum + 0,3% Triton in PBS. Goat serum (GS) was commonly used for blocking step and antibodies dilution, except when used with goat primary antibody, where newborn calf serum (NBCS) was used instead. On the next day, sections were washed 3 times 5min in PBS, and incubated 2h at room temperature in secondary antibodies, diluted in 3% Serum and 0,3% Triton in PBS. Primary and secondary antibodies dilution, species and provenance are listed in **Table 1** and **Table 2**. Following additional PBS washes, slides were mounted and counterstained with mounting medium [2% N-propylgallate (Sigma P3130-100G), 90% glycerol in PBS, 1 μ g/ml Hoechst (Invitrogen H3570)], and stored at -20°C. Pictures were taken using either an epifluorescence microscope (Zeiss Imager.M2) or a confocal microscope (Zeiss 710).

Primary Antibody	Specie	Source (ref)	Working dilution
α - BLBP	Rabbit polyclonal	Abcam (ab32423)	1/200
α - Calbindin D-28k	Rabbit polyclonal	SWANT (CB-38)	1/2500
α - Cleaved Caspase-3	Rabbit polyclonal	Cell Signaling (9661)	1/1000
α - COUP-TFI	Rabbit polyclonal	Studer lab	1/1000
α - GFAP	Mouse monoclonal	Sigma (G3893)	1/1000
α - GFAP	Rabbit polyclonal	DakoCytomation (Z0334)	1/1000
α - Ki-67	Rabbit polyclonal	Abcam (ab833)	1/100
α - Map2	Mouse monoclonal	Sigma	1/200
α - Mcm2	Rabbit polyclonal	Abcam (ab4461)	1/1000
α - NeuN	Mouse monoclonal	Millipore (MAB377)	1/100
α - NeuroD1 (N-19)	Goat polyclonal	Santa Cruz (sc-1084)	1/100
α - Pax6	Rabbit polyclonal	Millipore (AB5409)	1/500
α - Prox1	Rabbit polyclonal	AngioBio (11-002)	1/1000
α - Reelin	Mouse monoclonal	Chemicon (MAB5364)	1/500
α - Tbr1	Rabbit polyclonal	Abcam (ab31940)	1/1000
α - Tbr2	Chicken polyclonal	Millipore (AB15894)	1/500

Table 1. List of primary antibodies used in this study.

List of primary antibodies used in this study, with their species of origin, their source (commercial or not) and their working dilutions.

Secondary Antibody	Specie	Source	Working dilution
Anti-Chicken IgG Alexa 488 (green)	Goat	Fisher Scientific (10286672)	1/300
Anti-Goat IgG Alexa 594 (red)	Donkey	Fisher Scientific (10590523)	1/300
Anti-Mouse IgG Alexa 488/594 (green/red)	Goat	Fisher Scientific (10003482/10348652)	1/300
Anti-Rabbit IgG Alexa 488/594 (green/red)	Goat	Fisher Scientific (10779623/10789623)	1/300
Anti-Rabbit IgG biotinylated	Goat	Vector laboratories (pk-6101)	1/300

Table 2. List of secondary antibodies used in this study.

List of secondary antibodies used in this study, with their species of origin, their source (commercial or not) and their working dilutions.

C) Immunohistochemistry

For immunohistochemistry (IHC) procedures, mouse brain were post-fixed 2h in 4% PFA (*cf. Materials and Methods-II-A*) and immunolabelling were performed on 16µm cryosections. Slides, stored at -80°C, were dried at room temperature for at least 1h before being briefly washed in PBS. After 3 PBS washes of at least 5min each, slides were incubated with 1ml each of blocking solution [10% GS, 0,3% Triton in PBS] for 1h at RT. Sections were then incubated over-night at 4°C with 250µl/slide of primary antibody rabbit anti-COUP-TFI (Table 1), diluted in 3% Serum and 0,3% Triton in PBS. On the next day, sections were washed 3 times 5min in PBS, and incubated 2h at room temperature in secondary antibody anti-rabbit biotinylated (Table 1), diluted in 3% Serum and 0,3% Triton in PBS. Following 3 washes with PBS, slides followed the standard avidin-biotin complex reaction procedure by incubating sections with ABC reagent (Vector Laboratories pk-6101) [1/250 of A reagent and 1/250 of B reagent in PBS] for 1h at RT. After 3 additional washes in PBS, revelation was carried out using the DAB Peroxidase Substrate (Vector SK-4100), according to the manufacturer instructions. Reactions were monitored, stopped by washing with H₂O and then mounted with Aquatex mounting medium (Millipore 1.08562.0050). Pictures were taken using a brightfield microscope (Leica DM6000B) equipped with a color camera.

D) RNA probe synthesis and *In Situ* Hybridization

1) RNA probe synthesis

DNA plasmids were linearized by incubating in the linearization mix [10µg/µl DNA, 1X BSA, 1X Buffer, 50U restriction enzyme, in H₂O] for 2h at 37°C. The plasmids used in this study, their provenance and corresponding restriction enzyme are listed in Table 2. All restriction enzymes and their buffers were obtained either from Biolabs or from Promega. Linearized DNA was then purified with illustra MicroSpin S-200 HR Columns (GE Healthcare 27-5120-01) and linearization was confirmed by electrophoresis on a 1% agarose gel. Transcription reactions [2µl of purified linearized DNA, 2µl of Digoxigenin mix 10X (Roche Diagnostics 11277073910), 2µl of transcription buffer 10X, 0,5µl of RNase inhibitor (Invitrogen 100000840), 2µl RNA polymerase, in H₂O] were carried out at 37°C for 2h. The RNA polymerases used for each probe are listed in **Figure 2**, and were all obtained from Roche. Following a DNase treatment with DNase (RNase-free) from Qiagen (79254) for 1h at 37°C, the RNA probes were precipitated by adding 80µl of H₂O, 10µl of LiCl 4M and 300µl of EtOH absolute, for 20min at -80°C (or ON at -20°C), and centrifuging at 14000 rpm for 15min at 4°C. After two washes and centrifugations with EtOH 70%, the supernatant was carefully removed and the pellet was resuspended in 40µl of H₂O. Probes transcription was confirmed by electrophoresis on a 2% agarose gel, and stored at -20°C.

2) *In Situ* Hybridization

For *In Situ* Hybridization (ISH) procedures, mouse brain were fixed over-night in 4%PFA (*cf. Materials and Methods-II-A*) and experiments were performed on 16 µm cryosections (*cf. Materials and Methods-II-B*). Cryosections, stored at -80°C, were dried at room temperature for at least 1h before being briefly washed in PBS. Slides were then treated with RIPA buffer [150mM NaCl, 0,1% SDS, 1mM EDTA pH8, 50mM Tris pH8, 1% NP-40, 0,5% Na deoxycholate, in H₂O], 2 times 10 min at RT, post-fixed in PFA 4% in PBS, 15 min at RT,

and washed 3 times 5 minutes with PBS. Tissue was then incubated in Triethanolamine buffer [100mM Triethanolamine, 0,2% Acetic acid pH8, 0,25% Anhydride acetic, in H₂O] for 15 min at RT. Following 3 washes of 5 minutes in PBS, pre-hybridization step was performed by incubating slides in the warmed (at 70°C) hybridization solution [50% Formamide, 5X SSC, 5X Denhardt's, 500µg/ml Salmon sperm, 250µg/ml Yeast RNA, in H₂O] at RT for 1h. Each slide was then incubated with 1 to 2µl of probe, diluted in 250µl of hybridization solution, covered with a coverslip and left overnight at +70°C in a humidified chamber [50M Formamide, 5X SSC, in H₂O]. The probes used were the following: Cad8, COUP-TFII, CXCR4, LMO4 and Wnt5a.

The second day, tissues were incubated in post-hybridization solution [50% Formamide, 2X SSC, 0,1% Tween-20, in H₂O] for 2 times 1h at 70°C. After washing in MABT [100mM Maleic acid, 150mM NaCl, 0,1% Tween-20, in H₂O] for 2 times 5min and 1 time 20min at RT, the blocking step was performed by incubating sections in B2 buffer [10% Sheep Serum in MABT] (1ml / slide) for 1h at RT. Then, 200µl of antibody anti-DIG U-AP (Roche 11093274910), diluted at 1/2000 in B2 buffer, was applied on the slides, covered with parafilm and let ON at 4°C in a humidified chamber.

The third day, slides were washed 2 times 5min and 1 time 20min in MABT at RT, and incubated in B3 buffer [100mM Tris pH9.5, 50mM MgCl₂, 100mM NaCl, 0,1% Tween-20, in H₂O] for 30min at RT. Finally, the reaction was revealed by applying filtered NBT-BCIP (Sigma-Aldrich B1911) + 0,1% Tween-20 on the tissue, and let to develop in the dark at 4°C. The duration of the incubation was determined by the experimenter for each experiment, but *control* and *mutant* followed the same treatments. When the signal was estimated clearly visible, the reaction was stopped by washing the slides with PBST [PBS + 0.1% Tween-20] 3 times 5min at RT. Then, after briefly rinsing in H₂O, slides were mounted with Aquatex mounting medium (Millipore 1.08562.0050) and left to dry and stored at RT. Pictures were taken using a brightfield microscope (Leica DM6000B) equipped with a color camera, or with a black and white camera microscope (Zeiss Imager.M2).

E) Nissl Staining

Nissl Staining were realized on 2h-PFA-fixed tissues. 16µm thick cyosections, stored at -80°C, were dried at room temperature for at least 1h before processing. Tissues were post-fixed in 4% PFA for 10min and washed 3min in H₂O. The coloration step was performed by incubating slides in the coloration solution [0,025% Thionin, 0,025% Cresyl Violet, 100mM Sodium acetate, 8mM Acetic acid, in H₂O] for 5min at RT, under fume hood. Differentiation was done in the de-coloration solution [80% EtOH, 20% H₂O, and around 8 drops/500ml of solution of Acetic acid]. The duration of incubation was determined by the experimenter, and the differentiation was stopped when the signal was estimated clearly visible. Sections were then dehydrated by passage in 96% EtOH for 3 times 5min and minimum 2 times 5min in Xylen. Finally, slides were mounted using EUKITT mounting medium (GENTAUR 361894G), let to dry for several days in the dark under fume hood, and stored at RT. Pictures were taken using a brightfield microscope (Leica DM6000B) equipped with a color camera.

F) Axonal tracing by injection of lipophilic DiI

Tracing of entorhino-hippocampal projections was carried out by injecting approximately 80µl of DiI crystal (DiIC18(3); Molecular Probes) dissolved in DMSO in the entorhinal cortex of P8 *control* and *mutant* fixed brains (4% PFA ON). Brains were incubated for 6 weeks in 2% PFA at 37°C, embedded in 4% agarose, cut into 100 µm sections on a vibratome, counterstained with Hoechst (Invitrogen H3570) and mounted with mounting medium [2% N-propylgallate (Sigma P3130-100G), 90% glycerol in PBS, 1µg/ml Hoechst (Invitrogen H3570)], before storing at -20°C. Pictures were taken using either an epifluorescence microscope (Zeiss Imager.M2) for localization of the site of injection, or a confocal microscope (Zeiss 710) for visualizing fibers.

G) Imaging

IF were imaged using the Zeiss Imager.M2 epifluorescence microscope with the AxioVision software or the Zeiss 710 confocal microscope with the Zen software. Images were processed in with Adobe Photoshop CS6 software. IHC, ISH and Nissl staining were imaged using the Leica DM6000B brightfield microscope, equipped with a color camera.

H) Three-dimensional reconstruction

Adult brains representatives of hippocampal dysmorphism were coronally cryosectioned (20µm thickness) and stained for Nissl and pictures were taken on the Leica Stereomicroscope. Sections were identified with serial numbers and different HP components were labeled with a color-coded graphic pen. 3-D images were aligned and integrated with Amira 4.1.2-1 software to obtain 3D pictures.

IV / Quantification and Statistical analysis

Cell quantifications were performed on three coronal anatomically matched sections within the rostral hippocampus (septal pole). Different areas were delineated to count the cells, depending on the stage analyzed (**Figure 9**):

- At E16.5, three boxes of the same area were selected in *control* and *mutant* three dentate gyrus matrices (**Figure 9A**)
- At P0, the DG area was delineated and separated into two areas (**Figure 9B**): the upper blade (UB) and the lower blade (LB)
- At P7 and P14, the DG was split into 5 areas, corresponding to the layers of the dentate gyrus, visible with Hoechst staining (**Figure 9C**): the UB molecular layer (UBml), the UB granule cell layer (UBgcl), the Hilus (UB hilus + LB hilus), the LB granule cell layer (LBgcl) and the LB molecular layer (LBml)

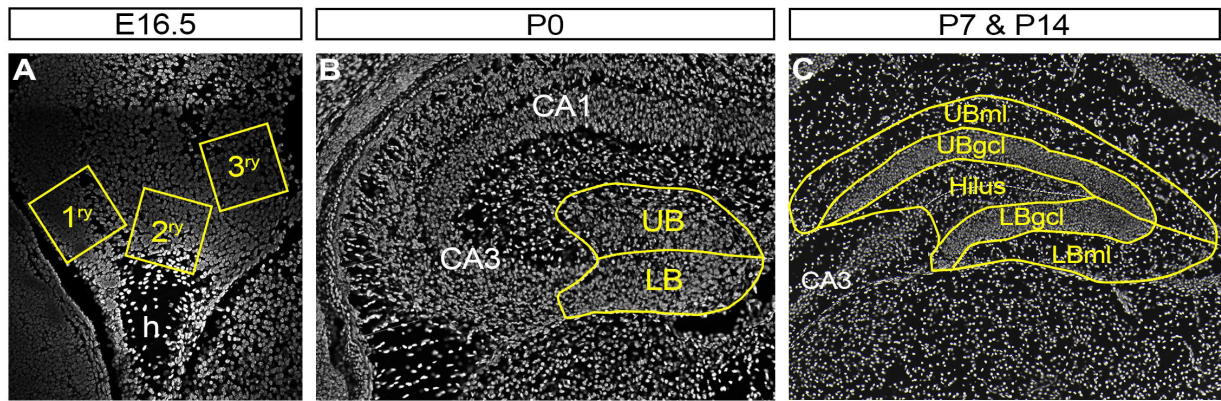


Figure 9. Counting methodology examples.

Representation of the area delineated for counting cells in the developing dentate gyrus. **A.** At E16.5, three boxes of same area were selected in the three matrices. **B.** At P0, the DG area was delineated and separated into two bins: the upper blade (*UB*) and the lower blade (*LB*). **C.** At P7 and P14, the DG was split into 5 areas, corresponding to the layers of the dentate gyrus: the UB molecular layer (*UBml*), the UB granule cell layer (*UBgcl*), the Hilus (UB hilus + LB hilus), the LB granule cell layer (*LBgcl*) and the LB molecular layer (*LBml*).

All the cell countings were made using the counting tool of Adobe Photoshop CS6 Extended software. Error bars reflect standard errors of the mean (SEM), calculated by dividing standard deviation (SD) by the square root of the sample number (n).

$$SEM = \frac{SD}{\sqrt{n}}$$

Statistical analyses were performed with a spreadsheet software (Numbers, Apple). A two-tailed paired Student's t-test, comparing each *mutant* to both *controls* of each genotype was used to analyze statistical significance (* $p < 0,05$; ** $p < 0,01$; *** $p < 0,001$).

CHAPTER 3

Results

I / COUP-TFI is expressed in the developing and adult hippocampus

1) COUP-TFI is expressed in the hippocampus in a low septal to high temporal gradient

COUP-TFI is expressed in the developing mouse hippocampus from its onset when the hippocampal plate starts to be generated (Qiu *et al.*, 1994b). As shown by immunohistochemistry using a well-established antibody against COUP-TFI raised in the Studer lab (Tripodi *et al.*, 2004) (**Figure 10**), COUP-TFI expression is found both in the ventricular zone (Hpn and dgn) and in the post-mitotic compartment of the developing hippocampus at E16.5 (**Figure 10A**). Notably, COUP-TFI is expressed at higher levels in the dentate gyrus neuroepithelium (dgn), or primary matrix (1ry), the primordium of the dentate gyrus, suggesting a specific role in DG formation. At P0, COUP-TFI is maintained in the developing Hp (CA fields) and DG in almost all cells (**Figure 10B**), although at different expression levels along the septo–temporal axis. This is more evident at P8 when COUP-TFI is highly expressed in the temporal pole of the hippocampus (caudo-ventral) and at a lower level in the septal pole (rostro-dorsal) (**arrowheads in Figure 10C**; Flore *et al.*, 2015 [manuscript in annexe]). A similar differential gene expression pattern along the longitudinal hippocampal axis has been already described for its homolog COUP-TFII (O'Reilly *et al.*, 2014), suggesting that both COUP-TF factors might be involved in distinct functions along this axis. Finally at adult stages, COUP-TFI expression is maintained in both the Hp pyramidal and DG granule cell layers (**Figure 10D**). High magnification views in the granule cell layer indicate that COUP-TFI is expressed in the subgranular zone (SGZ) where adult progenitors originate (**Figure 10D'-D''**), as demonstrated by its co-localization with the radial glia marker Pax6 (**arrowheads in Figure 10E**). Overall, these expression data suggest that COUP-TFI might play multiple roles during hippocampal development and maturity. My thesis work focuses mainly on the specific role of COUP-TFI during DG development and maturation.

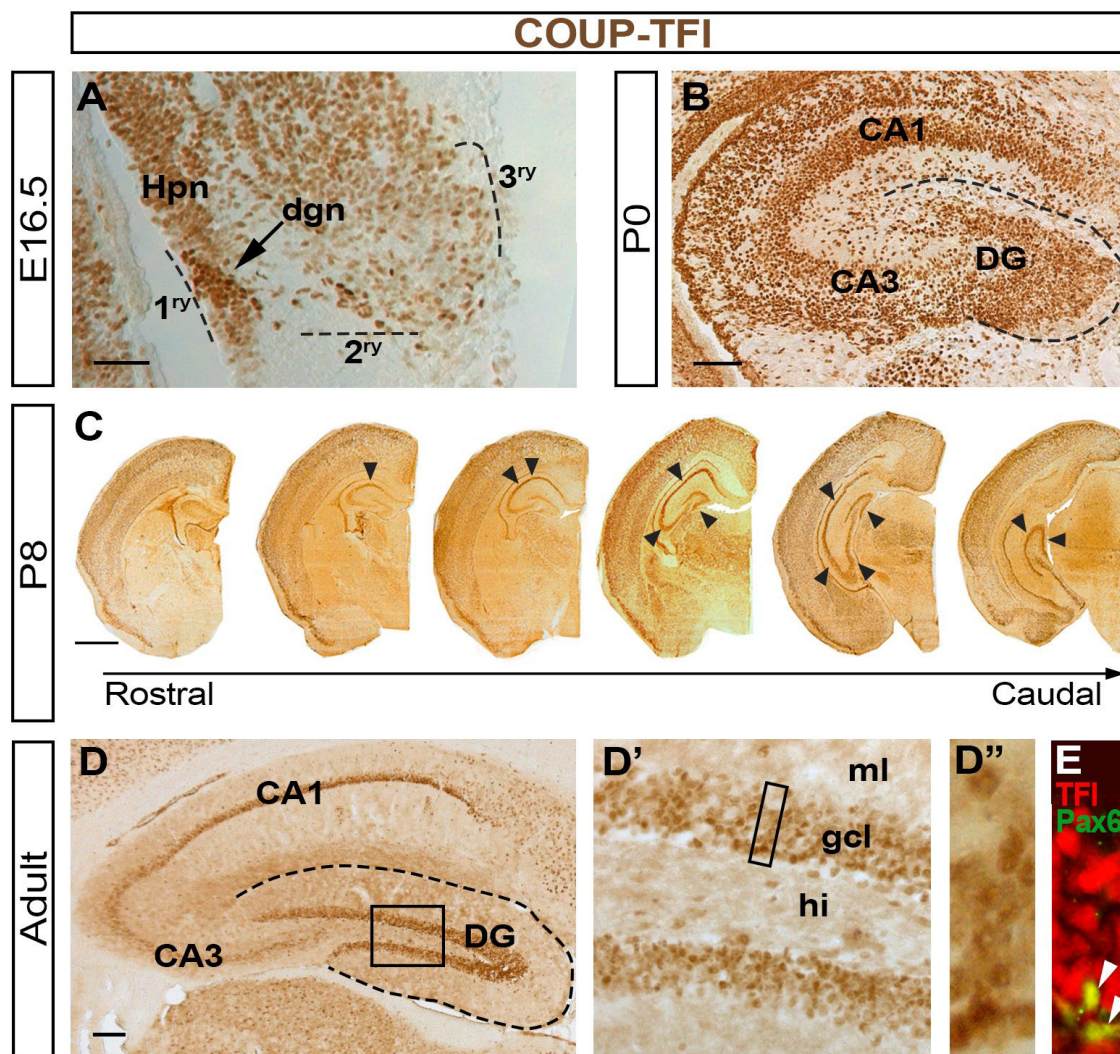


Figure 10. COUP-TFI is expressed in a gradient in the developing and adult hippocampus.

A-D''. Immunohistochemistries showing COUP-TFI protein expression in mouse hippocampus during development and in the adult. **A.** E16.5 hippocampal primordium: COUP-TFI is highly express in the dentate granule neuroepithelium (dgn). **B.** P0 hippocampus. **C.** P8 coronal sections of one hemisphere: COUP-TFI depict a rostro-caudal gradient of protein level in the hippocampus (arrowheads). **D.** Adult hippocampus: COUP-TFI is expressed in DG granule cells and Hp pyramidal cells. **D'.** Magnification of the box in D. **D''.** Magnification of the box in D' showing COUP-TFI expression in the granule cell layer. **E.** Immunofluorescence for COUP-TFI (in red) and the neural stem cell-like marker Pax6 (in green) show that COUP-TFI is also expressed in the SGZ, the adult neurogenic niche of the DG (co-expressing cells shown by white arrowheads). *1ry/2ry/3ry:* primary/secondary/tertiary matrix; *CA1/3:* cornus Ammonis field 1/3; *DG:* dentate gyrus; *dgn:* dentate granule neuroepithelium; *gcl:* granule cell layer; *Hpn:* hippocampus proper neuroepithelium; *hi:* hilus; *ml:* molecular layer. Scale bars = 50 μ m (A), 100 μ m (B, D), 1mm (C).

2) COUP-TFI expression is abolished in mitotic or post-mitotic cells in conditional mutants

To investigate the role of COUP-TFI during DG development, I took advantage of two conditional mutant (CKO) mouse lines already available in the Studer lab. Because constitutive *COUP-TFI* knock-outs (KO) resulted in embryonic lethality (Qiu *et al.*, 1997), I used a conditional inactivation approach to evaluate the function of COUP-TFI in the mouse developing DG. *COUP-TFI*-floxed mice (*COUP-TFI*^{fl/fl}) were mated either to *Emx1-Cre* or to *Nex-Cre* mice, reported to be active in cortical progenitor or post-mitotic cells, respectively (Gorski *et al.*, 2002; Goebbels *et al.*, 2006). In the resulting *COUP-TFI*^{fl/fl}:*EmxCre* mutant mice (referred as « *EmxCKO* »), COUP-TFI will be inactivated in dorsal cortical progenitors from embryonic day 9 (E9.5), and gene inactivation homogenously occurs all over the septo-temporal hippocampal axis from E11.5 onwards (Gorski *et al.*, 2002; Armentano *et al.*, 2007). Differently, in *COUP-TFI*^{fl/fl}:*NexCre* mutant mice (referred as « *NexCKO* ») COUP-TFI expression will be lost in post-mitotic cells from E11.5 (*cf. Chapter 2- Material and Methods*).

To validate the correct inactivation of COUP-TFI expression in the developing hippocampus of the two mutant mouse lines, I used the COUP-TFI antibody in coronal sections of *Control*, *NexCKO* and *EmxCKO* brains from E16.5 to P7 (**Figure 11**). At E16.5, COUP-TFI expression is still present in the ventricular zone (vz) of the *NexCKO* medio-caudal cortex, with a higher expression in progenitor cells of the dgn similar to *controls* (**arrows in Figure 11A-A'**). This is not the case for the *EmxCKO* mutant brain in which COUP-TFI expression is completely lost in the hippocampal primordium (**asterisks in Figure 11A''**). Similarly, at P0 COUP-TFI expression is clearly absent from the CA pyramidal cell layers of *NexCKO* and *EmxCKO* hippocampi, known to contain only post-mitotic cells (**blue asterisks in Figure 11B-B''**). As described in the introduction (**Figure 4C'**), the developing DG has the particularity to contain a second pool of progenitors in the 3rd matrix (future DG). Thus and as expected, *NexCKO* DG have decreased but still presence of COUP-TFI expression in the future dentate gyrus (**red asterisk in Figure 11B'**). On the contrary, *EmxCKO* hippocampi have a complete depletion of progenitors and post-mitotic hippocampal neurons (**red asterisks in Figure**

11B”). The persistence of the few spread COUP-TFI-expressing cells have been shown to be GABAergic interneurons (Flore *et al.*, 2015), which do not originate from the dorsal palium and therefore are not affected by the Cre-recombinase activity (Gorski *et al.*, 2002; Flore *et al.*, 2015). Finally, at P7 when the hippocampus is predominantly composed of post-mitotic neurons and COUP-TFI clearly labels the Hp pyramidal and DG granule cell layers, COUP-TFI is maintained only in mitotic cells of the DG in the *NexCKO* model, whereas no pyramidal or granule neurons express COUP-TFI in the *EmxCKO* hippocampus, except for interneurons (**red asterisks in Figure 11C-C**”). In summary, while COUP-TFI expression is maintained in cycling progenitors in the *NexCKO* mice, expression is completely abolished in all mitotic and post-mitotic pyramidal and granule cells in *EmxCKO* mice, allowing me in this way to discern the role of COUP-TFI in mitotic *versus* post-mitotic neurons during hippocampal development.

II / COUP-TFI is required in the growth and morphogenesis of the postnatal hippocampus and dentate gyrus

To investigate the functions of COUP-TFI in hippocampal and DG development, I have analyzed the morphogenesis of the two mutants at different developmental stages: from embryonic E16.5 to post-natal stages P0, P7, P14 and adult.

1) Lack of COUP-TFI leads to developmental malformations of the postnatal dentate gyrus

To visualize the overall morphology and layer organization of the hippocampus, I have used a classical Cresyl Violet staining (known as Nissl staining) that allows visualisation of all neuronal cell bodies on E16.5, P0, P7 and P14 coronal sections of *Control*, *NexCKO* and *EmxCKO* hippocampi (**Figure 12**).

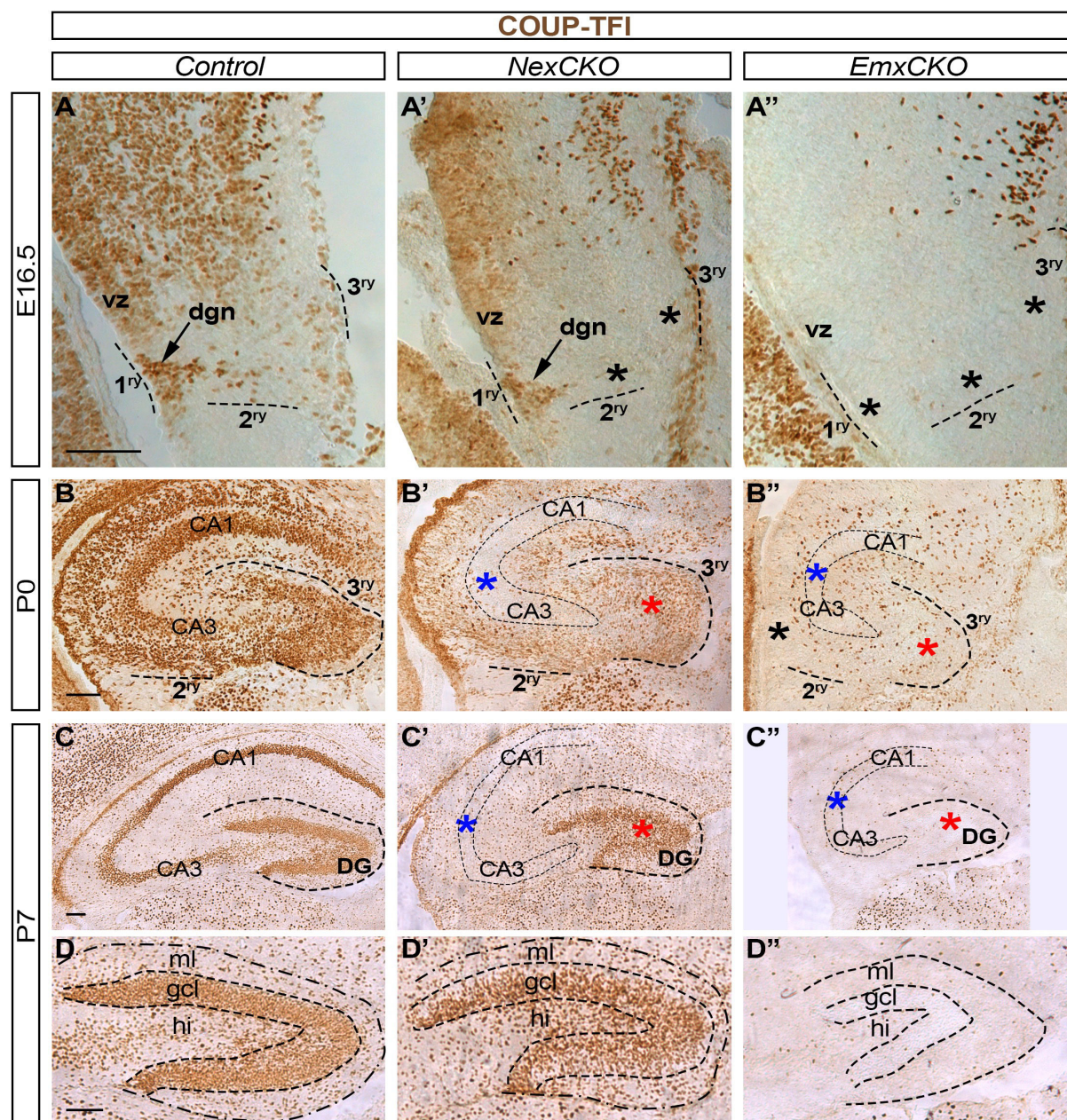
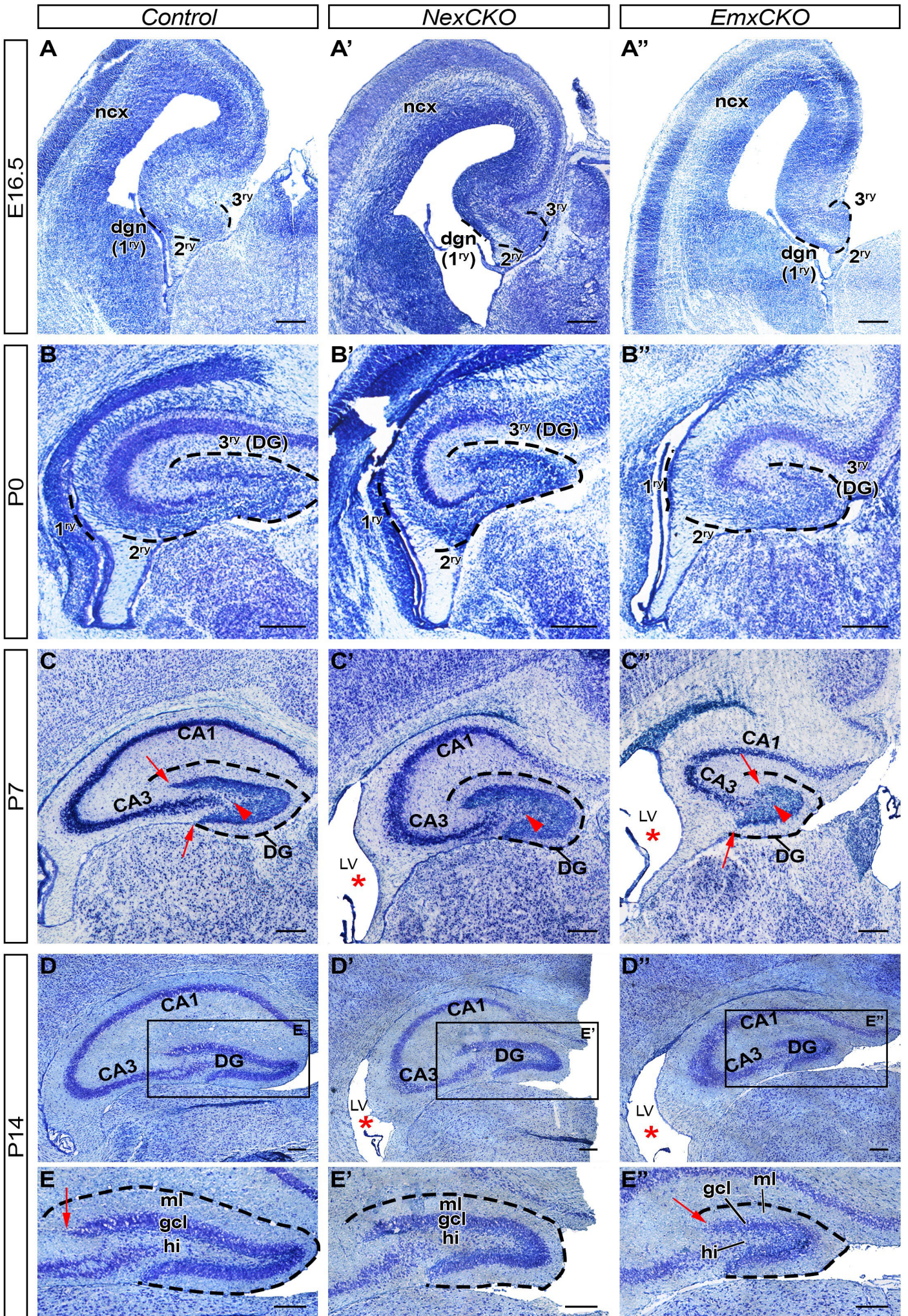


Figure 11. COUP-TFI loss of expression in *NexCKO* and *EmxCKO* mutant hippocampi.

Immunohistochemistries showing COUP-TFI expression in *Control* (A-D), *NexCKO* (A'-D') and *EmxCKO* (A''-D'') hippocampi during development. A-A''. At E16.5, COUP-TFI expression is lost in the 2ry and 3ry matrix of the *NexCKO* and in the 3 matrices in *EmxCKO* (asterisks in A'-A''). B-C'' At P0 and P7, COUP-TFI expression is absent from the pyramidal cell layer of *NexCKO* and *EmxCKO* (blue asterisks in B'-B'' and C'-C'') and from the *EmxCKO* ventricular zone (black asterisk in B''). *NexCKO* DG have a strongly reduced number of cells expressing COUP-TFI, which corresponds to mitotic cells (red asterisks in B' and C'), whereas *EmxCKO* have only few spared cells that retained COUP-TFI expression, which corresponds to interneurons (red asterisks in B'' and C''). D-D''. Magnifications of DG area from C-C''. 1ry/2ry/3ry: primary/secondary/tertiary matrix; CA1/3: cornus Ammonis field 1/3; DG: dentate gyrus; dgn: dentate granule neuroepithelium; gcl: granule cell layer; hi: hilus; ml: molecular layer vz: ventricular zone. Scale bars = 100 μ m.



< **Figure 12. COUP-TFI loss-of function induces growth impairment.**

Morphology of the hippocampus revealed by Nissl staining on coronal section of *Control* (A-E), *NexCKO* (A'-E') and *EmxCKO* (A''-E'') during development at E16.5 (A-A''), P0 (B-B''), P7 (C-C'') and P14 (D-D''). E-E'' are magnifications of the boxes in D-D'' showing DG layer organization. Both mutants have morphogenesis impairment, including altered blade length (red arrows), layer organization defects (red arrowheads) and lateral ventricle (LV) enlargement (red asterisks). Notably, *EmxCKO* exhibits the strongest phenotype. *Iry/2ry/3ry*: primary/secondary/tertiary matrix; *CA1/3*: cornus Ammonis field 1/3; *DG*: dentate gyrus; *dgn*: dentate granule neuroepithelium; *gcl*: granule cell layer; *hi*: hilus; *LV*: lateral ventricle; *ml*: molecular layer; *ncx*: neocortex. Scale bars = 200µm.

During early stages of DG development (E16.5) no obvious morphological defects of the dentate gyrus in the *EmxCKO* and *NexCKO* mutants were observed (**Figure 12A-A''**). The three matrices are well distinguishable and the cell density seems similar between *control* and *mutants*. At birth (P0), both *EmxCKO* and *NexCKO* hippocampi start to be slightly smaller than their littermate *controls* (**Figure 12B-B''**). This defect is more evident at P7 where both the hippocampus proper and the dentate gyrus are clearly smaller in *EmxCKO* compared to *Control* (**Figure 12C-C''**) and the size of the *NexCKO* hippocampus ranges between a *control* and *EmxCKO* one.

Beside a change in the overall size, mutant *NexCKO* DG have a more round C-shape, compared to the characteristic V-shape of the *Control* DG (**Figure 12C'**). This is even more exacerbated in the *EmxCKO* mutants in which the length of the upper and lower blades are altered. *EmxCKO* DG have a shorter upper blade and a longer lower blade compared to *controls* and *NexCKOs* at P7 (**red arrows in Figure 12C and C''**), suggesting a failure of granule cells accumulation during the primary dentate migration, in which the upper blade is formed before the lower blade. Regarding the laminar organization, while the three layers start to be distinguishable in the *control* DG at P7, both COUP-TFI-deficient mice show a defective layer organization where the three layers are less distinguishable. Indeed, while the molecular layer is visible, the delimitation between granule cell layer and hilus is less defined in the *NexCKO*, and is completely absent in *EmxCKO* (**arrowheads in Figure 12C-C''**). In the latter, the putative hilus appears full of cells, presumably due to granule cells that have failed to be organized in a thin and dense layer.

At P14, an age at which the hippocampus is normally completely formed, *NexCKO* and *EmxCKO* hippocampi are still smaller, with a more severe phenotype in the *EmxCKO* mutant (**Figure 12D-D''**). The *NexCKO* mutant shows an intermediate phenotype in both structures, the Hp proper and the DG. Since the DG contains numerous progenitors (mitotic cells) and several phases of cell divisions during its development, this might explain the more severe phenotype in *EmxCKO* than in *NexCKO* mice, which lack COUP-TFI expression only in post-mitotic cells. Moreover, at this age the DG lamination defect observed in the *NexCKO* brain seems to be improved when compared at earlier stage and at the one of the *EmxCKO*, suggesting that the defect observed at P7 might be partially rescued at P14. Nevertheless, the *NexCKO* DG shape is still rather different from *controls* but less severe than the DG shape of *EmxCKOs*. Finally, even if the lower blade has almost reached its normal size in the DG of P14 *EmxCKOs*, the upper blade is still very reduced compared to the *NexCKO* and *controls* (**red arrows in Figure 12E and E''**). These data collectively indicate that COUP-TFI plays a major role in progenitors than in post-mitotic cells during DG development.

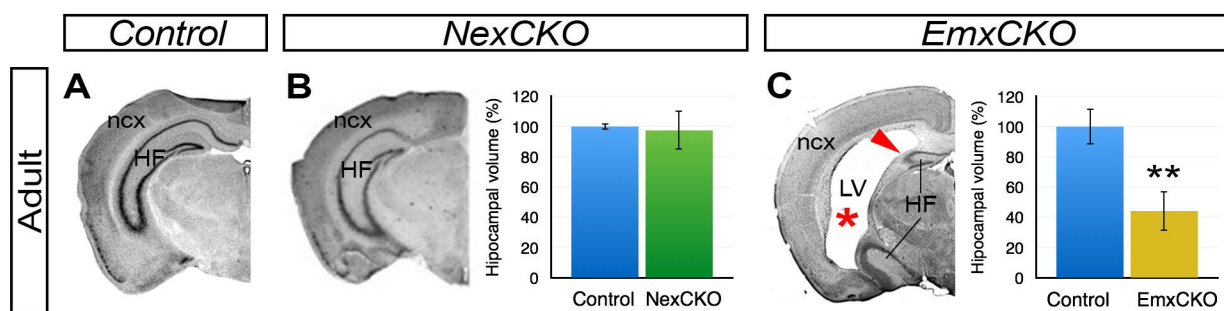


Figure 13. Developmental defects lead to strong hippocampal volume reduction in the adult *EmxCKO* brain but not in *NexCKO*.

Coronal section of adult brains stained with Nissl staining at the level of the hippocampus in *Control* (A), *NexCKO* (B) and *EmxCKO* (C). Hippocampal volume, expressed in percentages relative to *Control* volume are also presented in this figure and shows not significant differences in the *NexCKO* (B) and a strong reduction in *EmxCKO* (C). HF: hippocampal formation; LV: lateral ventricle; ncx: neocortex. ** $p < 0,01$.

Finally, I have evaluated and quantified the morphological defect in adult *EmxCKO* mice and compared it to *control* and *NexCKO* mice (**Figure 13C**; Flore *et al.*, 2015). Strikingly, at this age, *EmxCKO* mutant mice have a severely reduced hippocampal volume, of around 60% of its normal volume, while adult *NexCKO* show no significant defects in size and morphology (**Figure 13B**). In addition, the hippocampal volume reduction is accompanied by a huge enlargement of the lateral ventricle, particularly in adult *EmxCKO* brains (**red asterisk in Figure 13C**). However this defect is already visible at P0 and worsens at P7 and P14 (**red asterisks in Figure 12C'-C'' and D'-D''**) in both mutant mice. This could be a consequence either of the severe reduction of the hippocampus, and/or to another effect due to COUP-TFI loss, such as defective production of cerebrospinal fluid that could impact the pressure in the lateral ventricles.

Taken together, these results illustrate gradual growth impairments in the absence of COUP-TFI in progenitor cells, first observed at birth and then exacerbated from P7 to P14 and to adulthood. This suggests that the hippocampal development is affected by COUP-TFI loss more at post-natal than at pre-natal stages and can be explained by the fact that DG formation is known to take place predominantly post-natally. It also clearly shows that COUP-TFI acts more in progenitor than in post-mitotic cells during DG development, since the most severe phenotypic abnormalities are observed in *EmxCKO* mice.

2) COUP-TFI loss-of-function induces a more severe hippocampal and dentate gyrus impairment in the septal than the temporal pole

As previously described, COUP-TFI is expressed in a gradient along the longitudinal hippocampal axis (*cf. Results-I-1*). Since the septal/dorsal and temporal/ventral pole of the hippocampus have been demonstrated to possess distinct functions (Moser *et al.*, 1993; Moser *et al.*, 1995), it became important to quantify the morphological defect observed in *EmxCKO* adults along the entire longitudinal axis. To this purpose, consecutive coronal Nissl-stained sections were analyzed using the software Amira to produce a 3D representation of the whole *EmxCKO* hippocampus. By comparing the *mutant* to its littermate *control*, and measuring

hippocampal volume on each coronal section along the longitudinal axis, we found that whereas the septal/dorsal regions are dramatically affected (red arrows in **Figure 14E**, the most caudal parts are more similar to the *control* ones (**Figure 14**, Flore *et al.*, 2015).

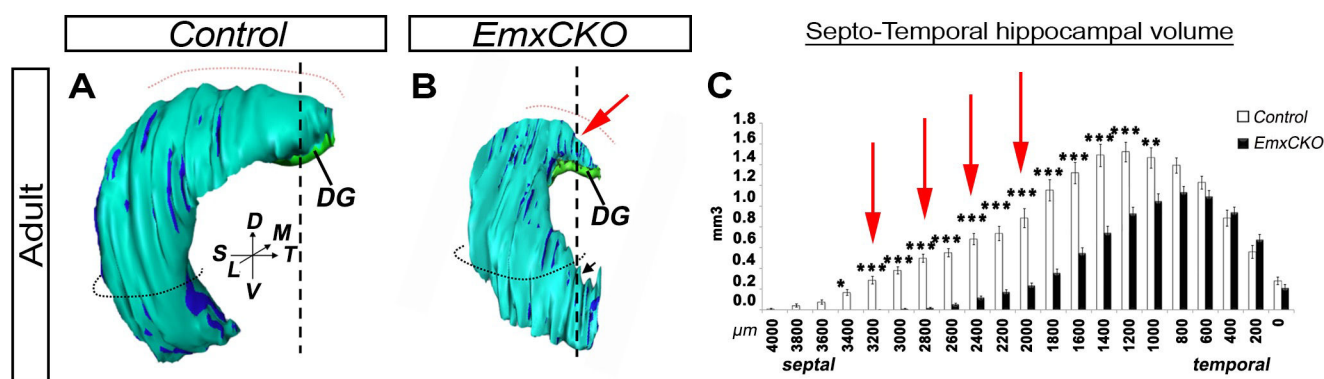


Figure 14. The septal pole of the hippocampus is particularly affected in *EmxCKO*.

A-B. 3D representations of the hippocampal formation in *Control* (A) and *EmxCKO* (B). Red arrow marks the strong volume reduction in the septal pole. **C.** Measures of the hippocampal volume along the septo-temporal axis in *Control* and *EmxCKO*, showing strong significant reductions in the septal sections (red arrows) while no significant differences are found in the temporal sections. *DG*: dentate gyrus; *D/V*: dorsal/ventral; *M/L*: medial/lateral; *S/T*: septal/temporal.

This is also observed in P7 and P14 mutant *EmxCKO* and *NexCKO* brains, in which I confirmed the impairment specific to the rostral/septal hippocampal pole. As shown in **Figure 15**, when coronal sections of *control* and *mutants* are matched according to their rostro-caudal axis, *NexCKO* and *EmxCKO* hippocampi become visible in more caudal regions than in *controls* (with a stronger impairment in *EmxCKO* mutant). In addition, the extent of the hippocampus varies between genotypes. For example, while the *control* septal hippocampus is found on 6 sections, the *NexCKO* one appears on 5 sections and the *EmxCKO* only on 4 sections at P7 (**Figure 15**). At P14, while the *control* septal hippocampus spans on 9 sections, it is only found in 7 and 5 sections of the *NexCKO* and *EmxCKO* mutants, respectively (**Figure 15**). Thus, this suggests that not only the hippocampal volume but also its longitudinal extension is specifically altered in the septal portion during post-natal development, and is consistent with the results obtained in adults (**Figure 14C**).

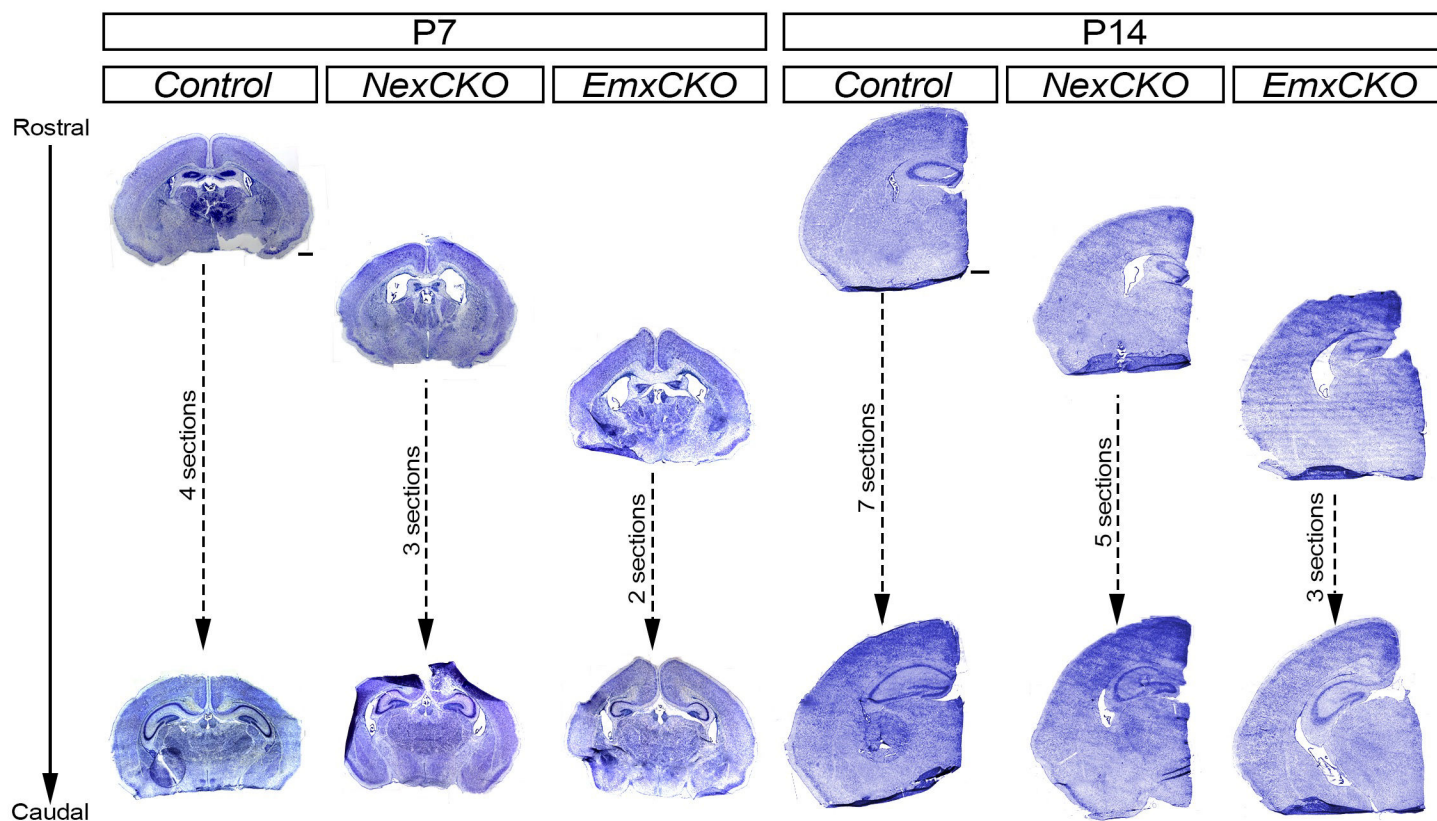
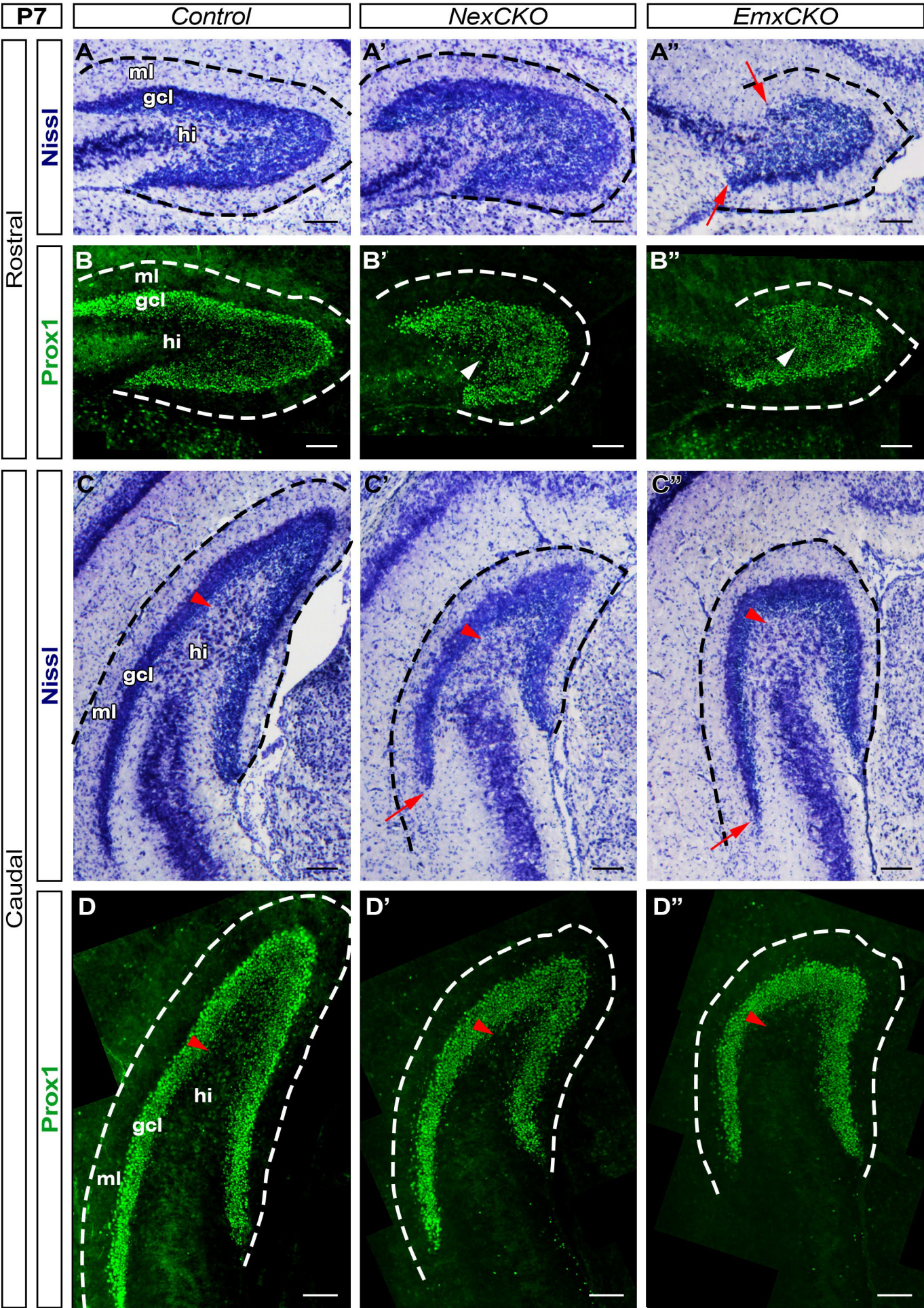


Figure 15. The number of coronal sections in the septal hippocampus is reduced in both *NexCKO* and *EmxCKO* during post-natal development.

Representation of the number of sections where the septal hippocampus is visible for each conditions, at P7 and P14 (in this situation, each section is 16 μ m thick and two consecutive sections are separated by 144 μ m). These data allows us to adjust our countings per section to the total amount of cells in septal DG. Scale bars = 500 μ m (same for all images of the same age).



< **Figure 16. *COUP-TFI* inactivation induces a disorganization of the rostral/septal DG lamination but not its temporal portion, in both *NexCKO* and *EmxCKO*.**

DG lamination is shown by Nissl staining (A-A'' and C-C'') and Prox1 immunofluorescence (B-B'' and D-D'') in rostral/septal pole (A-B'') and caudal/temporal pole (C-D'') at P7. The pial surface of the DG is delineated by a white or black dashed line in each panel. In the rostral/septal DG, *EmxCKO* exhibit an alteration of its blade lengths (red arrows in A'') and granule cells are abnormally located in the hilus of *NexCKO* and *EmxCKO* (white arrowheads in B' and B''). The temporal DG portion of *NexCKO* and *EmxCKO* exhibit a clear delimitation between granule cell layer and hilus (red arrowheads in C-D'') and a properly extended upper blade (red arrows in C' and C''). *CA3*: *cornus Ammonis field 3*; *gcl*: *granule cell layer*; *hi*: *hilus*; *ml*: *molecular layer*. Scale bars = 100 μ m.

To confirm that COUP-TFI loss differentially impacts the DG septal and temporal portions, I have compared the morphology and lamination of the dentate gyrus on adjacent P7 sections, which were either Nissl-stained or immunolabelled with Prox1, known to specifically label DG granule cells (Oliver *et al.*, 1993; Lavado *et al.*, 2010) (**Figure 16**). Using P7 coronal sections, the rostral sections correspond to the septal pole of the hippocampus, whereas the caudal sections correspond to the temporal pole. The DG morphology and lamination of P7 rostral portions have been reported in the very precedent section (*cf. Results-I-2*), as part of a time-course study. Thanks to Prox1 staining by IF, I was able to confirm here that cells populating the putative hilus in *NexCKO* and *EmxCKO* are indeed granule cells, since they express Prox1 (**Figure 16B,B''**). In addition, the lamination and blade length defects are less affected in both *NexCKO* and *EmxCKO* temporal hippocampi (**Figure 16C-D''**): granule cells (Prox1⁺) are well organized in a dense granule cell layer, the hilus is well distinguishable (**red arrowheads in Figure 16C-D''**), and the upper blade is longer than the lower blade (**red arrows in Figure 16C'-C''**), as it is in the *control* DG. Thus, as it is the case for the entire hippocampus, the dentate gyrus is more affected in its septal than in its temporal portion. However, it has to be noted, that differently from the whole hippocampal volume, the DG on its own is still smaller in *NexCKO* and *EmxCKO* (more severe) caudal portions compared to *control* ones.

Taken together, these results suggest that, despite the fact that COUP-TFI is highly expressed in the temporal pole, its loss affect less this region than the septal pole, leading to hypothesize that there might be a compensatory system in this portion.

In order to enlighten the role of COUP-TFI in the developing DG, and to avoid any putative compensatory system, I have chosen to focus my analysis on the septal pole of the DG, which shows the most severe abnormalities.

3) COUP-TFI is not involved in specifying the septal and temporal identities of the hippocampus

As described above, the septal hippocampus is strongly reduced and shifted posteriorly in the absence of COUP-TFI in progenitor cells (*EmxCKO* mutant). Thus, the reduced septal hippocampal portion in mutant mice might have resulted in a change of neuronal identity within the hippocampus. In order to address this issue, I have performed *in situ* hybridization of landmark markers on P7 sagittal sections, which allow me to identify both the dorsal (septal) and the ventral (temporal) hippocampus within the same section (**Figure 17**). Although increasing evidences of distinct functions between these two portions of the hippocampus are found together with differentially expressed genes, no specific markers for either the septal/dorsal or temporal/ventral hippocampus have been explicitly reported so far.

In this study, I have selected three molecular markers differentially expressed between septal/dorsal and temporal/ventral hippocampus: *Cadherin 8* (*Cad8*), a cell adhesion molecule playing crucial roles during morphogenesis of the CNS (Zhou *et al.*, 2001), the transcription factor *LMO4* (Sun *et al.*, 2005), and *COUP-TFII* (Fuentelba *et al.*, 2010), the homologue of COUP-TFI (**Figure 17**).

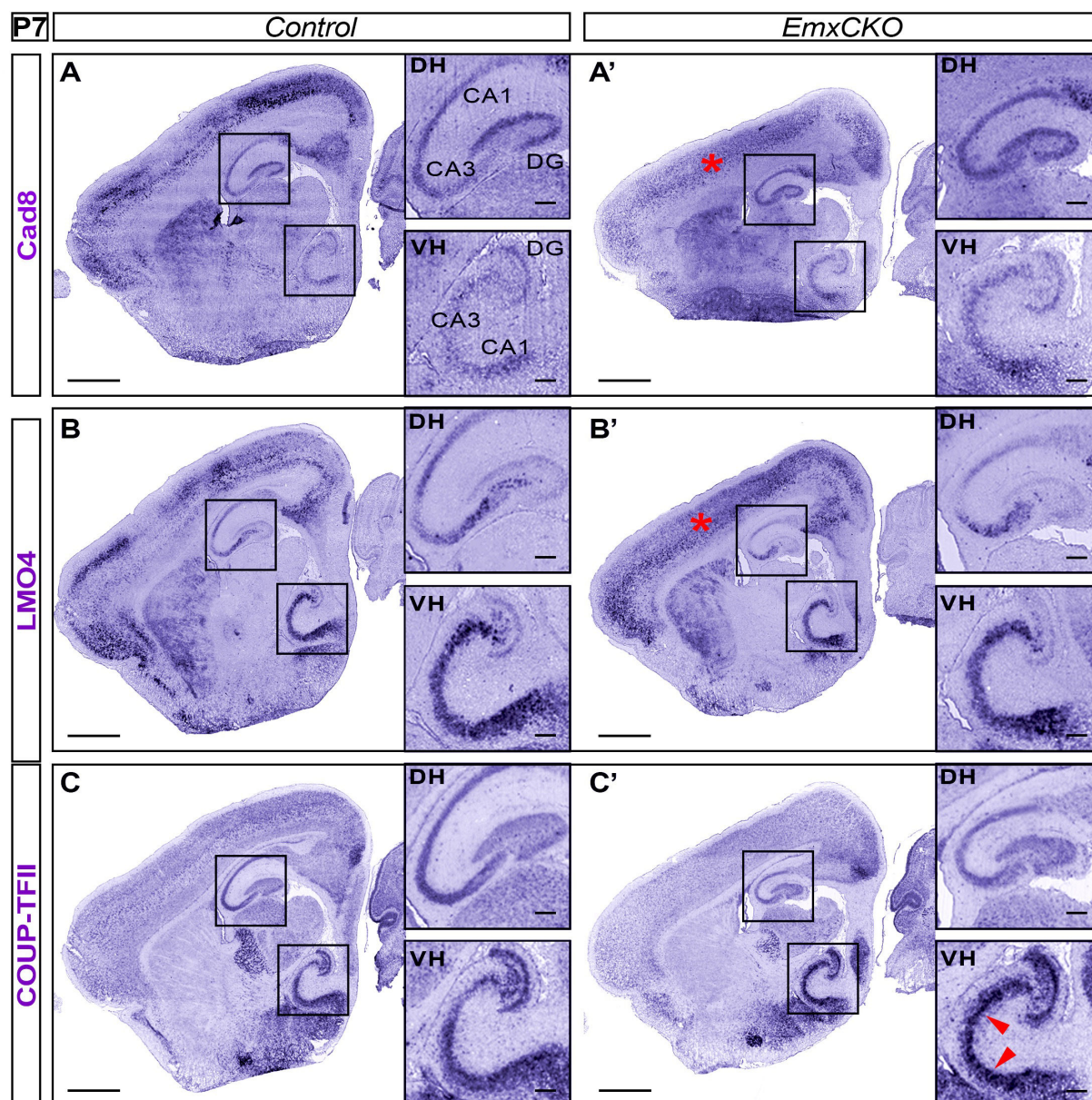


Figure 17. Preserved septo-temporal identity of COUP-TFI-deficient hippocampi.

Sagittal sections of P7 *Control* and *EmxCKO* brains hybridized with differentially expressed genes along the septo-temporal (dorso-ventral) hippocampal axis. Boxes indicate high magnification views of the dorsal (DH) and ventral (VH) hippocampus depicted to the right. **A-A'**. Cadherin8 (*Cdh8*) transcript is expressed at higher levels in the dorsal than in the ventral hippocampus. Despite the reduced DH volume in the mutant brain, *Cdh8* is still expressed at higher levels in the DH. **B-B'**. The LIM domain transcription factor *Lmo4* is expressed at higher levels in the VH than in the DH in *Control* and *EmxCKO* brains. **C-C'**. The orphan receptor COUP-TFII is highly expressed in the VH. Levels of COUP-TFII transcripts in VH are increased in *EmxCKO* (red arrowheads). Red asterisks in A' and B' indicate altered expression of *Cdh8* and *Lmo4* in the neocortex, which have been previously reported (Armentano *et al.*, 2007; Alfano *et al.*, 2014). *CA1/3*: *cornus Ammonis field 1/3*; *DG*: *dentate gyrus*; *DH*: *dorsal/septal hippocampus*; *VH*: *ventral/temporal hippocampus*. Scale bars = 1mm (low magnifications), 200 μ m (high magnifications).

In the *control* brain, *Cad8* transcript is expressed at a higher level in the dorsal hippocampus than in the ventral part, and is localized in DG granule cells as well as in pyramidal cells of the hippocampus proper (**Figure 17A**). In the absence of COUP-TFI in progenitors (*EmxCKO* mutants), *Cad8* mRNA is still observed in the same sub-regions of the dorsal hippocampus, and with a similar intensity in which *Cad8* is expressed at lower levels in the ventral hippocampus (**Figure 17A'**).

On the contrary, *LMO4 mRNA* appears at higher levels in the ventral hippocampus than in the dorsal one (**Figure 17B**). The dorsal signal is localized mainly in the pyramidal cell layer of the CA1 and CA3 fields, and seems weak or absent in the CA2 and DG. The strong ventral signal however is detected in all Hp fields. As for *Cad8*, the *LMO4 mRNA* pattern in *controls* is similar to the one in the *EmxCKO* hippocampus, showing higher expression in the ventral than dorsal hippocampus (**Figure 17B'**).

Finally, *COUP-TFII* transcript is expressed in all pyramidal and granule cell layers and at higher levels in the ventral than dorsal hippocampus (**Figure 17C**). In the *EmxCKO* brain, this low dorsal to high ventral gradient is also detected. Notably, COUP-TFII signal is not only maintained in the mutant hippocampus, but also increased in the ventral portion (**red arrowheads in Figure 17C'**), suggesting that COUP-TFII might compensate for some of the COUP-TFI functions in the ventral/temporal pole of the mutant, since both COUP-TFs share similar targets (Qiu *et al.*, 1994a).

Taken together, these results demonstrate that the septal and temporal identities are not affected in the absence of COUP-TFI function, suggesting that the dorsal volume reduction in the absence of COUP-TFI is caused by selective impairments of the septal domain, and not by an identity change between septal and temporal hippocampal portions.

III / COUP-TFI does not act on hem-derived signaling factors

The cortical hem controls hippocampal and dentate development at early stages of corticogenesis. It is mainly responsible for the developmental onset of the hippocampus, since it acts as a patterning center (Zhao *et al.*, 1999). To start deciphering the mechanisms leading to the growth impairment observed in *EmxCKO* mutants, I first assessed whether COUP-TFI was acting on this hem-derived patterning.

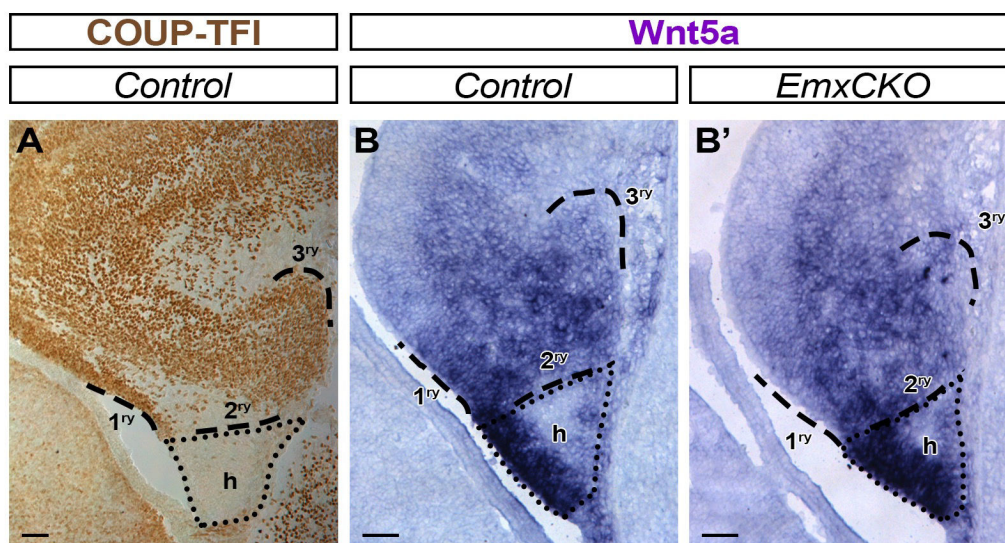


Figure 18. COUP-TFI does not alter hem-derived factors.

A. Immunohistochemistry indicates that COUP-TFI is not expressed in the cortical hem at E16.5. **B-B'.** COUP-TFI loss does not alter the hem-derived factor Wnt5a transcript levels or localization as seen by *in situ* hybridization. The cortical hem is delineated by a dotted line in all panels. *1ry/2ry/3ry*: primary/secondary/tertiary matrix; *h*: hem. Scale bars = 100 μ m

Immunohistochemistry using the COUP-TFI antibody shows that this factor is absent from the cortical hem region at E16.5, while it is highly expressed in the hippocampal plate and forming DG (**Figure 18A**). The Wnt member Wnt5a is expressed at high levels in the cortical hem and at lower levels in the forming Hp and DG (**Figure 18B**). No changes were observed in *Wnt5a* transcript levels of *EmxCKO* E16.5 embryos (**Figure 18B'**).

Together these data indicate that COUP-TFI does not affect the hem-derived signals during hippocampal formation.

IV / COUP-TFI is required in granule cell differentiation during DG development

In order to investigate whether and how COUP-TFI acts on granule cell differentiation, I have characterized the two *COUP-TFI* deficient mouse mutants for several key processes involved in DG development: the proliferation capacity throughout DG formation, the embryonic and post-natal phase of granule cell differentiation and the glia/neuron cell fate decision. To this goal, I have performed immunofluorescences for several members of the transcription factor cascade involved in all these processes and compared the two mouse mutants to littermate *controls* from E16.5 to P14. The comparison of the two *CKOs* will allow me to dissect the role of COUP-TFI in proliferating and/or differentiating cells during DG development.

1) COUP-TFI deficient mice have decreased proliferation in the developing dentate gyrus

First, to investigate whether the proliferative capacity of granule cell progenitors is altered in the absence of COUP-TFI, I have labelled cycling cells with the proliferation marker Ki67 during pre- and post-natal developing DG (**Figure 19**).

Comparison of the *NexCKO* and *EmxCKO* developing DGs shows a thinner Ki67⁺ ventricular zone (vz) in the 1st matrix of E16.5 *EmxCKO* mutants (**asterisk In Figure 19A**) compared to the one in *controls*. This is supported by the quantification of the cell cycle marker Ki67⁺ cells which are significantly decreased in the 1st matrix (**Figure 19a**; p=0,018), and less affected in the 2nd and 3rd matrix, although the number of Ki67⁺ cells tend to diminish in the 2nd matrix, showing a p value close to significance (**Figure 19a**; p=0,055). As a consequence, the number of progenitors (Ki67⁺) reaching the 3rd matrix at P0 is significantly decreased in this mutant (p=0,014) leading ultimately to a reduced pool of proliferative cells in the absence of COUP-TFI. Indeed, at P7, *EmxCKO* mutant hippocampi still have a strong depletion of about half of Ki67⁺ cells in the DG (**Figure 19c**; p<0,001).

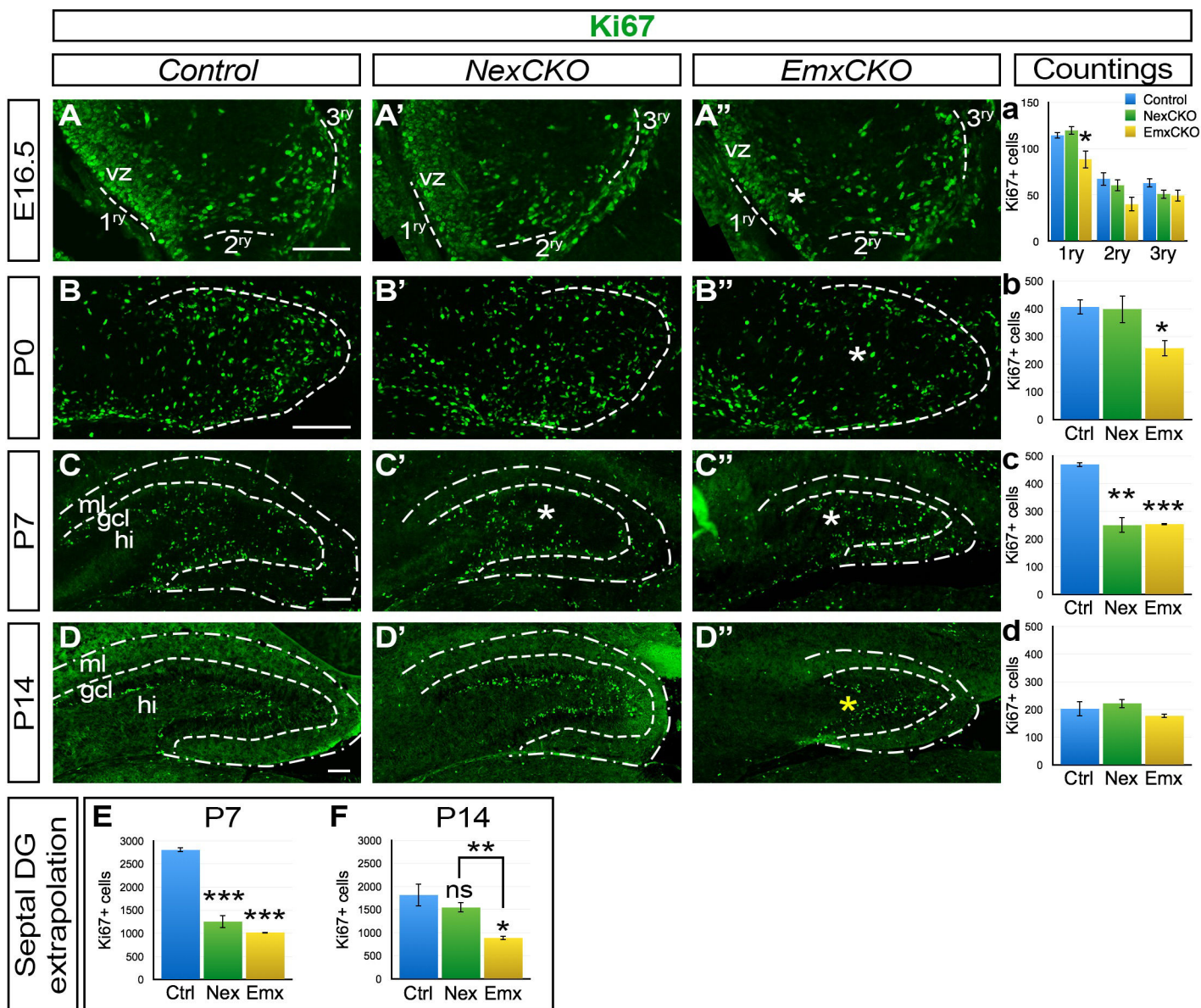


Figure 19. Decreased proliferation in COUP-TFI deficient DG.

A-D''. Immunofluorescences for the cell cycle marker Ki67 on *Control*, *NexCKO* and *EmxCKO* DG at E16.5 (A-A''), P0 (B-B''), P7 (C-C'') and P14 (D-D''). **a-d.** Number of Ki67+ cells per sections at each corresponding age. **E-F.** Extrapolation of the number of Ki67+ cells per section to the total septal DG, at P7 (E) and P14 (F). Asterisks in the IF pictures marks significant reduced number of proliferating cells, among which yellow asterisks indicate the significativity after extrapolation to the entire septal DG only. *1ry/2ry/3ry*: primary/secondary/tertiary matrix; *Ctrl*: Control; *Emx*: *EmxCKO* mutant; *gcl*: granule cell layer; *hi*: hilus; *ml*: molecular layer; *Nex*: *NexCKO* mutant; *vz*: ventricular zone. * $p < 0,05$; ** $p < 0,01$; *** $p < 0,001$. Scale bars = 100 μ m.

As expected, *NexCKO* mutants, in which COUP-TFI is ablated in post-mitotic cells only, do not show any significant differences with the *control* at E16.5 and P0 (**Figure 19a,b**). However and surprisingly, *NexCKO* appears to have a statistically significant decrease of Ki67+ cells in the dentate gyrus at P7 (**asterisks in Figure 19C'-C''** and **Figure 19c**; $p=0,0019$). This could be explained by an improper or delayed migration of progenitors cells in this mutant, leading to a defective accumulation in the dentate gyrus. In support of this hypothesis, P14 *NexCKO* DG show no significant differences in the number of Ki67+ cells with *Control* and *EmxCKO* brains (**Figure 19d**). Surprisingly, while the defective proliferation of *EmxCKOs* observed at E16.5 show cumulative consequences in P0 and P7 DG, and despite its smaller volume, no differences in the number of Ki67+ cells were found at P14 (**Figure 19d**).

It should be noted however that although the number of Ki67+ cells in *controls* and *mutants* are similar at P14, these countings reflect the density of labelled-cells within a section of septal DG (mean of 3 rostral coronal sections). Since the number of sections that compose the septal pole of the hippocampus is not the same in all conditions, as previously shown, (*cf. Results-II-2, Figure 15*), it becomes necessary to extrapolate the density of Ki67+ cells per section to the estimated total amount of rostral DG sections in all conditions (**Figure 19E-F**). In this way, the Ki67+ cell decrease is still confirmed at P7 in both mutants (**Figure 19E**; $p<0,001$ for P7 *NexCKO*; $p<0,001$ for P7 *EmxCKO*), and P14 *EmxCKO* septal DG parts have a significant decrease of proliferative Ki67+ cells when compared to *controls* (**Figure 19F**; $p=0,021$) and to *NexCKO* ($p=0,0057$).

Taken together, these results indicate that absence of COUP-TFI in mitotic cells affects their proliferative capacity in the developing DG.

2) COUP-TFI *EmxCKO* brains have a diminished number of intermediate progenitors (IPCs) during embryonic phases of granule cell differentiation

To investigate whether COUP-TFI acts on the transcription factor cascade involved in granule cell differentiation, I have labelled different members of this cascade, such as Pax6, Tbr2, ND1, Prox1, Tbr1 and NeuN, by IF at E16.5, a time at which no visible morphological defects are observed in the two COUP-TFI-deficient mutants.

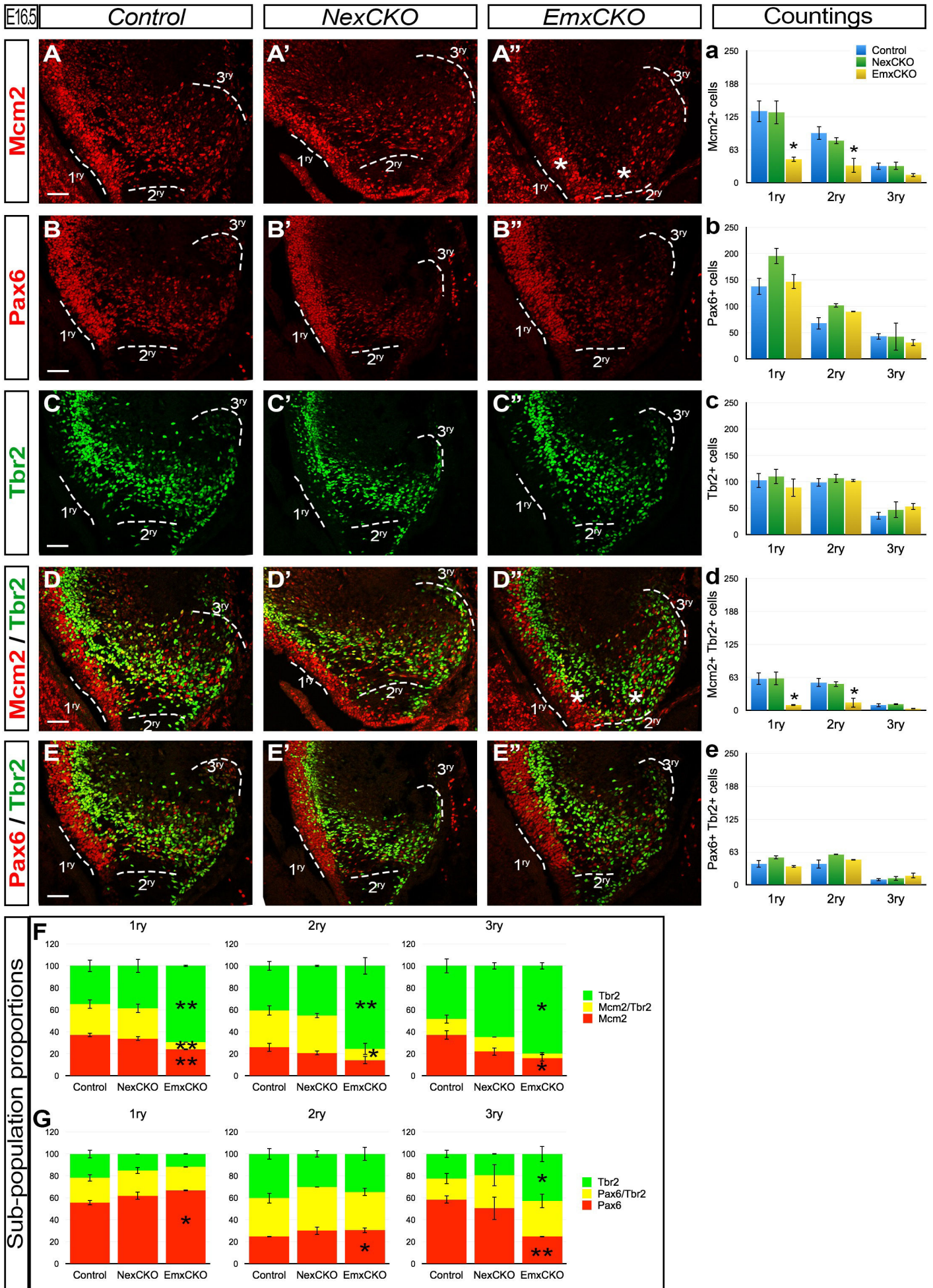
- Progenitors and IPCs

First, and in line with previous data reported above, the *NexCKO* mitotic cell populations are unaffected: no changes are observed in the number of Mcm2⁺ (a cell replication marker (Yan *et al.*, 1993)), Pax6⁺, Tbr2⁺ or double Mcm2/Tbr2⁺ and Pax6/Tbr2⁺ cells (**Figure 20**). In *EmxCKO* embryos, however, I obtained a significant reduction of the number of dividing cells in the 1^{ry} (p=0,019) and 2^{ry} (p=0,023) matrix (**Figure 20A-A''**, **a**), consistent with what was obtained with the cell proliferation marker Ki67 (*cf. previous section*), and confirming reduced cell proliferation in this mutant. In addition, although the number of single and double Pax6⁺ and Tbr2⁺ cell populations, which are considered apical progenitors and IPC (**Figure 5**), respectively, are found unchanged in the *EmxCKO* mutant at this age, the amount of dividing IPCs (double Mcm2/Tbr2⁺) is significantly reduced in the 1^{ry} (p=0,022) and 2^{ry} (p=0,026) matrix of the mutant embryos when compared to their littermates (**Figure 20D-D''**, **d**). This suggests that COUP-TFI alters the ratio between proliferating and neurogenic (no more proliferating) Tbr2⁺ cells in the DG primordium. To confirm this, I have analyzed the distribution of the different populations of single expressing Mcm2⁺, Tbr2⁺ and co-expressing double Mcm2/Tbr2⁺ cells in the two mutants and in the 3 matrices by normalizing the total amount of cells expressing either one or both of these markers to 100% and comparing their relative proportions in the different genotypes (**Figure 20F**). Thus, while the proportions remain constant between *NexCKO* and *Control*, in the 1^{ry} matrix of *EmxCKO* embryos the Mcm2⁺ single-expressing population (Mcm2⁺Tbr2⁻), representing the progenitors Tbr2 negative (not IPC) decreases from 37% to 24% (p=0,0021) whereas the double Mcm2/Tbr2⁺, representing the Tbr2⁺ proliferating population, decreases from 28% to 7% (p=0,0097) relative to the total population. As a consequence, Tbr2⁺ single-expressing cells increase

approximately from 35% to 70% ($p=0,0044$). This is also maintained in the 2^{ry} and 3^{ry} matrix of *EmxCKO* brains, with an increased $Mcm2^{-}Tbr2^{+}$ population ($p=0,0043$) at the expense of $Mcm2/Tbr2^{+}$ population ($p=0,02$). Finally, with a lower significance, *EmxCKO* 3^{ry} matrix also depict an expanded $Mcm2^{-}Tbr2^{+}$ population ($p=0,016$) at the expense of single $Mcm2^{+}$ single cell population ($p=0,016$). These results confirm that the amount of dividing IPC is decreased in the absence of COUP-TFI in progenitors at the expense of $Tbr2^{+}$ non-dividing cells. Thus, the majority of $Tbr2^{+}$ cells are not proliferating cells but are most probably IPC going through a differentiation process.

In the same manner, although the absolute number of $Pax6^{+}$ and $Pax6/Tbr2^{+}$ cells are not changed in the *EmxCKO* developing DG (**Figure 20b,e**), their proportions are altered (**Figure 20G**). Slight increases of the single $Pax6^{+}Tbr2^{-}$ sub-population are detected in the 1^{ry} ($p=0,033$) and 2^{ry} ($p=0,034$) matrices, whereas the 3^{ry} matrix has decreased $Pax6^{+}Tbr2^{-}$ ($p=0,0035$) and increased $Pax6^{-}Tbr2^{+}$ sub-populations ($p=0,043$). This implies that more proliferating progenitors expressing $Pax6$ and not $Tbr2$ are located in the 1^{ry} and 2^{ry} matrix of *EmxCKO* embryonic DGs.

Taken together, these results suggest that COUP-TFI might promote the proliferative capacity of IPC in the early developing DG by repressing the transition from apical progenitors ($Pax6^{+}$) to basal intermediate progenitors ($Tbr2^{+}$). Thus, in the absence of COUP-TFI, future granule cells are abnormally pushed toward a differentiating process at the expense of a proliferative state necessary for the expansion of granule cell numbers.



< **Figure 20. Mitotic cell populations during embryonic DG development.**

A-E''. Immunofluorescences on *Control*, *NexCKO* and *EmxCKO* DG at E16.5 for Mcm2 (A-A'), Pax6 (B-B''), Tbr2 (C-C''), co-expressing Mcm2/Tbr2 (D-D'') and Pax6/Tbr2 (E-E'). **a-e**. Number of cells expressing the corresponding marker per sections. Significant changes are reported on the corresponding IF picture (white asterisks). **F-G**. Sub-populations proportions in the 3 matrices from Mcm2/Tbr2 (F) and Pax6/Tbr2 (G) co-labelling. *1ry/2ry/3ry*: *primary/secondary/tertiary matrix*; * $p < 0,05$; ** $p < 0,01$. Scale bars = $50\mu\text{m}$ (same between all genotypes).

- Post-mitotic immature and mature granule cells

To validate my hypothesis that COUP-TFI-deficient progenitors tend to differentiate earlier than normal DG progenitors, I performed co-IF of Tbr2 and the early post-mitotic marker ND1 (**Figure 21A-B''**). By quantifying single and double ND1 and Tbr2/ND1-expressing cells in the 2^{ry} and 3^{ry} matrices, where early neurons are located at this stage, I observed a down-regulation of the number of early post-mitotic cells expressing ND1 in *EmxCKO* 2^{ry} and 3^{ry} matrices (**Figure 21a**), even if not reaching statistical significance. However, double Tbr2/ND1+ co-expressing cells, which correspond to a transitory mitotic to post-mitotic state, are slightly but significantly increased in the *EmxCKO* 3^{ry} matrix (**Figure 21b**). This suggests that more IPC reaching the 3^{ry} matrix already express the post-mitotic marker ND1 when lacking COUP-TFI. Similarly, a higher amount of these IPC also express Prox1 (**Figure 21d**) in the 3^{ry} matrix of *EmxCKO*, which is a marker that appears even after ND1 in granule cell differentiation, despite the fact that less Prox1+ cells seems to reach the 3^{ry} matrix in *EmxCKO* brains (**Figure 21c**).

However, more Prox1+ and double Tbr2/Prox1+ granule cells were found in the 2^{ry} and 3^{ry} matrix, respectively, of both *NexCKO* and *EmxCKO* (**Figure 21c,d**). Similarly, an increased amount of double ND1/Prox1+ cells was detected in the 2^{ry} matrix of both conditional mutants when compared to *controls* (**Figure 21e**), suggesting a combination of a migratory defect (more cells stuck in the 2^{ry} matrix) together with precocious differentiation (more post-mitotic neurons in the 3^{ry} matrix).

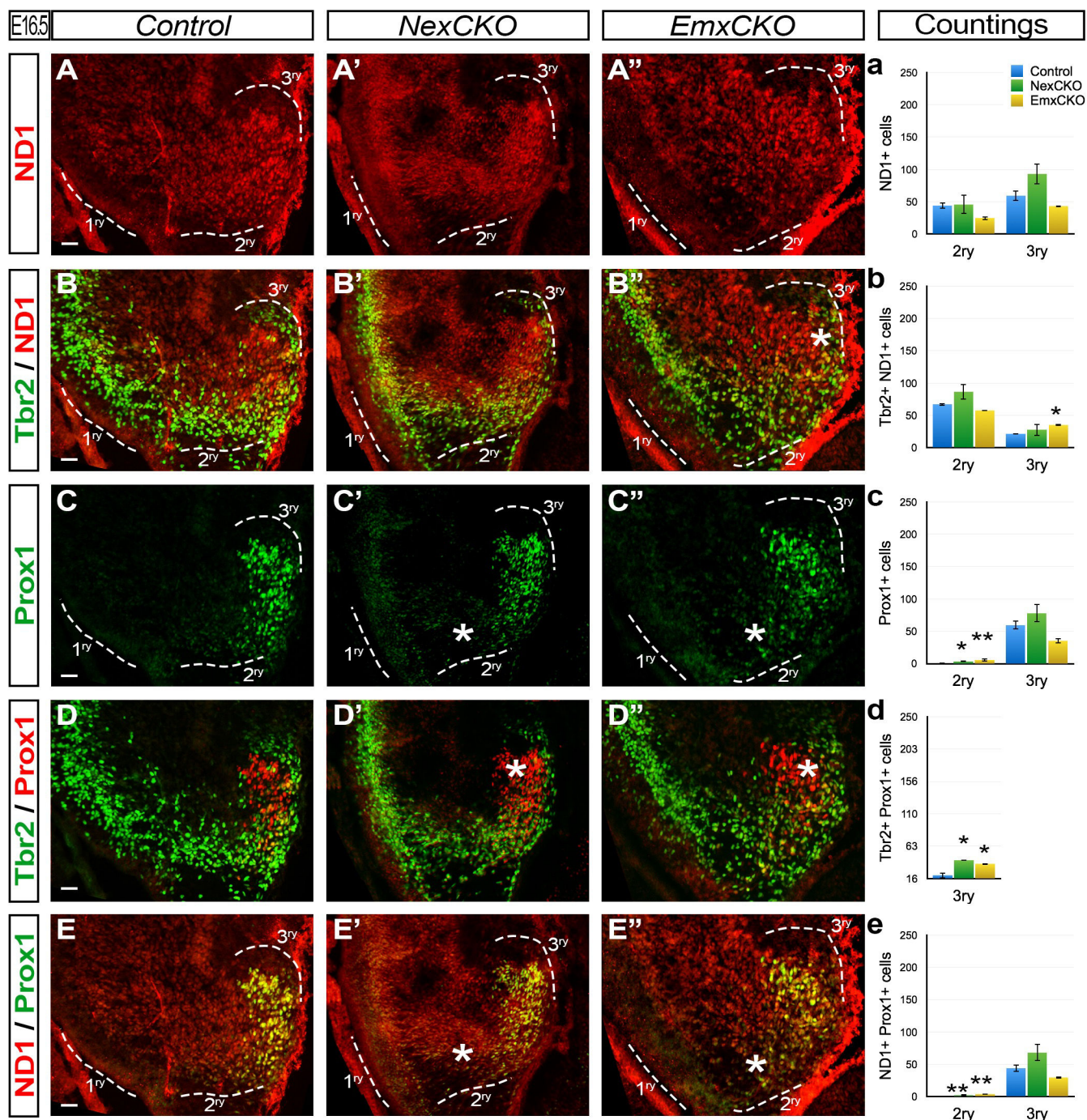


Figure 21. Late mitotic and early post-mitotic cell populations during embryonic DG development.

A-E''. Immunofluorescences on *Control*, *NexCKO* and *EmxCKO* DG at E16.5 for ND1 (A-A'), Tbr2/ND1 (B-B''), Prox1 (C-C''), Tbr2/Prox1 (D-D'') and ND1/Prox1 (E-E'). **a-e.** Number of cells expressing the corresponding marker per sections. Significant changes are reported on the corresponding IF picture (white asterisks). *1ry/2ry/3ry*: *primary/secondary/tertiary matrix*. * $p < 0,05$; ** $p < 0,01$. Scale bars = $50\mu\text{m}$ (same between all genotypes).

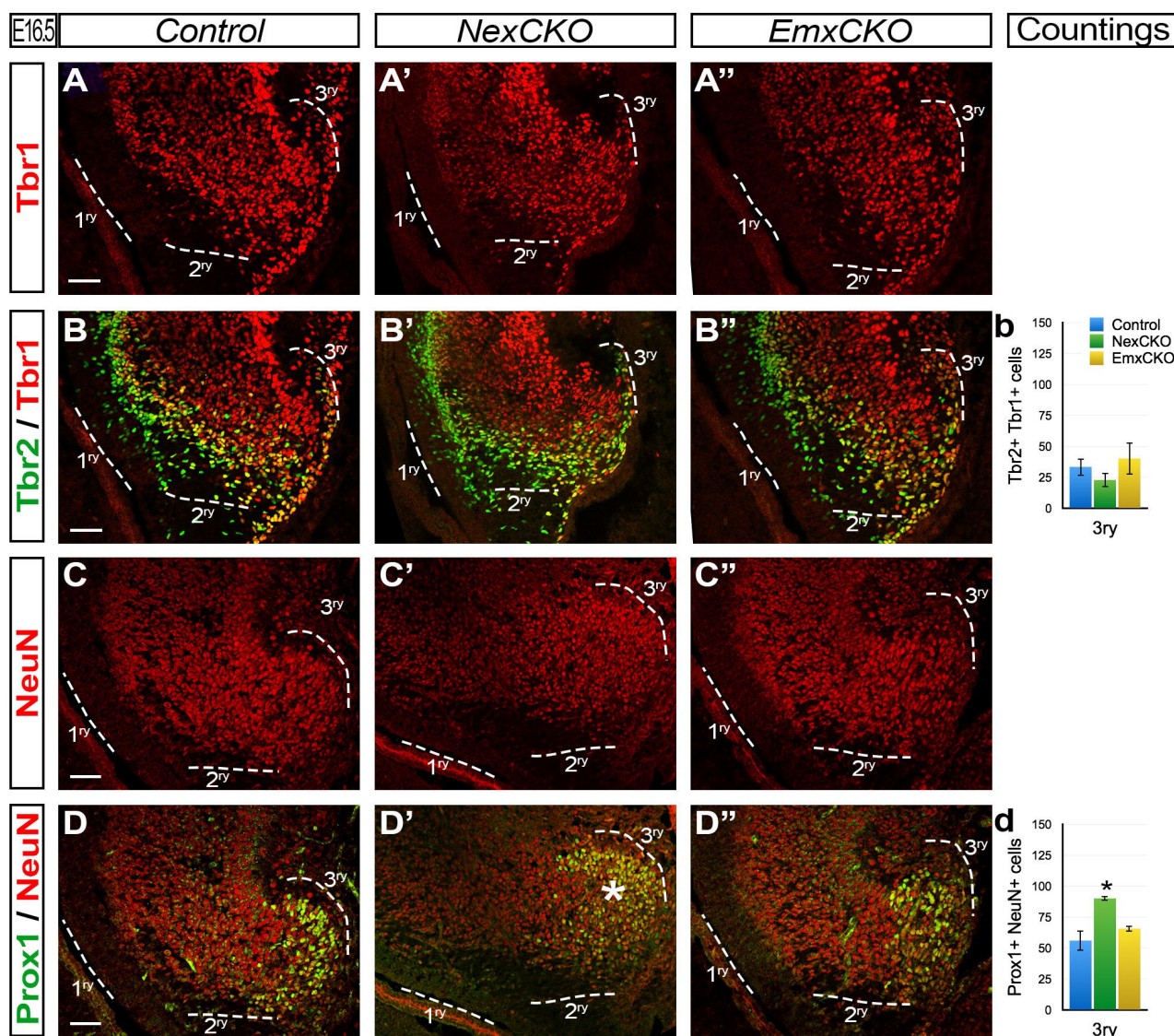


Figure 22. Post-mitotic cell populations during embryonic DG development.

A-D''. Immunofluorescences on *Control*, *NexCKO* and *EmxCKO* DG at E16.5 for Tbr1 (A-A'), Tbr2/Tbr1 (B-B''), NeuN (C-C''), and Prox1/NeuN (D-D''). **b and e**. Number of cells co-expressing Tbr2/Tbr1 (b) and Prox1/NeuN (d). Significant changes are reported on the corresponding IF picture (white asterisks). 1ry/2ry/3ry: primary/secondary/tertiary matrix; * $p < 0,05$. Scale bars = 50 μ m (same between all genotypes).

Finally, by further evaluating the type of neurons reaching the 3^{ry} matrix in *NexCKO* and *EmxCKO* DGs, cells were labelled with more mature differentiation markers, such as Tbr1 or NeuN (**Figure 22**). No visible changes were observed in their numbers and distributions, as well as in the amount of double Tbr2/Tbr1⁺ colocalizing cells (**Figure 22b**), most probably because of the low amount of post-mitotic granule cells at E16.5. However, the total number of double Prox1/NeuN⁺ cells, labelling late differentiating granule neurons, is significantly

increased in the 3rd matrix of *NexCKO* (**Figure 22D',d**), suggesting that post-mitotic expression of COUP-TFI might be required for the late differentiation process of DG granule cells.

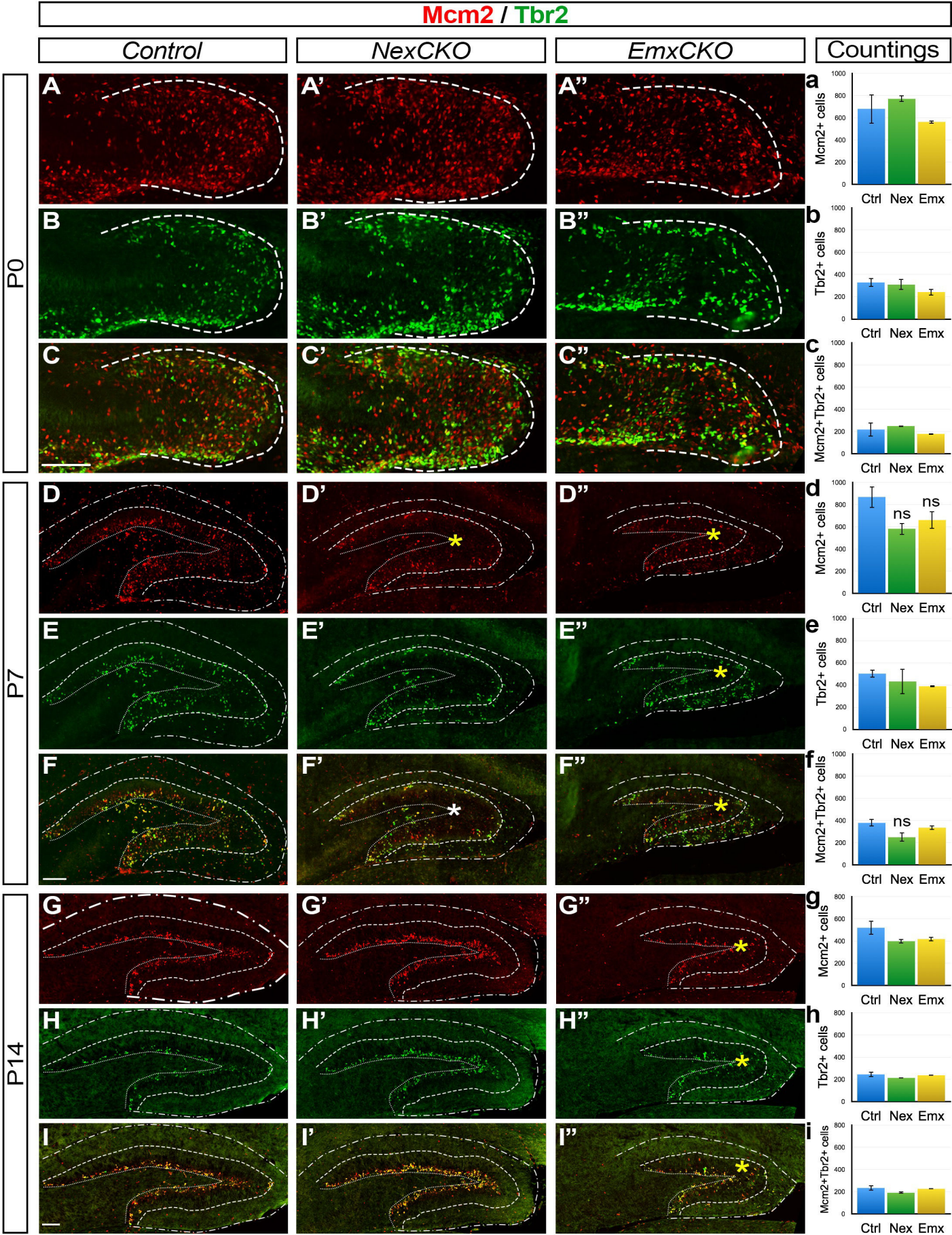
Taken together, my data show that early embryonic granule cell differentiation (at E16.5) is already altered in the *EmxCKO* model before morphological defects become apparent. On one hand, COUP-TFI inactivation in progenitors leads to a premature cell cycle exit and decreased IPC proliferation, suggesting that COUP-TFI might maintain a proper balance between progenitor self-renewal and differentiation. On the other hand, COUP-TFI inactivation in post-mitotic cells results in mild differentiation and migration impairments at E16.5. To further understand and discern the role of mitotic versus post-mitotic COUP-TFI function during DG granule cell differentiation, it becomes necessary to look at post-natal stages, when a higher amount of differentiated neurons are generated. This will be the aim of the next section.

3) Post-natal mitotic differentiation of granule cells and SGZ establishment are altered in the absence of COUP-TFI

To further investigate the reasons of the altered morphological defects observed in post-natal *NexCKO* and *EmxCKO* mutant DGs, I used the same battery of proliferating and differentiating markers used above, and evaluated their distribution in P0 to P14 mutants by comparing them to littermate *controls*. During this period, the majority of granule precursors and IPCs have reached the 3rd matrix where they undergo a further step of cell division before being positioned within the DG upper and lower blades.

- Progenitors and IPCs

First, I used single and double *Mcm2/Tbr2* IF to identify the mitotic and IPC population of the proliferating niche in the DG anlage (**Figure 23**). By counting single and double+ cells in all genotypes from P0 to P14, I found no obvious alteration in the absolute number of single *Mcm2+*, *Tbr2+* or double *Mcm2/Tbr2+* cells in both mutants (**Figure 23A-I**). However, as mentioned earlier, these countings correspond only to the number and density of labelled-cells per section and not to the whole DG. Since the volume of the forming rostral/septal DGs is different between *Controls*, *NexCKOs* and *EmxCKOs*, I extrapolated the cell number of single sections to the total number of septal DG sections in each conditions (**Figure 25**). The data showed that the proliferating *Mcm2+* cell population is reduced by half in *EmxCKO* at P7 (**Figure 25A**; $p=0,021$) and at P14 (**Figure 25F**; $p=0,016$). Similarly, the *Tbr2+* IPCs and dividing *Mcm2/Tbr2+* IPCs are significantly depleted in *EmxCKO* at both P7 and P14 (**Figure 25B-C and G-H**; *Tbr2+*: $p=0,021$ at P7 and $p=0,017$ at P14; *Mcm2/Tbr2+*: $p=0,017$ at P7 and $p=0,020$ at P14), indicating that the whole septal DG has reduced proliferative capacities in the absence of COUP-TFI. Surprisingly, both *Mcm2+* and co-expressing *Mcm2/Tbr2+* cells are also found reduced in *NexCKO* at P7 (**Figure 25A,C**; $p=0,032$ for *Mcm2+*; $p=0,015$ for *Mcm2/Tbr2+*), but this phenotype is not significant anymore at P14, consistent with the hypothesis that *NexCKO* mice have a delayed DG development which is rescued around P14.



< **Figure 23. Mitotic cell populations during post-natal DG development: Mcm2/Tbr2.**

A-I''. Immunofluorescences on *Control*, *NexCKO* and *EmxCKO* DG at P0 (A-C''), P7 (D-F'') and P14 (G-I'') for Mcm2 (in red), Tbr2 (in green), and co-expressing Mcm2/Tbr2. **a-i.** Number of cells expressing the corresponding marker per DG. Significant changes are reported on the corresponding IF picture with white asterisks and significant changes after extrapolation to the total septal DG (see **Figure 25**) are reported with yellow asterisks. Dashed and dotted lines delineate the DG (A-C'') and its 3 layers (D-I''). *Ctrl: Control; Emx: EmxCKO mutant; Nex: NexCKO mutant; ns: not significative.* Scale bars = 100 μ m (same between all genotypes).

Differently from Tbr2+ IPC cells, the density of single Pax6+ cells is reduced in P0, P7 and P14 *EmxCKO* DG sections (**Figure 24a,c,e**) and their total number is even more affected in the whole septal DG of *EmxCKO* at P7 (**Figure 25D**; p=0,0038) and P14 (**Figure 25I**; p<0,001). In addition, the total number of double Pax6/Tbr2+ cells is also affected in P7 (**Figure 25E**; p=0,013) and P14 *EmxCKO* brains (**Figure 25J**; p=0,013). This supports the reduced proliferation rate of COUP-TFI-deficient DG cells and is consistent with the gradual DG shrinkage observed with age (**Figure 12**).

Surprisingly, *NexCKO* P14 DGs also have decreased Pax6+ DG cell density (**Figure 25e**) and total cell number (**Figure 25I**; p=0,0023), whereas the double Pax6/Tbr2+ transitory population is not affected in these mice. This suggests that the reduced Pax6+ cell population in *NexCKO* mice is most probably a secondary effect due to the delay of migrating cells in reaching the 3rd matrix than to an intrinsic proliferative effect, differently from the *EmxCKO* mutants, which instead have a clear impairment in their proliferative capacity.

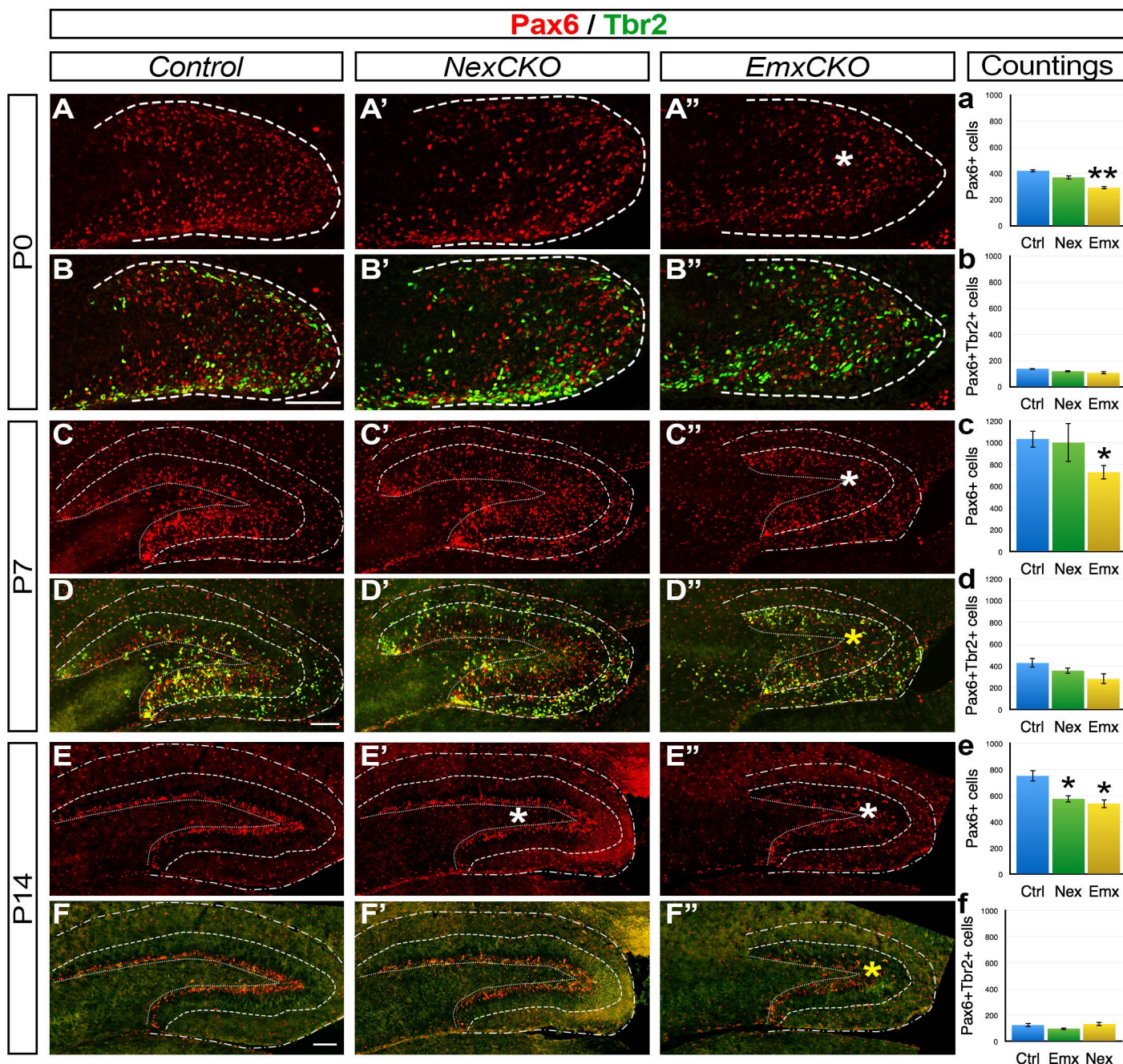


Figure 24. Mitotic cell populations during post-natal DG development: Pax6/Tbr2.

A-F''. Immunofluorescences on *Control*, *NexCKO* and *EmxCKO* DG at P0 (**A-B''**), P7 (**C-D''**) and P14 (**E-F''**) for Pax6 (in red), and co-expressing *Mcm2/Tbr2*. **a-f**. Number of cells expressing the corresponding marker per DG. Significant changes are reported on the corresponding IF picture with white asterisks and significant changes after extrapolation to the total septal DG (see **Figure 25**) are reported with yellow asterisks. Dashed and dotted lines delineate the 3 layers of the DG. *Ctrl*: Control; *Emx*: *EmxCKO* mutant; *Nex*: *NexCKO* mutant. * $p < 0,05$. Scale bars = 100 μ m.

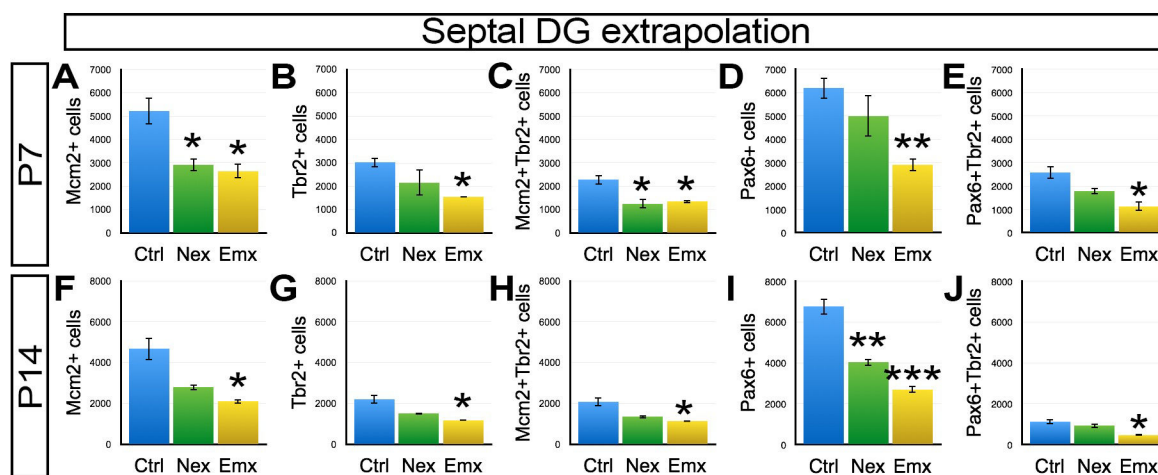


Figure 25. Reduced mitotic cell populations in COUP-TFI-deficient DG at post-natal stages.

All counting of cells per sections were extrapolated to the estimated number of sections with septal DG at P7 (A-E) and P14 (F-J). This thus represent the absolute number of cells expressing the marker of interest in the septal DG of *Control* (Ctrl), *NexCKO* mutant (Nex) and *EmxCKO* mutant (Emx). For the corresponding IF, refer to **Figure 23** and **Figure 24**. * $p < 0,05$; ** $p < 0,01$; *** $p < 0,001$.

Finally, by evaluating the proportion of the different single and double sub-populations, no drastic changes were observed in P0 to P7 *NexCKO* and *EmxCKO* DGs (**Figure 26**), differently from what was reported at E16.5 (*cf. Results-IV-2*). This clearly indicates that COUP-TFI acts more during the early pre-natal phases of granule cell proliferation and differentiation than during the post-natal phase of cell amplification.

- Post-mitotic immature and mature granule cells

To assess granule cell differentiation during post-natal DG development, I used Prox1, Tbr1 and NeuN IF in *Control*, *NexCKO* and *EmxCKO* P0 and P7 DGs (**Figure 27**, **Figure 28** and **Figure 29**). Since these experiments have been performed only twice, I was unable to precisely quantify all the different cell populations of the three genotypes. I will just give few quantitative results and an overview of what I observe in terms of granule cell distribution.

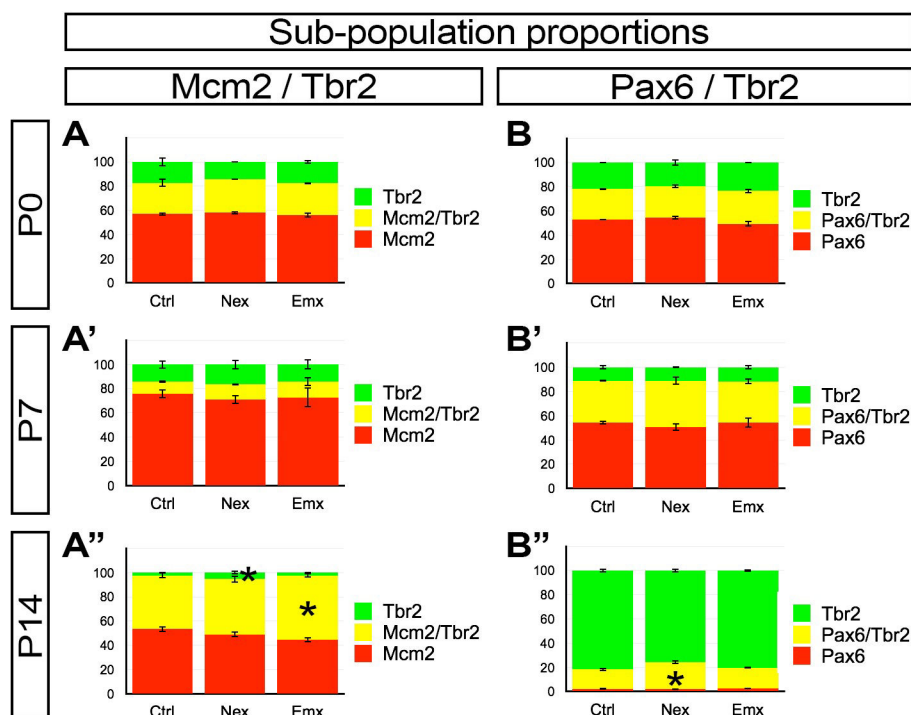


Figure 26. The proportion of mitotic cell sub-populations are not altered in *mutant* DG at post-natal stages.

A-A'. Sub-population distribution of single Mcm2, single Tbr2 and double Mcm2/Tbr2 cells at P0 (A) and P7 (A') in *Control* (Ctrl), *NexCKO* (Nex) and *EmxCKO* (Emx) DG. B-B'. Sub-population distribution of single Pax6, single Tbr2 and double Pax6/Tbr2 cells at P0 (B) and P7 (B') in *Control*, *NexCKO* and *EmxCKO* DG.

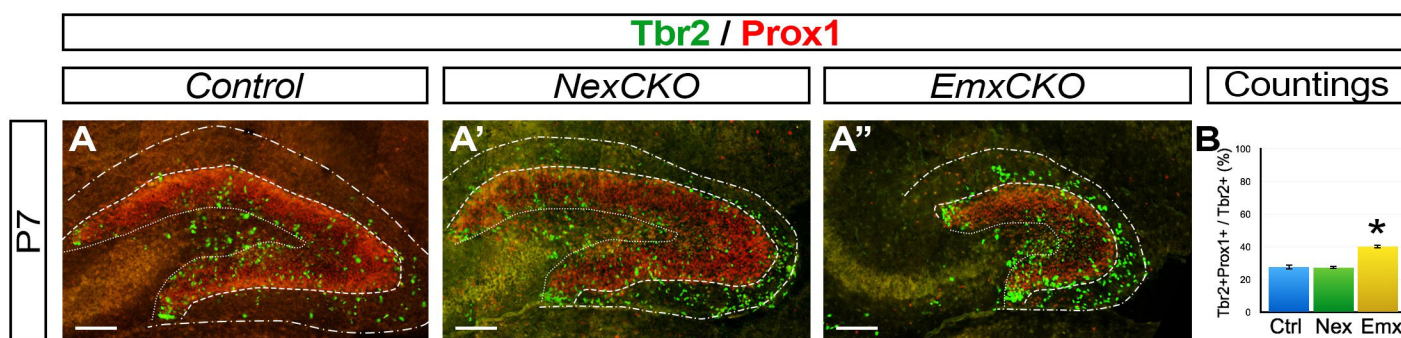


Figure 27. Early post-mitotic cell population Tbr2/Prox1+ in post-natal DG.

A-A". Immunofluorescences on *Control*, *NexCKO* and *EmxCKO* DG at P7 for co-expressing Tbr2/Prox1 cells. B. Percentage of Tbr2/Prox1+ cells among the Prox1+ population. Significant changes are reported on the corresponding IF picture with white asterisks and significant changes after extrapolation to the total septal DG (see **Figure 25**) are reported with yellow asterisks. Dashed and dotted lines delineate the DG (A-B'') and its 3 layers (C-F'') *Ctrl*: *Control*; *Emx*: *EmxCKO* mutant; *Nex*: *NexCKO* mutant. * $p < 0,05$; ** $p < 0,01$. Scale bars = 100 μ m (same between all genotypes).

First, by labelling the transition from IPC to post-mitotic cells with Tbr2 and Prox1 IF at P7 (**Figure 27**), I have shown that the percentage of double Tbr2/Prox1+ expressing cells among Tbr2+ population is increased in *EmxCKO* DG ($p=0,022$; **Figure 27B**), suggesting a precocious expression of early-post-mitotic marker Prox1 by IPC. Notably, this increase is not seen in *NexCKO* mutant.

At P0, a substantial number of Tbr1+ expressing cells are found in the future DG of both *NexCKO* and *EmxCKO* mutants (**Figure 28A-A''**). As expected with its smaller size, *EmxCKO* DG exhibit a reduced number of Tbr1+ granule cells (**asterisk in Figure 28A'' and Figure 28E**). However, no significative changes in the amount of Tbr2/Tbr1+ cells per section are observed (**Figure 28B-B'' and E'**), and no alterations of the sub-population proportions are detected (**Figure 28E''**). Additionally, when compared to *controls*, the distribution of these cells within the DG is altered in both mutants, even if more affected in the *EmxCKO* one (**Figure 28A''**). While *NexCKO* Tbr1+ cells are distributed quite similarly to the *control*, differentiated granule cells in the *EmxCKO* are spread all over the DG with no clear laminar organization (**asterisk in Figure 28A''**).

At P7, the distribution of Tbr1 cells within the DG of mutant mice resume the morphological defects seen with the Nissl (**Figure 28C-C''**), namely the imbalance between upper and lower blade length, more prominent in the *EmxCKO* in which the upper blade is strongly shortened (**arrows in Figure 28C''**), suggesting here again a migratory defect. At this age, when Tbr1 is expressed in the outer two-third of granule cell layer in both *controls* and *NexCKOs*, *EmxCKO* Tbr1+ cells seems more sparse in the granule cell layers and hilus (**arrowhead in Figure 28C''**). Moreover, *EmxCKO* upper blade appears to have a lower level of expression than the lower blade.

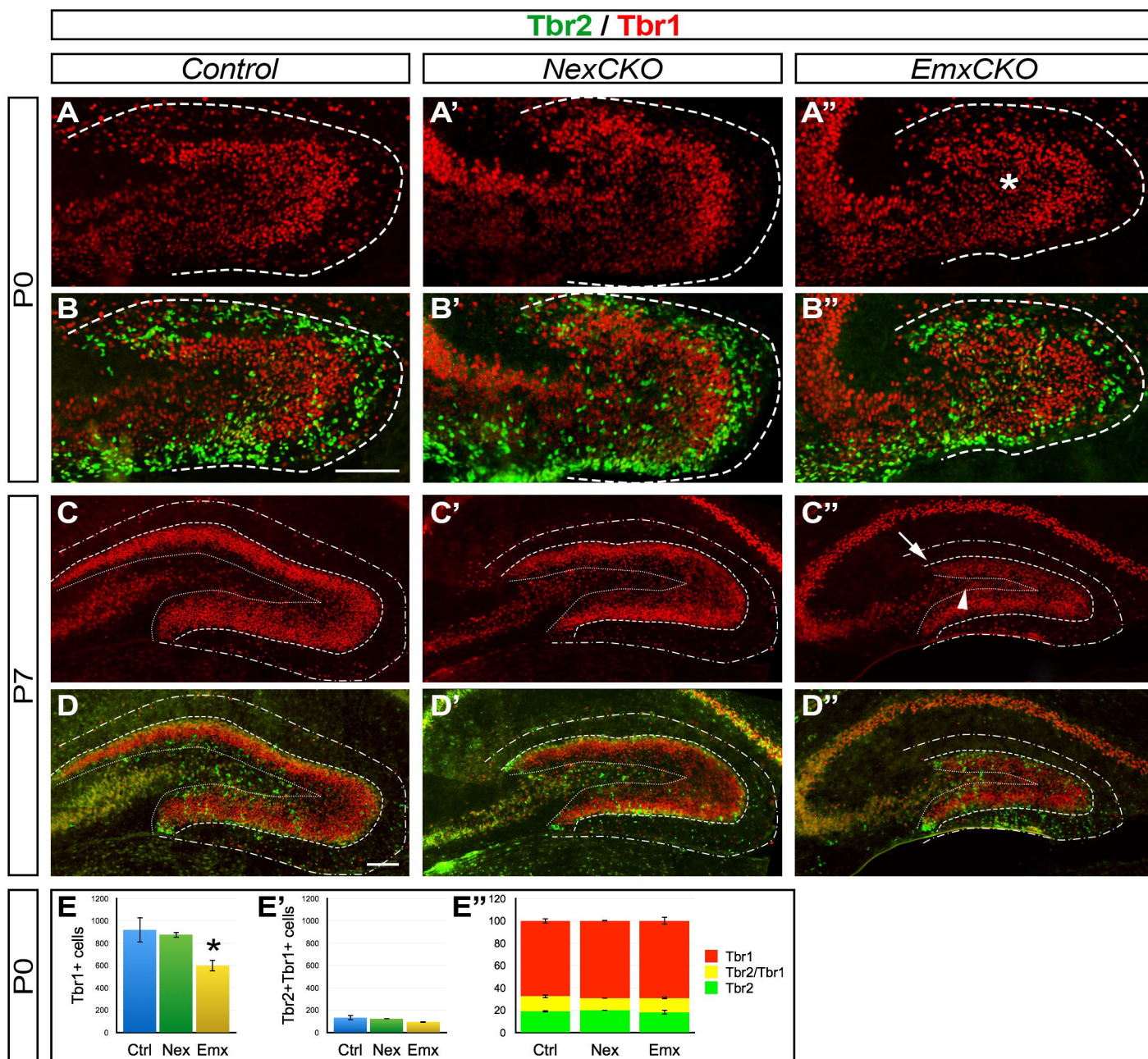
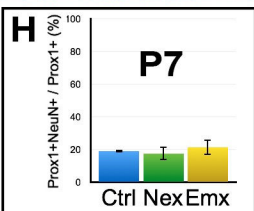
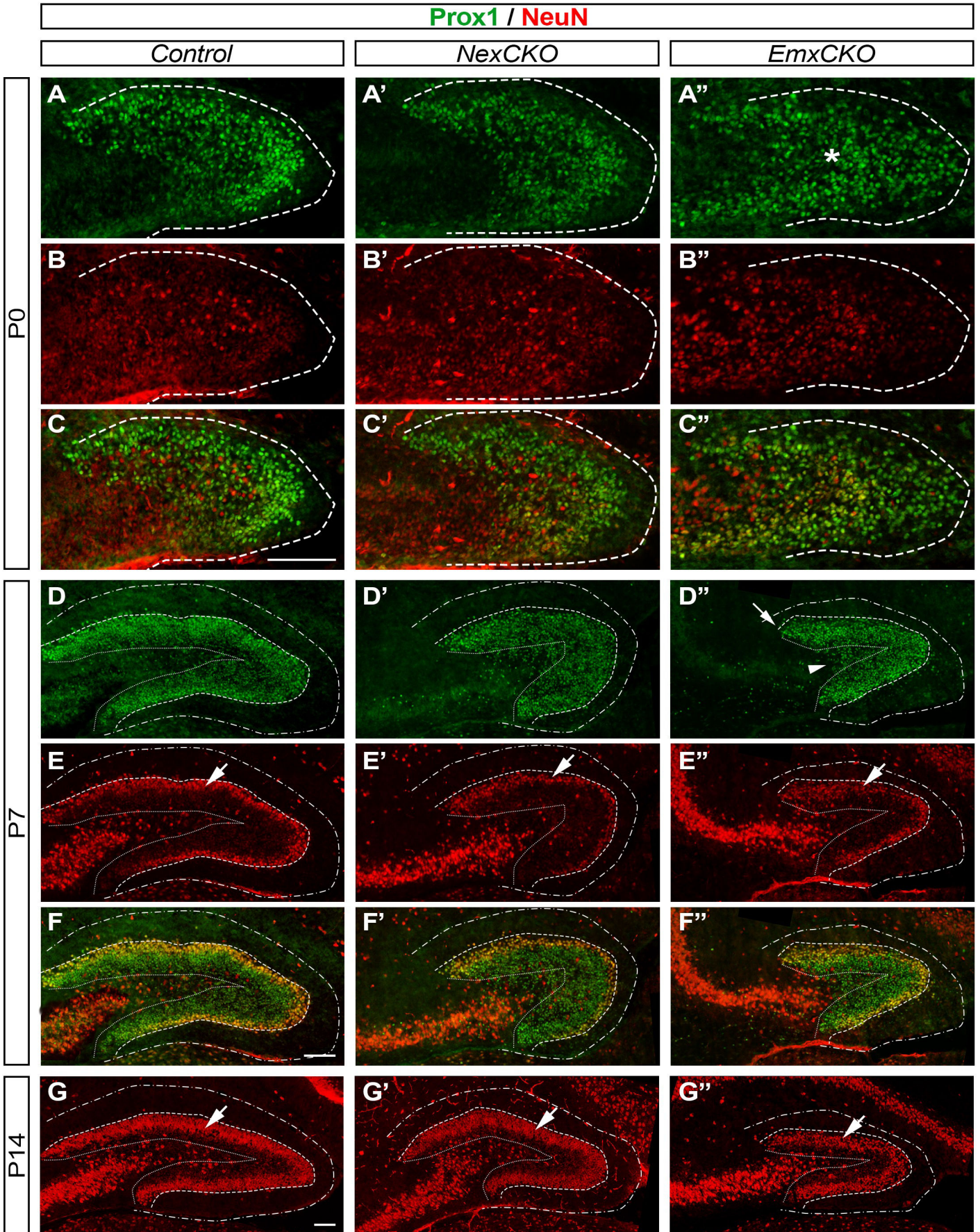


Figure 28. Post-mitotic cell population during post-natal DG development: Tbr2/Tbr1.

A-D''. Immunofluorescences on *Control*, *NexCKO* and *EmxCKO* DG at P0 (A-B'') and P7 (C-D'') for Tbr1 (in red) and the co-expressing Tbr2/Tbr1 cells. White arrow in C'' show the smaller upper blade of *EmxCKO*, and the arrowhead shows its disorganized DG lamination. **E-E''.** Number of Tbr1+ cells per DG (E), of Tbr2/Tbr1+ co-expressing cells per DG (E') and sub-population proportions (E''). Significant changes are reported on the corresponding IF picture with white asterisks. Dashed and dotted lines delineate the DG (A-B'') and its 3 layers (C-D''). *Ctrl*: *Control*; *Emx*: *EmxCKO* mutant; *Nex*: *NexCKO* mutant. * $p < 0,05$. Scale bars = 100µm (same between all genotypes).

Figure 29. Late post-mitotic cell populations during post-natal DG development: Prox1/NeuN.

Prox1 / NeuN

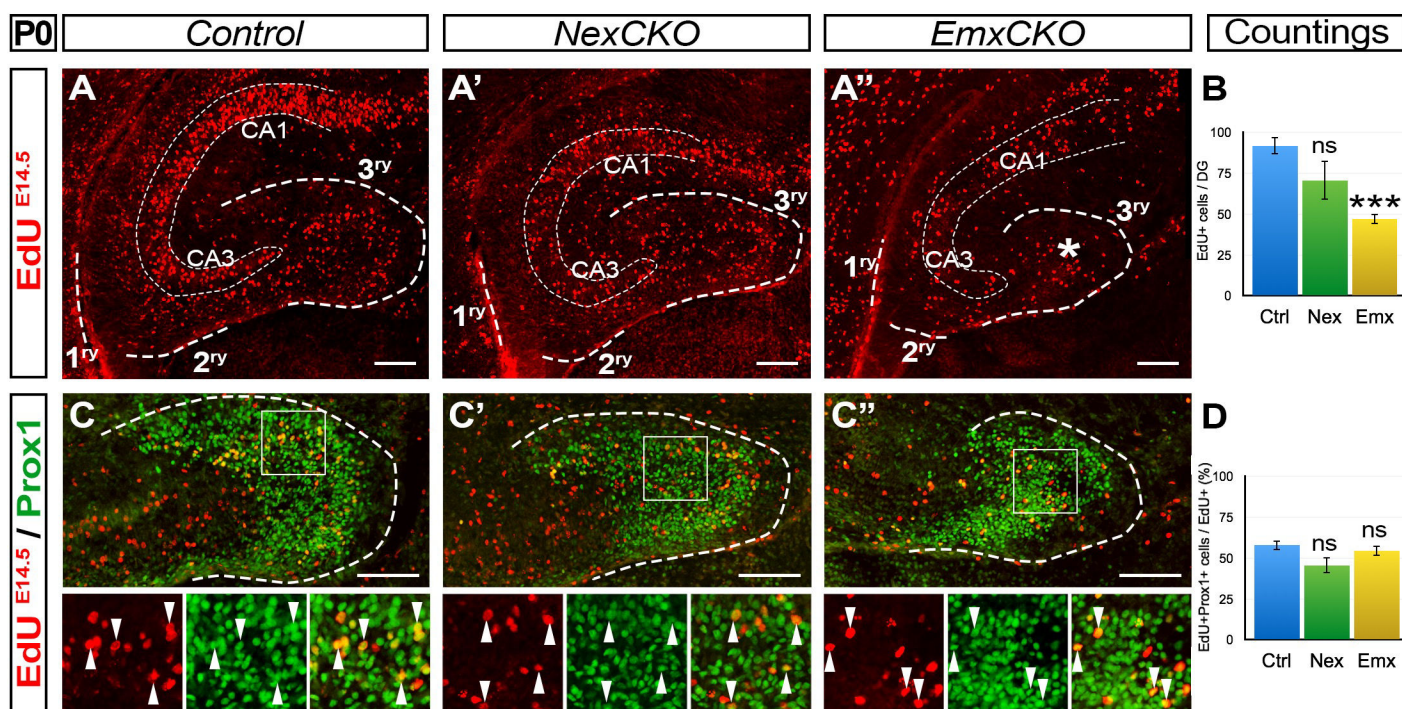


< **A-G**". Immunofluorescences on *Control*, *NexCKO* and *EmxCKO* DG at P0 (A-C"), P7 (D-F") and P14 (G-G") for Tbr1 (in red) and the co-expressing Tbr2/Prox1 cells. White arrow in D" show the smaller upper blade of *EmxCKO*, and the arrowhead shows its disorganized DG lamination. Arrows in E-E" and G-G" indicate the proper position of NeuN+ mature granule cells in all genotypes. **H.** Percentage of Prox1/NeuN+ cells among the Prox1+ population in the three conditions. Dashed and dotted lines delineate the DG (A-C") and its 3 layers (D-G"). *Ctrl*: *Control*; *Emx*: *EmxCKO* mutant; *Nex*: *NexCKO* mutant. Scale bars = 100 μ m (same between all genotypes).

Finally, to visualize immature and mature granule cells simultaneously, I performed IFs with Prox1 and NeuN antibodies on P0 to P14 *Control* and *mutant* DGs (**Figure 29**). At P0 and P7, similarly to Tbr1, Prox1+ expressing cells are found in the future DG of both *NexCKO* and *EmxCKO* mutants (**Figure 29A-A**"), although in a more disorganized way in *EmxCKO* mutants than in *Controls* (**asterisk in Figure 29A**" and **arrowhead in Figure 29D**"). In addition, NeuN, which marks more mature neurons, is correctly expressed in the outer layer of both blades where mature granule cells are normally positioned, in both mutants at P7 (**arrows in Figure 29E-E**"). Moreover, the percentage of double Prox1/NeuN+ expressing cells among the Prox1+ neurons show no significant differences between *controls* and *mutants* (**Figure 29H**), suggesting that the transition from post-mitotic immature to mature granule cells is not affected by COUP-TFI loss. At P14, more mature granule cells have been generated, and thus NeuN marks the outer two-third of the granule cell layer in both *controls* and *mutants* (**arrows in Figure 29G-G**"). Thus, despite their reduced size, immature (Prox1+) and mature (NeuN+) granule cells of P7 and P14 COUP-TFI mutants are properly located within both blades of the DG.

Taken together, these data show that despite the early differentiation and migration defects observed in perinatal *COUP-TFI* mutants, granule cells do differentiate into proper mature granule cells and get positioned at the expected locations. Thus, COUP-TFI seems mainly to act on mitotic granule cell amplification (progenitors and IPCs), and to a less extent on the post-mitotic phase of granule cell differentiation. This would also justify the severely reduced DG of *EmxCKO* mutant mice compared to the mild phenotype observed in the *NexCKO* mice.

4) The reduced DG cell population does differentiate into granule cells in the absence of COUP-TFI



Because COUP-TF genes have been reported to be involved in the cell fate switch between neurons and glia in the cortex by limiting the neurogenic period (*cf. Introduction-II-D-4-b*), I have first labelled the cells generated at E14.5 in the dgn and then quantified their number and challenged their fate in the DG of P0 *controls* and *COUP-TFI* mutant mice.

Pregnant females were injected with EdU at 14.5 dpc (days post coitum) to specifically label dividing cells of E14.5 old embryos. Pups were then sacrificed at birth (P0) and the number and distribution of EdU+ cells generated at E14.5 were counted in *controls* and *mutants* 3^{ry} matrix. A clear reduction of EdU+ cells is found in the *EmxCKO* but not *NexCKO* entire hippocampi (**asterisk in Figure 30A-A''**). The amount of EdU+ cells that reached the DG is indicated in **Figure 30B**: *EmxCKO* have around half less EdU+ cells in their DG, indicating that only 50% of the expected DG neurons were generated at E14.5 in the absence of COUP-TFI in mitotic cells, in line with the reduced proliferation observed at E16.5 (**Figure 19**).

To investigate the fate of these E14.5-generated cells, I performed co-labelling with the granule cell-specific marker Prox1 (**Figure 30C-C''**). Co-expressing EdU/Prox1+ cells were counted, and normalized on the total number of EdU+ cells that have reached the dentate gyrus (**Figure 30D**). The result shows no significant changes in the percentage of double

EdU/Prox1+ cells among the DG EdU+ cell population (**Figure 30D**). The remaining EdU+Prox1- cells are likely to be cells that have chosen a gliogenic fate. This indicates that despite the reduced proliferation rate in the embryonic ventricular zone of *EmxCKO* mice, *NexCKO* and *EmxCKO* cells that have exited the cell cycle after E14.5 (and thus are EdU+ cells) and reached the DG, have differentiated into Prox1+ granule cells in the same proportion that in *control* animals. This suggests that the balance between neurogenic *versus* gliogenic fate is not altered in *NexCKO* and *EmxCKO* mutant DG at early developmental stages.

Figure 30. *EmxCKO* early born DG neurons are less numerous, but differentiate in granule cells in the same proportion as the *Control*.

A-A''. Views of *Control*, *NexCKO* and *EmxCKO* hippocampi at P0, labelled with EdU. EdU fluorescence labels cells born at E14.5, the time of injection to the pregnant mother. The numbers of EdU+ cells in the entire hippocampus is clearly reduced (A''). **B**. Number of EdU+ cells that have reached the DG by P0. *EmxCKO* show a significant reduced number of early-born cells in the DG at birth, compared to *Control* of *NexCKO*. **C-C''**. Immunofluorescence for the granule cell marker Prox1 on *Control*, *NexCKO* and *EmxCKO* DG with E14.5-born cells labelled with EdU. Boxes area are presented in high magnification below and show co-localizing EdU/Prox1+ cells (arrowheads). **D**. Percentage of EdU/Prox1+ cells among all the EdU+ cells of the DG. No significant differences between the three genotypes are reported, which all show around 50% of EdU+ cells that became granule cells Prox1+. *Iry/2ry/3ry*: primary/secondary/tertiary matrix; *CA1/3*: cornus Ammonis field 1/3; *Ctrl*: *Control*; *Emx*: *EmxCKO* mutant; *Nex*: *NexCKO* mutant; *ns*: not significant. *** $p < 0,001$. Scale bars = 100 μ m.

Nevertheless, this result is preliminary and needs further investigation. Especially, cells need to be labelled by EdU injection at later stage, such as at E17.5, which is a time where gliogenesis peaks. Thus, this would allow us to assess whether the neurogenic period is prolonged in *COUP-TFI*-deficient mice, as it is the case when *COUP-TFI* and II are inactivated in cortical cells (Naka *et al.*, 2008).

V / Abnormal granule cell migration in COUP-TFI mutants

We have suggested earlier in this study that COUP-TFI might act on granule cell migration. In order to investigate this, I have analyzed different aspects of granule cell migration, such as the position of the cells along their migratory path, the possible guidance cues involved in this process, and the radial glia scaffold required in granule cell migration.

1) Impaired cell migration leads to the formation of ectopic clusters and altered laminar organization in COUP-TFI-deficient DG

- 2^{ry} matrix migratory stream

To follow granule cell migration, I have first used *Tbr2* as a marker since at P0 it labels migrating IPCs from the 1^{ry} to the 3^{ry} matrix (**Figure 31**). *Tbr2*-expressing cells are generated in the 1^{ry} matrix and migrate along the 2^{ry} matrix in a narrow stream before reaching the outermost region of the future DG in the 3^{ry} matrix (**Figure 31A**). The width of the migratory path does not seem to change in *NexCKOs* (**Figure 31A'**), but is drastically enlarged in *EmxCKO* DGs as seen by the expanded region ventral to the Hp pyramidal cell layer (**bar in Figure 31A''**). In addition, several *Tbr2*⁺ cells appear to migrate towards the hilar region (**arrows in Figure 31A''**) instead of the outer portion of the 3^{ry} matrix (along the pial surface) in P0 *EmxCKO* DGs. At P7, when all IPCs and post-mitotic granule cells have reached the DG anlage, *EmxCKOs* retain several *Tbr2*⁺ cells in the 2^{ry} matrix, suggesting that they have failed to reach the DG (**arrowheads in Figure 31B''**). These cells seem to differentiate *in loco* into *Prox1*- and *Tbr1*-expressing granule cells forming ectopic clusters of granule cells (**arrowheads in Figure 31C'' and D''**). These clusters of post-mitotic cells expressing *Tbr1* and *NeuN* at low levels are also present at P14 in the LB molecular layer of the *EmxCKO* DG (**arrowheads in Figure 31E'' and F''**). The presence of these clusters suggests that a subpopulation of IPCs has failed to migrate to the DG granule cell layer and has differentiated into granule cells in ectopic positions.

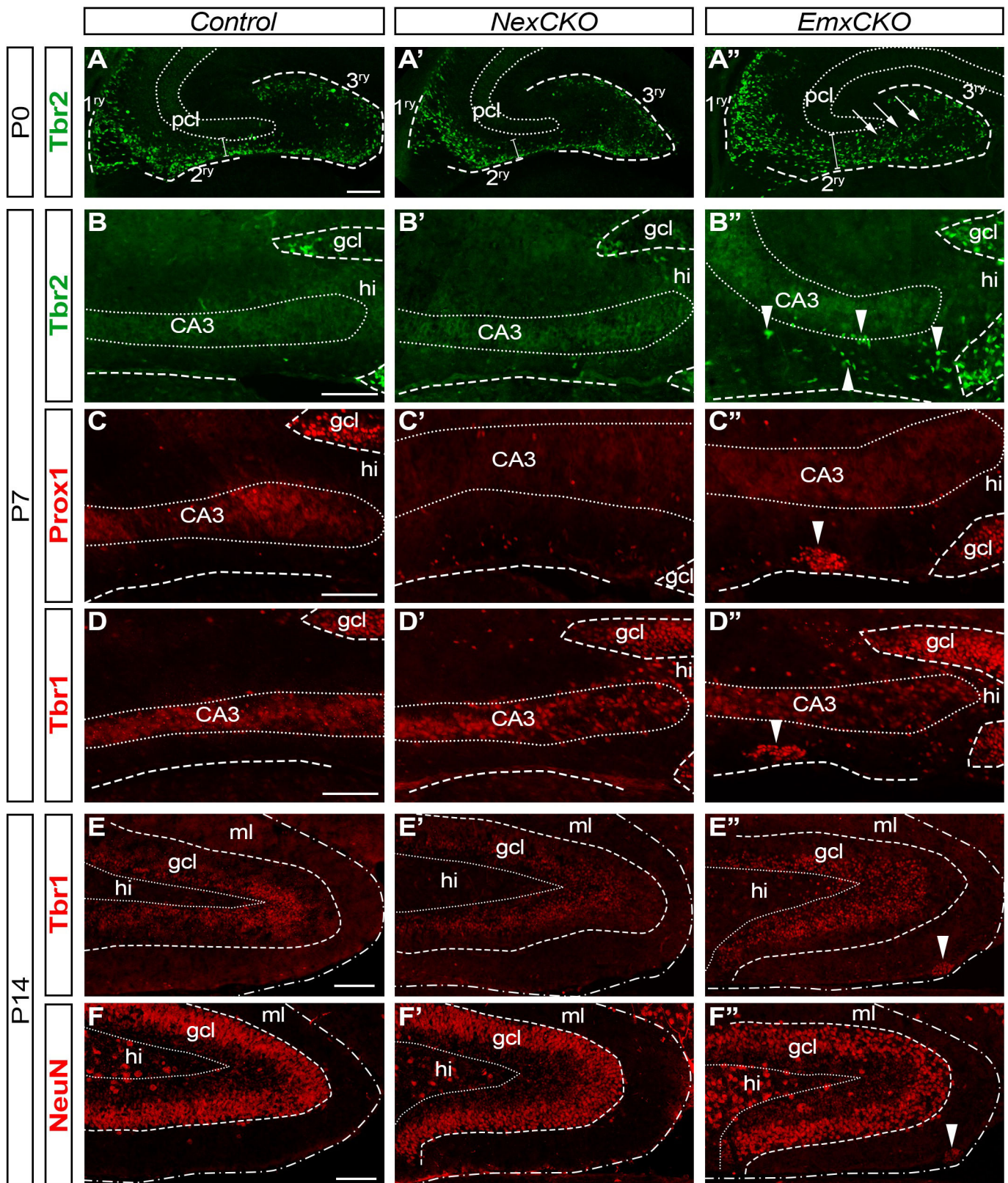


Figure 31. Impaired secondary migratory stream and presence of heterotopic clusters of post-mitotic cells during *EmxCKO* DG post-natal development.

A-B''. Immunofluorescences for Tbr2, labelling IPC in *Control*, *NexCKO* and *EmxCKO* developing DG, at P0 (A-A'') and P7 (B-B''). The migratory stream (2ry matrix) is enlarged (bars in A-A'') and more cells seem to cross the future DG in *EmxCKO* hippocampus (arrows in A''). At P7, many Tbr2+ cells are still migrating in the 2ry matrix of in *EmxCKO* (arrowheads in B'') whereas they have all

< (figure legend continuation) reached the DG in *Control* and *NexCKO*. **C-F''**. Immunofluorescences for post-mitotic markers Prox1, Tbr1 and NeuN in *Control*, *NexCKO* and *EmxCKO* post-natal DG, at P7 (C-D'') and P14 (E-F''). *EmxCKO* mutants have heterotypic clusters of post-mitotic cells (Prox1+, Tbr1+ and NeuN+) located in the 2ry matrix at P7 (C-D'') and in the lower blade molecular layer at P14 (E-E'') (arrowheads in C''-F''). *1ry/2ry/3ry*: primary/secondary/tertiary matrix; *CA3*: cornus Ammonis field 3; *gcl*: granule cell layer; *hi*: hilus; *ml*: molecular layer; *pcl*: pyramidal cell layer. Scale bars = 100µm (same between all genotypes).

- Layer distribution

Next, I evaluated whether the abnormal migratory path described in the *EmxCKO* and depicted by Tbr2+ expression (**Figure 31A-A''**) might affect the final laminar organization of the postnatal DG. To this purpose, I have subdivided the P0 3^{ry} matrix into upper blade (UB) and lower blade (LB), whereas at P7 and P14 the DG was split into UB molecular layer (UBml), UB granule cell layer (UBgcl), hilus, LB granule cell layer (LBgcl) and LB molecular layer (LBml) (*cf. Materials and Methods-IV*; **Figure 9**). Schema representing these subdivisions are depicted in **Figure 32 upper panel**. Are also indicated the figures of the corresponding IFs. All the cell counts were normalized on the total of cells expressing the marker of interest, which allows describing their laminar distribution independently of their number.

Thus, while at P0 the location of proliferating Ki67+ cells is similar in *control* and *mutant* 3^{ry} matrix with approximately 60% of the Ki67+ cells located in the LB (**Figure 32A** and **Figure 19B-B''**), both *NexCKO* and *EmxCKO* mutants have a partially disorganized distribution of cycling cells at P7: compared to control, *NexCKOs* have more Ki67+ cells in the LBgcl ($p=0,031$) and *EmxCKO* have less cells in the hilus ($p=0,022$) (**Figure 32A'**). However, at P14 Ki67+ cells of *NexCKOs* are again distributed similarly to *controls* (**Figure 32A''**), corroborating the hypothesis of a delayed DG organization that is rescued at P14. On the contrary, the laminar defects are maintained in the *EmxCKOs* at P14: significantly more cells are found in the LBml ($p=0,0049$) at the expense of the UBgcl which contains less cells ($p=0,0077$) (**Figure 32A''**; corresponding IF in **Figure 19D''**), in line with the morphological alterations and inverted length of upper and lower blades, as described in part *Results-II-1*.

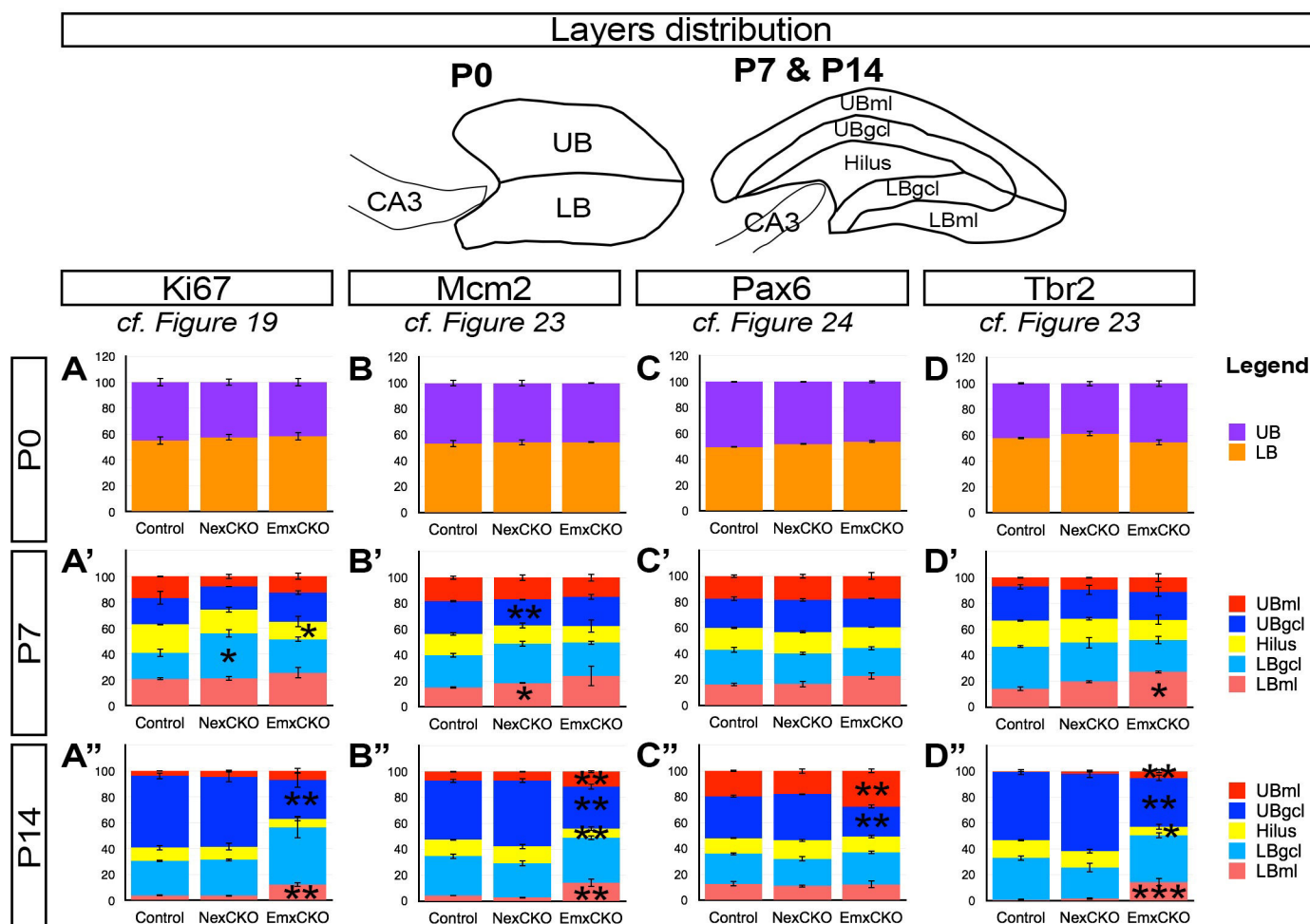


Figure 32. COUP-TFI inactivation leads to impairment in layers distribution of mitotic cells during post-natal development.

Upper panel. Schema representing the different counting area delimitating either upper and lower blades at P0, and the 3 layers at P7 and P14. **Lower panel (A-D'').** Layers distribution of Ki67+ (A-A''), Mcm2+ (B-B''), Pax6+ (C-C'') and Tbr2+ (D-D'') expressing cells in *Control*, *NexCKO* and *EmxCKO* DG. Figures to refer for the corresponding IFs are indicated. At P0 (A-D), no alterations are observed in the two mutants. At P7 (A'-D'), mild impairment in both *NexCKO* and *EmxCKO* are reported. Finally, at P14 (A''-D''), strong alteration of progenitors and IPC distribution in the DG are observed in *EmxCKO*, but not in *NexCKO* mutant. CA3: *corpus Ammonis*; LB: *lower blade*; LBgcl: *lower blade granule cell layer*; LBml: *lower blade molecular layer*; UB: *upper blade*; UBgcl: *upper blade granule cell layer*; UBml: *upper blade molecular layer*. * $p < 0,05$; ** $p < 0,01$; *** $p < 0,001$.

Similar results were obtained with the other cell marker Mcm2 and the IPC transcription factor Tbr2 (Figure 32B-B''; corresponding IFs in Figure 23). At first, no alterations of UB versus LB cell distribution were observed in either the Mcm2+ or Tbr2+ sub-populations at P0 (Figure 32B and corresponding IF in Figure 23A-B''). At P7, *NexCKOs* show a significant greater proportion of Mcm2+ cells in the LBml ($p=0,049$) and a consequent

reduction in the UBgcl ($p=0,0064$). *EmxCKOs* appear to have a similar tendency, as seen also in the IF (**Figure 23D''**) but without statistical significance for Mcm2+ cells, most probably due to a more widespread distribution of labelled cells which increases variability (see bigger error bars in **Figure 32B'**), but not for Tbr2+ cells which result to be more localized in the LBml than the LBgcl at this age ($p=0,021$) (**Figure 32D'** and corresponding IF in **Figure 23E''**). Finally at P14, the two sub-populations Mcm2+ and Tbr2+ are found in a higher proportion in the LBml of *EmxCKO* DGs (Mcm2+: $p=0,0029$; Tbr2+: $p=0,00043$), and in the UBml (Mcm2+: $p=0,0031$; Tbr2+: $p=0,0079$), at the expense of the Hilus (Mcm2+: $p=0,0071$; Tbr2+: $p=0,016$), and the UBgcl (Mcm2+: $p=0,0032$; Tbr2+: $p=0,0047$), compared with the *Control* (**Figure 32B'' and D''**; corresponding IFs in **Figure 23G-H''**). Moreover, as expected, the Mcm2+, and Tbr2+ populations are normally distributed in the *NexCKO* DG layers at P14 (**Figure 32B'' and D''**).

Similar results were obtained when analyzing layer distribution of Pax6+ cells: whereas P0 and P7 show no alterations (**Figure 32C-C'**), P14 *EmxCKO* have significantly more Pax6+ cells located in the UBml ($p=0,0032$), at the expense of cells located in the UBgcl ($p=0,0017$) (**Figure 32C''** and corresponding IF in **Figure 24E''**).

Taken together, these results demonstrate that COUP-TFI loss in post-mitotic cells (*NexCKO*) induces mild impairments of cycling cells into the different layers of the DG at P7, which is rescued later on at P14. However, since COUP-TFI is not inactivated in cycling cells in this mouse model, the weak and transient defects is most probably due to a non-cell-autonomous secondary consequence of COUP-TFI invalidation or to a delay in cell migration. On the contrary, COUP-TFI inactivation in mitotic cells (*EmxCKO*) induces a strong alteration in the distribution of cycling cells throughout the DG. These cells abnormally accumulate in the 2^{ry} matrix stream and subsequently in the molecular layer (predominantly of the lower blade) and form characteristic clusters or aggregates of post-mitotic cells, which is consistent with the mispositioning of post-mitotic cells that we previously reported (*cf. Results-IV-3*). These data suggest that COUP-TFI might act on the proliferation and migration of granule cell progenitors and IPCs, both during their journey through the 2^{ry} matrix and during their positioning and layer organization in the dentate gyrus.

2) Loss of COUP-TFI leads to altered guidance cues signaling

One of the important factors regulating granule cell migration are the guidance cues, which are secreted in the surrounding and either attract or repel migrating cells. The DG granule cells are known to depend on Reelin and SDF1/CXCR4 pathways to migrate to their proper locations during development (Bagri *et al.*, 2002; Lu *et al.*, 2002; Li *et al.*, 2009; Förster *et al.*, 2006).

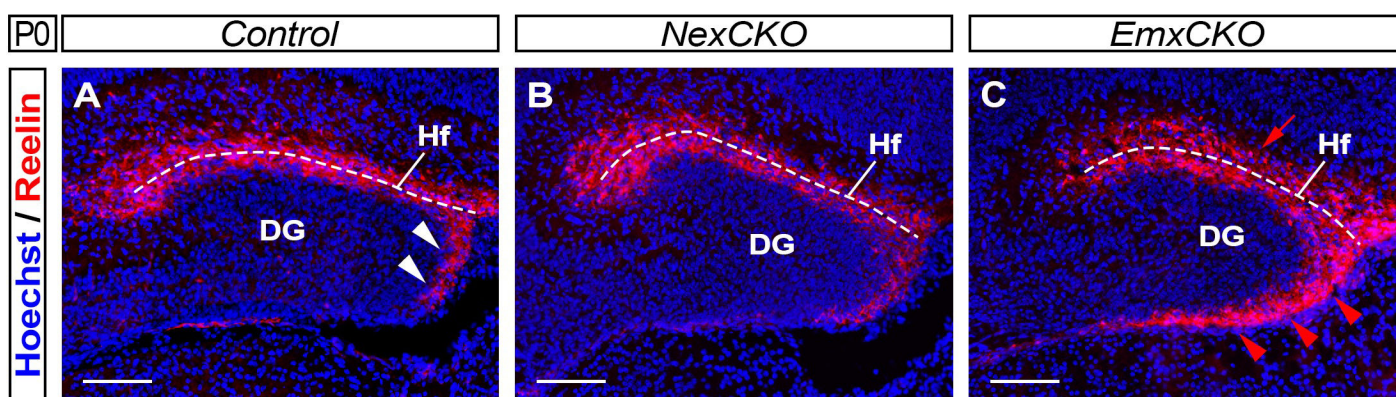


Figure 33. Reelin signal is altered in *EmxCKO* DG at birth.

Immunofluorescence for Reelin (in red) on P0 coronal sections at the level of the septal DG, and counterstained with Hoechst (in blue). In the *Control*, Reelin signal is detected in the hippocampal fissure (Hf) region (A) and at a lower extent in the most medial part of the lower blade molecular layer, close to the pia surface (white arrowheads). No alterations are observed in Reelin signal in *NexCKO* mutant (B), but *EmxCKO* exhibit a reduced signal in the Hf region (red arrow in C) and a strong increase in ectopic Reelin signal in the entire lower blade molecular layer (red arrowheads in C). Dashed lines delineate the hippocampal fissure in all panels. DG: dentate gyrus; Hf: hippocampal fissure. Scale bars = 100µm.

In the hippocampus, Reelin is secreted in the extracellular matrix by Cajal-Retzius cells around the hippocampal fissure (Haas *et al.*, 2002; Pesold *et al.*, 1998). Despite the fact that Cajal-Retzius cells do not express the transcription factor COUP-TFI (Studer *et al.*, 2005), I have observed an impairment in the distribution of Reelin⁺ cells in *EmxCKO* hippocampi (**Figure 33**). At P0, Reelin is normally highly expressed in the hippocampal fissure region (Hf) and to a lower extent in cells positioned in the ml of the lower blade and most probably migrating towards the hippocampal fissure (**arrowheads in Figure 33A**). While no obvious differences are observed in *NexCKOs* (**Figure 33A'**), *EmxCKOs* have a strong upregulation of

Reelin at the pial surface of the DG lower blade (**red arrowheads in Figure 33A''**), while cells expressing Reelin in the hippocampal fissure are more dispersed than in *controls* (**red arrow in Figure 33A''**). This phenotype could be a secondary effect of a defective migration process occurring in the *EmxCKO* DG. Thus, Cajal-Retzius cells, which originate in the cortical hem, would partially fail to invade the hippocampal fissure region and secrete Reelin in ectopic positions. Since granule cells respond to Reelin signaling, mis-positioning of this signal most-probably contributes to the granule cell migration impairment, and would explain the increase of ectopic mitotic and post-mitotic granule cells in the molecular layer of the lower blade that we illustrate above.

The other system known to strongly regulate granule cell migration is the chemokine/receptor couple SDF1/CXCR4 (Bagri *et al.*, 2002; Lu *et al.*, 2002). The ligand SDF1 is expressed by the meninges, whereas the receptor CXCR4 is expressed by migrating granule cells. Surprisingly, while the granule cell migratory defect observed in the COUP-TFI *EmxCKO* would at first instance predict a down-regulation of the receptor *CXCR4* expression, *in situ* hybridization revealed instead a strong up-regulation of transcript levels in the 2^{ry} and 3^{ry} matrix of P0 *EmxCKOs* (**red arrow in Figure 34**). This indicates that COUP-TFI normally modulates *CXCR4* expression levels in migrating granule cells and that either abnormally high levels or ectopic expression of *CXCR4* in low or non-expressing cells might perturb their migratory behavior by abnormally responding to SDF1 expressed by the meninges and Cajal-Retzius cells.

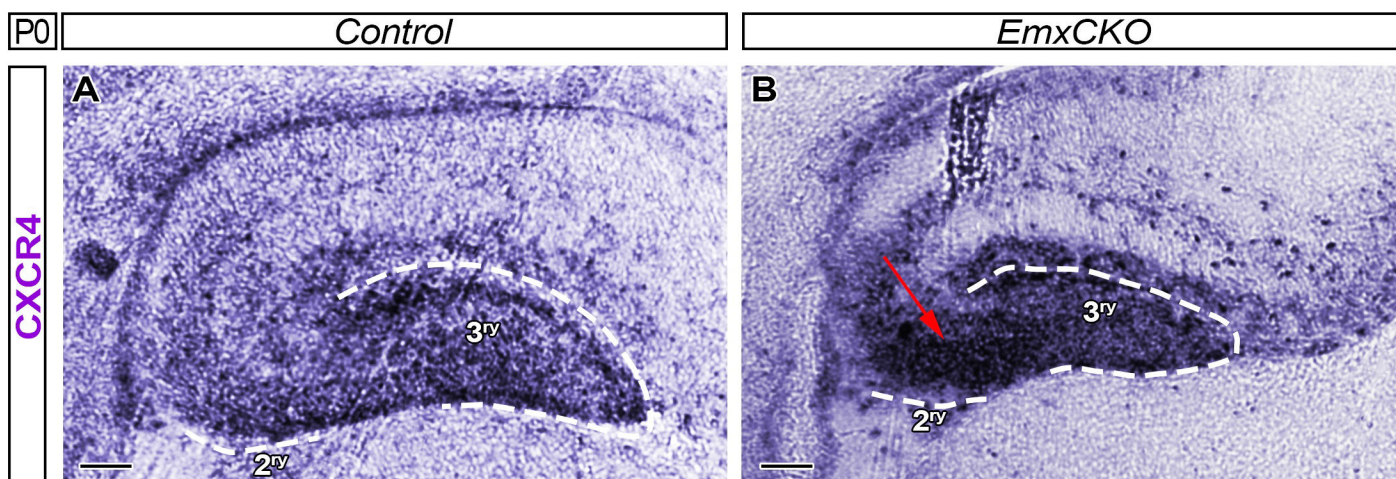
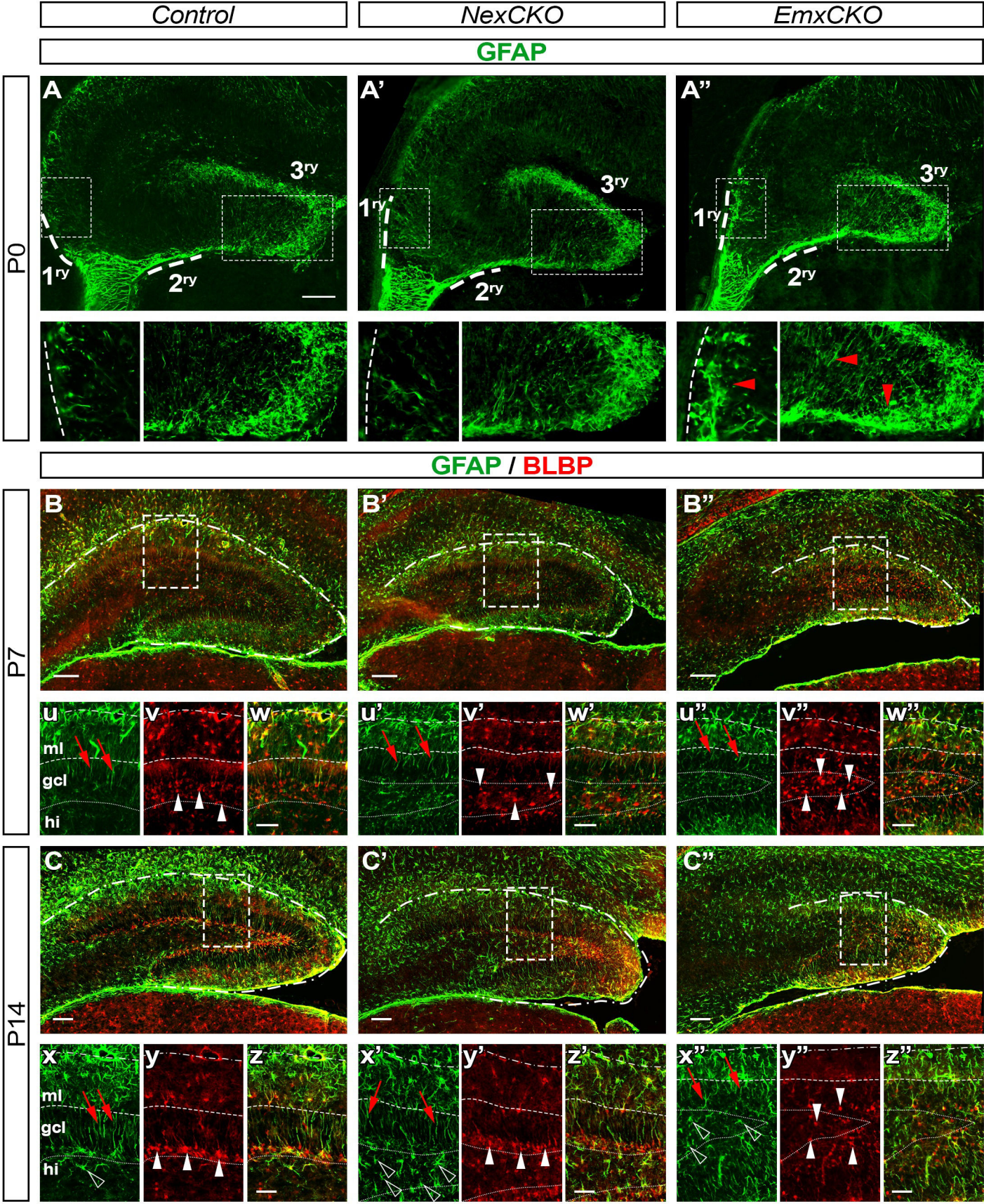


Figure 34. Increased CXCR4 transcript levels in *EmxCKO* 2^{ry} matrix at birth.

In situ hybridization detecting *CXCR4* mRNA levels in the developing DG at P0 in *Control* and *EmxCKO* mutant. *EmxCKO* exhibit a strong increase in *CXCR4* transcript expression in the 2ry matrix (red arrow in B). Dashed lines delineate the 2ry and 3ry matrices in the 2 panels. 2ry/3ry: secondary/tertiary matrix. Scale bars = 100 μ m.

3) Loss of COUP-TFI impacts the formation of radial glia scaffolds

One of the other factors required in DG granule cell migration is the presence of a fairly organized radial glia scaffold (Rickmann *et al.*, 1987; Sievers *et al.*, 1992), which supports cells to reach their targets during migration. To investigate whether this scaffold is impaired in both COUP-TFI-deficient models, I have labelled post-natal hippocampal sections with two markers of radial glia cells (RGC): GFAP and BLBP (**Figure 35**).



< **Figure 35. COUP-TFI inactivation leads to glia scaffold disorganization in post-natal DG.**

Upper panel (A-A''). GFAP immunofluorescence on *Control*, *NexCKO* and *EmxCKO* DG at P0. Radial glia scaffold (GFAP+) appear increased and disorganized in *EmxCKO* 1ry and 3ry matrices (red arrowheads in A'' high magnifications). **Lower panel (B-C'' and u-z'')**. Immunofluorescences for GFAP (in green) and BLBP (in red) on *Control*, *NexCKO* and *EmxCKO* DG at P7 (B-B'' and high magnifications u-w'') and P14 (C-C'' and high magnifications x-z''). Dashed lines in B-B'' and C-C'' delineate the DG. Dashed and dotted lines in thigh magnifications (u-w'' and x-z'') delineates the three layers of the DG upper blade. *EmxCKO mutant* exhibit defects in radial glia scaffold process (red arrows) and cell bodies localization (white arrows) at P7 and P14, while *NexCKO* appear to have only transient defects at P7. Empty arrowheads in x-x'' mark the astrocytic-shape cells GFAP+ found in the hilus. *1ry/2ry/3ry: primary/secondary/tertiary matrix; gcl: granule cell layer; hi: hilus; ml: molecular layer. Scale bars = 100μm (low magnifications), 50μm (high magnifications).*

At P0, GFAP-expressing RGCs are compacted in specific locations of the developing DG, such as the future fimbria, along the 2^{ry} matrix and at the outmost borders of the developing DG including the hippocampal fissure (**Figure 35A**). Very few GFAP+ cells are observed in the 1^{ry} matrix at this stage. No specific alterations are found in the 1^{ry} and 3^{ry} matrix of the *NexCKO* (**Figure 35A'** and **high magnifications**). On the contrary, more GFAP+ cells are found in the 1^{ry} matrix of *EmxCKO* DGs and the radial glia scaffold in the forming DG is severely disorganized in these mice, especially in the future lower blade and in the hilus where abnormally too many GFAP+ cells seem to cross the DG toward the hippocampal fissure (**Figure 35A''** and **arrowheads in high magnifications**). This suggests that COUP-TFI might act on the establishment of the radial glia scaffold necessary for granule cell migration and laminar distribution in the 3^{ry} matrix of the DG.

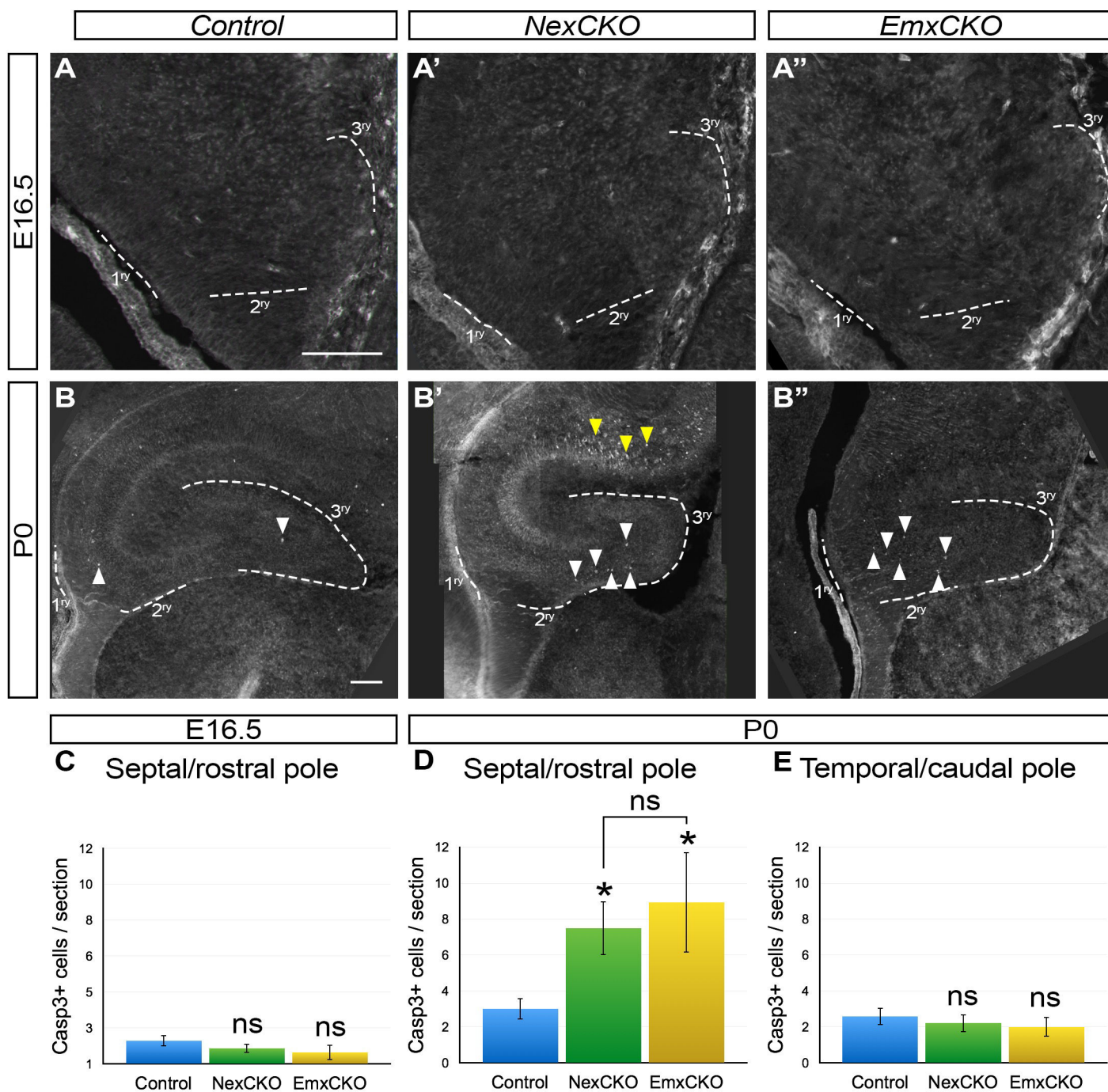
At P7, the RGC themselves have migrated across the DG and their cell bodies start to accumulate in the restricted area of the future adult neurogenic zone, the SGZ, as seen with BLBP IF (**arrowheads in Figure 35v**). Meanwhile, their processes extend along the granule cell layer (gcl), as seen by GFAP labelling (**red arrows in Figure 35u**), in order to set a new scaffold that will be used later by adult newborn granule cells to be integrated in the gcl. This new radial glia scaffold is fully established at P14, a stage when more SGZ cells can be detected (**arrowheads in Figure 35y**). At P7, in the *NexCKO* brains a prominent sub-population of RGCs is abnormally found in the hilus, as seen by their BLBP expression

(**arrowheads in Figure 35v'** and their process also appear rather disorganized, as seen with GFAP expression (**red arrows in Figure 35u'**). This phenotype seems to be rescued at P14 where RGCS are now properly located in the SGZ (**arrowheads in Figure 35y'**), and properly extend their processes across the gcl (**red arrows in Figure 35x**). In the *EmxCKO* however, RGCs appear poorly organized in both P7 and P14 DGs (**Figure 35B'',C''**): their cell bodies fail to be organized in a single layer in the SGZ, and remain spread through the DG (**arrowheads in Figure 35v'',y''**), and their processes lack the characteristic orientation and extension observed in *controls* (**red arrows in Figure 35u'',x''**). These results indicate that the establishment of the DG adult neurogenic niche (the SGZ), with RGCs at the border of the granule cell layer and hilus and a trans-granular scaffold, is specifically altered in *EmxCKO* brains, suggesting that the adult neurogenesis is most likely to be also affected in this mutant.

Moreover, we notice an increase in GFAP expression in the hilus of both mutants at P14 (**empty arrowheads in Figure 35x,x',x''**). This staining reminds us of astrocytes, which are also labelled by GFAP, suggesting either migratory defects or an increased gliogenesis.

VI / COUP-TFI inactivation leads to increased apoptosis in the newborn dentate gyrus

The drastic reduction of the hippocampus in the *EmxCKO* mutants might suggest a problem of cell survival and cell death. To thus investigate whether COUP-TFI plays a role in cell survival, I have performed a Caspase 3 (Casp3) IF on E16.5 and P0 coronal sections, and quantified the number of Casp3+ cells in all DG developing regions, comprising the three matrices (**Figure 36**).



At E16.5, very few Casp3⁺ cells are detected in all three conditions, and no significant difference has been found between *controls* and *mutants* (**Figure 36A-A'',C**). At P0, however, COUP-TFI *EmxCKOs* show a significant increase (around 3 times) of cell death in the developing septal DG, compared with *control* pups (**white arrowheads in Figure 36B'' and Figure 36D**: $p=0,037$). Surprisingly, I also found a statistically significant increased cell death in *NexCKO* mutant mice when compared to *controls* ($p=0,024$), although less severe than in *EmxCKO* mutants (**Figure 36D**). However, while Casp3⁺ cells are mainly found in the 3^{ry} matrix in the DG of *NexCKOs*, spread dying cells are instead located in the 2^{ry} matrix of *EmxCKO* mutants (**Figure 36B',B''**). This leads us to hypothesize that it is not the same cell population that undergoes apoptosis in the two types of mutant. Most likely, progenitors and IPCs stuck in the 2^{ry} matrix of *EmxCKO*, and post-mitotic and mature cells not properly integrated in the 3^{ry} matrix of *NexCKO* are depleted by apoptosis. Furthermore, no significant differences in cell death have been observed in the temporal/caudal portion of the hippocampus (**Figure E**), confirming a stronger effect of COUP-TFI loss in the septal/rostral portion of the DG.

Notably, *NexCKO* mutants have a prominent increase of apoptotic cells in the CA1/Subiculum region (**yellow arrowheads Figure 36B'**), implying that post-mitotic expression of COUP-TFI is important in the cell survival of this region. Surprisingly, this was not observed in *EmxCKO* mutants despite reduced growth in this region, suggesting either that cell death has occurred at an earlier stage in the *EmxCKO* mutant, or that the equivalent cells did not differentiate in *EmxCKOs*, while they probably reached a post-mitotic state in *NexCKO*, but could not properly survive. This reveals a particular aspect of COUP-TFI post-mitotic function in this region that will not be further investigated in this study.

At later stage, at P7, no or very few apoptotic cells were detected in all three conditions (data not shown), indicating that selected cell death occurs in a temporally controlled window. Taken together, these results demonstrate that COUP-TFI inactivation induces an increase of cell death in the perinatal septal DG, which could contribute in the shrinkage of this region. This impairment in cell survival might be either a direct effect of COUP-TFI or a consequence of improper granule cell migration and/or differentiation.

VII / COUP-TFI is required in the establishment and maturation of granule cell connectivity in the septal pole

Although the DG of *EmxCKO* hippocampi is smaller, and contains fewer cells, these cells do properly differentiate into granule cells, since they express *Prox1*, *Tbr1* and *NeuN*. However, in addition of expressing the proper combination of transcription factors, granule cells have to establish a proper connectivity loop in order to become fully mature and functional neurons.

1) COUP-TFI mitotic inactivation alters the septal but not the temporal perforant path fibers

The primary inputs to the hippocampus correspond to the perforant path fibers that originate from the entorhinal cortex. To evaluate whether this connection is modified in the absence of COUP-TFI, we have performed immunological detection of *Map2*, a microtubule-associated protein highly expressed in the perforant axons and CA1 dendrites (Steward and Halpain, 1999), on COUP-TFI *EmxCKO* brains and showed a strong downregulation of *Map2* mainly in the mutant septal hippocampus, but not in the temporal one (**arrowheads in Figure 37A-B'**, Flore *et al.*, 2015).

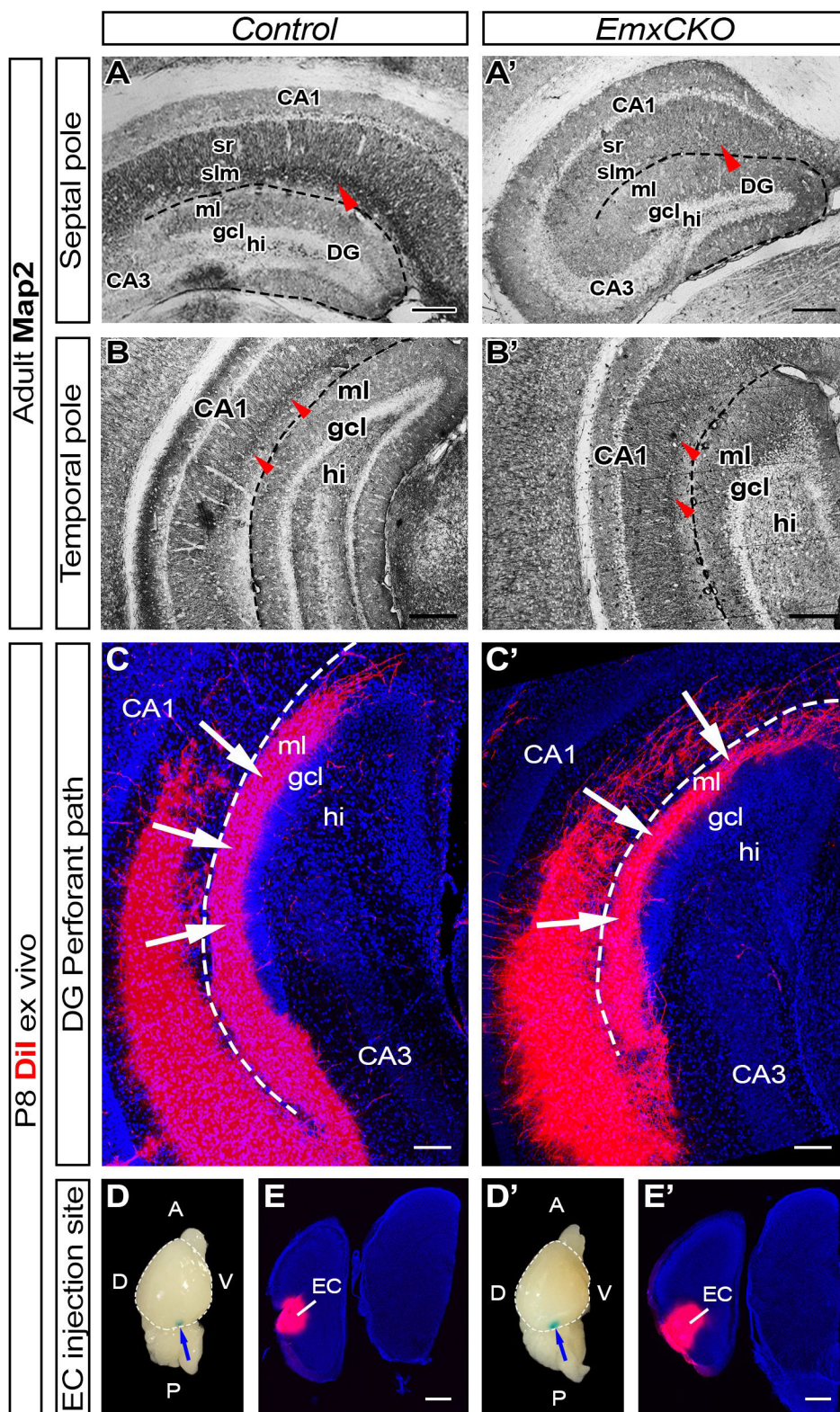


Figure 37. Impaired perforant path fibers in the septal *COUP-TFI EmxCKO* mutant hippocampus.

A-B'. Map2 immunohistochemistry on coronal sections of adult *Control* and *EmxCKO* septal (A-A') and temporal (B-B') hippocampus. Map2 labels CA1 pyramidal dendrites and entorhinal perforant path fibers. Map2 signal in *EmxCKO* is strongly decreased in the septal hippocampus (red arrowheads in A-A') and similar to *Control* in the temporal hippocampus (red arrowheads in B-B').

< (figure legend continuation) **C-C'**. Retrogradely DiI-labeled perforant paths in P8 *Control* (C) and *EmxCKO* mutant (C') temporal hippocampus. DiI-labeled fibers appear in red and cell nuclei are counterstained in blue with Hoechst **D-E'**. Site of DiI injection seen in whole hemibrain (blue arrows in D-D') and in coronal section at the level of the entorhinal cortex (E-E'). Dashed line delineate the DG hippocampal fissure in all panels. *CA1/3*: *cornu Ammonis field 1/3*; *DG*: *dentate gyrus*; *EC*: *entorhinal cortex*; *gcl*: *granule cell layer*; *hi*: *hilus*; *ml*: *molecular layer*; *sr*: *stratum radiatum*; *slm*: *stratum lucidum moleculare*. Scale bars = 100 μ m (A-C'), 500 μ m (E-E').

To confirm that connectivity between the entorhinal cortex and hippocampus was indeed maintained in the temporal *EmxCKO* DGs, as suggested by the Map2 staining, I performed an axonal tracing experiment on *Control* and *EmxCKO* post-mortem brains. The lipophilic tracer DiI was injected in the ventral entorhinal cortex (**Figure 37D-E'**) and let diffuse for several weeks, allowing a full labelling of the entorhinal axons to the DG molecular layer and CA1 (**Figure 37C-C'**). COUP-TFI mutant *EmxCKO* show a properly retrogradely labeled perforant path in the caudal/temporal hippocampus (**arrows in Figure 37C-C'**), confirming that entorhinal cortical afferences in this region are indeed well established. However, because of the position of the DiI, only perforant path fibers in the temporal hippocampus were labelled in this experiment. Since projections from the entorhinal cortex to the hippocampus are topographically organized in rodents (Van Groen *et al.*, 2003), septal perforant path fibers need to be further investigated by injecting DiI into a more lateral part of the entorhinal cortex that would support the Map2 septal staining described above.

Hence, COUP-TFI is mainly involved in the establishment of the perforant path fibers from the entorhinal cortex to the septal/rostral hippocampus.

2) COUP-TFI loss does not affect granule cell dendritic growth but induces an impairment of inner molecular layer fibers

My previous data showed impairment in granule cell maturation in the septal hippocampus primordially by molecular markers. In this last part of my thesis, I started to characterize the morphology of mature granule cells in P21 *Control* and *EmxCKO* brains. To this purpose, I

have crossed the *Thy1-H-YFP* transgenic line, in which a subset of granule cells is labelled by YFP (Feng *et al.*, 2000), with the *EmxCKO* line. Since Thy1 is a transmembrane protein, it is expressed in all compartments of the neuron, thus permitting to label the cell body, the dendrites and the axons of granule cells.

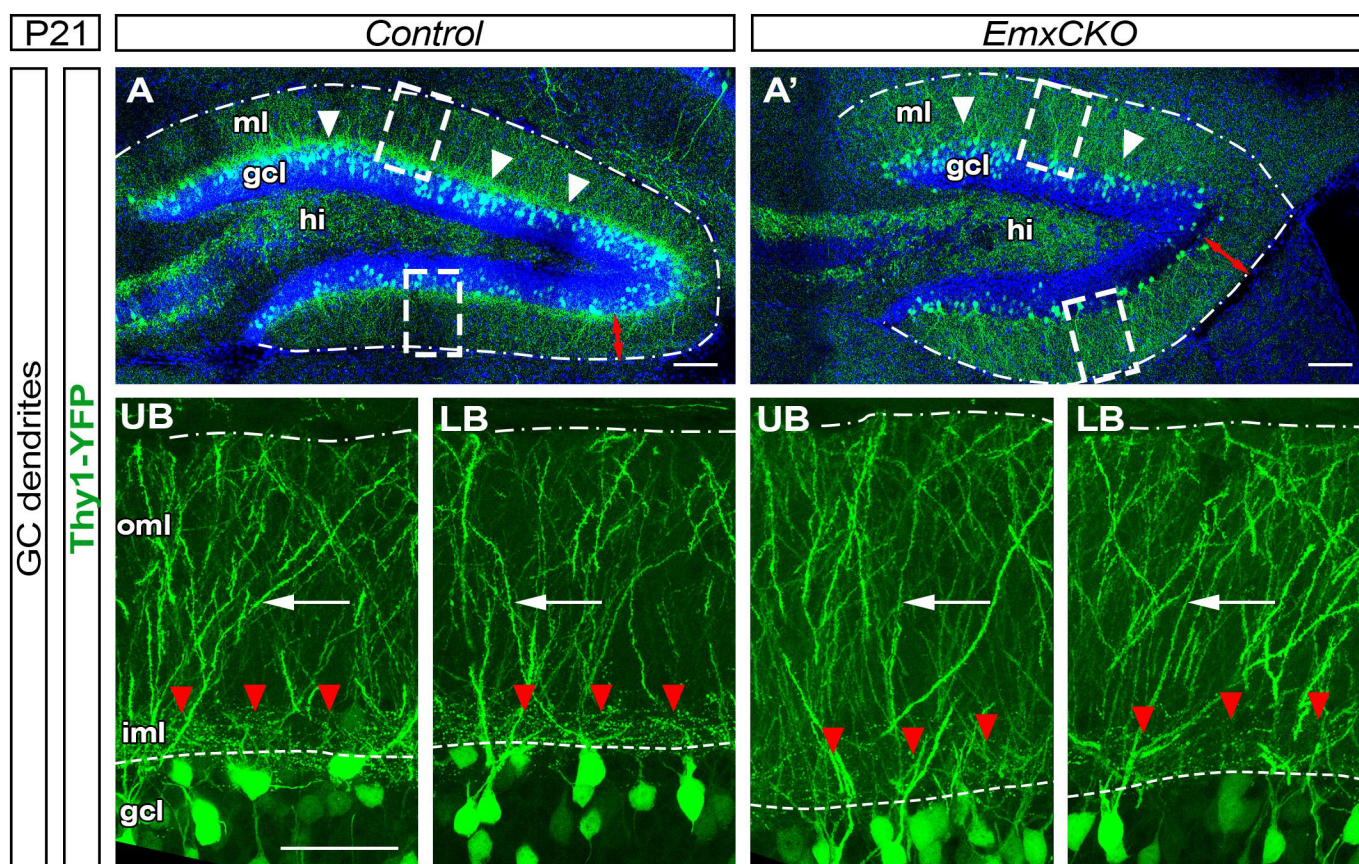


Figure 38. Granule cell dendritic arborization is not altered in the absence of COUP-TFI.

A-A'. View of the DG of Thy1-YFP *Control* and *EmxCKO*. High magnifications of the dashed box are presented in the lower panel for the two blades (UB and LB). Dendritic arborization of *EmxCKO* granule cells seems well developed (arrows in UB and LB high magnifications) although the length of their dendritic trees, and thus of the molecular layer, seems to be extended in *EmxCKO* mice (red arrows in A-A'). *EmxCKO* DG also exhibit a loss of YFP signal in the inner molecular layer (iml) (arrowheads in A-A' and high magnifications) *gcl*: granule cell layer; *hi*: hilus; *iml*: inner molecular layer; *LB*: lower blade; *ml*: molecular layer; *oml*: outer molecular layer; *UB*: upper blade. Scale bars = 100 μ m (A-A'), 50 μ m (UB and LB high magnifications).

At P21, several granule cells and their dendrites are labeled with YFP in both *Control* and *EmxCKO* hippocampi (**Figure 38A-A4**) and are correctly localized in the molecular layer. Magnifications of either the upper (UB) and lower blade (LB) show no obvious differences in the overall dendritic morphology in the *EmxCKO* DGs compared to *controls*: they extend correctly to the hippocampal fissure and seem fairly well organized (**white arrows in Figure 38UB and LB**), although the length of their dendritic trees, and thus of the molecular layer, seem to be extended in *EmxCKO* mice (**red arrows in Figure 38A-A'**). A more detailed morphological analysis using specific imaging softwares will be necessary to better assess the detailed morphology of single granule neurons in *mutant* mice of different ages and compare them with their *control* littermates.

Nevertheless, I have noticed a weaker if not absent signal of YFP in the inner molecular layer (iml) of *EmxCKO* DGs (**arrowheads in Figure 38A-A' and high magnifications**). This layer is known to contain mainly associational/commissural fibers from ipsi- and contra-lateral mossy cells, making synapses with the proximal dendrite of granule cells. Notably, our collaborators has recently shown that calretinin expression in mossy cells is missing in COUP-TFI-deficient hippocampi (Flore *et al.*, 2015). However, mossy cells, which cell bodies are located in the hilus, are not labelled by YFP in this mouse line. The inner molecular layer has also been shown to contain axons from the medial septum nucleus, in which few cells are indeed labelled by YFP (Porrero *et al.*, 2010 and data not shown), or fibers corresponding to granule cell collaterals (Haug, 1974), but these hypotheses need to be further investigated.

3) Mossy fibers are present but immature in the absence of COUP-TFI

With the help of the Thy1-YFP line, I was also able to visualize granule cell axons forming the so-called mossy fibers (**MF in Figure 39A**). Both in the *control* and *mutant* hippocampus, these fibers are found extending to the hilus and to the stratum lucidum, toward the dendrites of CA3 pyramidal cells (**arrows in Figure 39A-A'**). This suggests that granule cell axons properly form and project to their targets in the absence of COUP-TFI.

However, the expression of Calbindin, a calcium binding protein, normally found in these fibers is lost in the septal *EmxCKO* hippocampus at adult stage (**Figure 39B-B'**), suggesting that granule cells axons and synapses are most likely not properly mature although they can extend to their final targets.

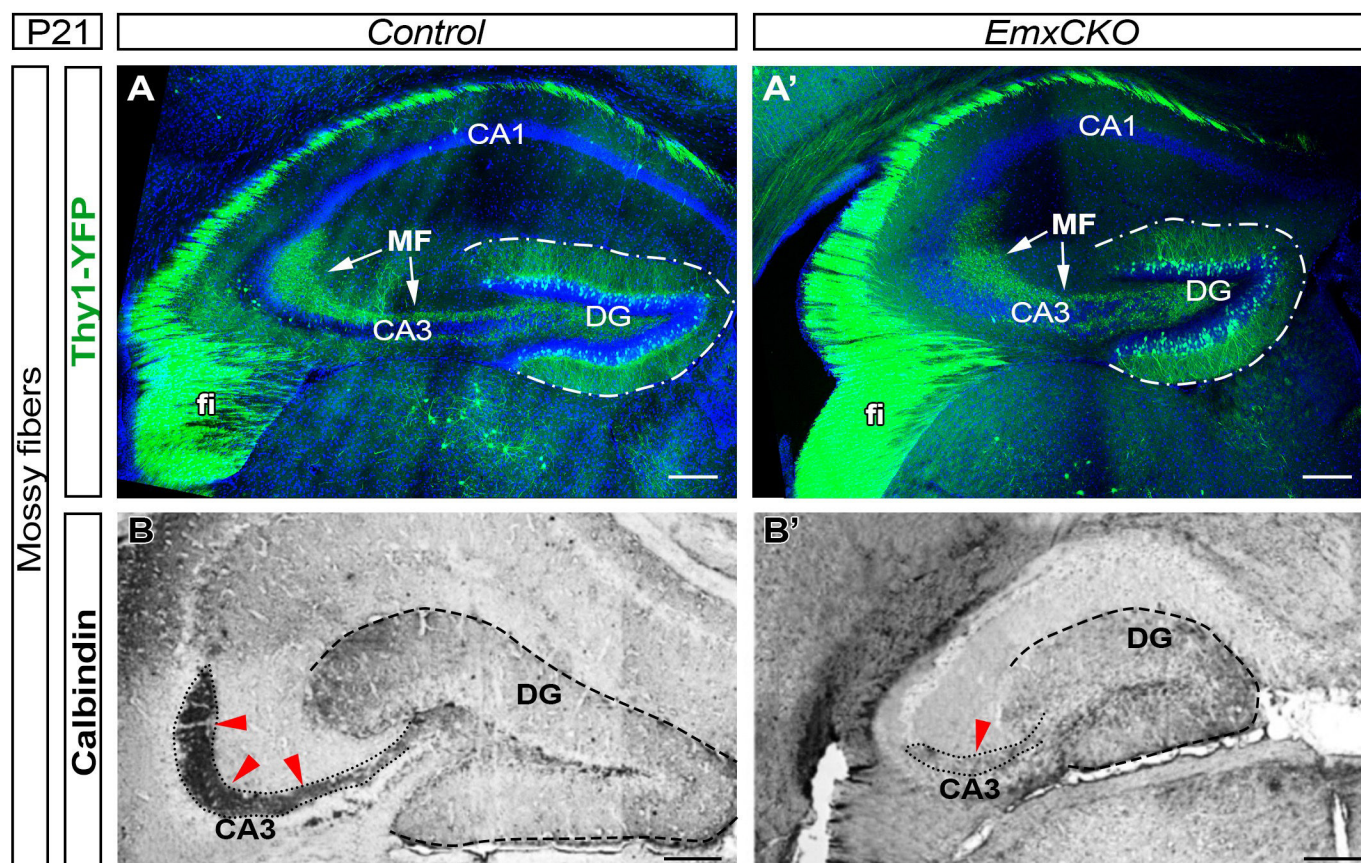


Figure 39. Mossy fibers are present but immature in *EmxCKO* mutant hippocampi.

A-A'. View of the hippocampi of Thy1-YFP *Control* and *EmxCKO*. Mossy fibers (MF) of DG granule cells that reach dendrites of the CA3 pyramidal cell layer are observable in both conditions (arrows). **B-B'**. Calbindin immunohistochemistry in coronal sections of the septal/rostral hippocampus, strongly labels MF in *Control*, whereas its signal is strongly altered in *EmxCKO* hippocampus (red arrowheads). CA1/3: cornu Ammonis field 1/3; DG: dentate gyrus; fi: fimbria; MF: mossy fibers. Scale bars = 200 μ m (A-A'), 100 μ m (B-B').

VIII / Behavior

The ultimate proof of whether a cell, structure and/or circuit are physiologically functional is to test their *in vivo* function in a physiological dynamic situation. With the help of our collaborators, we have challenged the behavioral consequences of a COUP-TFI-deficient underdeveloped hippocampus in adult mice (Flore *et al.*, 2015). Both the spatial and emotional memories, controlled by the septal/dorsal and temporal/ventral poles of the hippocampus, respectively, were tested on *control* and *EmxCKO* adult mice (Moser *et al.*, 1993; Moser *et al.*, 1995). Only a summary of these results is presented here, since the tests were not performed at iBV. More details can be found in the manuscript in annex (Flore *et al.*, 2015).

To test the spatial navigation memory, known to be under the control of the septal/dorsal hippocampus, *control* and *EmxCKO* mice were processed through the « water maze task ». This task revealed that *mutant* mice did learn to find the platform during training days, but were dramatically impaired in showing any preference for the target area (where the platform was previously located) during testing day, suggesting that COUP-TFI-deficient mice have impaired spatial memory. Notably, extension and volume of the hippocampus significantly correlated with this test and indicates that the impaired spatial memory is most probably due to the hippocampal dysmorphism observed in this mutant. It was also demonstrated that this effect is not linked to the sensory motor deficits associated with altered neocortical changes of COUP-TFI *EmxCKO* mice described before (Tomassy *et al.*, 2010).

Furthermore, by using the « one-trial inhibitory avoidance task » and the « spontaneous short-term object recognition task », our collaborators reported that COUP-TFI mutant mice do not show any impairments in their ability to form emotional memory, which is controlled by the temporal/ventral portion of the hippocampus.

Taken together, these behavioral data indicated that the hippocampal dysmorphism in *COUP-TFI EmxCKO* animals is associated to selective spatial memory impairments.

CHAPTER 4

Discussion and Perspectives

Discussion

The orphan nuclear receptor COUP-TFI is well described to act as a strong transcriptional regulator in the developing neocortex, playing, among others, key roles in neuronal migration, neurogenesis and neocortical arealization (Alfano *et al.*, 2014). In this study, I have shown that COUP-TFI is also required for the development of the hippocampus, and in particular of the dentate gyrus. Thus, this is the first evidence of COUP-TFI function in archicortical domains. To dissect the role of COUP-TFI in dentate gyrus development, I have characterized and compared two distinct COUP-TFI conditional knock-outs, the so-called *NexCKO* and *EmxCKO* mouse models, in which COUP-TFI is either inactivated in the progenitors or in the post-mitotic cells, respectively. Below in **Table 3** a summary of the different phenotypic alterations in the two models. These results will be discussed hereafter.

	<i>NexCKO</i> COUP-TFI post-mitotic inactivation	<i>EmxCKO</i> COUP-TFI mitotic inactivation
Morphology	Post-natal development: mild defects Adult: no morphological differences	Post-natal: gradual reduction Adult: strongly underdeveloped
Hem	N.D.	Unaffected
Proliferation	Unaffected	Decreased from embryonic stage
Granule cell mitotic differentiation	Unaffected	Impaired
Granule cell post-mitotic differentiation	Unaffected	Unaffected
Granule cell migration	Unaffected	Cell positioning, layer repartition and glia scaffold impaired Presence of heterotopic clusters
Apoptosis	Increased in DG septal pole	Increased in DG septal pole
Connectivity	N.D.	Perforant path: impaired in septal pole Granule cells dendrites: normal Mossy fibers: normal growth but not active
Behavior	N.D.	Spatial memory impaired Emotional memory unaffected

Table 3. Summary of the phenotypes observed in the two COUP-TFI-deficient models.

The effect of COUP-TFI inactivation in post-mitotic (*NexCKO*) or mitotic (*EmxCKO*) cells reported in this study are summarized in this table. *N.D.*: no data.

- **COUP-TFI gradient expression in progenitors is required for post-natal development and functional organization of the hippocampal septo-temporal axis**

COUP-TFI is expressed in the hippocampal primordium, both in the Hp neuroepithelium and in the DG neuroepithelium (dgn) with specifically high levels of expression in the latter one. Since COUP-TFI is expressed at the onset of DG development and maintained all along its formation, it was hypothesized that COUP-TFI might be an important factor for DG development from the earliest stages. Additionally, COUP-TFI is also expressed by the post-mitotic cells of the hippocampus, more particularly by pyramidal cells of the Hp and granule cells of the DG, and is maintained throughout development and adulthood (**Figure 10**). Thus, COUP-TFI acts both during development and adulthood as well as both, within the progenitors and differentiated cells. In order to distinguish these two putative roles, we have created two mutant mouse line that conditionally inactivate COUP-TFI expression, either in the cortical progenitors (*EmxCKO*) or solely in the cells that exited the cell cycle, called post-mitotic cells (*NexCKO*).

We have demonstrated that COUP-TFI expression along the septo-temporal axis of the hippocampus is not uniform (**Figure 10**). COUP-TFI expression exhibits a low septal (rostral/dorsal) to high temporal (caudal/ventral) gradient. Intriguingly, despite this observation, we have shown that the septal pole is particularly affected when COUP-TFI is depleted, while the temporal portion remains mildly impaired (**Figure 14** and **Figure 16**). This result is consistent with our collaborator's behavioral study (*cf. Result-VIII; Flore et al., 2015*) showing that the *EmxCKO* hippocampal dysmorphism is positively correlated with a selective spatial memory impairment, known to be controlled by the septal/dorsal hippocampus; this mutant instead has no gross impairments in emotional memory, controlled by the temporal/ventral portion of the hippocampus.

Thus, how comes that the portion in which COUP-TFI is expressed at its highest is instead the less affected? I would like to propose two possible explanations:

- The COUP-TFI homologue COUP-TFII, which share several targets, has increased expression levels in the temporal hippocampus of *EmxCKO* (**Figure 17**) suggesting that COUP-TFII might compensate for part of COUP-TFI function in this region, and thereby explaining why the hippocampal septal portion, in which COUP-TFII is expressed only at low levels, is more affected than the temporal pole. Double COUP-TFI and -II mutants, where both genes become inactivated in the same cortical cell types, would be extremely informative for supporting this hypothesis.

- Another plausible explanation for this phenotype could be that the connectivity is differentially impaired between septal and temporal pole of the dentate gyrus. Arrival of proper afferences plays a crucial role in the final patterning steps of the neocortex (Windrem and Finlay, 1991), and this might also apply for hippocampal morphogenesis. As a matter of fact, we have shown that depleting COUP-TFI in progenitors induces a loss of perforant path fibers reaching the septal hippocampus (**Figure 36** and Flore *et al.*, 2015), most probably due to the impaired entorhinal cortex observed in this mutant (Flore *et al.*, 2015), while the fibers reaching the temporal hippocampus are still present (**Figure 36**).

In the neocortex, COUP-TFI gradient expression is responsible for area patterning, along with other patterning genes such as Pax6, Sp8 and Emx2, by promoting caudal fate specification (Armentano *et al.*, 2007; Zhou *et al.*, 2001; Bishop *et al.*, 2000). Thus, it is reasonable to hypothesize that COUP-TFI also plays a role in the region-fate specification within the hippocampus. It is now well recognized that the hippocampus can be divided into separate structures or zones, both radially (CA fields and DG) and tangentially (along its septo-temporal axis). The latter subdivision is a rather recent observation, which arises from several studies showing that the septal and temporal poles of the hippocampus (often referred as the dorsal and ventral hippocampus) exhibit heterogeneity in terms of gene expression pattern, connectivity, and behavioral functions (*cf. Introduction-I-B-5*; reviewed in Fanselow and Dong, 2010). However, this work shows that the septal and temporal identities are not

affected by COUP-TFI loss (**Figure 17**), indicating that the septal volume reduction is caused by selective impairments of the septal domain, and not by an identity change along the septo-temporal axis. However, to specifically challenge COUP-TFI function in the fate specification of temporal identity, a COUP-TFI-overexpressing model in which the graded expression is lost at the expense of a forced and uniform expression would be worth analyzing.

Therefore, the hippocampal dysmorphism observed in *EmxCKO* mutant mice is more due to a growth impairment than to a change of fate, also because the hippocampus appears to have a gradual increasing reduction of its volume (**Figure 12**). While no obvious alterations are seen at embryonic stages, the post-natal development is particularly affected. This phenotype is not so surprising since it is known that most of the DG granule cells are generated after birth.

Unexpectedly however, *NexCKO* mutants also depict mild growth impairment, whereas its volume is not reduced at adult stage (**Figure 12** and **Figure 13**). The reasons of this apparent growth delay still remains unclear, since no strong defects have been observed in this mutant in terms of granule cell differentiation and migration. Nevertheless, I reported an alteration in cell survival by showing a transient cell death increase at perinatal stages (see below). Hence, even if apoptosis might reduce granule cell number at postnatal stages, this reduction would be compensated afterwards since most of granule cells are generated after birth.

- **COUP-TFI and hem-derived patterning**

The cortical hem controls DG development at the earliest stages (Galceran *et al.*, 2000; Lee *et al.*, 2000; Roelink, 2000), since it acts as a signaling center. It was therefore necessary to understand whether COUP-TFI acts on this hem-derived patterning. We demonstrated that COUP-TFI is not expressed in the cortical hem and that consequently the hem-produced signal Wnt5a is not changed in the absence of COUP-TFI (**Figure 18**), suggesting that COUP-TFI does not affect the hem-derived hippocampal formation onset. However, this result needs to be confirmed with other cortical hem factors, such as other members of the Wnt family. Additionally, even if we do not see any obvious alterations in the hem expression of morphogens, their signaling cascade could be affected by COUP-TFI loss and DG granule cells response to hem-derived signals could be changed.

For example, depletion of the Wnt signaling co-receptor LRP6 and the transcription factor Lef1 leads to DG morphological defects, due to a decreased number of mitotic precursors and abnormalities of the radial glial scaffold (Galceran *et al.*, 2000; Zhou *et al.*, 2004), which are defects that we also observe in the COUP-TFI-deficient mice. The β -catenin, a key mediator of the intracellular Wnt signaling, has also been involved in the development of the hippocampus (Machon *et al.*, 2003). Similarly, BMP-signaling, through function of its receptor Acvr1 (Activin receptor type I, also known as Alk2), also regulates DG neurogenesis by modulating Lef1 expression (Choe *et al.*, 2013).

Notably, some evidences of functional interactions between COUP-TFI and Wnt signaling have been reported in a previous report. The β -catenin pathway is repressed by COUP-TFI (Faedo *et al.*, 2008) but also directly by retinoic acid (Easwaran *et al.*, 1999), which is known to induce COUP-TFI expression (Clotman *et al.*, 1998). If and how COUP-TFI interact with Wnt signaling remains to be determined. Further studies, using down-stream factors of hem signals, are hence needed to investigate the role of COUP-TFI on hem early patterning.

- **COUP-TFI regulates the differentiation of DG granule progenitor cells**

In this study, I propose that COUP-TFI might regulate the balance between progenitor self-renewal and differentiation, by regulating the transition from progenitors to IPCs and promoting the proliferative capacity of IPCs in the early developing DG. Thus, in the *EmxCKO* mouse model, future granule cells are pushed toward a differentiating process, at the expense of a proliferative state necessary for expansion of granule cell number (*cf. Results-IV*). In this situation, a depletion of the progenitor pool and a defective amplification occurs, leading ultimately to a strongly reduced DG.

As mentioned in the Introduction, COUP-TFI and its fly homologue Svp have been shown to promote cell cycle exit and differentiation at the expense of progenitor pool maintenance (Kanai *et al.*, 2005; Maurange *et al.*, 2008; Armentano *et al.*, 2007). Our results in hippocampal development are therefore unexpected and contrast with these previous findings. The reasons of such a difference can be numerous and still need to be investigated. COUP-TFI could for example act on different target genes in this region, due to epigenetic factors, or be regulated by specific upstream local modulators, such as hem-derived patterning genes. Nonetheless, it demonstrates that the same transcription factor can have opposite effects on different part of the brain, most probably because of the different organization and development of the different regions. The number of layers, the cell composition, the mode of migration (inside-out *versus* outside-in), as well as the time of neurogenesis are fundamentally different between DG and neocortex, and could explain this discrepancy.

Despite the partial exhaustion of IPCs in *EmxCKO* mice, cells that have exited the cell cycle seem to properly differentiate into mature granule cells following the same sequence of transcription factor expression. However, the increased proportion of IPCs expressing early post-mitotic markers (ND1 and Prox1) suggests again that granule cells lacking COUP-TFI function are pushed toward a differentiating process, by precociously expressing post-mitotic markers. Notably, since this aspect of precocious Prox1 expression in IPC is also seen in *NexCKO* DG, we can deduce that COUP-TFI also acts post-mitotically in regulating expression of early post-mitotic transcription factor. Surprisingly however, late differentiation

process, such as the expression of mature granule cells markers (NeuN) does not seem to be altered, indicating that the maintained expression of COUP-TFI in mature granule cells might have a different function from modulating the granule differentiation process. For instance, we have provided some evidences of a role of COUP-TFI in the integration of granule cells into an active network (see below).

We have also reported in our two conditional COUP-TFI mutants a significant increase of apoptosis in the newborn DG (**Figure 35**). This increase is specific to the septal pole of the hippocampus, confirming the importance of COUP-TFI selective function along the hippocampal septo-temporal axis. Moreover, this excessive cell death correlates well with neocortical data in which inactivation of COUP-TFI leads to excessive cell death of subplate and layer IV neurons that failed to differentiate (Zhou *et al.*, 1999). However, the localization of these apoptotic cells differs between the two mutants. *EmxCKO* apoptotic cells are localized in the 2^{ly} matrix, within the granule cell migratory stream, suggesting that they might be IPCs or early post-mitotic cells, whereas *NexCKO* apoptotic cells are localized in the 3^{ly} matrix, corresponding to the DG anlage. Considering that COUP-TFI is ablated only in post-mitotic cells in this mutant, we can speculate that these apoptotic cells are post-mitotic immature granule cells. However, it remains to be determined more precisely which cell populations undergo abnormal cell death, and for which reason they do so. One possibility is that apoptotic cells might die because of their ectopic positions, due for example to a delay in differentiation and/or migration, and are unable to receive appropriate trophic factors to survive.

Could increased cell death also be due because of an imbalance between neurogenesis and gliogenesis, as suggested by a previous study (Naka *et al.*, 2008)? COUP-TF genes seem to limit the neurogenic period by promoting gliogenesis (cf. *Introduction-II-D-4-b*). Acute inactivation of both COUP-TFs prolongs neurogenesis and delays gliogenesis *in vitro* and *in vivo* and leads to an altered methylation pattern of the GFAP promoter, a crucial factor of glial fate specification (Naka *et al.*, 2008). Our preliminary data demonstrate that the cell fate decision of early-generated hippocampal cells does not appear to be altered in the two mutants, since granule cells are produced at the same rate as controls, at least from E14.5-

generated cells (**Figure 29**). Further studies are currently undergoing to determine whether at the time of gliogenesis, mutant mice would still produce granule cells, which would imply an extension of the neurogenic period. Surprisingly, we observed an increase of astrocytic-like cells in the hilus of *EmxCKO* DG at P14. If confirmed with the support of astrocyte-specific markers, this result would provide evidence of an unexpected role of COUP-TFI in promoting gliogenesis at the expense of, neurogenesis, which would contrast with the opposite effect previously reported in the neocortex. Notably however, we can also speculate that this putative increase of hilar astrocytes might be only due to a defective migration leading to mis-positioned astrocytes at late post-natal stages.

- **COUP-TFI regulates the migration of DG granule progenitor cells**

COUP-TFI is known to be associated with the migration behavior of various cell types during embryonic development and cancer (Tripodi *et al.*, 2004; Alfano *et al.*, 2011; Boudot *et al.*, 2014). This study supports this role in cell migration since migration of granule cells during DG development is altered in the absence of COUP-TFI in progenitors: a high number of IPCs is still found migrating in the 2^{ry} matrix at a stage when normally they are already positioned in the 3^{ry} matrix in controls (**Figure 30**). In addition, heterotopic clusters of post-mitotic cells are observed at late developmental stages (**Figure 30**), and the layer distribution of both mitotic and post-mitotic granule cells are severely altered, resulting in a less dense granule cells layer with spread progenitors and IPCs (**Figure 31**). The latter effect ultimately leads to a failed establishment of the SGZ, the adult neurogenic niche of the DG.

The reasons of this impaired migration appear to be multiple. First, radial glia scaffolds are altered: both at birth, when it is necessary for granule cells to reach their proper location in a densely packed granule cell layer, and at late developmental stages, when the trans-granular scaffold is used by adult-born granules to invade the granule cell layer. Second, guidance cues, such as Reelin and SDF1/CXCR4 pathways, are affected in the absence of COUP-TFI in progenitors. *EmxCKO* mutants exhibit a mis-positioned Reelin signal (and thus mis-positioned Cajal-Retizius secreting it) (**Figure 32**) and increased *CXCR4* mRNA expression

(**Figure 33**). Notably, altered SDF1/CXCR4 signaling has been associated with an invasion of breast cancer cells and is controlled by COUP-TFs (Boudot *et al.*, 2014). Differently from the previous study, *EmxCKO* mutants exhibit an increase in *CXCR4* expression, which most probably leads to an altered SDF1 signaling from the meninges and/or Cajal Retzius cells, and thus abnormal migration. Granule cells could also ectopically express CXCR4 during their migration, in line with their precocious differentiation. Again, migrating cells would abnormally respond to SDF1 and their migratory behavior affected. To determine the reasons and effects of the *CXCR4* mRNA up-regulation in *EmxCKO*, further investigation are needed, starting by analyzing protein levels and localisation, in addition to SDF1 expression levels.

All these effects are most likely to synergize and interact with each other. The abnormal position of Cajal-Retzius cells secreting Reelin and the increase of CXCR4 expression might be directly or indirectly linked and most likely affect the behavior of migrating granule cells and their positioning within the DG in *EmxCKO* mutant mice. For example, it is known that cortical meninges signals (including SDF1/CXCR4) and radial glia regulate Cajal–Retzius cell positioning in the early embryonic cerebral cortex (Borell and Marin, 2006; Paredes *et al.*, 2006; Kwon *et al.*, 2011) and reversely, Cajal-Retzius cells promote the radial alignment of the radial glia cells in the hippocampus (Förster *et al.*, 2002). Notably, I found some heterotypic clusters of post-mitotic cells in the molecular layer of COUP-TFI deficient DG that are characteristics of impaired cell migration and that remind us of those observed in *Lef1* and *ND1* mutants (Schwab *et al.*, 2000; Galceran *et al.*, 2000), and which have been reported to be associated with epilepsy (Liu *et al.*, 2000).

Thus, even if I cannot precisely define which of these mechanisms are directly modulated by COUP-TFI, a clear defect in cell migration associated with cell differentiation has emerged from my analysis. Further studies will be needed to clarify how and when the Reelin and SDF1/CXCR4 pathways are affected by COUP-TFI loss.

• COUP-TFI and the granule cell tri-synaptic circuit

We have shown that the granule cell cytoarchitecture does not appear to be strongly altered in the absence of COUP-TFI: correctly positioned granule cells exhibit a roughly well-organized dendritic arborization and have well-extended mossy fibers.

First, those granule cells that have managed to properly reach the granule cell layer in *EmxCKO* mutants develop a seemingly correct dendritic arborisation extending to the hippocampal fissure in the upper blade and to the pia membrane in the lower blade (**Figure 37**). Trophic interactions between afferent entorhinal fibers and granule cell dendrites are required for the maturation of distal granule cell dendritic segments (spine maturation) in the outer molecular layer, as this is affected in the absence of entorhinal input (Drakew *et al.*, 1999; Frotscher *et al.*, 2000). Dendritic tree arborization however, is independent from electrical activity and entorhinal inputs (Frotscher *et al.*, 2000). As described above, since COUP-TFI *EmxCKO* mutants depict a loss of perforant path fibers in the septal hippocampus (**Figure 36** and Flore *et al.*, 2015), it is very plausible that granule cell dendrites have an alteration in their spine maturation. Thus, a detailed morphological spine analysis will be needed to better characterize this phenotype.

Second, I have shown that granule cells axons forming the mossy fibers extend correctly to the CA2/CA3 distal ends of *EmxCKO* mutants (**Figure 38**). However, we have also demonstrated that these fibers almost completely fail to express the calcium-binding protein Calbindin, a marker of mature mossy fibers (**Figure 38**). Calbindin overexpression has been reported to enhance mossy fibers presynaptic function (Dumas *et al.*, 2004), suggesting that granule cell axons and synapses are most probably not mature in the *EmxCKO*, although they seem to correctly extend to their final target.

Our group previously showed that COUP-TFI-deficient primary hippocampal neurons have an abnormal distribution of actin- and tubulin-rich structures when cultured *in vitro*, leading to defects in axons and neurite formation and elongation (Armentano *et al.*, 2006). Thus, to further evaluate whether and how COUP-TFI acts during dendritic arborisation *in vivo*, it will

be necessary to perform a precise analysis by quantifying branching, spine numbers and lengths on GFP+ granule cells in *EmxCKO* mutant animals.

Furthermore, the use of the Thy1-eYFP-H mouse line revealed a missing signal in the inner molecular layer of the *EmxCKO* DG (**Figure 37**). This layer (also named supragranular band) is known to contain mostly associational/commissural fibers from ipsi- and contra-lateral mossy cells as well as axons from cholinergic cells of the medial septum and mossy fibers collaterals (Bayer, 1985; Matthews et al., 1987). The first population, the mossy cells, are not labeled by YFP in this line and can thus be excluded. Few cells of the medial septal nucleus are labelled by YFP (Porrero *et al.*, 2010 and data not shown) as well as a subpopulation of DG granule cells, that are known to possess mossy fibers collaterals to this supra granular area, although mainly in the temporal portion of the hippocampus (Haug, 1974). Consequently, we can hypothesize that either the septo-hippocampal projections and/or mossy fibers supragranular collaterals are affected in the absence of COUP-TFI. Previous studies of the lab showed impairments of the hippocampal commissure together with other axonal defects in a *COUP-TFI null* model (Armentano *et al.*, 2006). Further studies are of course required to clarify this issue. This would be quite informative since, on one hand, septo-hippocampal projections are one of the largest subcortical inputs to the hippocampus and play a critical role in learning and memory (Kesner, 1988; Bond *et al.*, 1989), and on the other hand, mossy fibers are known to undergo a reorganization in response to repeated seizures, mostly by enhancing these supragranular connections (Sutula *et al.*, 1988; Stanfield, 1989; Cavazos *et al.*, 1991; Golarai *et al.*, 1992).

Further studies are needed to understand in which extent granule cells are integrated in the neuronal network when COUP-TFI is missing. The amount of active synapses could be evaluated with specific markers such as PSD95 (post-synaptic density 95) and electrophysiological recording would bring added value to the study.

- **Concluding remarks:**

In summary, we have taken a mouse genetic approach and demonstrated that COUP-TFI is important for the development of the hippocampus, especially the dentate gyrus, one of the two major adult neurogenic regions. Mechanistically, COUP-TFI is important for proper differentiation of neural stem cells and intermediate progenitors by regulating cell cycle progression, transcription of related genes and neuronal migration, and act predominantly in progenitor cells. Notably, some of the functions of COUP-TFI suggested in this study contrast with its known role in other brain area, such as the neocortex, in which COUP-TFI acts predominantly post-mitotically to organize functional areas. Therefore, this suggests that the orphan nuclear receptor COUP-TFI possess specific and distinct functions in the hippocampus.

In our study, the COUP-TFI post-mitotic role remains more vague since its depletion in post-mitotic cells have only mild and transient defects in the hippocampus. We speculate that it could be instead involved in regulating cell survival, calcium-dependent neuronal activity or other refinement of granule cells properties. Intriguingly, some of the impairments found in this mutant partially affect mitotic cells, suggesting that COUP-TFI might also act in a non-cell autonomous manner.

In addition, our study shows that COUP-TFI graded expression is involved in shaping the morphology of the hippocampus and its subsequent function in spatial memory (attached manuscript).

Finally, COUP-TFI-dependent DG development appears also to affect the establishment of the adult neurogenic niche. Since COUP-TFI is also expressed in adult neural stem-like cells of the SGZ, it might play a direct role during adult neurogenesis. To challenge this, it will be necessary to inactivate COUP-TFI only in the SGZ through an inducible and cell-specific Cre recombinase.

To conclude, we have provided evidences for a crucial role of COUP-TFI in dentate gyrus formation and we thus propose COUP-TFI as a novel transcriptional regulator required in hippocampal development and function.

Perspectives

To further examine the influence of COUP-TFI in the development of the hippocampus, and the mechanisms involved in this process, I propose several experiments.

As mentioned above, I am currently working on confirming the absence of the septal perforant path, observed by the lack of Map2 staining in *EmxCKO* P7 mutants, with retrograde labelling experiment, after injection of the DiI tracer in the lateral entorhinal cortex, known to specifically connect to the septal hippocampus (Van Groen *et al.*, 2003). I am also investigating the plausible effect of COUP-TFI on the gliogenic switch by assessing the neurogenic *versus* gliogenic fate of late-born progenitors in postnatal *EmxCKO* DGs.

In addition, in a short-term view, I would investigate more in depth the relations between COUP-TFI and cortical-hem derived signals, by analyzing expression pattern of Wnt signaling downstream factors (Frizzled, LRP6, Lef1 etc), that could be altered in granule cells lacking COUP-TFI expression. More attention should also be given to decipher the impact of COUP-TFI inactivation on guidance cues, such as protein expression of CXCR4 and its ligand SDF1, and downstream effectors of the Reelin signaling pathway. It is also worth examining whether other factors regulating neuronal migration, such as those involved in the cytoskeletal machinery and the detachment of glia scaffold (*cf. Introduction-I-C-3b*), are altered in the absence of COUP-TFI.

In a more long-term view, I think that this work can lead to many other informative studies. Proper analysis of the granule cell cytoarchitecture, dendritic spine maturation, and electrophysiological properties would shed light on the role of COUP-TFI in regulating granule cell connectivity. Furthermore, analysis of a double COUP-TFI and COUP-TFII mutant or of a COUP-TFI-overexpressing model would unravel more precisely the role of COUP-TFs transcription factors in specifying the septo-temporal molecular and functional hippocampal axis.

Annexe

Manuscript
Flore *et al.*, 2015
(under review)

**Gradient COUP-TFI Expression is Required for Functional Organization
of the Hippocampal Septo-Temporal Longitudinal Axis**

**Flore Gemma^{1,2}, Di Ruberto Giuseppina², Joséphine Parisot^{3,4}, Sannino Sara¹, Russo Fabio¹,
Illingworth Elizabeth A.^{1,2}, Studer Michèle^{1,3,4*}, De Leonibus Elvira^{1,2*}**

¹Telethon Institute of Genetics and Medicine (TIGEM), Naples, Italy; ²Institute of Genetics and Biophysics, CNR, Naples, Italy; ³Institute of Biology Valrose, iBV, UMR INSERM1091/CNRS7277/UNS, Nice, France. ⁴University of Nice Sophia Antipolis (UNS), Valrose Campus, Nice, France.

*Co-corresponding

Corresponding authors:

Michèle Studer, Institute of Biology Valrose, Inserm U1091, CNRS UMR7277, UNS, Univ. of Nice Sophia Antipolis (UNS), 28 avenue Valrose, 06108 Nice Cedex 2 – France; Tél.: +33. 4.92.07.64.19 - Fax : +33. 4.92.07.64.02 e-mail: studer@unice.fr

Elvira De Leonibus, Telethon Institute of Genetics and Medicine, TIGEM, Via Campi Flegrei, 31, Pozzuoli (NA)-80078, Italy, Tel: +39-081-6132267, Fax: +39-081-7472037 e-mail: deleonibus@tigem.it

Running title: Hippocampal septo-temporal dysmorphogenesis.

Abstract

The hippocampus, a medial cortical structure, is subdivided into a distinct dorsal (septal) and ventral (temporal) portion, which is separated by an intermediate region lying on a longitudinal curvature. While the dorsal portion is more dedicated to spatial navigation and memory, the most ventral part processes emotional information. Genetic factors expressed in gradient during development seem to control the size and correct positioning of the hippocampus along its longitudinal axis; however, their roles in regulating differential growth and in supporting its anatomical and functional dissociation remain unexplored. Here, we challenge the *in vivo* function of the nuclear receptor COUP-TFI in controlling the hippocampal anatomical and functional properties along its longitudinal axis. Loss of cortical COUP-TFI function results in a progressive dysmorphic hippocampus with altered shape, volume and connectivity, particularly in its dorsal and intermediate regions. Notably, topographic inputs from the entorhinal cortex are strongly impaired in the dorsal portion of *COUP-TFI* mutants. These severe morphological changes are associated with selective spatial memory impairments. Together, these findings identify a novel transcriptional regulator required in the functional organization along the hippocampal septo-temporal axis supporting a genetic basis of the hippocampal volumetric growth with its final shape, circuit and type of memory function.

Keywords: hippocampus, septo-temporal longitudinal axis, COUP-TFI gradient expression, entorhinal connectivity, spatial memory.

Introduction

The hippocampus (HP) (*Cornu Ammonis* [CA1, CA3] and the dentate gyrus [DG]) is a limbic system structure in the medial temporal lobe of the mammalian telencephalon involved in memory formation. Functional studies have shown that the HP mediates behavioral tasks that depend on relating information from multiple sources (Kumaran D and EA Maguire 2005; Hannula DE *et al.* 2013). Animals with HP lesions are impaired in finding a hidden platform in water maze when relying on spatial strategies (Eichenbaum H *et al.* 1990), and in consolidating spatial information into long-term memory (Broadbent NJ *et al.* 2004; Ramos JM 2008). In contrast, the HP is not involved in behavioral tasks independent of relational information, such as finding a platform in the water maze signaled by a visual cue (Eichenbaum H *et al.* 1990).

Even small developmental and/or adulthood variations in the HP volume can have a dramatic impact on spatial memory ability, and are key features of neurodevelopmental psychiatric disorders (Mateffyova A *et al.* 2006; Arnold SJ *et al.* 2014). Multiple findings have suggested that the HP is not completely homogeneous along the dorso-ventral axis, also referred to septo (dorso)-temporal (ventral) longitudinal axis in rodents and antero-posterior axis in primates (for review see Strange BA *et al.* 2014). While the dorsal HP is more involved in spatial learning (Moser E *et al.* 1993; Moser MB *et al.* 1995), the ventral HP is required for non-spatial aspects of HP-dependent learning and emotional behaviors (Kheirbek MA *et al.* 2013; Wang ME *et al.* 2013). Neuronal ventral HP excitotoxic lesion is still one of the most used animal model of schizophrenia, as it resembles the neuropsychiatric deficits reported in humans (Lipska BK *et al.* 1993; Le Pen G *et al.* 2000; Ersland KM *et al.* 2012; Naert A *et al.* 2013; Arnold SJ *et al.* 2014; O'Reilly KC *et al.* 2014).

Anatomical and functional differences along the HP longitudinal axis are evolutionarily conserved, as reported in rats (Jung MW *et al.* 1994; Moser MB and EI Moser 2000; Vann SD *et al.* 2000; Bannerman DM *et al.* 2002), monkeys

(Colombo M *et al.* 1998), and humans (Small SA *et al.* 2001), suggesting that they might be genetically regulated. Several genetic factors, differentially expressed along the dorso-ventral HP axis, have been indeed identified (Leonardo ED *et al.* 2006; Lein ES *et al.* 2007; O'Reilly KC *et al.* 2014). However, whether regionalized-expressed genetic factors are causally linked to HP differential growth and to hippocampal functional dissociation along the longitudinal axis, is still unknown.

The transcription factor *COUP-TFI* (chicken ovalbumin upstream promoter transcription factor 1, also called *Nr2f1*) is a member of the nuclear hormone receptor superfamily of steroid hormone receptors, and is particularly interesting in this regard, because of its regionalized expression gradient in the cortex that results to be necessary and sufficient for neocortical areal organization and associated sensorimotor behavior (Tomassy GS *et al.* 2010; Alfano C *et al.* 2014). In this study, we hypothesized that COUP-TFI might belong to one of these genetic factors responsible for the differential growth and functional organization of the hippocampal longitudinal axis. To directly test this hypothesis, we characterized COUP-TFI expression along the HP longitudinal axis and challenged its role in HP functional organization in a genetically modified mouse model. Interestingly, we found that COUP-TFI is not only expressed in a low dorsal to high ventral gradient during HP postnatal development, but that its cortical ablation leads to severe HP dysmorphogenesis and connectivity impairments, and ultimately to selective impaired spatial memory. We thus provide the first evidence of a differentially expressed gene that acts by regulating volume, growth and functional organization of the septo-temporal longitudinal axis of the hippocampus.

Materials and Methods

Animals: *COUP-TFI^{fl/fl}/Emx1-Cre* (named also *CKO* or *mutant*) mice were generated and genotyped as previously described (Armentano M *et al.* 2006; Armentano M, SJ Chou, GS Tomassy, *et al.* 2007). *COUP-TFI^{lox/fox}* and *COUP-TFI^{lox/+}* mice are defined

as “controls” (*ctrl*) in this study since they have no detectable and quantitative defects and can be considered like wild-type mice. Midday of the day of the vaginal plug was embryonic day (E) 0.5. All experiments were conducted following guidelines of the Institutional Animal Care and Use Committee, CNR Animal Facility, Naples, Italy and European Union Guidelines. The experimenter was always blind to the treatment the animal had received.

Immunohistochemistry (IHC) and *in situ* Hybridization (ISH): Vibratome and cryostat sections were processed for immunohistochemistry and/or *in situ* hybridization as previously described (Armentano M, SJ Chou, GS Tomassy, et al. 2007). The following primary antibodies were used: mouse anti-human COUP-TFI (1:100, Abcam); rabbit anti-COUP-TFI (1:500) (Tripodi et al., 2004); rabbit anti-Calbindin D-28k (1:2500, SWANT), rabbit anti-Calretinin (1: 3000, SWANT) mouse monoclonal anti Map2 (1:200, Sigma) mouse monoclonal anti-SMI31 (1:500 Sternberger Monoclonals). For IHC, Biotinylated secondary antibodies (goat anti-rabbit, goat anti-mouse, (Vector Laboratories, Burlingame, CA, 1:200) were revealed by ABC-DAB reaction (Vector). Antisense RNA Probes were labelled using a DIG-RNA Labelling Kit (Roche). The following probes were used: *Cdh8*, *Lmo4*, *COUP-TFII*, *SCIP*, *KAI*, *GAD67*, *Id2*, *Neuropilin2 (Nrp2)*, *Fezf2*. COUP-TFI septo-temporal protein localization was quantified in 6 (3 females and 3 males) post-natal day 8 (P8) *control* hemi-brains. For each animal two septal slices (between 1600-2200 as reported in “*control*” of Figure 2D) and 3 temporal slices (between 400-1000) were sampled. Using the ImageJ graphic pen unit area (380µm² for each subfield) optical density (minus the slice background optical density) was measured in CA1, CA3 and DG. MAP2 was quantified in 3 *control* and 3 *CKO* hemi-brains at P8. This measure was taken in both genotypes starting from the first evidence of hippocampal tissue (see Figure 1C) by comparing them at different antero-posterior coordinates. Septal ranges (two slices) were between 2600-3200 vs. 1600-2000, while temporal ranges (3 slices) were 800-1600 vs 800-1400 for *control* and *CKO*, respectively (as reported in Figure 1C). Using the ImageJ graphic pen unit area (30µm²), optical density (minus the slice background optical density) was measured around the perforant path. Entorhinal cortex volume was quantified in 4 animals per genotype by measuring *Npn2* expression area in 4 consecutive (200 µm) hemi-brain sections at post-natal day 0 (P0).

Values are expressed as percentage from *control* values.

Axonal tracing by injection of lipophilic DiI

Tracing of entorhinal-hippocampal projections was carried out by injecting appr. 80µl of DiI crystal (DiI18(3); Molecular Probes) dissolved in DMSO in the entorhinal cortex of P8 *control* and *mutant* fixed brains. Brains were incubated for 6 weeks in 2% PFA at 37°C, embedded in 4% agarose, cut into 100 µm sections on a vibratome, counterstained with Hoechst (Invitrogen H3570), mounted in glycerol +phosphate buffer and photographed under fluorescent light.

Hippocampal volumetric analysis and field assessment:

Mice brains were vibratome-sectioned coronally with a thickness of 50µm and processed for Nissl staining, as previously described (Tomassy GS et al. 2010). For the adult HP phenotype, we evaluated the volume of the entire hippocampus and its rostro-caudal extension in coronal sections (one hemisphere, 28 *controls* and 41 *CKO*, 21 slices per animal). We also compared the septo-temporal volume distribution (average of the population ±SE for each rostro-caudal point) in *mutant* and *control* brains.

For P8 (4 *controls* and 3 *CKO* hemi-brains, 14 slices per animal), P0 (3 *controls* and 3 *CKO* hemi-brains, 10 slices per animal) and at E15.5 (4 *controls* and 4 *CKO*, 9 slices per animal in both hemispheres) brains were cryosectioned (20µm thickness) across the entire hippocampus, Nissl stained and evaluated at increments of 200µm using the ImageJ graphic pen. All evaluations previously described for adult animals were done during developmental stages. A second set of at least n=3 animals (9 slices per animal) was used to quantify the GAD67-positive cells in the HP at P8. For the CA1-CA3 field assessment (3 *controls* and 3 *CKO* hemi-brains, 11 slices per animal), the relative expressions of *SCIP* and *KAI* mRNA with respect to pyramidal layer extension were evaluated with ImageJ. For the evaluation of adult pyramidal layers cell density, n=6 animals per genotype were considered: two hemispheres (200 µm) in the septal domain and three hemispheres (every 200µm) in the temporal domain were analyzed for CA1 and CA3 cell density by 100µm² bins posed parallel to the pyramidal layer from the pyramidal/stratum radiatum border, and for 100µm unit of length. Quantification was performed exactly as described for MAP2.

For three-dimensional illustrations of the state of altered mutant HP, adult and P8 brains representatives of HP dysmorphism were coronally cryosectioned (20µm thickness at P8; 50µm thickness

floating in adults) and Nissl stained. Pictures were taken with a LEICA MZ 16 FA Stereomicroscope and converted from RGB to BW with Adobe Photoshop software. Sections were identified with serial numbers and different HP components were labeled with a color-coded graphic pen. 3-D images were aligned and integrated with Amira 4.1.2-1 software to obtain 3D pictures.

Statistical analysis: All the histological data were statistically analyzed and graphically represented using Statistica 10 and Microsoft Office Excel software, respectively. The error bars represent S.E.M. A two-tailed paired Student's *t*-test was used to analyze statistical significance. Data were normalized by defining the *control* value as 100%. Four-way ANOVA for repeated measures, with genotype (*Control* and *CKO*), gender (male and female) and HP subregions (CA1, CA3, DG), was used to analyze gene expression along different septo-temporal coordinates. As we have not detected any interaction between the factors gender and HP subfields, and the other factors, we grouped them together. Two-way ANOVA for repeated measures, with genotype (*Control* and *CKO*) as between group measure, and septo-temporal gradient as repeated measure was used to analyze HP volume and MAP2 expression along different septo-temporal coordinates. A Duncan *post hoc* test was used when appropriate to make direct comparisons.

Behavioral testing: A total of three-four months old 62 *controls* (34 females and 28 males) and 67 mutants (29 females and 38 males) were used for behavioral testings. They were divided into three subgroups. Two subgroups were tested in the spatial (11 *controls* and 27 *CKO*) and cue (16 *controls* and 11 *CKO*) versions of the water maze; a third group of animals (21 *controls* and 18 *CKO*) was subjected to the object recognition task on the first day, to the elevated plus maze on the second day, and to the passive avoidance task on the third and fourth day of testing. All behavioral tests were performed on mice under normal lighting conditions using previously established protocols. Before each behavioral task, animals were acclimatized to the testing room for at least 30 minutes. Before each test procedure, mice were placed in a waiting cage for at least 10 minutes before the beginning of the task; at the end of the measurement, they were placed back in their home cages.

Water maze apparatus: The tank (1.50 m diameter) was located in a cue-controlled environment (surrounded by many visual cues). The water

(temperature = 23 °C ± 1) was colored white and a platform (12 cm diameter) was placed in one of the four ideally present quadrants.

Visuo-spatial memory. Spatial memory testing procedure: the test consists in training the animals to use visuo-distal spatial cues (spatial map) in order to find a platform submerged below the surface of the water. 11 *controls* (5 males and 6 females) and 27 *CKO* mice (17 males and 10 females) were tested in the spatial water maze task. The position of the platform was kept constant during training, and it was randomized between different mice. During the 4 training days, the platform was submerged 1.5 cm below the water surface. Four sessions of three trials lasting 60 seconds each were performed each day for 4 consecutive days. The intertrial interval lasted about an hour. Animals were introduced to the tank in different quadrants each trial, in random order. If the animals did not reach the platform alone, they were accompanied to it. At the end of each trial, the animal was left on the platform for about 15 seconds. On the fifth day, a single probe trial of 60 seconds was performed, during which the platform was removed to assess the mice's memory of the platform position. Twenty-five of these animals (11 *controls* and 24 *CKO*) were used for volumetric assessment of the adult hippocampus at the end of behavioral testing.

Cue-memory procedure: the test consists in training the animals to use a cue (a flag) positioned on the top of the submerged platform to find it. Cue memory was tested in 15 *controls* (7 males and 8 females) and in 11 *CKO* (5 males and 6 females) mice, under exactly the same general conditions used to test spatial memory, with the addition of 2 further training days after the probe trial. The key differences between the spatial and the cue version of the task were: 1. No cues were present in the environment; 2. In each session, the position of the platform was displaced to 8 different points in the maze, and was visually signaled by a flag placed on the top of it. During testing, the platform was removed, and the flag placed in a further new place. Twenty-two (13 *controls* and 9 *CKO*) of these animals were used for assessment of volumetric measurements of the hippocampus.

Data collection: The latency to reach the platform was used as index of visuo-spatial performance during training days. In the probe trial we scored the number of target annulus (a 24 cm ring around the place where the platform was located during training) and compared them to the number of crossing in similar areas located in the other quadrants of the pool; a preference for the target annulus is considered as an indicator of functional memory.

Emotional memory: emotional memory was tested in the step-through inhibitory avoidance task (Ugo Basile, Italy) using a procedure identical to the one previously described (Manago F *et al.* 2009). Briefly, each mouse was placed in the light compartment, facing away from the dark compartment and the door leading to the dark compartment was automatically raised. When the mouse had stepped with all four paws into the dark compartment, the door was automatically closed and an electric foot-shock (0.5 mA, 50 Hz, 2 s) was delivered. Memory retention was tested recording step-through latency 24 hrs after training, following a similar procedure except that no shock was delivered. Cut-off was set at 60 s and 180 s for training and test, respectively.

Object memory: to test object memory, we used the spontaneous object memory task for mice with one-min delay and 3 identical object protocol, since we previously demonstrated that selective dorsal hippocampus lesions do not affect performance in this task (Sannino S *et al.* 2012). The other advantage of using this task in this study is that performance in this version of the task has never been clearly demonstrated to rely on the integrity of the prefrontal cortex (Mitchell JB and J Laiacina 1998; Yee BK 2000), and of other neocortical areas (Ennaceur A *et al.* 1997; Haijima A and Y Ichitani 2012). Animals were first habituated for 10 min to the empty open field (35×47×60 cm). After 1 min spent in their waiting cage, they were subjected to the study phase, during which they were allowed to explore for 10 min 3 identical objects (3-IOT) (Sannino S *et al.* 2012). During the 5 min test phase, the animal was exposed to identical copies of the familiar objects and one new object. We measured objects exploration, defined as the time in which the nose of the animal was in contact (2 cm from the object) with the object. The animal's behavior was recorded by a video-tracking system (Any-maze, Stoelting, USA) and analyzed by a trained observer.

Anxiety: Anxiety was measured in the plus-maze task for mice (Ugo Basile, Italy) in a 5 min trial. Distance, time and number of entries in the open and closed arm were recorded.

Data Collection and statistical analysis: The behavior was recorded with a video camera, located on the top of the mazes, and analyzed by a video-tracking (ANY-MAZE) program. ANOVA was used to analyze between subject factors genotype (*controls* and *CKO*) and gender (males and females). As we have never detected any interaction between the factor gender and the other factors, we grouped male and female mice

together. A Duncan *post-hoc* test was used, when appropriate, to make direct comparisons. Statistical significance was set at $p < 0.05$.

Results

COUP-TFI is expressed in a gradient and regulates hippocampal growth along the longitudinal axis

To investigate whether COUP-TFI could be involved in adult hippocampal morphogenesis and functionality, we first characterized COUP-TFI protein distribution in the postnatal HP at different ages. We previously reported strong COUP-TFI expression at E15.5 in the medio-caudal cortex where the hippocampal plate and dentate gyrus primordia develop (**Fig. 1A**) (Armentano M *et al.* 2006). Expression is maintained in the Ammon's horns and dentate gyrus from birth (P0) to adulthood (**Fig. 1A**), indicating that COUP-TFI might play multiple roles during hippocampal development and maturity. Similarly to what reported for its homolog COUP-TFII (or *Nr2f2*) (O'Reilly KC *et al.* 2014), COUP-TFI is expressed in a gradient fashion, which gradually increases dorso-ventrally along the anterior-posterior axis of all HP subfields [septo-temporal (F1/12=21.94; $p=0.0005$)] (**Fig. 1B, B'**) at P8, when the HP shows different connectivity and differential gene expression patterns along its longitudinal axis.

To directly test whether this expression gradient is required in the hippocampal differential morphogenesis and functional connectivity, we assessed HP formation in postnatal *COUP-TFI^{fl/fl}/Emx1-Cre* mice (or *COUP-TFI CKO*) in which COUP-TFI is inactivated in all cortical and archicortical neuronal progenitors (Armentano M, SJ Chou, GS Tomassy, *et al.* 2007; Alfano C *et al.* 2014). Gene inactivation in the mutant homogenously occurs all over the septo-temporal HP axis, consistently with a fully penetrant *Emx1-Cre* activity from E11.5 onwards (Gorski JA *et al.* 2002; Armentano M, SJ Chou, G Srubek Tomassy, *et al.* 2007). Quantification of the volume and total longitudinal extension of the *COUP-TFI* mutant HP (**Fig. 1C**) revealed an

overall volume reduction of 47% (total volume in *CKO*= $52.8 \pm 2.8\%$, $n=41$, compared to *controls*, $n=28$; two-tailed paired t-test; $p<0.0001$; **Fig. 1D**). Mutant mice have reduced septo-temporal volume, which is statistically different between adult *mutant* and *control* HP [genotype ($F1/19=64.16$; $p<0.0001$); septo-temporal coordinate ($F19/1273=194.74$; $p<0.0001$); genotype x septo-temporal coordinate ($F19/1273=20.05$; $p<0.0001$); **Fig. 1E**]. *Post-hoc* analysis confirms that whereas the septal/dorsal regions are dramatically affected, the most caudal parts are more similar to the *control* ones (**Fig. 1C, E**). Three-dimensional model representations of isolated *control* and *mutant* HP (**Fig. 1F**) better illustrate the strong decrease of the dorsal portion, which begins to occur at approximately the same rostro-caudal level of the ventral region, confirming that the majority of the septal pole is severely underdeveloped in *mutants*. The 3-D models also show that the HP appears caudo-ventrally shifted and rostro-dorsally poorly developed in *COUP-TFI CKO* compared to *control* mice (**Fig. 1F**). Thus, in the absence of COUP-TFI function, the hippocampus is caudally shifted and dramatically reduced in its dorsal portion.

To further investigate the onset and evolution of this morphological defect, we quantified the volume and extension of *control* and *mutant* HP at different developmental ages (**Fig. 2**). *COUP-TFI CKO* mice show a gradual reduction in HP volume during development, which peaks at postnatal ages (**Fig. 2**). While the *mutant* HP primordium volume is only slightly reduced (7%) at E15.5 (total volume in *CKO*= $93.1 \pm 11.9\%$, $n=4$, compared to *controls*, $n=4$; two-tailed paired t-test; $p=0.66$; **Fig. 2A, A'**), the total volume of the *mutant* HP decreases by about 30% when compared to *control* pups at P0 (**Fig. 2B**) even if not statistically significant (*CKO*= $69.5 \pm 17.2\%$, $n=3$; two-tailed paired t-test; $p=0.193$; **Fig. 2B'**). Detailed quantification of the volume distribution along the septo-temporal axis of the mutant HP at P0 supports a reduction of the dorsal portion, which again fails to show statistical significance when analyzed with repeated measures (**Fig. 2C**). However at P8, the overall shape of the mutant HP is

dramatically altered (**Fig. 2D**), showing little growth (the mutant volume is $52.6 \pm 3.1\%$, $n=3$, of that of the *control*, $n=4$; $p=0.0003$; two-tailed paired t-test; **Fig. 2D'**) and a clear imbalance between septal and temporal portions [genotype ($F1/5=78.96$; $p=0.003$); septo-temporal coordinates ($F5/65=16.56$; $p<0.0001$)], as supported by *post-hoc* analysis on quantitative volume distribution between *mutant* and *control* mice along the longitudinal axis (**Fig. 2E**). This is also illustrated in the 3-D models of *control* and *mutant* HP (**Fig. 2F**). Thus, a dorso-ventral imbalance, first evident at P0 and exacerbated at P8, becomes even more prominent in adult *mutant* HP, whose morphology is drastically altered when compared to that of *control* hippocampi.

In summary, these data indicate that impaired COUP-TFI function leads to the development of an asymmetric dysmorphic HP, which shows reduction in its dorsal portion, and suggest that *COUP-TFI* plays an imperative role in regulating proper HP growth along the septo-temporal axis during development.

Conserved septo-temporal identity of the *COUP-TFI* mutant hippocampus

The observed septal volume reduction and posterior shift of the HP in *mutant* mice might have resulted in a change of neuronal identity within the HP. To address this issue, we hybridized P8 *control* and *mutant* brains with molecular markers differentially expressed between dorsal and ventral HP (**Fig. 3**). Sagittal sections and high magnifications of dorsal and ventral hippocampi show that the normally higher expression of *Cdh8* in dorsal HP is maintained in *COUP-TFI CKO* brains of the same age (**Fig. 3A**), even if the dorsal HP is reduced, as described above (**Fig. 2D, D'**). Similarly, higher expression of *Lmo4* in the ventral HP and lower expression in the dorsal HP are maintained in the mutant ventral HP (**Fig. 3B**), supporting a conserved septo-temporal identity of the mutant HP despite its dorsal volume reduction. Notably, the low dorsal to high expression gradient of *COUP-TFII* is not only maintained in the *mutant* HP, but also exacerbated in the ventral portion where *COUP-TFII* is expressed at higher levels

than in *controls* (**Fig. 3C**). This suggests that COUP-TFII might compensate for some of the COUP-TFI functions in the ventral/temporal pole of the mutant HP. Taken together these data confirm that dorsal volume reduction due to the absence of COUP-TFI is caused by selective impairments of the septal domain, and not by an identity change between septal and temporal hippocampal portions.

Normal field specification and neuronal distribution in the dysmorphic hippocampus

We next investigated whether neuronal density and field specification were altered in the *COUP-TFI mutant* HP. Notably, P8 and adult *control* and *COUP-TFI*-deficient septal and temporal hippocampi maintain a comparable neuronal density and cell number within the CA fields and DG, despite the difference in size of *mutant* brains (**Fig. 4A-D**). Expression of the two complementary field specification markers, *KAI* and *SCIP*, in the pyramidal neurons of CA3 and CA1, respectively (Tole S *et al.* 1997), are also not altered (**Fig. 4E-F**) indicating that the distribution and the relative subdivision into CA1 and CA3 fields are not affected in the dysmorphic *COUP-TFI*-deficient HP.

Expression of COUP-TFI is abolished in pyramidal neurons of the dorsal and ventral hippocampus (**Fig. 4G**), but not in GABAergic interneurons, identified by the expression of the glutamate decarboxylase *GAD67* (**Fig. 4G, H**); this because hippocampal interneurons, which normally originate from subpallial regions, are not under the activity of the *Emx1-Cre* (Gorski JA *et al.* 2002) and thus still express *COUP-TFI* (Armentano M, SJ Chou, GS Tomassy, *et al.* 2007). Statistical analysis confirmed a normal number and distribution of *GAD67*-expressing cells within the different strata of P8 *COUP-TFI CKO* hippocampi (**Fig. 4H, I**), consistent with a cell-autonomous inactivation of *COUP-TFI* in pyramidal neurons. Taken together, these data indicate that, despite the dramatic morphological hippocampal dysmorphism observed in the absence of COUP-TFI function, the CA field allocation and the distribution of excitatory and inhibitory hippocampal populations are properly assigned.

Impaired connectivity in dorsal portions of the dysmorphic hippocampus is linked to abnormal entorhinal cortex

Normal cell density does not imply proper function. We thus assessed the hippocampal connectivity network that forms a closed loop in which the perforant path, composed by entorhinal cortical axons transmitting sensory information to the DG and CA fields (Steward O and SA Scoville 1976; Ruth RE *et al.* 1982), represents the unique direct connection between the HP and the cortex (**Fig. 5A**). The other paths involve ipsilateral (associational) and contralateral (commissural) intrahippocampal connections (Super H and E Soriano 1994). To determine the connectivity pattern in the dysmorphic HP, path-specific markers were used on adult *control* and *COUP-TFI CKO* hippocampi along their septo-temporal axes (**Fig. 5A, B**). No expression of calbindin, which labels ipsilateral mossy fibers projecting to CA3 pyramidal neurons, and calretinin, specifically expressed in hilar mossy cells projecting to the contralateral DG (Liu Y *et al.* 1996; Blasco-Ibanez JM and TF Freund 1997), is found in the septal/dorsal portion of dysmorphic HP (**Fig. 5C**); however, in more temporal sections, expression levels of calbindin and calretinin are less affected and more comparable between *controls* and *mutant* brains (**Fig. 5D**). Similarly, Schaffer collateral axons projecting from the ipsilateral or contralateral CA3 neurons to the CA1 region, fail to express SMI31 in the septal/dorsal mutant HP (**Fig. 5C**). MAP2, a microtubule-associated protein highly expressed in the perforant axons and CA1 dendrites (**Fig. 5E**) (Steward O and S Halpain 1999), is strongly downregulated in the mutant septal HP. Statistical analysis on the quantification of MAP2 protein levels shows significant differences in terms of genotype ($F_{1/4}=248.78$; $p<0.0001$), septo-temporal areas ($F_{1/4}=35.27$; $p=0.044$) and of the interaction between the two ($F_{1/4}=11.07$; $p=0.02$). *Post-hoc* analysis reveals that MAP2 expression is significantly reduced in *mutants* as compared to the *control* group at both septo-temporal levels (**Fig. 5E-G**); nevertheless, in the *CKO* group, but not in the *control* group, the expression in the

temporal region is significantly higher compared to that in the septal portion, suggesting a milder defect in the ventral than dorsal area (**Fig. 5F,G**). This is also confirmed by DiI axonal tracing, in which the perforant paths to the DG and to the CA1 are properly retrogradely labeled in *COUP-TFI CKO* ventral hippocampi (**Fig. 5H**). Taken together these findings consistently suggest a correlation between connectivity and growth, and support a functional role for COUP-TFI in differentially regulating dorsal *versus* ventral portions of the developing HP.

It is well known that projections from the entorhinal cortex (EC) to the HP are topographically organized in rodents and follow a dorsolateral to ventromedial gradient in the EC that corresponds to the dorsoventral axis of termination in the HP (van Groen T *et al.* 2003). Thus, altered connectivity to the dorsal HP of mutants might be due to abnormal development of the dorsal EC. To test this hypothesis, we first assessed COUP-TFI expression in the EC and then EC-specific markers in *COUP-TFI* mutant brains. Interestingly, coronal sections at P0 show a dramatic reduction of COUP-TFI expression at the rhinal fissure (red arrowhead in **Fig. 6A**), where the dorsal portion of the EC starts to appear, as also supported by the dorsal expression boundary of *Nrp2*, a molecular marker for the EC (Chen H *et al.* 1997) (**Fig. 6C**). However, COUP-TFI is highly expressed in the ventral part of the EC in more caudal sections (black arrow in **Fig. 6A**). Sagittal views further support this abrupt COUP-TFI downregulation at the transition between dorsal EC and neocortex, and re-expression in the most ventromedial part of the EC (**Fig. 6B**). This is also corroborated by the complementary expression patterns of *Nrp2* and *Fezf2*, a neocortical-specific marker (Molyneaux BJ *et al.* 2005), which nicely delimitate paleocortical and neocortical tissues, respectively (**Fig. 6D**). Thus, similar to the neocortex and the HP, COUP-TFI is expressed in a gradient in the developing EC, suggesting that it might control topographic entorhinal to hippocampal connectivity in the dorsal portion of the HP. Indeed, dorsalmost *Nrp2* expression is drastically downregulated and *Fezf2* is ventrally shifted in the absence of cortical COUP-TFI function (**Fig.**

6C, D), in line with impaired dorsolateral EC and caudally shifted neocortex. Quantification of the *Nrp2* expression area in the EC (**Fig. 6C'**) confirms that COUP-TFI mice have a significant [genotype (F1/6=6.5; p=0.04)] reduced EC volume as compared to *control* animals.

Overall, these data illustrate that COUP-TFI shares a common expression gradient between EC and HP, and suggests that its expression is required in the formation of a proper topographic circuit between dorsal EC and dorsal HP.

Impaired spatial memory defects are correlated to abnormal hippocampal growth

In light of the septal to temporal hippocampal dysmorphism, we tested whether *COUP-TFI* mutant mice had any impairment in spatial memory, known to be controlled by the septal/dorsal HP pole (Moser E *et al.* 1993; Moser MB *et al.* 1995). Different groups of adult *COUP-TFI CKO* and their littermates *control* mice were subjected to the spatial and cued versions of the water maze. In the spatial version, animal had to retrieve the position of the submerged platform using visual distal cues surrounding the pool. Two-way ANOVA for repeated measures revealed that *COUP-TFI CKO* as well as *control* mice reduce the time required finding the platform during the training days (Training days: F3/108=15.249; p<0.0001) (**Fig. 7A**). However, *mutant* mice have a higher approaching latency compared to *controls* (Genotype: F1/36=3.24; p=0.07). On the testing day, *COUP-TFI CKO* mice are dramatically impaired in showing any preference for the quadrant [Quadrant time (F3/108=6.402; p<0.0005); Quadrant time x Genotype (F3/108=2.958; p=0.03), two-way ANOVA for repeated measures] and annulus ("?" point in **Fig. 7B**) where the platform was previously located (**Fig. 7B**), when compared to the other annulus areas of the tank [Annulus crossing (F3/108=13.992; p<0.0001); Annulus crossing x Genotype (F3/108=5.52; two-way ANOVA for repeated measures; p=0.001)]. This is also reflected by a significant reduction in the percentage of target annulus crossings (Genotype: F1/36=4.3; one-way ANOVA; p=0.04) (**Fig. 7C**), suggesting that *COUP-TFI*

CKO mice have impaired spatial memory. To assess whether abnormal target annulus crossing was caused by the abnormal HP differential growth due to *COUP-TFI* deficiency, we used simple regression to correlate the percentage of the target annulus crossings with the extension and volume of the HP. We found that both of these measures significantly correlate with the percentage of annulus crossings on the testing day (Extension: $R=0.343$; $p=0.03$; Volume: $R=0.358$; simple regression analysis; $p=0.03$) (**Fig. 7D, E**), indicating that impaired spatial memory might most probably due to the hippocampal dysmorphism observed in *COUP-TFI CKO* mice.

Next, to exclude that this effect was not secondary to sensory-motor deficits associated with altered neocortical changes (Tomassy GS *et al.* 2010), different groups of animals were subjected to a cue version of the water maze. In this case, the position of the submerged platform was labeled by a visual cue, and the use of spatial information was limited. Two-way ANOVA for repeated measures show that both groups exhibit similar reduced latency in reaching the platform during the four training days (**Fig. 7F**), and when the platform is removed, both groups focus their searching below the cue (Annulus: $F_{6/144}=25.055$; one-way ANOVA; $p<0.0001$) (**Fig. 7G**). This indicates that the sensory-motor deficits associated to the previously described neocortical defects of *COUP-TFI CKO* mice (Armentano M, SJ Chou, G Srubek Tomassy, *et al.* 2007; Tomassy GS *et al.* 2010) are most likely not contributing to the spatial memory deficits reported here.

Since the ventral hippocampus has been implicated in non-spatial aspects of hippocampal-dependent learning and emotional behaviors (Kheirbek MA *et al.* 2013; Wang ME *et al.* 2013), we subjected other groups of mice to the one-trial inhibitory avoidance task, which probes animals' ability to form emotional memory. *COUP-TFI mutant* mice fail to show any impairment and, similarly to *control* animals, they increase the step-through latency from the training day to the testing day performed 24 hr later (Day: $F_{1/25}=44.93$; $p<0.0001$), indicating that they learned to avoid the shocked compartment (**Fig.**

7H). Similarly, when they are tested for their ability to recognize a new object from a familiar one in the spontaneous short-term object recognition task, mutant mice do not show any significant difference from *controls*. Both groups explore the new object significantly more than the familiar ones during the study (*control*= 26 ± 2.4 ; *COUP-TFI CKO*= 22 ± 2.1) and the test phase (object type: $F_{2/72}= 18.31$; $p<0.0001$) (**Fig. 7I**). This is consistent with previous findings showing that dorsal HP lesions generally spare short-term recognition memory, when the same (Sannino S *et al.* 2012) or similar behavioral protocols are used (Broadbent NJ *et al.* 2004; Ainge JA *et al.* 2006; Dere E *et al.* 2007).

Finally, we tested basal level of anxiety in the elevated plus maze task; we found no significant difference between genotypes in the percentage of time and distance spent in the open arm (**Fig. 7J**), as well as in the total distance and arm entries (data not shown). Taken together, our behavioral data confirm that the hippocampal dysmorphism in *COUP-TFI CKO* animals is associated to selective spatial memory impairment.

Discussion

Our study provides to our knowledge, the first experimental evidence of a neurodevelopmental genetic program controlling HP development along its septal/dorsal to temporal/ventral axis. We find that the nuclear receptor *COUP-TFI* is expressed in the hippocampus in a dorso-ventral gradient, and that its developmental loss leads to a dysmorphic HP, in which the size of the septal pole is specifically reduced and connectivity strongly impaired. We also identified gradient *COUP-TFI* expression in the EC and an impaired perforant path projecting to the dorsal HP in the absence of cortical *COUP-TFI* function. These data strongly support a role for this transcriptional regulator in establishing and/or maintaining proper connectivity between cortex and HP. Importantly, these distinct morphological and anatomical changes are associated with selective impairment in spatial memory

formation, consistently with a functional dissociation between the dorsal and ventral HP.

Unraveling the molecular mechanisms required in proper hippocampal anatomical and functional organization along its longitudinal axis is becoming a priority issue, in particular after the identification of a whole series of genes differentially enriched in the dorsal or ventral HP from birth to adulthood (O'Reilly KC *et al.* 2014), and their contribution in neuropsychiatric developmental disorders. Indeed, recent anatomical and connectivity studies have shown that at birth (i) the hippocampus is shortened along its dorso-ventral axis; (ii) the ventral regions remain ventral similarly to the adult HP, and (iii) the terminal distribution of EC input along the dorso-ventral hippocampal axis reflects the adult topography. In addition, the most ventral one-third of the hippocampus is the one that seems to differ more than the other two third in terms of intrinsic connectivity, electrophysiological properties, behavioral function, and genetic program (O'Reilly KC *et al.* 2014; Strange BA *et al.* 2014). Thus, altering differentially expressed genes along the longitudinal axis will contribute in our understanding on how the HP undergoes major volumetric increase in length and curvature from P0 to P15, and whether changes in HP curvature might be due to changes in HP volume along the dorso-ventral axis.

In this study, we have abolished the function of a differentially expressed gene, the transcriptional regulator COUP-TFI, expressed in a gradient fashion in the postnatal developing HP and EC, two functionally related structures during HP circuit formation. We previously reported that gradient cortical expression of COUP-TFI is required in neocortical organization and thalamo-cortical topographic connectivity by regulating identity, size and position of functional areas during corticogenesis (reviewed in Alfano C and M Studer 2013). In this study, we demonstrate that gradient archicortical COUP-TFI expression is involved in setting up the anatomical and functional architecture along the hippocampal longitudinal axis.

Interestingly, COUP-TFI mutant adult hippocampi have a shape similar to neonatal HP,

since it is shortened, lacks the normal HP curvature but preserves a proper ventral pole-“the most ventral one-third”, which is located more posterior than age-matched control brains, and has reduced size and volume in its dorsal portion. Although this phenotype already appears at birth, it becomes fully established at P8, an age when the hippocampal length and growth are substantially increasing and which will ultimately dictate its final curvature and shape (O'Reilly KC *et al.* 2014). Various mechanisms might be involved in this morphological dysmorphism, ranging from alteration in regional growth to reduced cortical connectivity. Since the “intermediate” portion, a transitional structure with mixed dorsal and ventral features, seems crucial for obtaining an optimal HP volume and shape during the first postnatal week (O'Reilly KC *et al.* 2014), we propose that the graded COUP-TFI expression might be involved in modulating the volume of intermediate and ventral portions thus allowing the dorsal part to properly expand (O'Reilly KC *et al.* 2014; Strange BA *et al.* 2014). As for the neocortex (Faedo A *et al.* 2008), COUP-TFI might be required in controlling the spatio-temporal regulation of the balance between progenitor proliferation and differentiation. Accordingly, we observed altered neurogenesis in the prospective hippocampus at E15.5 (G.F., J.P. and M.S., manuscript in preparation). In addition, maintenance and even higher expression of the homolog COUP-TFII in the ventral HP might compensate for the lack of COUP-TFI in this region, thus allowing proper ventral growth at the expense of dorsal parts.

Absence of EC afferent projections might be another contributor of the septal/dorsal reduction, which gets worse with age becoming dramatic in adult *COUP-TFI* mutant mice. Neurogenesis is strictly correlated with the topographical organization of entorhinal-HP reciprocal connections. The dorsal EC preferentially connects with the dorsal part of the HP, whereas portions of the EC positioned more ventrally connect to ventral parts of the HP (Witter MP *et al.* 2000). Our molecular analysis indicates an important reduction of the dorsal EC portion at the expense of neocortical tissue at P0,

whereas part of the ventral EC seems to be preserved. Connectivity impairments appeared also graded along the longitudinal axis of the mutant HP, in accordance with a gradient- rather than absolute-like HP organization along its dorso-ventral axis (Scorzin JE *et al.* 2008; Strange BA *et al.* 2014). The topographic EC to HP connectivity defects at early postnatal ages might thus contribute to the severe septal HP reduction observed in *COUP-TFI* adult mutants.

The hippocampus is crucial for spatial memory formation. Accordingly, the findings we report in this study show that *COUP-TFI* mutant mice have a specific impairment in spatial memory formation that correlates well with their HP volume reduction, as indicated by our regression analysis. We previously showed that these mice have no major impairments in open field exploratory activity as well as in neuromotor performance in the hanging wire and rotarod task (Tomassy GS *et al.* 2010). In contrast, they were affected in fine motor-skill learning tasks, such as the adhesive-removal and the skilled-reaching tasks.

In the aim to dissociate neocortical from archicortical dependent behavioral defects, we used a spatial water maze procedure based on distal landmarks. This procedure relies on the integrity of the HP and is not affected by prefrontal and parietal cortex functional deactivation (Save E and B Poucet 2000; Mogensen J *et al.* 2004; Lopez J *et al.* 2012). At the same time, the lack of effect on the visual cue and on the spontaneous object recognition task confirmed that in *COUP-TFI CKO* mice the sensory-motor defects related to neocortical dysfunctions are very specific and involve fine sensory-motor skills. Spontaneous object short-term recognition memory task, differently from the instrumental visual object discrimination task (Kesner RP *et al.* 1996), has never been clearly demonstrated to rely on the integrity of the prefrontal cortex (Mitchell JB and J Laiacina 1998; Yee BK 2000), and of other neocortical areas (Ennaceur A *et al.* 1997; Haijima A and Y Ichitani 2012). On the contrary, it relies on the integrity of the perirhinal cortex, in particular of its most caudal part (Albasser MM *et al.* 2009),

which seems not to be affected in *COUP-TF CKO* mice.

Thus, the lack of impairment in the visual water maze and the correlation between the spatial memory impairment with altered HP volume and gross morphology, strongly suggest that the spatial memory defect here reported is not secondary to the sensory-motor deficit associated with altered neocortical patterning (Tomassy GS *et al.* 2010). The selectivity of the spatial memory defects, in the absence of major changes in anxiety observed in mutant mice, is consistent with a dramatic dorsal HP volume reduction and altered connectivity between EC and HP (Steffenach HA *et al.* 2005), and no major changes in the functionality of the ventral HP. This is in line with the observation that absence of cortical *COUP-TFI* during development differently affects the dorsal and ventral HP portions, indicating that HP development and functional specification along its septo-temporal axis is indeed controlled by different genetic developmental programs, as previously suggested in a study involving quantitative trait loci (Martin MV *et al.* 2006). Although we cannot completely exclude that the ventral HP is affected in *COUP-TFI* mutant mice, our study supports a major role for this transcriptional regulator in patterning the septal/dorsal HP portion and its connectivity with the dorsal EC during development and in early postnatal stages.

In conclusion, this study shows that the archicortical expression gradient of a transcription factor, such as *COUP-TFI*, can regulate HP volume and connectivity along its dorsal-to-ventral axis and, ultimately, HP-dependent behavioral functions. To our knowledge, this is the first experimental evidence supporting the anatomical and functional dorso-ventral HP dissociation on a genetic developmental basis. *COUP-TFI* loss of function causes optic atrophy with intellectual disability (Al-Kateb H *et al.* 2013; Bosch DG *et al.* 2014). Furthermore *COUP-TFI* expression has been found to be strongly associated with childhood general cognitive ability and mental retardation (Webber C *et al.* 2009; Erslund KM *et al.* 2012). Our findings pave the way for investigating *COUP-TFI* mutations and associated changes in

septo-temporal volumetric distribution in children with neurodevelopmental cognitive impairments. It is also highly interesting in this regard that COUP-TFI is deregulated in fetuses of pregnant women-smokers (Fowler PA *et al.* 2014), as compared to non-smokers, suggesting it might be a pathway of teratogenic effects on HP growth and function.

ACKNOWLEDGEMENTS

We would like to thank Prof Andrea Mele, Dr. Ingrid Bethus, Prof Menno Witter, Dr. Olivier DeShaux, Dr. Helene Marie for carefully reading the manuscript, and Alexis Burton for English language revision. E. Giordano for animal husbandry, and the IGB Microscopy Core Facility for technical support. This work was supported by the Italian Telethon Foundation, by the French Government (National Research Agency, ANR) under grant number R09125AA and TMSP14TELC to MS, and TMSTHMTELC to MS-EDL, Gemma Flore was supported by fellowships from Fondazione Telethon (TCP04006) and Ministerial European (PON01_02342) grants.

Financial disclosure: The authors declare no competing financial interests

References

Ainge JA, Heron-Maxwell C, Theofilas P, Wright P, de Hoz L, Wood ER. 2006. The role of the hippocampus in object recognition in rats: examination of the influence of task parameters and lesion size. *Behav Brain Res* 167:183-195.

Al-Kateb H, Shimony JS, Vineyard M, Manwaring L, Kulkarni S, Shinawi M. 2013. NR2F1 haploinsufficiency is associated with optic atrophy, dysmorphism and global developmental delay. *Am J Med Genet A* 161A:377-381.

Albasser MM, Davies M, Futter JE, Aggleton JP. 2009. Magnitude of the object recognition deficit associated with perirhinal cortex damage in rats: Effects of varying the lesion extent and the duration of the sample period. *Behav Neurosci* 123:115-124.

Alfano C, Magrinelli E, Harb K, Hevner RF, Studer M. 2014. Postmitotic control of sensory area

specification during neocortical development. *Nature communications* 5:5632.

Alfano C, Studer M. 2013. Neocortical arealization: evolution, mechanisms, and open questions. *Developmental neurobiology* 73:411-447.

Armentano M, Chou SJ, Tomassy GS, Leingartner A, O'Leary DD, Studer M. 2007. COUP-TFI regulates the balance of cortical patterning between frontal/motor and sensory areas. *Nat Neurosci* 10:1277-1286.

Armentano M, Filosa A, Andolfi G, Studer M. 2006. COUP-TFI is required for the formation of commissural projections in the forebrain by regulating axonal growth. *Development* 133:4151-4162.

Arnold SJ, Ivleva EI, Gopal TA, Reddy AP, Jeon-Slaughter H, Sacco CB, Francis AN, Tandon N, Bidesi AS, Witte B, Poudyal G, Pearlson GD, Sweeney JA, Clementz BA, Keshavan MS, Tamminga CA. 2014. Hippocampal Volume Is Reduced in Schizophrenia and Schizoaffective Disorder But Not in Psychotic Bipolar I Disorder Demonstrated by Both Manual Tracing and Automated Parcellation (FreeSurfer). *Schizophr Bull.*

Bannerman DM, Deacon RM, Offen S, Friswell J, Grubb M, Rawlins JN. 2002. Double dissociation of function within the hippocampus: spatial memory and hyponeophagia. *Behav Neurosci* 116:884-901.

Blasco-Ibanez JM, Freund TF. 1997. Distribution, ultrastructure, and connectivity of calretinin-immunoreactive mossy cells of the mouse dentate gyrus. *Hippocampus* 7:307-320.

Bosch DG, Boonstra FN, Gonzaga-Jauregui C, Xu M, de Ligt J, Jhangiani S, Wiszniewski W, Muzny DM, Yntema HG, Pfundt R, Vissers LE, Spruijt L, Blokland EA, Chen CA, Baylor-Hopkins Center for Mendelian G, Lewis RA, Tsai SY, Gibbs RA, Tsai MJ, Lupski JR, Zoghbi HY, Cremers FP, de Vries BB, Schaaf CP. 2014. NR2F1 mutations cause optic atrophy with intellectual disability. *Am J Hum Genet* 94:303-309.

Broadbent NJ, Squire LR, Clark RE. 2004. Spatial memory, recognition memory, and the hippocampus. *Proc Natl Acad Sci U S A* 101:14515-14520.

Chen H, Chedotal A, He Z, Goodman CS, Tessier-Lavigne M. 1997. Neuropilin-2, a novel member of the neuropilin family, is a high affinity receptor for the

- semaphorins Sema E and Sema IV but not Sema III. *Neuron* 19:547-559.
- Colombo M, Fernandez T, Nakamura K, Gross CG. 1998. Functional differentiation along the anterior-posterior axis of the hippocampus in monkeys. *J Neurophysiol* 80:1002-1005.
- Dere E, Huston JP, De Souza Silva MA. 2007. The pharmacology, neuroanatomy and neurogenetics of one-trial object recognition in rodents. *Neurosci Biobehav Rev* 31:673-704.
- Eichenbaum H, Stewart C, Morris RG. 1990. Hippocampal representation in place learning. *J Neurosci* 10:3531-3542.
- Ennaceur A, Neave N, Aggleton JP. 1997. Spontaneous object recognition and object location memory in rats: the effects of lesions in the cingulate cortices, the medial prefrontal cortex, the cingulum bundle and the fornix. *Exp Brain Res* 113:509-519.
- Ersland KM, Christoforou A, Stansberg C, Espeseth T, Mattheisen M, Mattingsdal M, Hardarson GA, Hansen T, Fernandes CP, Giddaluru S, Breuer R, Strohmaier J, Djurovic S, Nothen MM, Rietschel M, Lundervold AJ, Werge T, Cichon S, Andreassen OA, Reinvang I, Steen VM, Le Hellard S. 2012. Gene-based analysis of regionally enriched cortical genes in GWAS data sets of cognitive traits and psychiatric disorders. *PLoS One* 7:e31687.
- Faedo A, Tomassy GS, Ruan Y, Teichmann H, Krauss S, Pleasure SJ, Tsai SY, Tsai MJ, Studer M, Rubenstein JL. 2008. COUP-TFI coordinates cortical patterning, neurogenesis, and laminar fate and modulates MAPK/ERK, AKT, and beta-catenin signaling. *Cereb Cortex* 18:2117-2131.
- Fowler PA, Childs AJ, Courant F, MacKenzie A, Rhind SM, Antignac JP, Le Bizec B, Filis P, Evans F, Flannigan S, Maheshwari A, Bhattacharya S, Monteiro A, Anderson RA, O'Shaughnessy PJ. 2014. In utero exposure to cigarette smoke dysregulates human fetal ovarian developmental signalling. *Human reproduction* 29:1471-1489.
- Gorski JA, Talley T, Qiu M, Puelles L, Rubenstein JL, Jones KR. 2002. Cortical excitatory neurons and glia, but not GABAergic neurons, are produced in the *Emx1*-expressing lineage. *J Neurosci* 22:6309-6314.
- Hajjima A, Ichitani Y. 2012. Dissociable anterograde amnesic effects of retrosplenial cortex and hippocampal lesions on spontaneous object recognition memory in rats. *Hippocampus* 22:1868-1875.
- Hannula DE, Libby LA, Yonelinas AP, Ranganath C. 2013. Medial temporal lobe contributions to cued retrieval of items and contexts. *Neuropsychologia* 51:2322-2332.
- Jung MW, Wiener SI, McNaughton BL. 1994. Comparison of spatial firing characteristics of units in dorsal and ventral hippocampus of the rat. *J Neurosci* 14:7347-7356.
- Kesner RP, Hunt ME, Williams JM, Long JM. 1996. Prefrontal cortex and working memory for spatial response, spatial location, and visual object information in the rat. *Cerebral cortex* 6:311-318.
- Kheirbek MA, Drew LJ, Burghardt NS, Costantini DO, Tannenholz L, Ahmari SE, Zeng H, Fenton AA, Hen R. 2013. Differential control of learning and anxiety along the dorsoventral axis of the dentate gyrus. *Neuron* 77:955-968.
- Kumaran D, Maguire EA. 2005. The human hippocampus: cognitive maps or relational memory? *J Neurosci* 25:7254-7259.
- Le Pen G, Grottick AJ, Higgins GA, Martin JR, Jenck F, Moreau JL. 2000. Spatial and associative learning deficits induced by neonatal excitotoxic hippocampal damage in rats: further evaluation of an animal model of schizophrenia. *Behavioural pharmacology* 11:257-268.
- Lein ES, Hawrylycz MJ, Ao N, Ayres M, Bensinger A, Bernard A, Boe AF, Boguski MS, Brockway KS, Byrnes EJ, Chen L, Chen TM, Chin MC, Chong J, Crook BE, Czaplinska A, Dang CN, Datta S, Dee NR, Desaki AL, Desta T, Diep E, Dolbeare TA, Donelan MJ, Dong HW, Dougherty JG, Duncan BJ, Ebbert AJ, Eichele G, Estin LK, Faber C, Facer BA, Fields R, Fischer SR, Fliss TP, Frensley C, Gates SN, Glattfelder KJ, Halverson KR, Hart MR, Hohmann JG, Howell MP, Jeung DP, Johnson RA, Karr PT, Kawal R, Kidney JM, Knapik RH, Kuan CL, Lake JH, Laramée AR, Larsen KD, Lau C, Lemon TA, Liang AJ, Liu Y, Luong LT, Michaels J, Morgan JJ, Morgan RJ, Mortrud MT, Mosqueda NF, Ng LL, Ng R, Orta GJ, Overly CC, Pak TH, Parry SE, Pathak SD,

- Pearson OC, Puchalski RB, Riley ZL, Rockett HR, Rowland SA, Royall JJ, Ruiz MJ, Sarno NR, Schaffnit K, Shapovalova NV, Sivisay T, Slaughterbeck CR, Smith SC, Smith KA, Smith BI, Sodt AJ, Stewart NN, Stumpf KR, Sunkin SM, Sutram M, Tam A, Teemer CD, Thaller C, Thompson CL, Varnam LR, Visel A, Whitlock RM, Wohnoutka PE, Wolkey CK, Wong VY, Wood M, Yaylaoglu MB, Young RC, Youngstrom BL, Yuan XF, Zhang B, Zwingman TA, Jones AR. 2007. Genome-wide atlas of gene expression in the adult mouse brain. *Nature* 445:168-176.
- Leonardo ED, Richardson-Jones JW, Sibille E, Kottman A, Hen R. 2006. Molecular heterogeneity along the dorsal-ventral axis of the murine hippocampal CA1 field: a microarray analysis of gene expression. *Neuroscience* 137:177-186.
- Lipska BK, Jaskiw GE, Weinberger DR. 1993. Postpubertal emergence of hyperresponsiveness to stress and to amphetamine after neonatal excitotoxic hippocampal damage: a potential animal model of schizophrenia. *Neuropsychopharmacology : official publication of the American College of Neuropsychopharmacology* 9:67-75.
- Liu Y, Fujise N, Kosaka T. 1996. Distribution of calretinin immunoreactivity in the mouse dentate gyrus. I. General description. *Exp Brain Res* 108:389-403.
- Lopez J, Herbeaux K, Cosquer B, Engeln M, Muller C, Lazarus C, Kelche C, Bontempi B, Cassel JC, de Vasconcelos AP. 2012. Context-dependent modulation of hippocampal and cortical recruitment during remote spatial memory retrieval. *Hippocampus* 22:827-841.
- Manago F, Castellano C, Oliverio A, Mele A, De Leonibus E. 2009. Role of dopamine receptors subtypes, D1-like and D2-like, within the nucleus accumbens subregions, core and shell, on memory consolidation in the one-trial inhibitory avoidance task. *Learn Mem* 16:46-52.
- Martin MV, Dong H, Vallera D, Lee D, Lu L, Williams RW, Rosen GD, Cheverud JM, Csernansky JG. 2006. Independent quantitative trait loci influence ventral and dorsal hippocampal volume in recombinant inbred strains of mice. *Genes Brain Behav* 5:614-623.
- Mateffyova A, Otahal J, Tsenov G, Mares P, Kubova H. 2006. Intrahippocampal injection of endothelin-1 in immature rats results in neuronal death, development of epilepsy and behavioral abnormalities later in life. *Eur J Neurosci* 24:351-360.
- Mitchell JB, Laiacona J. 1998. The medial frontal cortex and temporal memory: tests using spontaneous exploratory behaviour in the rat. *Behav Brain Res* 97:107-113.
- Mogensen J, Lauritsen KT, Elvertorp S, Hasman A, Moustgaard A, Wortwein G. 2004. Place learning and object recognition by rats subjected to transection of the fimbria-fornix and/or ablation of the prefrontal cortex. *Brain research bulletin* 63:217-236.
- Molyneaux BJ, Arlotta P, Hirata T, Hibi M, Macklis JD. 2005. Fezl is required for the birth and specification of corticospinal motor neurons. *Neuron* 47:817-831.
- Moser E, Moser MB, Andersen P. 1993. Spatial learning impairment parallels the magnitude of dorsal hippocampal lesions, but is hardly present following ventral lesions. *J Neurosci* 13:3916-3925.
- Moser MB, Moser EI. 2000. Pretraining and the function of hippocampal long-term potentiation. *Neuron* 26:559-561.
- Moser MB, Moser EI, Forrest E, Andersen P, Morris RG. 1995. Spatial learning with a minislab in the dorsal hippocampus. *Proc Natl Acad Sci U S A* 92:9697-9701.
- Naert A, Gantois I, Laeremans A, Vreysen S, Van den Bergh G, Arckens L, Callaerts-Vegh Z, D'Hooge R. 2013. Behavioural alterations relevant to developmental brain disorders in mice with neonatally induced ventral hippocampal lesions. *Brain research bulletin* 94:71-81.
- O'Reilly KC, Flatberg A, Islam S, Olsen LC, Kruge IU, Witter MP. 2014. Identification of dorsal-ventral hippocampal differentiation in neonatal rats. *Brain Struct Funct*.
- Ramos JM. 2008. Hippocampal damage impairs long-term spatial memory in rats: comparison between electrolytic and neurotoxic lesions. *Physiol Behav* 93:1078-1085.
- Ruth RE, Collier TJ, Routtenberg A. 1982. Topography between the entorhinal cortex and the dentate septotemporal axis in rats: I. Medial and

- intermediate entorhinal projecting cells. *J Comp Neurol* 209:69-78.
- Sannino S, Russo F, Torromino G, Pendolino V, Calabresi P, De Leonibus E. 2012. Role of the dorsal hippocampus in object memory load. *Learn Mem* 19:211-218.
- Save E, Poucet B. 2000. Involvement of the hippocampus and associative parietal cortex in the use of proximal and distal landmarks for navigation. *Behav Brain Res* 109:195-206.
- Scorzin JE, Kaaden S, Quesada CM, Muller CA, Fimmers R, Urbach H, Schramm J. 2008. Volume determination of amygdala and hippocampus at 1.5 and 3.0T MRI in temporal lobe epilepsy. *Epilepsy Res* 82:29-37.
- Small SA, Nava AS, Perera GM, DeLaPaz R, Mayeux R, Stern Y. 2001. Circuit mechanisms underlying memory encoding and retrieval in the long axis of the hippocampal formation. *Nat Neurosci* 4:442-449.
- Steffenach HA, Witter M, Moser MB, Moser EI. 2005. Spatial memory in the rat requires the dorsolateral band of the entorhinal cortex. *Neuron* 45:301-313.
- Steward O, Halpain S. 1999. Lamina-specific synaptic activation causes domain-specific alterations in dendritic immunostaining for MAP2 and CAM kinase II. *J Neurosci* 19:7834-7845.
- Steward O, Scoville SA. 1976. Cells of origin of entorhinal cortical afferents to the hippocampus and fascia dentata of the rat. *J Comp Neurol* 169:347-370.
- Strange BA, Witter MP, Lein ES, Moser EI. 2014. Functional organization of the hippocampal longitudinal axis. *Nat Rev Neurosci* 15:655-669.
- Super H, Soriano E. 1994. The organization of the embryonic and early postnatal murine hippocampus. II. Development of entorhinal, commissural, and septal connections studied with the lipophilic tracer DiI. *J Comp Neurol* 344:101-120.
- Tole S, Christian C, Grove EA. 1997. Early specification and autonomous development of cortical fields in the mouse hippocampus. *Development* 124:4959-4970.
- Tomassy GS, De Leonibus E, Jabaudon D, Lodato S, Alfano C, Mele A, Macklis JD, Studer M. 2010. Area-specific temporal control of corticospinal motor neuron differentiation by COUP-TFI. *Proc Natl Acad Sci U S A* 107:3576-3581.
- van Groen T, Miettinen P, Kadish I. 2003. The entorhinal cortex of the mouse: organization of the projection to the hippocampal formation. *Hippocampus* 13:133-149.
- Vann SD, Brown MW, Erichsen JT, Aggleton JP. 2000. Fos imaging reveals differential patterns of hippocampal and parahippocampal subfield activation in rats in response to different spatial memory tests. *J Neurosci* 20:2711-2718.
- Wang ME, Fraize NP, Yin L, Yuan RK, Petsagourakis D, Wann EG, Muzzio IA. 2013. Differential roles of the dorsal and ventral hippocampus in predator odor contextual fear conditioning. *Hippocampus* 23:451-466.
- Webber C, Hehir-Kwa JY, Nguyen DQ, de Vries BB, Veltman JA, Ponting CP. 2009. Forging links between human mental retardation-associated CNVs and mouse gene knockout models. *PLoS genetics* 5:e1000531.
- Witter MP, Naber PA, van Haefen T, Machielsen WC, Rombouts SA, Barkhof F, Scheltens P, Lopes da Silva FH. 2000. Cortico-hippocampal communication by way of parallel parahippocampal-subicular pathways. *Hippocampus* 10:398-410.
- Yee BK. 2000. Cytotoxic lesion of the medial prefrontal cortex abolishes the partial reinforcement extinction effect, attenuates prepulse inhibition of the acoustic startle reflex and induces transient hyperlocomotion, while sparing spontaneous object recognition memory in the rat. *Neuroscience* 95:675-689.

Figures

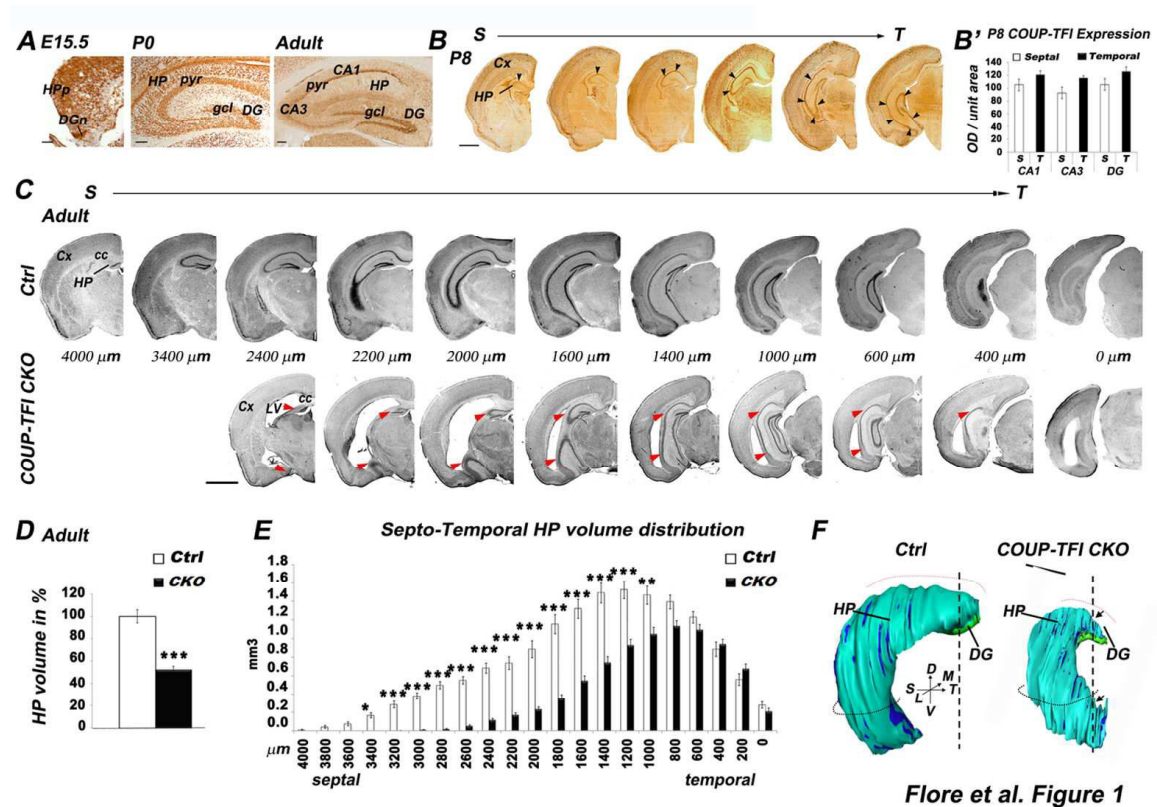
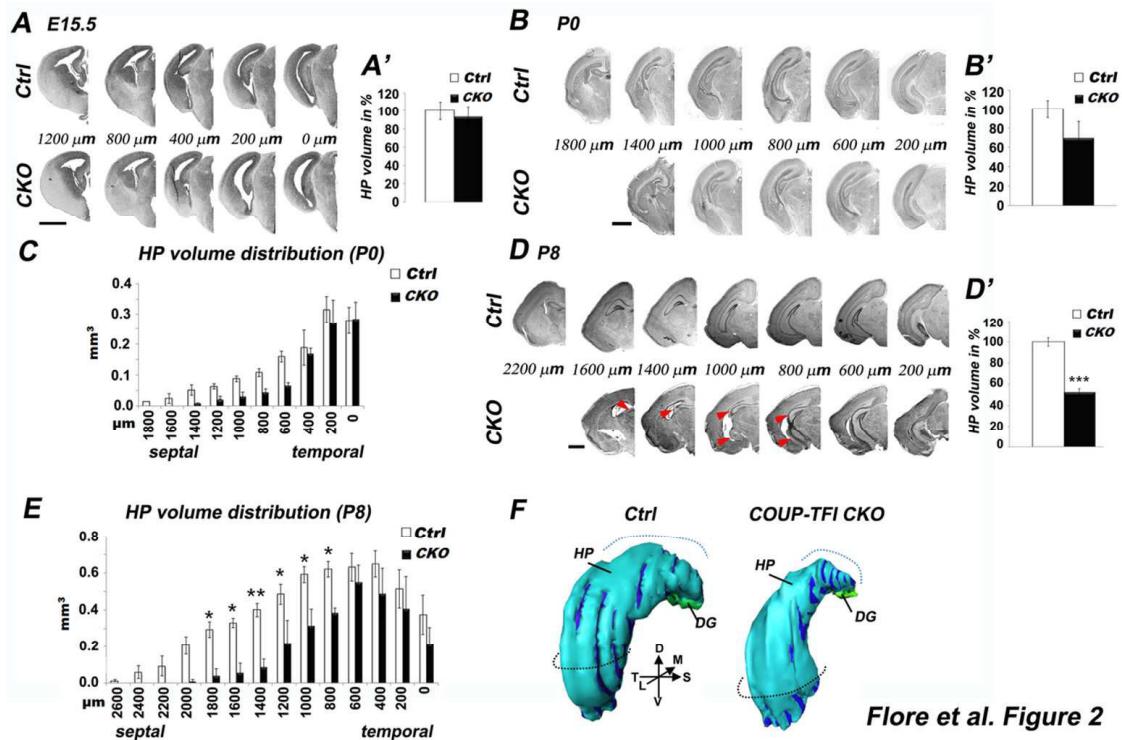


Figure 1. Absence of cortical COUP-TFI expression gradient leads to a dysmorphic hippocampus (HP) in adult mice. (A) COUP-TFI protein localization in mouse E15.5 and P0 coronal sections and in adult sagittal sections. (B, B') Black arrowheads indicate the increased graded dorsal to ventral COUP-TFI hippocampal expression from rostral to caudal coronal sections of a P8 representative brain (B), quantified as optical density (OD)/unit area expression in septal and temporal sections (B'). (C) Representative Nissl-stained sections of adult hippocampus in control (*Ctrl*) and *COUP-TFI CKO* mice at different antero-posterior sections (0µm representing the most caudal slice where the hippocampus is present). Red arrowheads indicate the reduction and caudal shift of the dorsal hippocampus in the mutant, compared to *control* brains of the same age. In contrast, the ventral part is comparable to that of *control* animals, although posteriorly shifted. (D, E) Histograms reporting the total hippocampal volume quantification and the hippocampal septo-temporal volume extension in percentage. (F) 3D reconstructions of the hippocampal hemispheres in *control* and *COUP-TFI CKO* mice highlight the overall reduction of the mutant HP and the imbalance between dorsal and ventral portions, leading to a “drop-like” dysmorphism in the mutant HP. Dashed lines indicate that the dorsal portion emerges almost at the same level as the ventral one in mutant brains (black arrows in *COUP-TFI-CKO*). Values are indicated in average ± S.E.M. Duncan post-hoc values: *CKO* vs. *Ctrl* * $p \leq 0.05$; ** $p \leq 0.01$; *** $p \leq 0.001$. Scale bars: (A) 50µm (E15.5); 50µm (P0); 100µm (Adult); (B) 1mm; (C) 2mm. HP, hippocampus; HPp, hippocampal primordium; DGn, Dentate Gyrus neuroepithelium; pyr, pyramidal layer; DG, Dentate Gyrus; CA1, CA3, Cornus Ammonis fields 1,3; gcl, granule cells layer; LV, Lateral ventricle; CC, corpus callosum; Cx, Cortex.



Flore et al. Figure 2

Figure 2. Postnatal hippocampal development is compromised by conditional inactivation of *COUP-TFI*. (A, B, D) Representative Nissl-stained sections of the hippocampal plate in *control* (*Ctrl*) and *COUP-TFI CKO* (*CKO*) mice show no abnormalities in embryonic mutant brains (A), but a trend of hippocampal decreased volume at birth (B, C), which becomes significant at P8 (D), (0 μ m representing the most caudal section where the hippocampus is present). Red arrowheads indicate the dramatic hippocampal defect evident in mutant mice at P8. (A', B', D') Histograms indicating the total hippocampal volume in percentage of *control* and *COUP-TFI CKO* mice at the different developmental ages, E15.5 (A'), P0 (B') and P8 (D'). At P0, although the hippocampal volume is reduced in *CKO* as compared to *control* mice, the difference does not reach statistical significance (B, B'). (C, E) Histograms representing the hippocampal rostro-caudal extension (%) in *control* and *COUP-TFI CKO* mice at P0 and P8. The overall volume (D, D'), the rostro-caudal extension and the dorsal hippocampus (E) are significantly reduced in P8 *CKO* dorsal/septal HP, with minor differences in the ventral/temporal region. (F) 3D reconstructions of the left hippocampal hemisphere in *control* and *COUP-TFI CKO* highlight the poor development of the dorsal *mutant* portion compared to the ventral one, which is more similar to *controls*. Values are indicated in average \pm S.E.M. Duncan *post-hoc* test, *p* values: **p* \leq 0.05; ***p* \leq 0.01; ****p* \leq 0.001 *CKO* vs. *Ctrl*, within slice. Scale bars: (A, B, D) 1mm. HP, hippocampus; DG, Dentate Gyrus.

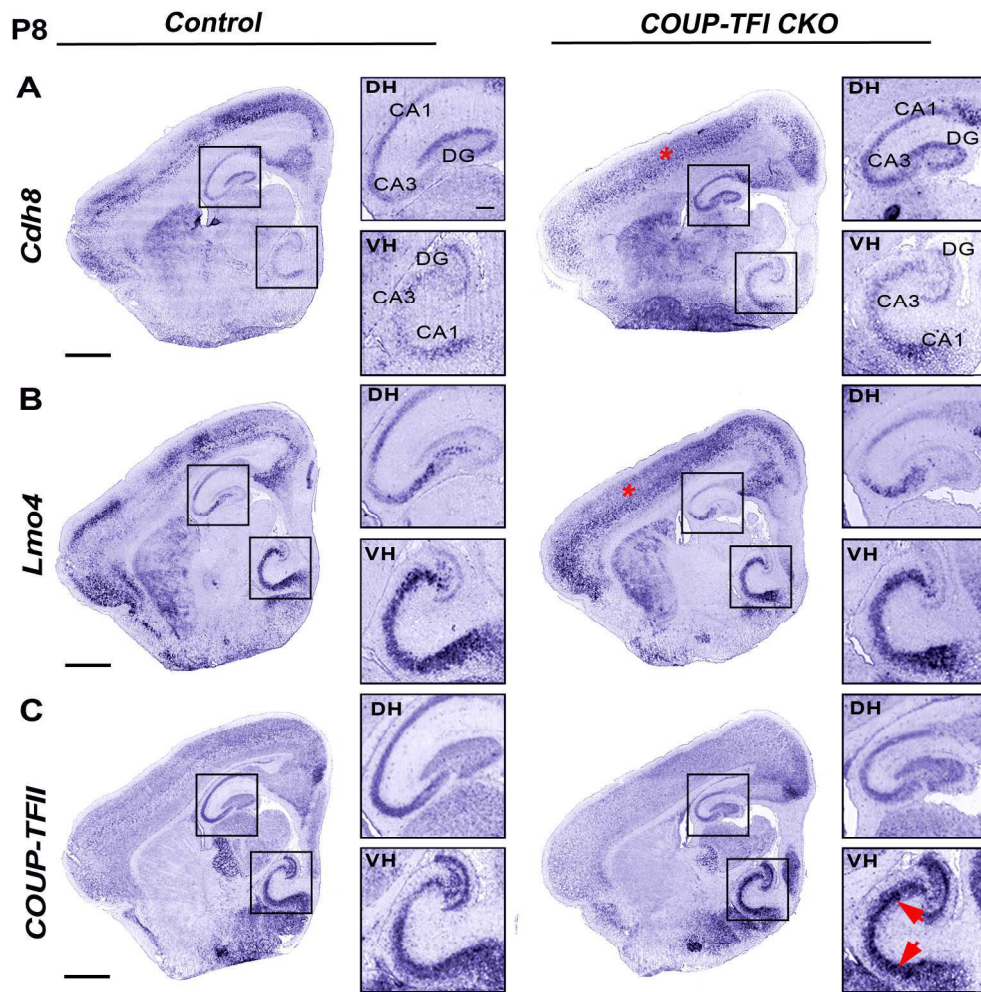
Flore *et al.* Figure 3

Figure 3. Preserved dorso-ventral identity of *COUP-TFI*-deficient hippocampi. (A-C) Para-sagittal sections of P8 *control* and *COUP-TFI CKO* brains hybridized with differentially expressed genes along the longitudinal hippocampal axis. Boxes indicate high magnification views of the dorsal (DH) and ventral (VH) hippocampus depicted to the right. (A) *Cadherin8* (*Cdh8*) transcript is expressed at higher levels in the dorsal than in the ventral hippocampus. Despite the reduced DH volume in the mutant brain, *Cdh8* is still expressed at higher levels in the DH. (B) The LIM domain transcription factor *Lmo4* is expressed at higher levels in the VH than in the DH in *controls* and *COUP-TFI CKO* brains. (C) The orphan receptor *COUP-TFII* is highly expressed in the VH. Levels of *COUP-TFII* expression in VH are increased in *COUP-TFI CKO* (indicated by red arrowheads). Red asterisks indicate altered expression of *Cdh8* and *Lmo4* in the neocortex, which have been previously reported (Armentano *et al.* 2007; Alfano *et al.* 2014). Scale bars: (A, B, C) 1mm.

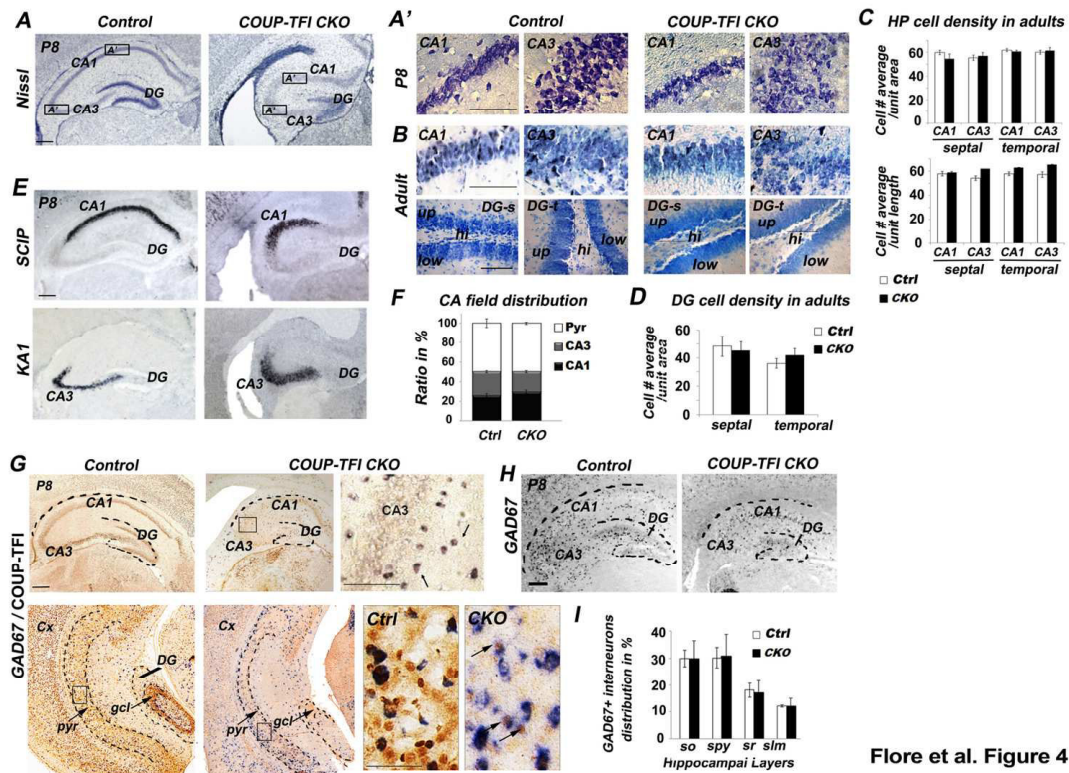
Flore *et al.* Figure 4

Figure 4. Adult *COUP-TFI CKO* hippocampi have preserved field specification, pyramidal cell density and GABAergic interneuron distribution. (A) Nissl staining of P8 coronal sections through the HP of *control* and *COUP-TFI CKO mutant* brains. Boxes indicate high magnification views of CA1 and CA3 and depicted in (A'). (B) Details of CA1, CA3 and DG in Nissl-stained adult *control* and *mutant* hippocampal coronal sections. (C, D) Histogram indicating neuronal cell density within the pyramidal layer of adult *control* and *CKO* hippocampi. The cell number and cell density *per unit area* and *per unit length* are comparable between the two genotypes in septal and temporal regions of CA1, CA3 (C) and DG (D). (E) Coronal sections of P8 *control* and *COUP-TFI CKO* HP taken at the same level and hybridized with *SCIP* for CA1 and *KAI1* for CA3. (F) Histogram indicating the field percentage representation within the pyramidal layer of *control* and *COUP-TFI CKO* HP. (G) Double *GAD67 in situ hybridization* (in blue)/*COUP-TFI immunohistochemistry* (in brown) on P8 coronal sections through septal (above) and temporal (below) HP. Boxes indicate high magnification views depicted to the right. In *mutants*, *COUP-TFI* co-labels solely with *GAD67*. (H) *In situ hybridization* of *GAD67* on P8 coronal sections of *control* and *COUP-TFI CKO* septal HP. (I) Histogram representing the percentage distribution of *GAD67+* neurons in *control* and *COUP-TFI CKO* HP. Values are indicated as average \pm S.E.M. Scale bars: (A,E,G,H) 250 μ m; (A',B) 100 μ m; (High mags in G, H) 500 μ m. Cx, cortex; HP, hippocampus; DG, Dentate Gyrus; CA1, CA3, Cornus Ammonis fields 1, 3; gcl, granule cell layer; pyr, pyramidal layer; so, stratum oriens; spy, stratum pyramidale; sr, stratum radiatum; slm, stratum lucidum moleculare; up, upper blade; low, lower blade, hi, hilus.

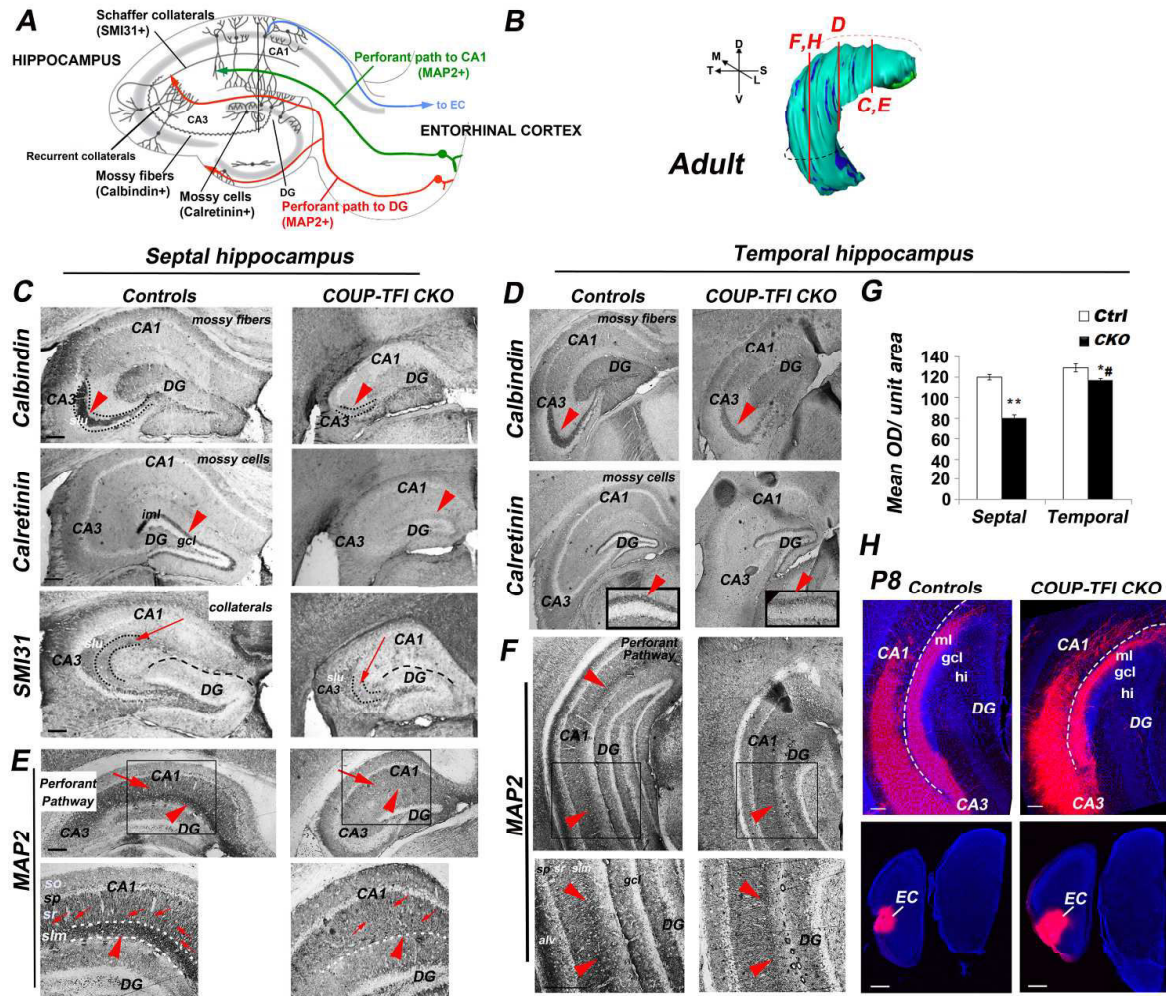
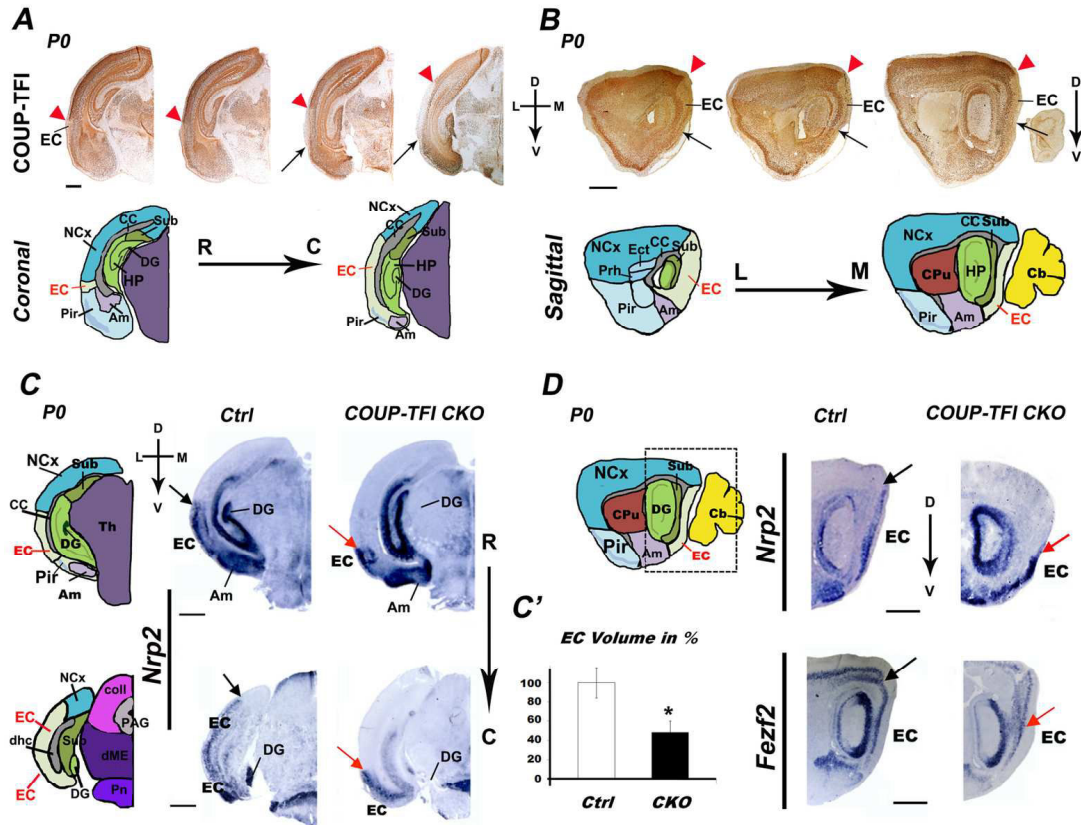
Flore *et al.* Figure 5

Figure 5. Impaired connectivity in the dorsal *COUP-TFI* mutant hippocampus. (A) Diagram of hippocampal anatomy and connectivity (modified from *Tutorial on neural systems modeling*, Sinauer Associates, Inc, 2010) mapping out the major circuits within the HP and between the HP and entorhinal cortex (EC). (B) 3-D reconstruction of a normal HP (taken from Fig. 1F) indicating the planes of sections shown in C to H. (C-F) Immunohistochemistry on coronal sections of adult *control* and *COUP-TFI CKO* dorsal (C, E) and ventral (D, F) HP. (C) Dotted lines and arrowheads indicate the calbindin-expressing stratum lucidum moleculare (slu) layer of mossy fibers axons. Red arrowheads indicate calretinin-expressing terminals of commissural fibers originating from hilar mossy cells, which normally reach the contralateral DG inner molecular layer (iml) of granule cells dendrites. SMI31-expressing CA3 axons, which normally form the Schaffer collaterals (dotted lines and red arrows) in the associative pathway; dashed lines indicate the DG upper blade border. (E) MAP2 normally labels CA1 pyramidal dendrites (arrows) and axons of the entorhinal perforant pathway (arrowheads). Boxes depict high magnification views of the CA1 regions label with MAP2 and illustrated below. (D) Calbindin is expressed at lower levels in the mossy fibers of *COUP-TFI* mutants at more ventral levels (arrowheads) when compared to *controls*. However, Calretinin is still expressed in commissural fibers of mutant HP at more ventral levels (arrowheads in insets). (F) Axonal MAP2 staining of the perforant path and in CA1 dendrites is partially maintained in ventral mutant HP (arrowheads). Boxes depict high magnification views of the CA1 region illustrated below. (G) Quantification of optical density (OD)/unit area of the perforant path labeled by MAP2 in dorsal (septal) and ventral sections (temporal). Values are indicated as average \pm S.E.M. Duncan post-hoc test,

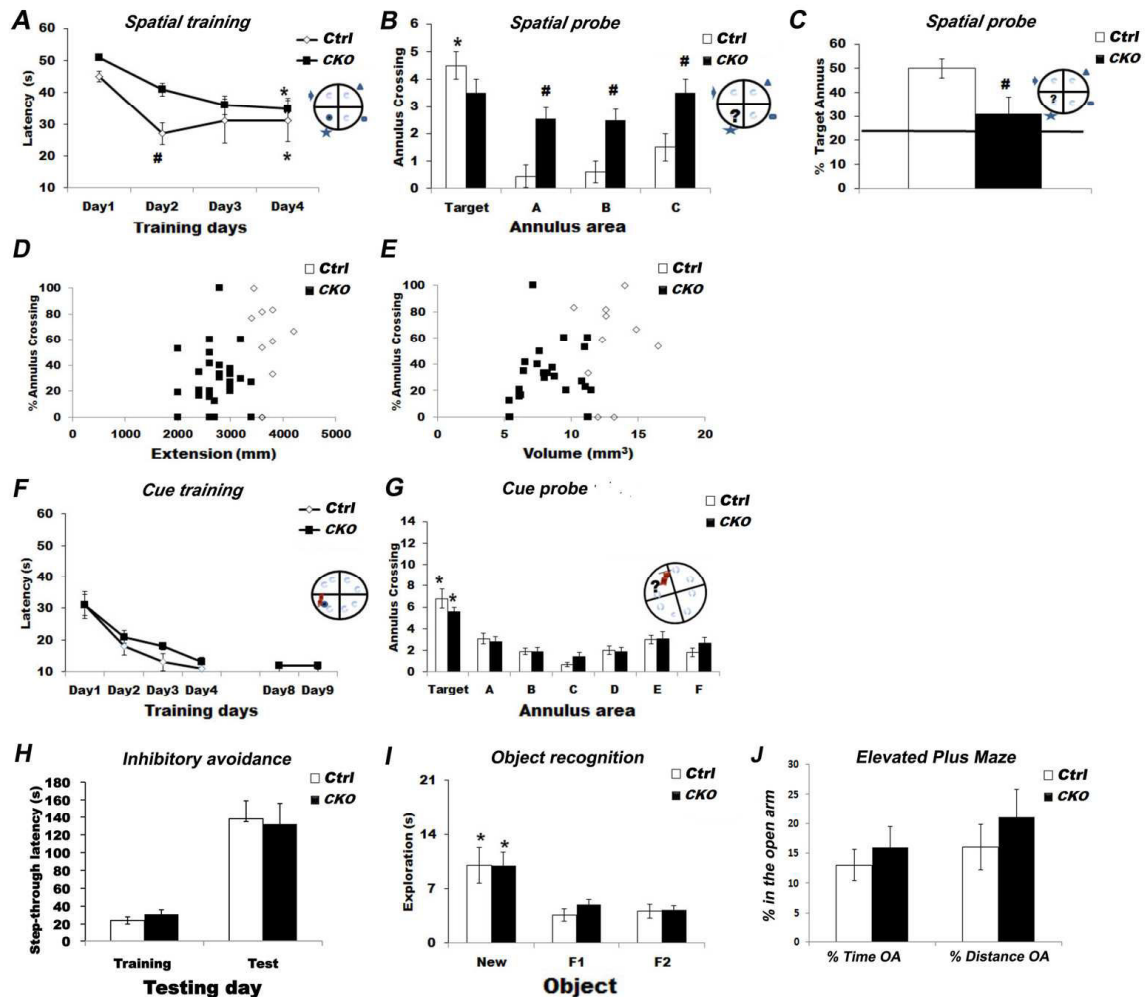
* $p < 0.05$, ** $p < 0.05$ *CKO* vs. *ctrl* within septo-temporal area, # $p < 0.05$ temporal vs. septal, within genotype. (H) Retrogradely DiI-labeled perforant paths in P8 *control* and *mutant* ventral HP. Below, region of the entorhinal cortex in which the DiI has been injected. Scale bars: (C-F, H above) $100\mu\text{m}$; (H below) $500\mu\text{m}$; HP, hippocampus; DG, Dentate Gyrus, EC, entorhinal cortex; hi, hilus; alv, alveus; gcl, granule cell layer; so, stratum oriens; sp, stratum pyramidale; sg, stratum granulosum; ml, molecular layer; sr, stratum radiatum; slm, stratum lucidum molecolare.



Flore *et al.* Figure 6

Figure 6. Reduced entorhinal cortex in *COUP-TFI* *CKO* mutants. (A-B) P0 brains stained with COUP-TFI antibody indicate a dorso-ventral gradient of expression for COUP-TFI in the entorhinal cortex (EC). Rostral to caudal coronal sections indicate an abruptly reduced expression at the level of the dorsal entorhinal cortex (red arrowheads), partially reestablished in the most ventromedial part at rostro-caudal levels (black arrows). Below schematics of the sections (A). Serial sagittal sections confirm the dorsal to ventral COUP-TFI gradient in the EC. Red arrowheads point to the neocortical to entorhinal cortical transition, and black arrows indicate the gradual-reestablishment of COUP-TFI expression in the most ventral EC region. Below schematics of the sections (B). (C-D) Paleocortical (*Nrp2*) and neocortical (*Fezf2*) marker expression in *control* and *COUP-TFI* *CKO* brains. *Nrp2* *in situ* hybridization on coronal sections at medial and caudal levels indicates reduced *Nrp2* expression in the *mutant* EC (compare black and red arrows). To the left schematics of the sections (C). (C') Histogram reports quantification of the EC volume in *control* and *COUP-TFI* *CKO* mice expressed in percentage (%). *Nrp2* and *Fezf2* *in situ* hybridization on sagittal sections indicate expanded expression of *Fezf2* at the expense of *Nrp2* in mutant dorsal EC (compare black and red arrows) (D). Values are indicated as average \pm S.E.M. * $p < 0.05$ *CKO* vs. *ctrl*. Scale bars: A, $200\mu\text{m}$; B-D, $500\mu\text{m}$. AM, amygdaloid nuclei, DG, Dentate Gyrus, fi, fimbria; Cpu, Caudato Putamen; CC, Corpus Callosum, Ncx, Neocortex, Pir, Piriform cortex; Sub,

subiculum;; EC, Entorhinal Cortex; Ect, entorhinal cortex; Prh, perirhinal cortex; coll, colliculus; PAG, Periaqueductal Gray; dME, deep Mesencephalic nucleus;; dhc, dorsal hippocampal commissure, Pn, pontine nuclei.



Flore et al. Figure 7

Figure 7. *COUP-TFI CKO* mice have impaired spatial memory but preserved visual-cue memory. (A-C) Behavior of *control* and *COUP-TFI CKO* mice in the spatial version of the water maze task. (A) *COUP-TFI CKO* mice show an increase in latency and time to reach the hidden platform during training. (B, C) During the probe trial, they have a random searching behavior with no preference (number of annulus crossing) and correct annulus (target). (D, E) Correlation between the percentage of target annulus searching on the probe trial with hippocampal extension (D) and volume (E) in *COUP-TFI CKO* (filled square) and *control* animals (open square). Both these histological measurements were significantly correlated with the percentage of crossing in the target annulus. * $p < 0.05$ Day 4 vs Day1 (A) or Target vs other annulus (B) within genotype; # $p < 0.05$ *COUP-TFI CKO* vs *controls*. (F-I) Behavior of *control* and *COUP-TFI CKO* mice in the cue version of the water maze task. (F) *COUP-TFI CKO* and *control* animals use the same time (s) to reach the cue signaled (flag) platform during training days. (G) Both groups show a clear preference for searching (number of annulus crossing) the platform in the correct annulus (target), when tested 1 day after the last training day. Values are indicated as average \pm S.E.M. * $p < 0.05$ Target vs other annulus (B) within genotype; # $p < 0.05$ *COUP-TFI CKO* vs *controls*.

(H-J) *COUP-TFI CKO* and *control* mice in the one-trial inhibitory avoidance **(H)** in object recognition **(I)**, and in the plus maze **(J)** tasks. **(H)** *COUP-TFI CKO* and *control* groups showed comparable step-through latency (s) during both training and testing (1 day after training) in the one trial inhibitory avoidance task, suggesting that *CKO* had intact capacity to form emotional long-term memory. **(I)** *COUP-TFI CKO* and *control* mice showed comparable new object exploration time (s) as compared to two familiar objects during the test phase of the object recognition task, suggesting that mutant mice had retained intact object recognition memory. **(J)** *COUP-TFI CKO* and *control* mice showed no significantly different percentage time and distance in the open arm of the plus-maze task, indicating that their anxiety level was comparable. Values are indicated as average \pm S.E.M. * $p < 0.05$ New vs familiar objects, within genotype.

References

- Abrous, D. N., Koehl, M. and Moal, L. M.** (2005) 'Adult neurogenesis: from precursors to network and physiology', *Physiological reviews*.
- Akirav, I., Kozenicky, M., Tal, D., Sandi, C., Venero, C. and Richter-Levin, G.** (2004) 'A facilitative role for corticosterone in the acquisition of a spatial task under moderate stress', *Learning & memory (Cold Spring Harbor, N.Y.)*, 11(2), pp. 188-195.
- Al-Kateb, H., Shimony, J. S., Vineyard, M., Manwaring, L., Kulkarni, S. and Shinawi, M.** (2013) 'NR2F1 haploinsufficiency is associated with optic atrophy, dysmorphism and global developmental delay', *American journal of medical genetics. Part A*, 161A(2), pp. 377-381.
- Alcántara, S., Ruiz, M., D'Arcangelo, G., Ezan, F., de Lecea, L., Curran, T., Sotelo, C. and Soriano, E.** (1998) 'Regional and cellular patterns of reelin mRNA expression in the forebrain of the developing and adult mouse', *The Journal of neuroscience : the official journal of the Society for Neuroscience*, 18(19), pp. 7779-7799.
- Alfano, C., Magrinelli, E., Harb, K. and Studer, M.** (2014) 'The nuclear receptors COUP-TF: a long-lasting experience in forebrain assembly', *Cellular and molecular life sciences : CMLS*, 71(1), pp. 43-62.
- Alfano, C., Viola, L., Heng, J. I., Pirozzi, M., Clarkson, M., Flore, G., De Maio, A., Schedl, A., Guillemot, F. and Studer, M.** (2011) 'COUP-TFI promotes radial migration and proper morphology of callosal projection neurons by repressing Rnd2 expression', *Development (Cambridge, England)*, 138(21), pp. 4685-4697.
- Alfonso, L., Oleg, V. L., Lionel, M. L. C., Suzanne, J. B. and Guillermo, O.** (2010) 'Prox1 Is Required for Granule Cell Maturation and Intermediate Progenitor Maintenance During Brain Neurogenesis', *PLoS Biology*, 8(8).
- Altman, J.** (1962) 'Are new neurons formed in the brains of adult mammals?', *Science (New York, N.Y.)*, 135(3509).
- Altman, J.** (1969) 'Autoradiographic and histological studies of postnatal neurogenesis. IV. Cell proliferation and migration in the anterior forebrain, with special reference to persisting neurogenesis in the olfactory bulb', *The Journal of comparative neurology*, 137(4), pp. 433-457.
- Altman, J. and Bayer, S. A.** (1990a) 'Mosaic organization of the hippocampal neuroepithelium and the multiple germinal sources of dentate granule cells', *The Journal of comparative neurology*, 301(3), pp. 325-342.
- Altman, J. and Bayer, S. A.** (1990b) 'Prolonged sojourn of developing pyramidal cells in the intermediate zone of the hippocampus and their settling in the stratum pyramidale', *The Journal of comparative neurology*, 301(3), pp. 343-364.
- Altman, J. and Bayer, S. A.** (1990c) 'Migration and distribution of two populations of hippocampal granule cell precursors during the perinatal and postnatal periods', *The Journal of comparative neurology*, 301(3), pp. 365-381.
- Altman, J. and Das, G. D.** (1965) 'Autoradiographic and histological evidence of postnatal hippocampal neurogenesis in rats', *The Journal of comparative neurology*, 124(3), pp. 319-335.
- Alvarez-Buylla, A. and Lim, D. A.** (2004) 'For the long run: maintaining germinal niches in the adult brain', *Neuron*, 41(5), pp. 683-686.
- Amador-Arjona, A., Cimadamore, F., Huang, C.-T. T., Wright, R., Lewis, S., Gage, F. H. and Terskikh, A. V.** (2015) 'SOX2 primes the epigenetic landscape in neural precursors enabling proper gene activation during hippocampal neurogenesis', *Proceedings of the National Academy of Sciences of the United States of America*, 112(15), pp. 45.
- Amaral, D. G. and Dent, J. A.** (1981) 'Development of the mossy fibers of the dentate gyrus: I. A light and electron microscopic study of the mossy fibers and their expansions', *The Journal of comparative neurology*, 195(1), pp. 51-86.

- Amaral, D. G., Insausti, R. and Cowan, W. M.** (1984) 'The commissural connections of the monkey hippocampal formation', *The Journal of comparative neurology*, 224(3), pp. 307-336.
- Amaral, D. G. and Witter, M. P.** (1989) 'The three-dimensional organization of the hippocampal formation: a review of anatomical data', *Neuroscience*, 31(3), pp. 571-591.
- Amrein, I., Slomianka, L. and Lipp, H.-P. P.** (2004) 'Granule cell number, cell death and cell proliferation in the dentate gyrus of wild-living rodents', *The European journal of neuroscience*, 20(12), pp. 3342-3350.
- Andersen, P., Bliss, T. V., Lomo, T., Olsen, L. I. and Skrede, K. K.** (1969) 'Lamellar organization of hippocampal excitatory pathways', *Acta physiologica Scandinavica*, 76(1).
- Angevine, J. B.** (1965) 'Time of neuron origin in the hippocampal region. An autoradiographic study in the mouse', *Experimental neurology. Supplement*, pp. 70.
- Armentano, M., Chou, S.-J. J., Tomassy, G. S., Leingärtner, A., O'Leary, D. D. and Studer, M.** (2007) 'COUP-TFI regulates the balance of cortical patterning between frontal/motor and sensory areas', *Nature neuroscience*, 10(10), pp. 1277-1286.
- Armentano, M., Filosa, A., Andolfi, G. and Studer, M.** (2006) 'COUP-TFI is required for the formation of commissural projections in the forebrain by regulating axonal growth', *Development (Cambridge, England)*, 133(21), pp. 4151-4162.
- Arnold, S. J., Huang, G.-J. J., Cheung, A. F., Era, T., Nishikawa, S.-I., Bikoff, E. K., Molnár, Z., Robertson, E. J. and Groszer, M.** (2008) 'The T-box transcription factor Eomes/Tbr2 regulates neurogenesis in the cortical subventricular zone', *Genes & development*, 22(18), pp. 2479-2484.
- Artavanis-Tsakonas, S., Rand, M. D. and Lake, R. J.** (1999) 'Notch signaling: cell fate control and signal integration in development', *Science (New York, N.Y.)*, 284(5415), pp. 770-776.
- Avram, D., Ishmael, J. E., Nevriy, D. J., Peterson, V. J., Lee, S. H., Dowell, P. and Leid, M.** (1999) 'Heterodimeric interactions between chicken ovalbumin upstream promoter-transcription factor family members ARP1 and ear2', *The Journal of biological chemistry*, 274(20), pp. 14331-14336.
- Bagri, A., Gurney, T., He, X., Zou, Y.-R. R., Littman, D. R., Tessier-Lavigne, M. and Pleasure, S. J.** (2002) 'The chemokine SDF1 regulates migration of dentate granule cells', *Development (Cambridge, England)*, 129(18), pp. 4249-4260.
- Baimbridge, K. G. and Miller, J. J.** (1982) 'Immunohistochemical localization of calcium-binding protein in the cerebellum, hippocampal formation and olfactory bulb of the rat', *Brain research*, 245(2), pp. 223-229.
- Bajetto, A., Bonavia, R., Barbero, S., Florio, T. and Schettini, G.** (2001) 'Chemokines and their receptors in the central nervous system', *Frontiers in neuroendocrinology*, 22(3), pp. 147-184.
- Baker, K. B. and Kim, J. J.** (2002) 'Effects of stress and hippocampal NMDA receptor antagonism on recognition memory in rats', *Learning & memory (Cold Spring Harbor, N.Y.)*, 9(2), pp. 58-65.
- Bani-Yaghoob, M., Tremblay, R. G., Lei, J. X., Zhang, D., Zurakowski, B., Sandhu, J. K., Smith, B., Ribocco-Lutkiewicz, M., Kennedy, J., Walker, P. R. and Sikorska, M.** (2006) 'Role of Sox2 in the development of the mouse neocortex', *Developmental biology*, 295(1), pp. 52-66.
- Baraban, S. C.** (2007) 'Emerging epilepsy models: insights from mice, flies, worms and fish', *Current opinion in neurology*, 20(2), pp. 164-168.
- Barkovich, A. J., Koch, T. K. and Carrol, C. L.** (1991) 'The spectrum of lissencephaly: report of ten patients analyzed by magnetic resonance imaging', *Annals of neurology*, 30(2), pp. 139-146.
- Bartholomä, A. and Nave, K. A.** (1994) 'NEX-1: a novel brain-specific helix-loop-helix protein with autoregulation and sustained expression in mature cortical neurons', *Mechanisms of development*, 48(3), pp. 217-228.
- Baulac, M., De Grissac, N., Hasboun, D., Oppenheim, C., Adam, C., Arzimanoglou, A., Semah, F., Lehericy, S., Clémenceau, S. and Berger, B.** (1998) 'Hippocampal developmental

- changes in patients with partial epilepsy: magnetic resonance imaging and clinical aspects', *Annals of neurology*, 44(2), pp. 223-233.
- Bayer, S. A.** (1980a) 'Development of the hippocampal region in the rat. I. Neurogenesis examined with 3H-thymidine autoradiography', *The Journal of comparative neurology*, 190(1), pp. 87-114.
- Bayer, S. A.** (1980b) 'Development of the hippocampal region in the rat. II. Morphogenesis during embryonic and early postnatal life', *The Journal of comparative neurology*, 190(1), pp. 115-134.
- Bayer, S. A.** (1985) 'Hippocampal region In G. Paxinos (Ed.) The Rat Nervous System Vol1; Forebrain and Midbrain', *New York, Academic Press* pp. 335-352.
- Bedogni, F., Hodge, R. D., Elsen, G. E., Nelson, B. R., Daza, R. A., Beyer, R. P., Bammler, T. K., Rubenstein, J. L. and Hevner, R. F.** (2010) 'Tbr1 regulates regional and laminar identity of postmitotic neurons in developing neocortex', *Proceedings of the National Academy of Sciences of the United States of America*, 107(29), pp. 13129-13134.
- Bellenchi, G. C., Gurniak, C. B., Perlas, E., Middei, S., Ammassari-Teule, M. and Witke, W.** (2007) 'N-cofilin is associated with neuronal migration disorders and cell cycle control in the cerebral cortex', *Genes & development*, 21(18), pp. 2347-2357.
- Benito-Sipos, J., Ulvklo, C., Gabilondo, H., Baumgardt, M., Angel, A., Torroja, L. and Thor, S.** (2011) 'Seven up acts as a temporal factor during two different stages of neuroblast 5-6 development', *Development (Cambridge, England)*, 138(24), pp. 5311-5320.
- Berrodin, T. J., Marks, M. S., Ozato, K., Linney, E. and Lazar, M. A.** (1992) 'Heterodimerization among thyroid hormone receptor, retinoic acid receptor, retinoid X receptor, chicken ovalbumin upstream promoter transcription factor, and an endogenous liver protein', *Molecular endocrinology (Baltimore, Md.)*, 6(9), pp. 1468-1478.
- Bishop, K. M., Goudreau, G. and O'Leary, D. D.** (2000) 'Regulation of area identity in the mammalian neocortex by Emx2 and Pax6', *Science (New York, N.Y.)*, 288(5464), pp. 344-349.
- Blaabjerg, M. and Zimmer, J.** (2007) 'The dentate mossy fibers: structural organization, development and plasticity', *Progress in brain research*, 163, pp. 85-107.
- Blackstad, T. W.** (1956) 'Commissural connections of the hippocampal region in the rat, with special reference to their mode of termination', *The Journal of comparative neurology*, 105(3).
- Blackstad, T. W., Brink, K., Hem, J. and Jeune, B.** (1970) 'Distribution of hippocampal mossy fibers in the rat. An experimental study with silver impregnation methods', *The Journal of comparative neurology*, 138(4), pp. 433-449.
- Bobinski, M., de Leon, M. J., Wegiel, J., Desanti, S., Convit, A., Saint Louis, L. A., Rusinek, H. and Wisniewski, H. M.** (2000) 'The histological validation of post mortem magnetic resonance imaging-determined hippocampal volume in Alzheimer's disease', *Neuroscience*, 95(3), pp. 721-725.
- Bond, N. W., Walton, J. and Pruss, J.** (1989) 'Restoration of memory following septo-hippocampal grafts: a possible treatment for Alzheimer's disease', *Biological psychology*, 28(1), pp. 67-87.
- Borello, U., Madhavan, M., Vilinsky, I., Faedo, A., Pierani, A., Rubenstein, J. and Campbell, K.** (2014) 'Sp8 and COUP-TF1 reciprocally regulate patterning and Fgf signaling in cortical progenitors', *Cerebral cortex (New York, N.Y. : 1991)*, 24(6), pp. 1409-1421.
- Borello, U. and Pierani, A.** (2010) 'Patterning the cerebral cortex: traveling with morphogens', *Current opinion in genetics & development*, 20(4), pp. 408-415.
- Borrell, V. and Marín, O.** (2006) 'Meninges control tangential migration of hem-derived Cajal-Retzius cells via CXCL12/CXCR4 signaling', *Nature neuroscience*, 9(10), pp. 1284-1293.
- Bosch, D. G. G., Boonstra, F. N., Gonzaga-Jauregui, C., Xu, M., de Ligt, J., Jhangiani, S., Wiszniewski, W., Muzny, D. M., Yntema, H. G., Pfundt, R., Vissers, L. E., Spruijt, L., Blokland, E. A., Chen, C.-A. A., Baylor-Hopkins Center for Mendelian, G., Lewis, R. A.,**

- Tsai, S. Y., Gibbs, R. A., Tsai, M.-J. J., Lupski, J. R., Zoghbi, H. Y., Cremers, F. P., de Vries, B. B. and Schaaf, C. P. (2014) 'NR2F1 mutations cause optic atrophy with intellectual disability', *American journal of human genetics*, 94(2), pp. 303-309.
- Boudot, A., Kerdivel, G., Lecomte, S., Flouriot, G., Desille, M., Godey, F., Leveque, J., Tas, P., Le Dréan, Y. and Pakdel, F. (2014) 'COUP-TFI modifies CXCL12 and CXCR4 expression by activating EGF signaling and stimulates breast cancer cell migration', *BMC cancer*, 14, pp. 407.
- Bouilleret, V., Ridoux, V., Depaulis, A., Marescaux, C., Nehlig, A. and Le Gal La Salle, G. (1999) 'Recurrent seizures and hippocampal sclerosis following intrahippocampal kainate injection in adult mice: electroencephalography, histopathology and synaptic reorganization similar to mesial temporal lobe epilepsy', *Neuroscience*, 89(3), pp. 717-729.
- Boyle, M. P., Bernard, A., Thompson, C. L., Ng, L., Boe, A., Mortrud, M., Hawrylycz, M. J., Jones, A. R., Hevner, R. F. and Lein, E. S. (2011) 'Cell-type-specific consequences of Reelin deficiency in the mouse neocortex, hippocampus, and amygdala', *The Journal of comparative neurology*, 519(11), pp. 2061-2089.
- Braak, H., Braak, E. and Bohl, J. (1993) 'Staging of Alzheimer-related cortical destruction', *European neurology*, 33(6), pp. 403-408.
- Brandt, M. D., Jessberger, S., Steiner, B., Kronenberg, G., Reuter, K., Bick-Sander, A., von der Behrens, W. and Kempermann, G. (2003) 'Transient calretinin expression defines early postmitotic step of neuronal differentiation in adult hippocampal neurogenesis of mice', *Molecular and cellular neurosciences*, 24(3), pp. 603-613.
- Brodal, A. (1947) 'The hippocampus and the sense of smell; a review', *Brain : a journal of neurology*, 70(Pt 2).
- Brodal, A. (1981) 'Neurological anatomy in relation to clinical medicine. Third edition', *New York, Oxford University Press*, 10(6).
- Brown, J., Cooper-Kuhn, C. M., Kempermann, G., Van Praag, H., Winkler, J., Gage, F. H. and Kuhn, H. G. (2003) 'Enriched environment and physical activity stimulate hippocampal but not olfactory bulb neurogenesis', *The European journal of neuroscience*, 17(10), pp. 2042-2046.
- Brown, K. K., Alkuraya, F. S., Matos, M., Robertson, R. L., Kimonis, V. E. and Morton, C. C. (2009) 'NR2F1 deletion in a patient with a de novo paracentric inversion, inv(5)(q15q33.2), and syndromic deafness', *American journal of medical genetics. Part A*, 149A(5), pp. 931-938.
- Butt, S. J., Fuccillo, M., Nery, S., Noctor, S., Kriegstein, A., Corbin, J. G. and Fishell, G. (2005) 'The temporal and spatial origins of cortical interneurons predict their physiological subtype', *Neuron*, 48(4), pp. 591-604.
- Bylund, M., Andersson, E., Novitsch, B. G. and Muhr, J. (2003) 'Vertebrate neurogenesis is counteracted by Sox1-3 activity', *Nature neuroscience*, 6(11), pp. 1162-1168.
- Cameron, H. A. and Gould, E. (1994) 'Adult neurogenesis is regulated by adrenal steroids in the dentate gyrus', *Neuroscience*, 61(2), pp. 203-209.
- Campbell, S., Marriott, M., Nahmias, C. and MacQueen, G. M. (2004) 'Lower hippocampal volume in patients suffering from depression: a meta-analysis', *The American journal of psychiatry*, 161(4), pp. 598-607.
- Cardoso, C., Boys, A., Parrini, E., Mignon-Ravix, C., McMahon, J. M., Khantane, S., Bertini, E., Pallesi, E., Missirian, C., Zuffardi, O., Novara, F., Villard, L., Giglio, S., Chabrol, B., Slater, H. R., Moncla, A., Scheffer, I. E. and Guerrini, R. (2009) 'Periventricular heterotopia, mental retardation, and epilepsy associated with 5q14.3-q15 deletion', *Neurology*, 72(9), pp. 784-792.
- Casanova, J., Helmer, E., Selmi-Ruby, S., Qi, J. S., Au-Fliegner, M., Desai-Yajnik, V., Koudinova, N., Yarm, F., Raaka, B. M. and Samuels, H. H. (1994) 'Functional evidence for ligand-

- dependent dissociation of thyroid hormone and retinoic acid receptors from an inhibitory cellular factor', *Molecular and cellular biology*, 14(9), pp. 5756-5765.
- Castillo, P. E., Malenka, R. C. and Nicoll, R. A.** (1997) 'Kainate receptors mediate a slow postsynaptic current in hippocampal CA3 neurons', *Nature*, 388(6638), pp. 182-186.
- Cavazos, J. E., Golarai, G. and Sutula, T. P.** (1991) 'Mossy fiber synaptic reorganization induced by kindling: time course of development, progression, and permanence', *The Journal of neuroscience : the official journal of the Society for Neuroscience*, 11(9), pp. 2795-2803.
- Caviness, V. S.** (1973) 'Time of neuron origin in the hippocampus and dentate gyrus of normal and reeler mutant mice: an autoradiographic analysis', *The Journal of comparative neurology*, 151(2), pp. 113-120.
- Cebolla, B. and Vallejo, M.** (2006) 'Nuclear factor-I regulates glial fibrillary acidic protein gene expression in astrocytes differentiated from cortical precursor cells', *Journal of neurochemistry*, 97(4), pp. 1057-1070.
- Celio, M. R.** (1990) 'Calbindin D-28k and parvalbumin in the rat nervous system', *Neuroscience*, 35(2), pp. 375-475.
- Chiu, Y.-C. C., Algase, D., Whall, A., Liang, J., Liu, H.-C. C., Lin, K.-N. N. and Wang, P.-N. N.** (2004) 'Getting lost: directed attention and executive functions in early Alzheimer's disease patients', *Dementia and geriatric cognitive disorders*, 17(3), pp. 174-180.
- Choe, Y., Kozlova, A., Graf, D. and Pleasure, S. J.** (2013) 'Bone morphogenic protein signaling is a major determinant of dentate development', *The Journal of neuroscience : the official journal of the Society for Neuroscience*, 33(16), pp. 6766-6775.
- Cholfin, J. A. and Rubenstein, J. L.** (2008) 'Frontal cortex subdivision patterning is coordinately regulated by Fgf8, Fgf17, and Emx2', *The Journal of comparative neurology*, 509(2), pp. 144-155.
- Christensen, T., Bisgaard, C. F., Nielsen, H. B. and Wiborg, O.** (2010) 'Transcriptome differentiation along the dorso-ventral axis in laser-captured microdissected rat hippocampal granular cell layer', *Neuroscience*, 170(3), pp. 731741.
- Christophe, G., François, G. and Carlos, M. P.** (2008) 'Neurogenin 2 has an essential role in development of the dentate gyrus', *Development*, 135(11), pp. 2031-2041.
- Chédotal, A. and Rijli, F. M.** (2009) 'Transcriptional regulation of tangential neuronal migration in the developing forebrain', *Current opinion in neurobiology*, 19(2), pp. 139-145.
- Claiborne, B. J., Amaral, D. G. and Cowan, W. M.** (1986) 'A light and electron microscopic analysis of the mossy fibers of the rat dentate gyrus', *The Journal of comparative neurology*, 246(4), pp. 435-458.
- Clotman, F., Van Maele-Fabry, G. and Picard, J. J.** (1998) 'All-trans-retinoic acid upregulates the expression of COUP-TFI in early-somite mouse embryos cultured in vitro', *Neurotoxicology and teratology*, 20(6), pp. 591-599.
- Conrad, C. D., Lupien, S. J. and McEwen, B. S.** (1999) 'Support for a bimodal role for type II adrenal steroid receptors in spatial memory', *Neurobiology of learning and memory*, 72(1), pp. 39-46.
- Convit, A., De Leon, M. J., Tarshish, C., De Santi, S., Tsui, W., Rusinek, H. and George, A.** (1997) 'Specific hippocampal volume reductions in individuals at risk for Alzheimer's disease', *Neurobiology of aging*, 18(2), pp. 131-138.
- Cooney, A. J., Leng, X., Tsai, S. Y., O'Malley, B. W. and Tsai, M. J.** (1993) 'Multiple mechanisms of chicken ovalbumin upstream promoter transcription factor-dependent repression of transactivation by the vitamin D, thyroid hormone, and retinoic acid receptors', *The Journal of biological chemistry*, 268(6), pp. 4152-4160.
- Cooney, A. J., Tsai, S. Y., O'Malley, B. W. and Tsai, M. J.** (1992) 'Chicken ovalbumin upstream promoter transcription factor (COUP-TF) dimers bind to different GGTC A response elements,

- allowing COUP-TF to repress hormonal induction of the vitamin D3, thyroid hormone, and retinoic acid receptors', *Molecular and cellular biology*, 12(9), pp. 4153-4163.
- Corbin, J. G., Nery, S. and Fishell, G.** (2001) 'Telencephalic cells take a tangent: non-radial migration in the mammalian forebrain', *Nature neuroscience*, 4 Suppl, pp. 1177-1182.
- Corbo, J. C., Deuel, T. A., Long, J. M., LaPorte, P., Tsai, E., Wynshaw-Boris, A. and Walsh, C. A.** (2002) 'Doublecortin is required in mice for lamination of the hippocampus but not the neocortex', *The Journal of neuroscience : the official journal of the Society for Neuroscience*, 22(17), pp. 7548-7557.
- Cordero, M. I., Venero, C., Kruyt, N. D. and Sandi, C.** (2003) 'Prior exposure to a single stress session facilitates subsequent contextual fear conditioning in rats. Evidence for a role of corticosterone', *Hormones and behavior*, 44(4), pp. 338-345.
- Cossart, R., Bernard, C. and Ben-Ari, Y.** (2005) 'Multiple facets of GABAergic neurons and synapses: multiple fates of GABA signalling in epilepsies', *Trends in neurosciences*, 28(2), pp. 108-115.
- Cui, Z., Gerfen, C. R. and Young, W. S.** (2013) 'Hypothalamic and other connections with dorsal CA2 area of the mouse hippocampus', *The Journal of comparative neurology*, 521(8), pp. 1844-1866.
- Dedovic, K., Duchesne, A., Andrews, J., Engert, V. and Pruessner, J. C.** (2009) 'The brain and the stress axis: the neural correlates of cortisol regulation in response to stress', *NeuroImage*, 47(3), pp. 864-871.
- Del Río, J. A., Heimrich, B., Borrell, V., Förster, E., Drakew, A., Alcántara, S., Nakajima, K., Miyata, T., Ogawa, M., Mikoshiba, K., Derer, P., Frotscher, M. and Soriano, E.** (1997) 'A role for Cajal-Retzius cells and reelin in the development of hippocampal connections', *Nature*, 385(6611), pp. 70-74.
- des Portes, V., Francis, F., Pinard, J. M., Desguerre, I., Moutard, M. L., Snoeck, I., Meiners, L. C., Capron, F., Cusmai, R., Ricci, S., Motte, J., Echenne, B., Ponsot, G., Dulac, O., Chelly, J. and Beldjord, C.** (1998) 'doublecortin is the major gene causing X-linked subcortical laminar heterotopia (SCLH)', *Human molecular genetics*, 7(7), pp. 1063-1070.
- Deuel, T. A., Liu, J. S., Corbo, J. C., Yoo, S.-Y. Y., Rorke-Adams, L. B. and Walsh, C. A.** (2006) 'Genetic interactions between doublecortin and doublecortin-like kinase in neuronal migration and axon outgrowth', *Neuron*, 49(1), pp. 41-53.
- Diamond, D. M., Fleshner, M., Ingersoll, N. and Rose, G. M.** (1996) 'Psychological stress impairs spatial working memory: relevance to electrophysiological studies of hippocampal function', *Behavioral neuroscience*, 110(4), pp. 661-672.
- Diamond, D. M. and Park, C. R.** (2000) 'Predator exposure produces retrograde amnesia and blocks synaptic plasticity. Progress toward understanding how the hippocampus is affected by stress', *Annals of the New York Academy of Sciences*, 911, pp. 453-455.
- Diep, D. B., Hoen, N., Backman, M., Machon, O. and Krauss, S.** (2004) 'Characterisation of the Wnt antagonists and their response to conditionally activated Wnt signalling in the developing mouse forebrain', *Brain research. Developmental brain research*, 153(2), pp. 261-270.
- Dobyns, W. B., Andermann, E., Andermann, F., Czapansky-Beilman, D., Dubeau, F., Dulac, O., Guerrini, R., Hirsch, B., Ledbetter, D. H., Lee, N. S., Motte, J., Pinard, J. M., Radtke, R. A., Ross, M. E., Tampieri, D., Walsh, C. A. and Truwit, C. L.** (1996) 'X-linked malformations of neuronal migration', *Neurology*, 47(2), pp. 331-339.
- Doe, C. Q.** (2008) 'Neural stem cells: balancing self-renewal with differentiation', *Development (Cambridge, England)*, 135(9), pp. 1575-1587.
- Donmez, F. Y., Yildirim, M., Erkek, N., Demir Karacan, C. and Coskun, M.** (2009) 'Hippocampal abnormalities associated with various congenital malformations', *Child's nervous system :*

- ChNS : official journal of the International Society for Pediatric Neurosurgery*, 25(8), pp. 933-939.
- Drakew, A., Frotscher, M. and Heimrich, B.** (1999) 'Blockade of neuronal activity alters spine maturation of dentate granule cells but not their dendritic arborization', *Neuroscience*, 94(3), pp. 767-774.
- Duan, D., Fu, Y., Paxinos, G. and Watson, C.** (2013) 'Spatiotemporal expression patterns of Pax6 in the brain of embryonic, newborn, and adult mice', *Brain structure & function*, 218(2), pp. 353-372.
- Dulabon, L., Olson, E. C., Taglienti, M. G., Eisenhuth, S., McGrath, B., Walsh, C. A., Kreidberg, J. A. and Anton, E. S.** (2000) 'Reelin binds alpha3beta1 integrin and inhibits neuronal migration', *Neuron*, 27(1), pp. 33-44.
- Dumas, T. C., Powers, E. C., Tarapore, P. E. and Sapolsky, R. M.** (2004) 'Overexpression of calbindin D(28k) in dentate gyrus granule cells alters mossy fiber presynaptic function and impairs hippocampal-dependent memory', *Hippocampus*, 14(6), pp. 701-709.
- Easwaran, V., Pishvaian, M., Salimuddin and Byers, S.** (1999) 'Cross-regulation of beta-catenin-LEF/TCF and retinoid signaling pathways', *Current biology : CB*, 9(23), pp. 1415-1418.
- Eckenhoff, M. F. and Rakic, P.** (1984) 'Radial organization of the hippocampal dentate gyrus: a Golgi, ultrastructural, and immunocytochemical analysis in the developing rhesus monkey', *The Journal of comparative neurology*, 223(1), pp. 1-21.
- Ekstrom, A. D., Kahana, M. J., Caplan, J. B., Fields, T. A., Isham, E. A., Newman, E. L. and Fried, I.** (2003) 'Cellular networks underlying human spatial navigation', *Nature*, 425(6954), pp. 184-188.
- Englund, C., Fink, A., Lau, C., Pham, D., Daza, R. A., Bulfone, A., Kowalczyk, T. and Hevner, R. F.** (2005) 'Pax6, Tbr2, and Tbr1 are expressed sequentially by radial glia, intermediate progenitor cells, and postmitotic neurons in developing neocortex', *The Journal of neuroscience : the official journal of the Society for Neuroscience*, 25(1), pp. 247-251.
- Eriksson, P. S., Perfilieva, E., Björk-Eriksson, T., Alborn, A. M., Nordborg, C., Peterson, D. A. and Gage, F. H.** (1998) 'Neurogenesis in the adult human hippocampus', *Nature medicine*, 4(11), pp. 1313-1317.
- Faedo, A., Tomassy, G. S., Ruan, Y., Teichmann, H., Krauss, S., Pleasure, S. J., Tsai, S. Y., Tsai, M.-J. J., Studer, M. and Rubenstein, J. L.** (2008) 'COUP-TFI coordinates cortical patterning, neurogenesis, and laminar fate and modulates MAPK/ERK, AKT, and beta-catenin signaling', *Cerebral cortex (New York, N.Y. : 1991)*, 18(9), pp. 2117-2131.
- Fanselow, M. S. and Dong, H.-W. W.** (2010) 'Are the dorsal and ventral hippocampus functionally distinct structures?', *Neuron*, 65(1), pp. 7-19.
- Faux, C., Rakic, S., Andrews, W. and Britto, J. M.** (2012) 'Neurons on the move: migration and lamination of cortical interneurons', *Neuro-Signals*, 20(3), pp. 168-189.
- Favaro, R., Valotta, M., Ferri, A. L., Latorre, E., Mariani, J., Giachino, C., Lancini, C., Tosetti, V., Ottolenghi, S., Taylor, V. and Nicolis, S. K.** (2009) 'Hippocampal development and neural stem cell maintenance require Sox2-dependent regulation of Shh', *Nature neuroscience*, 12(10), pp. 1248-1256.
- Feng, G., Mellor, R. H., Bernstein, M., Keller-Peck, C., Nguyen, Q. T., Wallace, M., Nerbonne, J. M., Lichtman, J. W. and Sanes, J. R.** (2000) 'Imaging neuronal subsets in transgenic mice expressing multiple spectral variants of GFP', *Neuron*, 28(1), pp. 41-51.
- Ferri, A. L., Cavallaro, M., Braidà, D., Di Cristofano, A., Canta, A., Vezzani, A., Ottolenghi, S., Pandolfi, P. P., Sala, M., DeBiasi, S. and Nicolis, S. K.** (2004) 'Sox2 deficiency causes neurodegeneration and impaired neurogenesis in the adult mouse brain', *Development (Cambridge, England)*, 131(15), pp. 3805-3819.

- Fjose, A., Weber, U. and Mlodzik, M.** (1995) 'A novel vertebrate svp-related nuclear receptor is expressed as a step gradient in developing rhombomeres and is affected by retinoic acid', *Mechanisms of development*, 52(2-3), pp. 233-246.
- Fleck, M. W., Hirotsune, S., Gambello, M. J., Phillips-Tansey, E., Soares, G., Mervis, R. F., Wynshaw-Boris, A. and McBain, C. J.** (2000) 'Hippocampal abnormalities and enhanced excitability in a murine model of human lissencephaly', *The Journal of neuroscience : the official journal of the Society for Neuroscience*, 20(7), pp. 2439-2450.
- Flore, G., Di Ruberto, G., Parisot, J., Sannino, S., Russo, F., Studer, M. and De Leonibus, E.** (2015) 'Gradient COUP-TFI Expression is Required for Functional Organization of the Hippocampal Septo-Temporal Longitudinal Axis (manuscript in annexe)', *Cerebral Cortex*.
- Förster, E., Jossin, Y., Zhao, S., Chai, X., Frotscher, M. and Goffinet, A. M. M.** (2006) 'Recent progress in understanding the role of Reelin in radial neuronal migration, with specific emphasis on the dentate gyrus', *The European journal of neuroscience*, 23(4), pp. 901-909.
- Förster, E., Tielsch, A., Saum, B., Weiss, K. H., Johanssen, C., Graus-Porta, D., Müller, U. and Frotscher, M.** (2002) 'Reelin, Disabled 1, and beta 1 integrins are required for the formation of the radial glial scaffold in the hippocampus', *Proceedings of the National Academy of Sciences of the United States of America*, 99(20), pp. 13178-13183.
- Foy, M. R., Stanton, M. E., Levine, S. and Thompson, R. F.** (1987) 'Behavioral stress impairs long-term potentiation in rodent hippocampus', *Behavioral and neural biology*, 48(1), pp. 138-149.
- Frantz, G. D., Bohner, A. P., Akers, R. M. and McConnell, S. K.** (1994) 'Regulation of the POU domain gene SCIP during cerebral cortical development', *The Journal of neuroscience : the official journal of the Society for Neuroscience*, 14(2), pp. 472-485.
- Freund, T. F. and Buzsáki, G.** (1996) 'Interneurons of the hippocampus', *Hippocampus*, 6(4), pp. 347-470.
- Frotscher, M.** (1992) 'Application of the Golgi/electron microscopy technique for cell identification in immunocytochemical, retrograde labeling, and developmental studies of hippocampal neurons', *Microscopy research and technique*, 23(4), pp. 306-323.
- Frotscher, M., Drakew, A. and Heimrich, B.** (2000) 'Role of afferent innervation and neuronal activity in dendritic development and spine maturation of fascia dentata granule cells', *Cerebral cortex (New York, N.Y. : 1991)*, 10(10), pp. 946-951.
- Frotscher, M., Zhao, S. and Förster, E.** (2007) 'Development of cell and fiber layers in the dentate gyrus', *Progress in brain research*, 163, pp. 133-142.
- Fuentealba, L. C., Obernier, K. and Alvarez-Buylla, A.** (2012) 'Adult neural stem cells bridge their niche', *Cell stem cell*, 10(6), pp. 698-708.
- Fuentealba, P., Klausberger, T., Karayannis, T., Suen, W. Y., Huck, J., Tomioka, R., Rockland, K., Capogna, M., Studer, M., Morales, M. and Somogyi, P.** (2010) 'Expression of COUP-TFII nuclear receptor in restricted GABAergic neuronal populations in the adult rat hippocampus', *The Journal of neuroscience : the official journal of the Society for Neuroscience*, 30(5), pp. 1595-1609.
- Fukaya, M., Yamazaki, M., Sakimura, K. and Watanabe, M.** (2005) 'Spatial diversity in gene expression for VDCCgamma subunit family in developing and adult mouse brains', *Neuroscience research*, 53(4), pp. 376-383.
- Fukuchi-Shimogori, T. and Grove, E. A.** (2003) 'Emx2 patterns the neocortex by regulating FGF positional signaling', *Nature neuroscience*, 6(8), pp. 825-831.
- Furuta, Y., Piston, D. W. and Hogan, B. L.** (1997) 'Bone morphogenetic proteins (BMPs) as regulators of dorsal forebrain development', *Development (Cambridge, England)*, 124(11), pp. 2203-2212.

- Gaarskjaer, F. B.** (1978) 'Organization of the mossy fiber system of the rat studied in extended hippocampi. II. Experimental analysis of fiber distribution with silver impregnation methods', *The Journal of comparative neurology*, 178(1), pp. 73-88.
- Gaarskjaer, F. B.** (1985) 'The development of the dentate area and the hippocampal mossy fiber projection of the rat', *Journal of Comparative Neurology*.
- Galceran, J., Miyashita-Lin, E. M., Devaney, E., Rubenstein, J. L. and Grosschedl, R.** (2000) 'Hippocampus development and generation of dentate gyrus granule cells is regulated by LEF1', *Development (Cambridge, England)*, 127(3), pp. 469-482.
- Galeeva, A., Treuter, E., Tomarev, S. and Peltto-Huikko, M.** (2007) 'A prospero-related homeobox gene Prox-1 is expressed during postnatal brain development as well as in the adult rodent brain', *Neuroscience*, 146(2), pp. 604-616.
- Garcia, R., Musleh, W., Tocco, G., Thompson, R. F. and Baudry, M.** (1997) 'Time-dependent blockade of STP and LTP in hippocampal slices following acute stress in mice', *Neuroscience letters*, 233(1), pp. 41-44.
- Garel, S., Huffman, K. J. and Rubenstein, J. L.** (2003) 'Molecular regionalization of the neocortex is disrupted in Fgf8 hypomorphic mutants', *Development (Cambridge, England)*, 130(9), pp. 1903-1914.
- Gay, F., Baráth, P., Desbois-Le Péron, C., Métivier, R., Le Guével, R., Birse, D. and Salbert, G.** (2002) 'Multiple phosphorylation events control chicken ovalbumin upstream promoter transcription factor I orphan nuclear receptor activity', *Molecular endocrinology (Baltimore, Md.)*, 16(6), pp. 1332-1351.
- Ge, W., He, F., Kim, K. J., Bianchi, B., Coskun, V., Nguyen, L., Wu, X., Zhao, J., Heng, J. I., Martinowich, K., Tao, J., Wu, H., Castro, D., Sobeih, M. M., Corfas, G., Gleeson, J. G., Greenberg, M. E., Guillemot, F. and Sun, Y. E.** (2006) 'Coupling of cell migration with neurogenesis by proneural bHLH factors', *Proceedings of the National Academy of Sciences of the United States of America*, 103(5), pp. 1319-1324.
- Germain, P., Staels, B., Dacquet, C., Spedding, M. and Laudet, V.** (2006) 'Overview of nomenclature of nuclear receptors', *Pharmacological reviews*, 58(4), pp. 685-704.
- Goebbels, S., Bormuth, I., Bode, U., Hermanson, O., Schwab, M. H. and Nave, K.-A. A.** (2006) 'Genetic targeting of principal neurons in neocortex and hippocampus of NEX-Cre mice', *Genesis (New York, N.Y. : 2000)*, 44(12), pp. 611-621.
- Golarai, G., Cavazos, J. E. and Sutula, T. P.** (1992) 'Activation of the dentate gyrus by pentylentetrazol evoked seizures induces mossy fiber synaptic reorganization', *Brain research*, 593(2), pp. 257-264.
- Good, M.** (2002) 'Spatial memory and hippocampal function: where are we now?', *Psicológica: Revista de metodología y psicología*
- Gorski, J. A., Talley, T., Qiu, M., Puellas, L., Rubenstein, J. L. and Jones, K. R.** (2002) 'Cortical excitatory neurons and glia, but not GABAergic neurons, are produced in the Emx1-expressing lineage', *The Journal of neuroscience : the official journal of the Society for Neuroscience*, 22(15), pp. 6309-6314.
- Gottlieb, D. I. and Cowan, W. M.** (1973) 'Autoradiographic studies of the commissural and ipsilateral association connection of the hippocampus and dentate gyrus of the rat. I. The commissural connections', *The Journal of comparative neurology*, 149(4), pp. 393-422.
- Götz, M. and Barde, Y.-A. A.** (2005) 'Radial glial cells defined and major intermediates between embryonic stem cells and CNS neurons', *Neuron*, 46(3), pp. 369-372.
- Götz, M., Stoykova, A. and Gruss, P.** (1998) 'Pax6 controls radial glia differentiation in the cerebral cortex', *Neuron*, 21(5), pp. 1031-1044.

- Gould, E., Cameron, H. A., Daniels, D. C., Woolley, C. S. and McEwen, B. S.** (1992) 'Adrenal hormones suppress cell division in the adult rat dentate gyrus', *The Journal of neuroscience : the official journal of the Society for Neuroscience*, 12(9), pp. 3642-3650.
- Gould, E., McEwen, B. S., Tanapat, P., Galea, L. A. and Fuchs, E.** (1997) 'Neurogenesis in the dentate gyrus of the adult tree shrew is regulated by psychosocial stress and NMDA receptor activation', *The Journal of neuroscience : the official journal of the Society for Neuroscience*, 17(7), pp. 2492-2498.
- Gould, E. and Tanapat, P.** (1997) 'Lesion-induced proliferation of neuronal progenitors in the dentate gyrus of the adult rat', *Neuroscience*, 80(2), pp. 427-436.
- Gould, E., Vail, N., Wagers, M. and Gross, C. G.** (2001) 'Adult-generated hippocampal and neocortical neurons in macaques have a transient existence', *Proceedings of the National Academy of Sciences of the United States of America*, 98(19), pp. 10910-10917.
- Gould, E., Woolley, C. S., Cameron, H. A., Daniels, D. C. and McEwen, B. S.** (1991) 'Adrenal steroids regulate postnatal development of the rat dentate gyrus: II. Effects of glucocorticoids and mineralocorticoids on cell birth', *The Journal of comparative neurology*, 313(3), pp. 486-493.
- Graham, V., Khudyakov, J., Ellis, P. and Pevny, L.** (2003) 'SOX2 functions to maintain neural progenitor identity', *Neuron*, 39(5), pp. 749-765.
- Gray, J. and Jeffrey, A.** (1971) 'The psychology of fear and stress', *World University Library New York: McGraw-Hill*, (5).
- Gray, J. A. and McNaughton, N.** (2000) 'The neuropsychology of anxiety: an Enquiry into the Functions of the Septo-hippocampal System, Second Edition', (*Oxford: Oxford University Press*).
- Gray, J. R.** (2001) 'Emotional modulation of cognitive control: approach-withdrawal states double-dissociate spatial from verbal two-back task performance', *Journal of experimental psychology. General*, 130(3), pp. 436-452.
- Grove, E. A., Tole, S., Limon, J., Yip, L. and Ragsdale, C. W.** (1998) 'The hem of the embryonic cerebral cortex is defined by the expression of multiple Wnt genes and is compromised in Gli3-deficient mice', *Development (Cambridge, England)*, 125(12), pp. 2315-2325.
- Guy, B., Michael, P., Charlotta, L., Randal, M., Sharon, M., Erica, L., Anindita, S., Shubha, T., Richard, M. G. and Linda, J. R.** (2008) 'Specific Glial Populations Regulate Hippocampal Morphogenesis', *The Journal of Neuroscience*, 28(47), pp. 12328-12340.
- Haas, C. A., Dudeck, O., Kirsch, M., Huszka, C., Kann, G., Pollak, S., Zentner, J. and Frotscher, M.** (2002) 'Role for reelin in the development of granule cell dispersion in temporal lobe epilepsy', *The Journal of neuroscience : the official journal of the Society for Neuroscience*, 22(14), pp. 5797-5802.
- Haddad, I. A., Ordovas, J. M., Fitzpatrick, T. and Karathanasis, S. K.** (1986) 'Linkage, evolution, and expression of the rat apolipoprotein A-I, C-III, and A-IV genes', *The Journal of biological chemistry*, 261(28), pp. 13268-13277.
- Hall, R. K., Sladek, F. M. and Granner, D. K.** (1995) 'The orphan receptors COUP-TF and HNF-4 serve as accessory factors required for induction of phosphoenolpyruvate carboxykinase gene transcription by glucocorticoids', *Proceedings of the National Academy of Sciences of the United States of America*, 92(2), pp. 412-416.
- Harrison, P. J.** (2004) 'The hippocampus in schizophrenia: a review of the neuropathological evidence and its pathophysiological implications', *Psychopharmacology*, 174(1), pp. 151-162.
- Haug, F. M.** (1974) 'Light microscopical mapping of the hippocampal region, the pyriform cortex and the corticomedial amygdaloid nuclei of the rat with Timm's sulphide silver method. I. Area dentata, hippocampus and subiculum', *Zeitschrift für Anatomie und Entwicklungsgeschichte*, 145(1), pp. 1-27.

- Hayashi, K., Kubo, K.-I., Kitazawa, A. and Nakajima, K.** (2015) 'Cellular dynamics of neuronal migration in the hippocampus', *Frontiers in neuroscience*, 9, pp. 135.
- Heinrich, C., Nitta, N., Flubacher, A., Müller, M., Fahrner, A., Kirsch, M., Freiman, T., Suzuki, F., Depaulis, A., Frotscher, M. and Haas, C. A.** (2006) 'Reelin deficiency and displacement of mature neurons, but not neurogenesis, underlie the formation of granule cell dispersion in the epileptic hippocampus', *The Journal of neuroscience : the official journal of the Society for Neuroscience*, 26(17), pp. 4701-4713.
- Helmstaedter, M., de Kock, C. P., Feldmeyer, D., Bruno, R. M. and Sakmann, B.** (2007) 'Reconstruction of an average cortical column in silico', *Brain research reviews*, 55(2), pp. 193-203.
- Heng, J. I., Nguyen, L., Castro, D. S., Zimmer, C., Wildner, H., Armant, O., Skowronska-Krawczyk, D., Bedogni, F., Matter, J. M., Hevner, R. and Guillemot, F.** (2008) 'Neurogenin 2 controls cortical neuron migration through regulation of Rnd2'. *Nature*, 455, pp. 114-118.
- Henke, P. G.** (1990) 'Hippocampal pathway to the amygdala and stress ulcer development', *Brain research bulletin*, 25(5), pp. 691-695.
- Herman, J. P., Ostrander, M. M., Mueller, N. K. and Figueiredo, H.** (2005) 'Limbic system mechanisms of stress regulation: hypothalamo-pituitary-adrenocortical axis', *Progress in neuro-psychopharmacology & biological psychiatry*, 29(8), pp. 1201-1213.
- Hevner, R. F.** (2006) 'From radial glia to pyramidal-projection neuron: transcription factor cascades in cerebral cortex development', *Molecular neurobiology*, 33(1), pp. 33-50.
- Hevner, R. F., Shi, L., Justice, N., Hsueh, Y., Sheng, M., Smiga, S., Bulfone, A., Goffinet, A. M., Campagnoni, A. T. and Rubenstein, J. L.** (2001) 'Tbr1 regulates differentiation of the preplate and layer 6', *Neuron*, 29(2), pp. 353-366.
- Hodge, R. D., Nelson, B. R., Kahoud, R. J., Yang, R., Mussar, K. E., Reiner, S. L. and Hevner, R. F.** (2012) 'Tbr2 is essential for hippocampal lineage progression from neural stem cells to intermediate progenitors and neurons', *The Journal of neuroscience : the official journal of the Society for Neuroscience*, 32(18), pp. 6275-6287.
- Houser, C. R.** (1990) 'Granule cell dispersion in the dentate gyrus of humans with temporal lobe epilepsy', *Brain research*, 535(2), pp. 195-204.
- Hébert, J. M., Mishina, Y. and McConnell, S. K.** (2002) 'BMP signaling is required locally to pattern the dorsal telencephalic midline', *Neuron*, 35(6), pp. 1029-1041.
- Ishizuka, N., Weber, J. and Amaral, D. G.** (1990) 'Organization of intrahippocampal projections originating from CA3 pyramidal cells in the rat', *The Journal of comparative neurology*, 295(4), pp. 580-623.
- Isshiki, T., Pearson, B., Holbrook, S. and Doe, C. Q.** (2001) 'Drosophila neuroblasts sequentially express transcription factors which specify the temporal identity of their neuronal progeny', *Cell*, 106(4), pp. 511-521.
- Jack, C. R., Petersen, R. C., Xu, Y. C., Waring, S. C., O'Brien, P. C., Tangalos, E. G., Smith, G. E., Ivnik, R. J. and Kokmen, E.** (1997) 'Medial temporal atrophy on MRI in normal aging and very mild Alzheimer's disease', *Neurology*, 49(3), pp. 786-794.
- Jacobson, L. and Sapolsky, R.** (1991) 'The role of the hippocampus in feedback regulation of the hypothalamic-pituitary-adrenocortical axis', *Endocrine reviews*, 12(2), pp. 118-134.
- Jarrard, L. E.** (1983) 'Selective hippocampal lesions and behavior: effects of kainic acid lesions on performance of place and cue tasks', *Behavioral neuroscience*, 97(6), pp. 873-889.
- Jazin, E. E., Söderström, S., Ebendal, T. and Larhammar, D.** (1997) 'Embryonic expression of the mRNA for the rat homologue of the fusin/CXCR-4 HIV-1 co-receptor', *Journal of neuroimmunology*, 79(2), pp. 148-154.

- Jin, K., Peel, A. L., Mao, X. O., Xie, L., Cottrell, B. A., Henshall, D. C. and Greenberg, D. A.** (2004) 'Increased hippocampal neurogenesis in Alzheimer's disease', *Proceedings of the National Academy of Sciences of the United States of America*, 101(1), pp. 343-347.
- Jonk, L. J., de Jonge, M. E., Pals, C. E., Wissink, S., Vervaart, J. M., Schoorlemmer, J. and Kruijer, W.** (1994) 'Cloning and expression during development of three murine members of the COUP family of nuclear orphan receptors', *Mechanisms of development*, 47(1), pp. 81-97.
- Kakimoto, T., Katoh, H. and Negishi, M.** (2004) 'Identification of splicing variants of Rapostlin, a novel RND2 effector that interacts with neural Wiskott-Aldrich syndrome protein and induces neurite branching', *The Journal of biological chemistry*, 279(14), pp. 14104-14110.
- Kanai, M. I., Okabe, M. and Hiromi, Y.** (2005) 'seven-up Controls switching of transcription factors that specify temporal identities of Drosophila neuroblasts', *Developmental cell*, 8(2), pp. 203-213.
- Kanatani, S., Yozu, M., Tabata, H. and Nakajima, K.** (2008) 'COUP-TFII is preferentially expressed in the caudal ganglionic eminence and is involved in the caudal migratory stream', *The Journal of neuroscience : the official journal of the Society for Neuroscience*, 28(50), pp. 13582-13591.
- Kaplan, M. S. and Hinds, J. W.** (1977) 'Neurogenesis in the adult rat: electron microscopic analysis of light radioautographs', *Science (New York, N.Y.)*, 197(4308), pp. 1092-1094.
- Karalay, O., Doberauer, K., Vadodaria, K. C., Knobloch, M., Berti, L., Miquelajauregui, A., Schwark, M., Jagasia, R., Taketo, M. M., Tarabykin, V., Lie, D. C. and Jessberger, S.** (2011) 'Prospero-related homeobox 1 gene (Prox1) is regulated by canonical Wnt signaling and has a stage-specific role in adult hippocampal neurogenesis', *Proceedings of the National Academy of Sciences of the United States of America*, 108(14), pp. 5807-5812.
- Kato, A. S., Siuda, E. R., Nisenbaum, E. S. and Bredt, D. S.** (2008) 'AMPA receptor subunit-specific regulation by a distinct family of type II TARPs', *Neuron*, 59(6), pp. 986-996.
- Kee, N. J., Preston, E. and Wojtowicz, J. M.** (2001) 'Enhanced neurogenesis after transient global ischemia in the dentate gyrus of the rat', *Experimental brain research*, 136(3), pp. 313-320.
- Kempermann, G., Jessberger, S., Steiner, B. and Kronenberg, G.** (2004) 'Milestones of neuronal development in the adult hippocampus', *Trends in neurosciences*, 27(8), pp. 447-452.
- Kempermann, G., Kuhn, H. G. and Gage, F. H.** (1997) 'More hippocampal neurons in adult mice living in an enriched environment', *Nature*, 386(6624), pp. 493-495.
- Kerjan, G., Koizumi, H., Han, E. B., Dubé, C. M., Djakovic, S. N., Patrick, G. N., Baram, T. Z., Heinemann, S. F. and Gleason, J. G.** (2009) 'Mice lacking doublecortin and doublecortin-like kinase 2 display altered hippocampal neuronal maturation and spontaneous seizures', *Proceedings of the National Academy of Sciences of the United States of America*, 106(16), pp. 6766-6771.
- Kesner, R. P.** (1988) 'Reevaluation of the contribution of the basal forebrain cholinergic system to memory', *Neurobiology of aging*, 9(5-6), pp. 609-616.
- Kim, J. J. and Diamond, D. M.** (2002) 'The stressed hippocampus, synaptic plasticity and lost memories', *Nature reviews. Neuroscience*, 3(6), pp. 453-462.
- Kim, K. K., Adelstein, R. S. and Kawamoto, S.** (2009) 'Identification of neuronal nuclei (NeuN) as Fox-3, a new member of the Fox-1 gene family of splicing factors', *The Journal of biological chemistry*, 284(45), pp. 31052-31061.
- Kliwer, S. A., Umesono, K., Heyman, R. A., Mangelsdorf, D. J., Dyck, J. A. and Evans, R. M.** (1992) 'Retinoid X receptor-COUP-TF interactions modulate retinoic acid signaling', *Proceedings of the National Academy of Sciences of the United States of America*, 89(4), pp. 1448-1452.
- Klüver, H. and Bucy, P. C.** (1937) "'Psychic blindness" and other symptoms following bilateral temporal lobectomy in Rhesus monkeys', *American Journal of Physiology*.

- Kohara, K., Pignatelli, M., Rivest, A. J., Jung, H.-Y. Y., Kitamura, T., Suh, J., Frank, D., Kajikawa, K., Mise, N., Obata, Y., Wickersham, I. R. and Tonegawa, S.** (2014) 'Cell type-specific genetic and optogenetic tools reveal hippocampal CA2 circuits', *Nature neuroscience*, 17(2), pp. 269-279.
- Krishnan, V., Pereira, F. A., Qiu, Y., Chen, C. H., Beachy, P. A., Tsai, S. Y. and Tsai, M. J.** (1997) 'Mediation of Sonic hedgehog-induced expression of COUP-TFII by a protein phosphatase', *Science (New York, N.Y.)*, 278(5345), pp. 1947-1950.
- Kuhn, H. G., Dickinson-Anson, H. and Gage, F. H.** (1996) 'Neurogenesis in the dentate gyrus of the adult rat: age-related decrease of neuronal progenitor proliferation', *The Journal of neuroscience : the official journal of the Society for Neuroscience*, 16(6), pp. 2027-2033.
- Kullmann, D. M.** (2011) 'Interneuron networks in the hippocampus', *Current opinion in neurobiology*, 21(5), pp. 709-716.
- Kwon, H. J., Ma, S. and Huang, Z.** (2011) 'Radial glia regulate Cajal-Retzius cell positioning in the early embryonic cerebral cortex', *Developmental biology*, 351(1), pp. 25-34.
- Ladias, J. A., Hadzopoulou-Cladaras, M., Kardassis, D., Cardot, P., Cheng, J., Zannis, V. and Cladaras, C.** (1992) 'Transcriptional regulation of human apolipoprotein genes ApoB, ApoCIII, and ApoAII by members of the steroid hormone receptor superfamily HNF-4, ARP-1, EAR-2, and EAR-3', *The Journal of biological chemistry*, 267(22), pp. 15849-15860.
- Ladias, J. A. and Karathanasis, S. K.** (1991) 'Regulation of the apolipoprotein AI gene by ARP-1, a novel member of the steroid receptor superfamily', *Science (New York, N.Y.)*, 251(4993), pp. 561-565.
- Lakshmi, S., Anindita, S., Ashwin, S. S., Bhavana, M., Hari, P., Michael, P., Edwin, S. M., Ingolf, B., Richard, M. G., Linda, J. R. and Shubha, T.** (2011) 'Transcription factor Lhx2 is necessary and sufficient to suppress astrogliogenesis and promote neurogenesis in the developing hippocampus', *Proceedings of the National Academy of Sciences*, 108(27).
- Lavdas, A. A., Grigoriou, M., Pachnis, V. and Parnavelas, J. G.** (1999) 'The medial ganglionic eminence gives rise to a population of early neurons in the developing cerebral cortex', *The Journal of neuroscience : the official journal of the Society for Neuroscience*, 19(18), pp. 7881-7888.
- Lavi, E., Strizki, J. M., Ulrich, A. M., Zhang, W., Fu, L., Wang, Q., O'Connor, M., Hoxie, J. A. and González-Scarano, F.** (1997) 'CXCR-4 (Fusin), a co-receptor for the type 1 human immunodeficiency virus (HIV-1), is expressed in the human brain in a variety of cell types, including microglia and neurons', *The American journal of pathology*, 151(4), pp. 1035-1042.
- Lazennec, G., Kern, L., Valotaire, Y. and Salbert, G.** (1997) 'The nuclear orphan receptors COUP-TF and ARP-1 positively regulate the trout estrogen receptor gene through enhancing autoregulation', *Molecular and cellular biology*, 17(9), pp. 5053-5066.
- Lee, S., Hjerling-Leffler, J., Zaghera, E., Fishell, G. and Rudy, B.** (2010) 'The largest group of superficial neocortical GABAergic interneurons expresses ionotropic serotonin receptors', *The Journal of neuroscience : the official journal of the Society for Neuroscience*, 30(50), pp. 16796-16808.
- Lee, S. M., Tole, S., Grove, E. and McMahon, A. P.** (2000) 'A local Wnt-3a signal is required for development of the mammalian hippocampus', *Development (Cambridge, England)*, 127(3), pp. 457-467.
- Lemaire, V., Koehl, M., Le Moal, M. and Abrous, D. N.** (2000) 'Prenatal stress produces learning deficits associated with an inhibition of neurogenesis in the hippocampus', *Proceedings of the National Academy of Sciences of the United States of America*, 97(20), pp. 11032-11037.
- Leng, X., Cooney, A. J., Tsai, S. Y. and Tsai, M. J.** (1996) 'Molecular mechanisms of COUP-TF-mediated transcriptional repression: evidence for transrepression and active repression', *Molecular and cellular biology*, 16(5), pp. 2332-2340.

- Leonardo, E. D., Richardson-Jones, J. W., Sibille, E., Kottman, A. and Hen, R.** (2006) 'Molecular heterogeneity along the dorsal–ventral axis of the murine hippocampal CA1 field: a microarray analysis of gene expression', *Neuroscience*, 137(1), pp. 1771-86.
- Li, G., Fang, L., Fernández, G. and Pleasure, S. J.** (2013) 'The ventral hippocampus is the embryonic origin for adult neural stem cells in the dentate gyrus', *Neuron*, 78(4), pp. 658-672.
- Li, G., Kataoka, H., Coughlin, S. R. and Pleasure, S. J.** (2009) 'Identification of a transient subpial neurogenic zone in the developing dentate gyrus and its regulation by Cxcl12 and reelin signaling', *Development (Cambridge, England)*, 136(2), pp. 327-335.
- Li, G. and Pleasure, S. J.** (2005) 'Morphogenesis of the dentate gyrus: what we are learning from mouse mutants', *Developmental neuroscience*, 27(2-4), pp. 93-99.
- Li, G. and Pleasure, S. J.** (2007) 'Genetic regulation of dentate gyrus morphogenesis', *Progress in brain research*, 163, pp. 143-152.
- Li, Q., Bian, S., Hong, J., Kawase-Koga, Y., Zhu, E., Zheng, Y., Yang, L. and Sun, T.** (2011) 'Timing specific requirement of microRNA function is essential for embryonic and postnatal hippocampal development', *PloS one*, 6(10).
- Li, X. G., Somogyi, P., Ylinen, A. and Buzsáki, G.** (1994) 'The hippocampal CA3 network: an in vivo intracellular labeling study', *The Journal of comparative neurology*, 339(2), pp. 181-208.
- Lie, D.-C. C., Colamarino, S. A., Song, H.-J. J., Désiré, L., Mira, H., Consiglio, A., Lein, E. S., Jessberger, S., Lansford, H., Dearie, A. R. and Gage, F. H.** (2005) 'Wnt signalling regulates adult hippocampal neurogenesis', *Nature*, 437(7063), pp. 1370-1375.
- Ligon, K. L., Echelard, Y., Assimacopoulos, S., Danielian, P. S., Kaing, S., Grove, E. A., McMahon, A. P. and Rowitch, D. H.** (2003) 'Loss of Emx2 function leads to ectopic expression of Wnt1 in the developing telencephalon and cortical dysplasia', *Development (Cambridge, England)*, 130(10), pp. 2275-2287.
- Lin, F.-J. J., Qin, J., Tang, K., Tsai, S. Y. and Tsai, M.-J. J.** (2011) 'Coup d'Etat: an orphan takes control', *Endocrine reviews*, 32(3), pp. 404-421.
- Liu, M., Pleasure, S. J., Collins, A. E., Noebels, J. L., Naya, F. J., Tsai, M. J. and Lowenstein, D. H.** (2000a) 'Loss of BETA2/NeuroD leads to malformation of the dentate gyrus and epilepsy', *Proceedings of the National Academy of Sciences of the United States of America*, 97(2), pp. 865-870.
- Liu, Q., Dwyer, N. D. and O'Leary, D. D.** (2000b) 'Differential expression of COUP-TFI, CHL1, and two novel genes in developing neocortex identified by differential display PCR', *The Journal of neuroscience : the official journal of the Society for Neuroscience*, 20(20), pp. 7682-7690.
- Liu, Y., Fujise, N. and Kosaka, T.** (1996) 'Distribution of calretinin immunoreactivity in the mouse dentate gyrus. I. General description', *Experimental brain research*, 108(3), pp. 389-403.
- Liu, Y. H. and Teng, C. T.** (1991) 'Characterization of estrogen-responsive mouse lactoferrin promoter', *The Journal of biological chemistry*, 266(32), pp. 21880-21885.
- Lo Nigro, C., Chong, C. S., Smith, A. C., Dobyns, W. B., Carrozzo, R. and Ledbetter, D. H.** (1997) 'Point mutations and an intragenic deletion in LIS1, the lissencephaly causative gene in isolated lissencephaly sequence and Miller-Dieker syndrome', *Human molecular genetics*, 6(2), pp. 157-164.
- Lorente de Nó, R.** (1934) 'Studies on the structure of the cerebral cortex. II. Continuation of the study of the ammonic system', *Studies on the structure of the cerebral cortex. II. Continuation of the study of the ammonic system*.
- LoTurco, J. J. and Bai, J.** (2006) 'The multipolar stage and disruptions in neuronal migration', *Trends in neurosciences*, 29(7), pp. 407-413.
- Lu, M., Grove, E. A. and Miller, R. J.** (2002) 'Abnormal development of the hippocampal dentate gyrus in mice lacking the CXCR4 chemokine receptor', *Proceedings of the National Academy of Sciences of the United States of America*, 99(10), pp. 7090-7095.

- Lu, X. P., Salbert, G. and Pfahl, M.** (1994) 'An evolutionary conserved COUP-TF binding element in a neural-specific gene and COUP-TF expression patterns support a major role for COUP-TF in neural development', *Molecular endocrinology (Baltimore, Md.)*, 8(12), pp. 1774-1788.
- Lütolf, S., Radtke, F., Aguet, M., Suter, U. and Taylor, V.** (2002) 'Notch1 is required for neuronal and glial differentiation in the cerebellum', *Development (Cambridge, England)*, 129(2), pp. 373-385.
- Lutz, B., Kuratani, S., Cooney, A. J., Wawersik, S., Tsai, S. Y., Eichele, G. and Tsai, M. J.** (1994) 'Developmental regulation of the orphan receptor COUP-TF II gene in spinal motor neurons', *Development (Cambridge, England)*, 120(1), pp. 25-36.
- Lydia, D., Antoine, T. and Serge, M.** (2006) 'The development of hippocampal interneurons in rodents', *Hippocampus*, 16(12), pp. 1032-1060.
- Ma, Q., Jones, D., Borghesani, P. R., Segal, R. A., Nagasawa, T., Kishimoto, T., Bronson, R. T. and Springer, T. A.** (1998) 'Impaired B-lymphopoiesis, myelopoiesis, and derailed cerebellar neuron migration in CXCR4- and SDF-1-deficient mice', *Proceedings of the National Academy of Sciences of the United States of America*, 95(16), pp. 9448-9453.
- Machon, O., Backman, M., Machonova, O., Kozmik, Z., Vacik, T., Andersen, L. and Krauss, S.** (2007) 'A dynamic gradient of Wnt signaling controls initiation of neurogenesis in the mammalian cortex and cellular specification in the hippocampus', *Developmental biology*, 311(1), pp. 223-237.
- Machon, O., van den Bout, C. J., Backman, M., Kemler, R. and Krauss, S.** (2003) 'Role of beta-catenin in the developing cortical and hippocampal neuroepithelium', *Neuroscience*, 122(1), pp. 129-143.
- Maekawa, M., Takashima, N., Arai, Y., Nomura, T., Inokuchi, K., Yuasa, S. and Osumi, N.** (2005) 'Pax6 is required for production and maintenance of progenitor cells in postnatal hippocampal neurogenesis', *Genes to cells : devoted to molecular & cellular mechanisms*, 10(10), pp. 1001-1014.
- Magariños, A. M. and McEwen, B. S.** (1995) 'Stress-induced atrophy of apical dendrites of hippocampal CA3c neurons: involvement of glucocorticoid secretion and excitatory amino acid receptors', *Neuroscience*, 69(1), pp. 89-98.
- Maguire, E. A., Gadian, D. G., Johnsrude, I. S., Good, C. D., Ashburner, J., Frackowiak, R. S. and Frith, C. D.** (2000) 'Navigation-related structural change in the hippocampi of taxi drivers', *Proceedings of the National Academy of Sciences of the United States of America*, 97(8), pp. 4398-4403.
- Malberg, J. E. and Duman, R. S.** (2003) 'Cell proliferation in adult hippocampus is decreased by inescapable stress: reversal by fluoxetine treatment', *Neuropsychopharmacology : official publication of the American College of Neuropsychopharmacology*, 28(9), pp. 1562-1571.
- Manent, J.-B. B., Jorquera, I., Ben-Ari, Y., Aniksztejn, L. and Represa, A.** (2006) 'Glutamate acting on AMPA but not NMDA receptors modulates the migration of hippocampal interneurons', *The Journal of neuroscience : the official journal of the Society for Neuroscience*, 26(22), pp. 5901-5909.
- Marchetti, G., Escuin, S., van der Flier, A., De Arcangelis, A., Hynes, R. O. and Georges-Labouesse, E.** (2010) 'Integrin alpha5beta1 is necessary for regulation of radial migration of cortical neurons during mouse brain development', *The European journal of neuroscience*, 31(3), pp. 399-409.
- Marco, T., Alessandro, F., Maria, A. and Michèle, S.** (2004) 'The COUP-TF nuclear receptors regulate cell migration in the mammalian basal forebrain', *Development (Cambridge, England)*, 131(24), pp. 6119-6129.
- Marín, O. and Rubenstein, J. L.** (2001) 'A long, remarkable journey: tangential migration in the telencephalon', *Nature reviews. Neuroscience*, 2(11), pp. 780-790.

- Marín-Padilla, M.** (1998) 'Cajal-Retzius cells and the development of the neocortex', *Trends in neurosciences*, 21(2), pp. 64-71.
- Markakis, E. A. and Gage, F. H.** (1999) 'Adult-generated neurons in the dentate gyrus send axonal projections to field CA3 and are surrounded by synaptic vesicles', *The Journal of comparative neurology*, 406(4), pp. 449-460.
- Martin, L. A., Tan, S.-S. S. and Goldowitz, D.** (2002) 'Clonal architecture of the mouse hippocampus', *The Journal of neuroscience : the official journal of the Society for Neuroscience*, 22(9), pp. 3520-3530.
- Matthews, D. A., Salvaterra, P. M., Crawford, G. D., Houser, C. R. and Vaughn, J. E.** (1987) 'An immunocytochemical study of choline acetyltransferase-containing neurons and axon terminals in normal and partially deafferented hippocampal formation', *Brain research*, 402(1), pp. 30-43.
- Maurange, C., Cheng, L. and Gould, A. P.** (2008) 'Temporal transcription factors and their targets schedule the end of neural proliferation in *Drosophila*', *Cell*, 133(5), pp. 891-902.
- McBain, C. J. and Fisahn, A.** (2001) 'Interneurons unbound', *Nature reviews. Neuroscience*, 2(1), pp. 11-23.
- McEwen, B. S., Stephenson, B. S. and Krey, L. C.** (1980) 'Radioimmunoassay of brain tissue and cell nuclear corticosterone', *Journal of neuroscience methods*, 3(1), pp. 57-65.
- McEwen, B. S., Weiss, J. M. and Schwartz, L. S.** (1968) 'Selective retention of corticosterone by limbic structures in rat brain', *Nature*, 220(5170), pp. 911-912.
- McGrath, K. E., Koniski, A. D., Maltby, K. M., McGann, J. K. and Palis, J.** (1999) 'Embryonic expression and function of the chemokine SDF-1 and its receptor, CXCR4', *Developmental biology*, 213(2), pp. 442-456.
- Mettler, U., Vogler, G. and Urban, J.** (2006) 'Timing of identity: spatiotemporal regulation of hunchback in neuroblast lineages of *Drosophila* by Seven-up and Prospero', *Development (Cambridge, England)*, 133(3), pp. 429-437.
- Michael, P., Guy, B., John, H., Sharon, M., Charlotta, L., Erica, L., Anindita, S., Aaron, G. S., Randal, X. M., Glen, M. B., Shubha, T., Richard, M. G., Timothy, L. B. and Linda, J. R.** (2010) 'NFIA Controls Telencephalic Progenitor Cell Differentiation through Repression of the Notch Effector *Hes1*', *The Journal of Neuroscience*, 30(27), pp. 9127-9139.
- Miller, F. D. and Gauthier, A. S. S.** (2007) 'Timing is everything: making neurons versus glia in the developing cortex', *Neuron*, 54(3), pp. 357-369.
- Mishkin, M.** (1954) 'Visual discrimination performance following partial ablations of the temporal lobe. II. Ventral surface vs. hippocampus', *Journal of comparative and physiological psychology*, 47(3).
- Miyajima, N., Kadowaki, Y., Fukushige, S., Shimizu, S., Semba, K., Yamanashi, Y., Matsubara, K., Toyoshima, K. and Yamamoto, T.** (1988) 'Identification of two novel members of erbA superfamily by molecular cloning: the gene products of the two are highly related to each other', *Nucleic acids research*, 16(23), pp. 11057-11074.
- Miyata, T., Maeda, T. and Lee, J. E.** (1999) 'NeuroD is required for differentiation of the granule cells in the cerebellum and hippocampus', *Genes & development*, 13(13), pp. 1647-1652.
- Miyoshi, G., Hjerling-Leffler, J., Karayannis, T., Sousa, V. H., Butt, S. J., Battiste, J., Johnson, J. E., Machold, R. P. and Fishell, G.** (2010) 'Genetic fate mapping reveals that the caudal ganglionic eminence produces a large and diverse population of superficial cortical interneurons', *The Journal of neuroscience : the official journal of the Society for Neuroscience*, 30(5), pp. 1582-1594.
- Mizoguchi, K., Kunishita, T., Chui, D. H. and Tabira, T.** (1992) 'Stress induces neuronal death in the hippocampus of castrated rats', *Neuroscience letters*, 138(1), pp. 157-160.

- Mlodzik, M., Hiromi, Y., Weber, U., Goodman, C. S. and Rubin, G. M.** (1990) 'The Drosophila seven-up gene, a member of the steroid receptor gene superfamily, controls photoreceptor cell fates', *Cell*, 60(2), pp. 211-224.
- Montenegro, M. A., Kinay, D., Cendes, F., Bernasconi, A., Bernasconi, N., Coan, A. C., Li, L. M., Guerreiro, M. M., Guerreiro, C. A., Lopes-Cendes, I., Andermann, E., Dubeau, F. and Andermann, F.** (2006) 'Patterns of hippocampal abnormalities in malformations of cortical development', *Journal of neurology, neurosurgery, and psychiatry*, 77(3), pp. 367-371.
- Moser, E., Moser, M. B. and Andersen, P.** (1993) 'Spatial learning impairment parallels the magnitude of dorsal hippocampal lesions, but is hardly present following ventral lesions', *The Journal of neuroscience : the official journal of the Society for Neuroscience*, 13(9), pp. 3916-3925.
- Moser, E. I., Kropff, E. and Moser, M.-B. B.** (2008) 'Place cells, grid cells, and the brain's spatial representation system', *Annual review of neuroscience*, 31, pp. 69-89.
- Moser, M. B., Moser, E. I., Forrest, E., Andersen, P. and Morris, R. G.** (1995) 'Spatial learning with a minislab in the dorsal hippocampus', *Proceedings of the National Academy of Sciences of the United States of America*, 92(21), pp. 9697-9701.
- Mullen, R. J., Buck, C. R. and Smith, A. M.** (1992) 'NeuN, a neuronal specific nuclear protein in vertebrates', *Development (Cambridge, England)*, 116(1), pp. 201-211.
- Muramatsu, R., Ikegaya, Y., Matsuki, N. and Koyama, R.** (2007) 'Neonatal born granule cells numerically dominate adult mice dentate gyrus', *Neuroscience*, 148(3), pp. 593-598.
- Muzio, L., Di Benedetto, B., DiBenedetto, B., Stoykova, A., Boncinelli, E., Gruss, P. and Mallamaci, A.** (2002) 'Emx2 and Pax6 control regionalization of the pre-neuronogenic cortical primordium', *Cerebral cortex (New York, N.Y. : 1991)*, 12(2), pp. 129-139.
- Muzio, L., Soria, J. M., Pannese, M., Piccolo, S. and Mallamaci, A.** (2005) 'A mutually stimulating loop involving emx2 and canonical wnt signalling specifically promotes expansion of occipital cortex and hippocampus', *Cerebral cortex (New York, N.Y. : 1991)*, 15(12), pp. 2021-2028.
- Müller, M. C., Osswald, M., Tinnes, S., Häussler, U., Jacobi, A., Förster, E., Frotscher, M. and Haas, C. A.** (2009) 'Exogenous reelin prevents granule cell dispersion in experimental epilepsy', *Experimental neurology*, 216(2), pp. 390-397.
- Naka, H., Nakamura, S., Shimazaki, T. and Okano, H.** (2008) 'Requirement for COUP-TFI and II in the temporal specification of neural stem cells in CNS development', *Nature neuroscience*, 11(9), pp. 1014-1023.
- Nakajima, K., Mikoshiba, K., Miyata, T., Kudo, C. and Ogawa, M.** (1997) 'Disruption of hippocampal development in vivo by CR-50 mAb against reelin', *Proceedings of the National Academy of Sciences of the United States of America*, 94(15), pp. 8196-8201.
- Nakamura, K., Yamashita, Y., Tamamaki, N., Katoh, H., Kaneko, T. and Negishi, M.** (2006) 'In vivo function of Rnd2 in the development of neocortical pyramidal neurons'. *Neurosci. Res.* 54, pp. 149-153.
- Nakano, Y., Kohno, T., Hibi, T., Kohno, S., Baba, A., Mikoshiba, K., Nakajima, K. and Hattori, M.** (2007) 'The extremely conserved C-terminal region of Reelin is not necessary for secretion but is required for efficient activation of downstream signaling', *The Journal of biological chemistry*, 282(28), pp. 20544-20552.
- Namba, T., Mochizuki, H., Onodera, M., Mizuno, Y., Namiki, H. and Seki, T.** (2005) 'The fate of neural progenitor cells expressing astrocytic and radial glial markers in the postnatal rat dentate gyrus', *The European journal of neuroscience*, 22(8), pp. 1928-1941.
- Namba, T., Mochizuki, H., Onodera, M., Namiki, H. and Seki, T.** (2007) 'Postnatal neurogenesis in hippocampal slice cultures: early in vitro labeling of neural precursor cells leads to efficient neuronal production', *Journal of neuroscience research*, 85(8), pp. 1704-1712.

- Namba, T., Mochizuki, H., Suzuki, R., Onodera, M., Yamaguchi, M., Namiki, H., Shioda, S. and Seki, T. (2011) 'Time-lapse imaging reveals symmetric neurogenic cell division of GFAP-expressing progenitors for expansion of postnatal dentate granule neurons', *PloS one*, 6(9).
- Namihira, M., Kohyama, J., Semi, K., Sanosaka, T., Deneen, B., Taga, T. and Nakashima, K. (2009) 'Committed neuronal precursors confer astrocytic potential on residual neural precursor cells', *Developmental cell*, 16(2), pp. 245-255.
- Nery, S., Fishell, G. and Corbin, J. G. (2002) 'The caudal ganglionic eminence is a source of distinct cortical and subcortical cell populations', *Nature neuroscience*, 5(12), pp. 1279-1287.
- Neuman, K., Soosaar, A., Nornes, H. O. and Neuman, T. (1995) 'Orphan receptor COUP-TF I antagonizes retinoic acid-induced neuronal differentiation', *Journal of neuroscience research*, 41(1), pp. 39-48.
- O'Keefe, J. and Dostrovsky, J. (1971) 'The hippocampus as a spatial map. Preliminary evidence from unit activity in the freely-moving rat', *Brain research*, 34(1), pp. 171-175.
- O'Keefe, J. and Nadel, L. (1978) 'The hippocampus as a cognitive map', *Oxford: Clarendon Press*.
- O'Leary, D. D., Chou, S.-J. J. and Sahara, S. (2007) 'Area patterning of the mammalian cortex', *Neuron*, 56(2), pp. 252-269.
- O'Reilly, K., Flatberg, A., Islam, S., Olsen, L., Kruge, I. and Witter, M. (2014) 'Identification of dorsal-ventral hippocampal differentiation in neonatal rats', *Brain Structure and Function*.
- Ohshima, T., Hirasawa, M., Tabata, H., Mutoh, T., Adachi, T., Suzuki, H., Saruta, K., Iwasato, T., Itohara, S., Hashimoto, M., Nakajima, K., Ogawa, M., Kulkarni, A. B. and Mikoshiba, K. (2007) 'Cdk5 is required for multipolar-to-bipolar transition during radial neuronal migration and proper dendrite development of pyramidal neurons in the cerebral cortex', *Development (Cambridge, England)*, 134(12), pp. 2273-2282.
- Ohshima, T., Ogura, H., Tomizawa, K., Hayashi, K., Suzuki, H., Saito, T., Kamei, H., Nishi, A., Bibb, J. A., Hisanaga, S.-I., Matsui, H. and Mikoshiba, K. (2005) 'Impairment of hippocampal long-term depression and defective spatial learning and memory in p35 mice', *Journal of neurochemistry*, 94(4), pp. 917-925.
- Ohshima, T., Ward, J. M., Huh, C. G., Longenecker, G., Veeranna, Pant, H. C., Brady, R. O., Martin, L. J. and Kulkarni, A. B. (1996) 'Targeted disruption of the cyclin-dependent kinase 5 gene results in abnormal corticogenesis, neuronal pathology and perinatal death', *Proceedings of the National Academy of Sciences of the United States of America*, 93(20), pp. 11173-11178.
- Okano, H. J. and Darnell, R. B. (1997) 'A hierarchy of Hu RNA binding proteins in developing and adult neurons', *The Journal of neuroscience : the official journal of the Society for Neuroscience*, 17(9), pp. 3024-3037.
- Oliver, G., Sosa-Pineda, B., Geisendorf, S., Spana, E. P., Doe, C. Q. and Gruss, P. (1993) 'Prox 1, a prospero-related homeobox gene expressed during mouse development', *Mechanisms of development*, 44(1), pp. 3-16.
- Olson, E. C., Kim, S. and Walsh, C. A. (2006) 'Impaired neuronal positioning and dendritogenesis in the neocortex after cell-autonomous Dab1 suppression', *The Journal of neuroscience : the official journal of the Society for Neuroscience*, 26(6), pp. 1767-1775.
- Olton, D. S. and Becker, J. T. (1979) 'Hippocampus, space, and memory', *Behavioral and Brain*.
- Osumi, N. (2001) 'The role of Pax6 in brain patterning', *The Tohoku journal of experimental medicine*, 193(3), pp. 163-174.
- Papez, J. W. (1937) 'A proposed mechanism of emotion', *The Journal of neuropsychiatry and clinical neurosciences*, 38.
- Paredes, M. F., Li, G., Berger, O., Baraban, S. C. and Pleasure, S. J. (2006) 'Stromal-derived factor-1 (CXCL12) regulates laminar position of Cajal-Retzius cells in normal and dysplastic

- brains', *The Journal of neuroscience : the official journal of the Society for Neuroscience*, 26(37), pp. 9404-9412.
- Parent, J. M., Yu, T. W., Leibowitz, R. T., Geschwind, D. H., Sloviter, R. S. and Lowenstein, D. H.** (1997) 'Dentate granule cell neurogenesis is increased by seizures and contributes to aberrant network reorganization in the adult rat hippocampus', *The Journal of neuroscience : the official journal of the Society for Neuroscience*, 17(10), pp. 3727-3738.
- Paulweber, B., Brooks, A. R., Nagy, B. P. and Levy-Wilson, B.** (1991) 'Identification of a negative regulatory region 5' of the human apolipoprotein B promoter', *The Journal of biological chemistry*, 266(32), pp. 21956-21961.
- Pearce, J. M., Roberts, A. D. and Good, M.** (1998) 'Hippocampal lesions disrupt navigation based on cognitive maps but not heading vectors', *Nature*, 396(6706), pp. 75-77.
- Pellegrini, M., Mansouri, A., Simeone, A., Boncinelli, E. and Gruss, P.** (1996) 'Dentate gyrus formation requires Emx2', *Development (Cambridge, England)*, 122(12), pp. 3893-3898.
- Pereira, F. A., Qiu, Y., Tsai, M. J. and Tsai, S. Y.** (1995) 'Chicken ovalbumin upstream promoter transcription factor (COUP-TF): expression during mouse embryogenesis', *The Journal of steroid biochemistry and molecular biology*, 53(1-6), pp. 503-508.
- Pereira, F. A., Tsai, M. J. and Tsai, S. Y.** (2000) 'COUP-TF orphan nuclear receptors in development and differentiation', *Cellular and molecular life sciences : CMLS*, 57(10), pp. 1388-1398.
- Perissi, V., Aggarwal, A., Glass, C. K., Rose, D. W. and Rosenfeld, M. G.** (2004) 'A corepressor/coactivator exchange complex required for transcriptional activation by nuclear receptors and other regulated transcription factors', *Cell*, 116(4), pp. 511-526.
- Pesold, C., Impagnatiello, F., Pisu, M. G., Uzunov, D. P., Costa, E., Guidotti, A. and Caruncho, H. J.** (1998) 'Reelin is preferentially expressed in neurons synthesizing gamma-aminobutyric acid in cortex and hippocampus of adult rats', *Proceedings of the National Academy of Sciences of the United States of America*, 95(6), pp. 3221-3226.
- Pickens, B. S., Teets, B. W., Soprano, K. J. and Soprano, D. R.** (2013) 'Role of COUP-TFI during retinoic acid-induced differentiation of P19 cells to endodermal cells', *Journal of cellular physiology*, 228(4), pp. 791-800.
- Pleasure, S. J., Anderson, S., Hevner, R., Bagri, A., Marin, O., Lowenstein, D. H. and Rubenstein, J. L.** (2000a) 'Cell migration from the ganglionic eminences is required for the development of hippocampal GABAergic interneurons', *Neuron*, 28(3), pp. 727-740.
- Pleasure, S. J., Collins, A. E. and Lowenstein, D. H.** (2000b) 'Unique expression patterns of cell fate molecules delineate sequential stages of dentate gyrus development', *The Journal of neuroscience : the official journal of the Society for Neuroscience*, 20(16), pp. 6095-6105.
- Porrero, C., Rubio-Garrido, P., Avendaño, C. and Clascá, F.** (2010) 'Mapping of fluorescent protein-expressing neurons and axon pathways in adult and developing Thy1-eYFP-H transgenic mice', *Brain research*, 1345, pp. 59-72.
- Power, R. F., Lydon, J. P., Conneely, O. M. and O'Malley, B. W.** (1991) 'Dopamine activation of an orphan of the steroid receptor superfamily', *Science (New York, N.Y.)*, 252(5012), pp. 1546-1548.
- Power, S. C. and Cereghini, S.** (1996) 'Positive regulation of the vHNF1 promoter by the orphan receptors COUP-TF1/Ear3 and COUP-TFII/Arp1', *Molecular and cellular biology*, 16(3), pp. 778-791.
- Puelles, L.** (2011) 'Pallio-pallial tangential migrations and growth signaling: new scenario for cortical evolution?', *Brain, behavior and evolution*, 78(1), pp. 108-127.
- Pugh, C. R., Tremblay, D., Fleshner, M. and Rudy, J. W.** (1997) 'A selective role for corticosterone in contextual-fear conditioning', *Behavioral neuroscience*, 111(3), pp. 503-511.
- Qiu, Y., Cooney, A. J., Kuratani, S., DeMayo, F. J., Tsai, S. Y. and Tsai, M. J.** (1994b) 'Spatiotemporal expression patterns of chicken ovalbumin upstream promoter-transcription

- factors in the developing mouse central nervous system: evidence for a role in segmental patterning of the diencephalon', *Proceedings of the National Academy of Sciences of the United States of America*, 91(10), pp. 4451-4455.
- Qiu, Y., Krishnan, V., Zeng, Z., Gilbert, D. J., Copeland, N. G., Gibson, L., Yang-Feng, T., Jenkins, N. A., Tsai, M. J. and Tsai, S. Y.** (1995) 'Isolation, characterization, and chromosomal localization of mouse and human COUP-TF I and II genes', *Genomics*, 29(1), pp. 240-246.
- Qiu, Y., Pereira, F. A., DeMayo, F. J., Lydon, J. P., Tsai, S. Y. and Tsai, M. J.** (1997) 'Null mutation of mCOUP-TFI results in defects in morphogenesis of the glossopharyngeal ganglion, axonal projection, and arborization', *Genes & development*, 11(15), pp. 1925-1937.
- Qiu, Y., Tsai, S. Y. and Tsai, M. J.** (1994a) 'COUP-TF an orphan member of the steroid/thyroid hormone receptor superfamily', *Trends in endocrinology and metabolism: TEM*, 5(6), pp. 234-239.
- Raisman, G., Cowan, W. M. and Powell, T. P. S.** (1965) 'The extrinsic afferent, commissural and association fibres of the hippocampus', *Brain*.
- Rakic, P.** (1978) 'Neuronal migration and contact guidance in the primate telencephalon', *Postgraduate medical journal*, 54 Suppl 1, pp. 25-40.
- Ramos-Moreno, T., Galazo, M. J., Porrero, C., Martínez-Cerdeño, V. and Clascá, F.** (2006) 'Extracellular matrix molecules and synaptic plasticity: immunomapping of intracellular and secreted Reelin in the adult rat brain', *The European journal of neuroscience*, 23(2), pp. 401-422.
- Ramón y Cajal, S.** (1893) 'Estructura del asta de Ammon y fascia dentata', *Ann Soc Esp Hist Nat*, 22.
- Rawlins, J. N. and Olton, D. S.** (1982) 'The septo-hippocampal system and cognitive mapping', *Behavioural brain research*, 5(4), pp. 331-358.
- Raymond, K.** (2013) 'Neurobiological foundations of an attribute model of memory', *Comparative Cognition & Behavior Reviews*, 8, pp. 2959.
- Rebecca, D. H., Thomas, D. K., Susanne, A. W., Juan, M. E., Caitlin, R., Grigori, E., Gerd, K. and Robert, F. H.** (2008) 'Intermediate Progenitors in Adult Hippocampal Neurogenesis: Tbr2 Expression and Coordinate Regulation of Neuronal Output', *The Journal of Neuroscience*, 28(14), pp. 3707-3717.
- Reiner, O., Carrozzo, R., Shen, Y., Wehnert, M., Faustinella, F., Dobyns, W. B., Caskey, C. T. and Ledbetter, D. H.** (1993) 'Isolation of a Miller-Dieker lissencephaly gene containing G protein beta-subunit-like repeats', *Nature*, 364(6439), pp. 717-721.
- Reue, K., Leff, T. and Breslow, J. L.** (1988) 'Human apolipoprotein CIII gene expression is regulated by positive and negative cis-acting elements and tissue-specific protein factors', *The Journal of biological chemistry*, 263(14), pp. 6857-6864.
- Rickmann, M., Amaral, D. G. and Cowan, W. M.** (1987) 'Organization of radial glial cells during the development of the rat dentate gyrus', *The Journal of comparative neurology*, 264(4), pp. 449-479.
- Roelink, H.** (2000) 'Hippocampus formation: an intriguing collaboration', *Current biology : CB*, 10(7), pp. 81.
- Rolls, E. T.** (1996) 'A theory of hippocampal function in memory', *Hippocampus*, 6(6), pp. 601-620.
- Rottman, J. N., Widom, R. L., Nadal-Ginard, B., Mahdavi, V. and Karathanasis, S. K.** (1991) 'A retinoic acid-responsive element in the apolipoprotein AI gene distinguishes between two different retinoic acid response pathways', *Molecular and cellular biology*, 11(7), pp. 3814-3820.
- Roybon, L., Hjalt, T., Stott, S., Guillemot, F., Li, J.-Y. Y. and Brundin, P.** (2009) 'Neurogenin2 directs granule neuroblast production and amplification while NeuroD1 specifies neuronal fate during hippocampal neurogenesis', *PloS one*, 4(3).

- Sahara, S., Kawakami, Y., Izpisua Belmonte, J. C. and O'Leary, D. D.** (2007) 'Sp8 exhibits reciprocal induction with Fgf8 but has an opposing effect on anterior-posterior cortical area patterning', *Neural development*, 2, pp. 10.
- Sakurai, K. and Osumi, N.** (2008) 'The neurogenesis-controlling factor, Pax6, inhibits proliferation and promotes maturation in murine astrocytes', *The Journal of neuroscience : the official journal of the Society for Neuroscience*, 28(18), pp. 4604-4612.
- Sanada, K., Gupta, A. and Tsai, L.-H. H.** (2004) 'Disabled-1-regulated adhesion of migrating neurons to radial glial fiber contributes to neuronal positioning during early corticogenesis', *Neuron*, 42(2), pp. 197-211.
- Sapolsky, R. M., Krey, L. C. and McEwen, B. S.** (1985) 'Prolonged glucocorticoid exposure reduces hippocampal neuron number: implications for aging', *The Journal of neuroscience : the official journal of the Society for Neuroscience*, 5(5), pp. 1222-1227.
- Sasaki, S., Shionoya, A., Ishida, M., Gambello, M. J., Yingling, J., Wynshaw-Boris, A. and Hirotsune, S.** (2000) 'A LIS1/NUDEL/cytoplasmic dynein heavy chain complex in the developing and adult nervous system', *Neuron*, 28(3), pp. 681-696.
- Savaskan, N. E., Alvarez-Bolado, G., Glumm, R., Nitsch, R., Skutella, T. and Heimrich, B.** (2002) 'Impaired postnatal development of hippocampal neurons and axon projections in the Emx2-/- mutants', *Journal of neurochemistry*, 83(5), pp. 1196-1207.
- Scharfman, H. E.** (2004) 'Functional implications of seizure-induced neurogenesis', *Advances in experimental medicine and biology*, 548, pp. 192-212.
- Schlessinger, A. R., Cowan, W. M. and Gottlieb, D. I.** (1975) 'An autoradiographic study of the time of origin and the pattern of granule cell migration in the dentate gyrus of the rat', *The Journal of comparative neurology*, 159(2), pp. 149-175.
- Schreiner, L. and Kling, A.** (1956) 'Rhencephalon and behavior', *The American journal of physiology*, 184(3).
- Schuh, T. J. and Kimelman, D.** (1995) 'COUP-TFI is a potential regulator of retinoic acid-modulated development in Xenopus embryos', *Mechanisms of development*, 51(1), pp. 39-49.
- Schwab, M. H., Bartholomae, A., Heimrich, B., Feldmeyer, D., Druffel-Augustin, S., Goebbels, S., Naya, F. J., Zhao, S., Frotscher, M., Tsai, M. J. and Nave, K. A.** (2000) 'Neuronal basic helix-loop-helix proteins (NEX and BETA2/Neuro D) regulate terminal granule cell differentiation in the hippocampus', *The Journal of neuroscience : the official journal of the Society for Neuroscience*, 20(10), pp. 3714-3724.
- Scott, D. K., Mitchell, J. A. and Granner, D. K.** (1996) 'The orphan receptor COUP-TF binds to a third glucocorticoid accessory factor element within the phosphoenolpyruvate carboxykinase gene promoter', *The Journal of biological chemistry*, 271(50), pp. 31909-31914.
- Scoville, W. B. and Milner, B.** (2000) 'Loss of recent memory after bilateral hippocampal lesions. 1957', *The Journal of neuropsychiatry and clinical neurosciences*, 12(1), pp. 103-113.
- Seri, B., García-Verdugo, J. M. M., Collado-Morente, L., McEwen, B. S. and Alvarez-Buylla, A.** (2004) 'Cell types, lineage, and architecture of the germinal zone in the adult dentate gyrus', *The Journal of comparative neurology*, 478(4), pp. 359-378.
- Sessa, A., Mao, C.-A. A., Hadjantonakis, A.-K. K., Klein, W. H. and Broccoli, V.** (2008) 'Tbr2 directs conversion of radial glia into basal precursors and guides neuronal amplification by indirect neurogenesis in the developing neocortex', *Neuron*, 60(1), pp. 56-69.
- Shibata, H., Nawaz, Z., Tsai, S. Y., O'Malley, B. W. and Tsai, M. J.** (1997) 'Gene silencing by chicken ovalbumin upstream promoter-transcription factor I (COUP-TFI) is mediated by transcriptional corepressors, nuclear receptor-corepressor (N-CoR) and silencing mediator for retinoic acid receptor and thyroid hormone receptor (SMRT)', *Molecular endocrinology (Baltimore, Md.)*, 11(6), pp. 714-724.

- Shiraishi, Y., Mizutani, A., Yuasa, S., Mikoshiba, K. and Furuichi, T.** (2004) 'Differential expression of Homer family proteins in the developing mouse brain', *The Journal of comparative neurology*, 473(4), pp. 582-599.
- Shors, T. J.** (2001) 'Acute stress rapidly and persistently enhances memory formation in the male rat', *Neurobiology of learning and memory*, 75(1), pp. 10-29.
- Shu, T., Butz, K. G., Plachez, C., Gronostajski, R. M. and Richards, L. J.** (2003) 'Abnormal development of forebrain midline glia and commissural projections in Nfia knock-out mice', *The Journal of neuroscience : the official journal of the Society for Neuroscience*, 23(1), pp. 203-212.
- Sibbe, M., Förster, E., Basak, O., Taylor, V. and Frotscher, M.** (2009) 'Reelin and Notch1 cooperate in the development of the dentate gyrus', *The Journal of neuroscience : the official journal of the Society for Neuroscience*, 29(26), pp. 8578-8585.
- Sievers, J., Hartmann, D., Pehlemann, F. W. and Berry, M.** (1992) 'Development of astroglial cells in the proliferative matrices, the granule cell layer, and the hippocampal fissure of the hamster dentate gyrus', *The Journal of comparative neurology*, 320(1), pp. 1-32.
- Simona, L., Giulio, S. T., Elvira De, L., Yoryani, G. U., Gennaro, A., Maria, A., Audrey, T., Jose, M. G., Paola, A., Liset Menendez de la, P. and Michèle, S.** (2011) 'Loss of COUP-TFI alters the balance between caudal ganglionic eminence- and medial ganglionic eminence-derived cortical interneurons and results in resistance to epilepsy', *The Journal of neuroscience : the official journal of the Society for Neuroscience*, 31(12), pp. 4650-4662.
- Simpson, T. I. and Price, D. J.** (2002) 'Pax6; a pleiotropic player in development', *BioEssays : news and reviews in molecular, cellular and developmental biology*, 24(11), pp. 1041-1051.
- Sisodiya, S. M., Ragge, N. K., Cavalleri, G. L., Hever, A., Lorenz, B., Schneider, A., Williamson, K. A., Stevens, J. M., Free, S. L., Thompson, P. J., van Heyningen, V. and Fitzpatrick, D. R.** (2006) 'Role of SOX2 mutations in human hippocampal malformations and epilepsy', *Epilepsia*, 47(3), pp. 534-542.
- Sloviter, R. S.** (1989) 'Calcium-binding protein (calbindin-D28k) and parvalbumin immunocytochemistry: localization in the rat hippocampus with specific reference to the selective vulnerability of hippocampal neurons to seizure activity', *The Journal of comparative neurology*, 280(2), pp. 183-196.
- Smith, S. J. and Augustine, G. J.** (1988) 'Calcium ions, active zones and synaptic transmitter release', *Trends in neurosciences*, 11(10), pp. 458-464.
- Solstad, T., Boccarda, C. N., Kropff, E., Moser, M.-B. B. and Moser, E. I.** (2008) 'Representation of geometric borders in the entorhinal cortex', *Science (New York, N.Y.)*, 322(5909), pp. 1865-1868.
- Soriano, E., Cobas, A. and Fairén, A.** (1986) 'Asynchronism in the neurogenesis of GABAergic and non-GABAergic neurons in the mouse hippocampus', *Brain research*, 395(1), pp. 88-92.
- Soriano, E., Cobas, A. and Fairén, A.** (1989a) 'Neurogenesis of glutamic acid decarboxylase immunoreactive cells in the hippocampus of the mouse. I: Regio superior and regio inferior', *The Journal of comparative neurology*, 281(4), pp. 586-602.
- Soriano, E., Cobas, A. and Fairén, A.** (1989b) 'Neurogenesis of glutamic acid decarboxylase immunoreactive cells in the hippocampus of the mouse. II: Area dentata', *The Journal of comparative neurology*, 281(4), pp. 603-611.
- Soriano, E. and Del Río, J. A. A.** (2005) 'The cells of cajal-retzius: still a mystery one century after', *Neuron*, 46(3), pp. 389-394.
- Sousa, V. H. and Fishell, G.** (2010) 'Sonic hedgehog functions through dynamic changes in temporal competence in the developing forebrain', *Current opinion in genetics & development*, 20(4), pp. 391-399.

- Squire, L. R.** (1992) 'Memory and the hippocampus: a synthesis from findings with rats, monkeys, and humans', *Psychological review*, 99(2), pp. 195-231.
- Squire, L. R. and Schacter, D. L.** (2002) 'The Neuropsychology of Memory, 3rd Edition', *Guilford Press*.
- Squire, L. R., Stark, C. E. and Clark, R. E.** (2004) 'The medial temporal lobe', *Annual review of neuroscience*, 27, pp. 279-306.
- Stanfield, B. B.** (1989) 'Excessive intra- and supragranular mossy fibers in the dentate gyrus of tottering (tg/tg) mice', *Brain research*, 480(1-2), pp. 294-299.
- Stanfield, B. B. and Cowan, W. M.** (1979a) 'The development of the hippocampus and dentate gyrus in normal and reeler mice', *The Journal of comparative neurology*, 185(3), pp. 423-459.
- Stanfield, B. B. and Cowan, W. M.** (1979b) 'The morphology of the hippocampus and dentate gyrus in normal and reeler mice', *The Journal of comparative neurology*, 185(3), pp. 393-422.
- Stanfield, B. B. and Trice, J. E.** (1988) 'Evidence that granule cells generated in the dentate gyrus of adult rats extend axonal projections', *Experimental brain research*, 72(2), pp. 399-406.
- Starkman, M. N., Gebarski, S. S., Berent, S. and Scheingart, D. E.** (1992) 'Hippocampal formation volume, memory dysfunction, and cortisol levels in patients with Cushing's syndrome', *Biological psychiatry*, 32(9), pp. 756-765.
- Stensaas, L. J.** (1967) 'The development of hippocampal and dorsolateral pallial region of the cerebral hemisphere in fetal rabbits. V. Sixty millimeter stage, glial cell morphology', *The Journal of comparative neurology*, 131(4), pp. 423-436.
- Steward, O. and Scoville, S. A.** (1976) 'Retrograde labeling of central nervous pathways with tritiated or Evans blue-labeled bovine serum albumin', *Neuroscience letters*, 3(4), pp. 191-196.
- Storm, E. E., Garel, S., Borello, U., Hebert, J. M., Martinez, S., McConnell, S. K., Martin, G. R. and Rubenstein, J. L.** (2006) 'Dose-dependent functions of Fgf8 in regulating telencephalic patterning centers', *Development (Cambridge, England)*, 133(9), pp. 1831-1844.
- Studer, M., Filosa, A. and Rubenstein, J. L.** (2005) 'The nuclear receptor COUP-TFI represses differentiation of Cajal-Retzius cells', *Brain research bulletin*, 66(4-6), pp. 394-401.
- Sun, T., Patoine, C., Abu-Khalil, A., Visvader, J., Sum, E., Cherry, T. J., Orkin, S. H., Geschwind, D. H. and Walsh, C. A.** (2005) 'Early asymmetry of gene transcription in embryonic human left and right cerebral cortex', *Science (New York, N.Y.)*, 308(5729), pp. 1794-1798.
- Supèr, H. and Soriano, E.** (1994) 'The organization of the embryonic and early postnatal murine hippocampus. II. Development of entorhinal, commissural, and septal connections studied with the lipophilic tracer DiI', *The Journal of comparative neurology*, 344(1), pp. 101-120.
- Supèr, H. and Uylings, H. B.** (2001) 'The early differentiation of the neocortex: a hypothesis on neocortical evolution', *Cerebral cortex (New York, N.Y. : 1991)*, 11(12), pp. 1101-1109.
- Sutula, T., He, X. X., Cavazos, J. and Scott, G.** (1988) 'Synaptic reorganization in the hippocampus induced by abnormal functional activity', *Science (New York, N.Y.)*, 239(4844), pp. 1147-1150.
- Swanson, L. W., Wyss, J. M. and Cowan, W. M.** (1978) 'An autoradiographic study of the organization of intrahippocampal association pathways in the rat', *The Journal of comparative neurology*, 181(4), pp. 681-715.
- Tabata, H. and Nakajima, K.** (2003) 'Multipolar migration: the third mode of radial neuronal migration in the developing cerebral cortex', *The Journal of neuroscience : the official journal of the Society for Neuroscience*, 23(31), pp. 9996-10001.
- Takeuchi, A. and O'Leary, D. D.** (2006) 'Radial migration of superficial layer cortical neurons controlled by novel Ig cell adhesion molecule MDGA1', *The Journal of neuroscience : the official journal of the Society for Neuroscience*, 26(17), pp. 4460-4464.
- Takiguchi-Hayashi, K., Sekiguchi, M., Ashigaki, S., Takamatsu, M., Hasegawa, H., Suzuki-Migishima, R., Yokoyama, M., Nakanishi, S. and Tanabe, Y.** (2004) 'Generation of reelin-

- positive marginal zone cells from the caudomedial wall of telencephalic vesicles', *The Journal of neuroscience : the official journal of the Society for Neuroscience*, 24(9), pp. 2286-2295.
- Tanaka, D. H. and Nakajima, K.** (2012a) 'GABAergic interneuron migration and the evolution of the neocortex', *Development, growth & differentiation*, 54(3), pp. 366-372.
- Tanaka, D. H. and Nakajima, K.** (2012b) 'Migratory pathways of GABAergic interneurons when they enter the neocortex', *The European journal of neuroscience*, 35(11), pp. 1655-1660.
- Tanaka, T., Koizumi, H. and Gleeson, J. G.** (2006) 'The doublecortin and doublecortin-like kinase 1 genes cooperate in murine hippocampal development', *Cerebral cortex (New York, N.Y. : 1991)*, 16 Suppl 1, pp. 73.
- Tanapat, P., Hastings, N. B., Reeves, A. J. and Gould, E.** (1999) 'Estrogen stimulates a transient increase in the number of new neurons in the dentate gyrus of the adult female rat', *The Journal of neuroscience : the official journal of the Society for Neuroscience*, 19(14), pp. 5792-5801.
- Tanapat, P., Hastings, N. B., Rydel, T. A., Galea, L. A. and Gould, E.** (2001) 'Exposure to fox odor inhibits cell proliferation in the hippocampus of adult rats via an adrenal hormone-dependent mechanism', *The Journal of comparative neurology*, 437(4), pp. 496-504.
- Tomassy, G. S., De Leonibus, E., Jabaudon, D., Lodato, S., Alfano, C., Mele, A., Macklis, J. D. and Studer, M.** (2010) 'Area-specific temporal control of corticospinal motor neuron differentiation by COUP-TFI', *Proceedings of the National Academy of Sciences of the United States of America*, 107(8), pp. 3576-3581.
- Tomohiko, I., Aki, M., Hiroshi, K., Hideki, E. and Fumio, M.** (2012) 'Prox1 postmitotically defines dentate gyrus cells by specifying granule cell identity over CA3 pyramidal cell fate in the hippocampus', *Development*, 139(16), pp. 3051-3062.
- Tran, P., Zhang, X. K., Salbert, G., Hermann, T., Lehmann, J. M. and Pfahl, M.** (1992) 'COUP orphan receptors are negative regulators of retinoic acid response pathways', *Molecular and cellular biology*, 12(10), pp. 4666-4676.
- Trommsdorff, M., Gotthardt, M., Hiesberger, T., Shelton, J., Stockinger, W., Nimpf, J., Hammer, R. E., Richardson, J. A. and Herz, J.** (1999) 'Reeler/Disabled-like disruption of neuronal migration in knockout mice lacking the VLDL receptor and ApoE receptor 2', *Cell*, 97(6), pp. 689-701.
- Tsai, S. Y. and Tsai, M. J.** (1997) 'Chick ovalbumin upstream promoter-transcription factors (COUP-TFs): coming of age', *Endocrine reviews*, 18(2), pp. 229-240.
- Uesugi, K., Oinuma, I., Katoh, H. and Negishi, M.** (2009) 'Different requirement for Rnd GTPases of R-Ras GAP activity of Plexin-C1 and Plexin-D1', *The Journal of biological chemistry*, 284(11), pp. 6743-6751.
- van der Wees, J., Matharu, P. J., de Roos, K., Destrée, O. H., Godsave, S. F., Durston, A. J. and Sweeney, G. E.** (1996) 'Developmental expression and differential regulation by retinoic acid of Xenopus COUP-TF-A and COUP-TF-B', *Mechanisms of development*, 54(2), pp. 173-184.
- van Groen, T., Miettinen, P. and Kadish, I.** (2003) 'The entorhinal cortex of the mouse: organization of the projection to the hippocampal formation', *Hippocampus*, 13(1), pp. 133-149.
- van Praag, H., Schinder, A. F., Christie, B. R., Toni, N., Palmer, T. D. and Gage, F. H.** (2002) 'Functional neurogenesis in the adult hippocampus', *Nature*, 415(6875), pp. 1030-1034.
- Wang, L. H., Ing, N. H., Tsai, S. Y., O'Malley, B. W. and Tsai, M. J.** (1991) 'The COUP-TFs compose a family of functionally related transcription factors', *Gene expression*, 1(3), pp. 207-216.
- Wang, L. H., Tsai, S. Y., Cook, R. G., Beattie, W. G., Tsai, M. J. and O'Malley, B. W.** (1989) 'COUP transcription factor is a member of the steroid receptor superfamily', *Nature*, 340(6229), pp. 163-166.

- Wang, L. H., Tsai, S. Y., Sagami, I., Tsai, M. J. and O'Malley, B. W. (1987) 'Purification and characterization of chicken ovalbumin upstream promoter transcription factor from HeLa cells', *The Journal of biological chemistry*, 262(33), pp. 16080-16086.
- Weiskrantz, L. (1956) 'Behavioral changes associated with ablation of the amygdaloid complex in monkeys', *Journal of comparative and physiological psychology*, 49(4).
- Wenzel, H. J., Robbins, C. A., Tsai, L. H. and Schwartzkroin, P. A. (2001) 'Abnormal morphological and functional organization of the hippocampus in a p35 mutant model of cortical dysplasia associated with spontaneous seizures', *The Journal of neuroscience : the official journal of the Society for Neuroscience*, 21(3), pp. 983-998.
- Westenbroek, C., Den Boer, J. A., Veenhuis, M. and Ter Horst, G. J. (2004) 'Chronic stress and social housing differentially affect neurogenesis in male and female rats', *Brain research bulletin*, 64(4), pp. 303-308.
- Widom, R. L., Rhee, M. and Karathanasis, S. K. (1992) 'Repression by ARP-1 sensitizes apolipoprotein AI gene responsiveness to RXR alpha and retinoic acid', *Molecular and cellular biology*, 12(8), pp. 3380-3389.
- Windrem, M.S., and Finlay, B.L. (1991). 'Thalamic ablations and neo- cortical development: alterations of cortical cytoarchitecture and cell number'. *Cerebral Cortex*, 1, pp. 230-240.
- Witter, M. P. and Amaral, D. G. (2004) 'Hippocampal Formation. The Rat Nervous System (G. Paxinos, Third Edition)', *Elsevier Academic press*.
- Witter, M. P., Groenewegen, H. J., Lopes da Silva, F. H. and Lohman, A. H. (1989) 'Functional organization of the extrinsic and intrinsic circuitry of the parahippocampal region', *Progress in neurobiology*, 33(3), pp. 161-253.
- Woolley, C. S., Gould, E. and McEwen, B. S. (1990) 'Exposure to excess glucocorticoids alters dendritic morphology of adult hippocampal pyramidal neurons', *Brain research*, 531(1-2), pp. 225-231.
- Woon, F. L., Sood, S. and Hedges, D. W. (2010) 'Hippocampal volume deficits associated with exposure to psychological trauma and posttraumatic stress disorder in adults: a meta-analysis', *Progress in neuro-psychopharmacology & biological psychiatry*, 34(7), pp. 1181-1188.
- Yan, H., Merchant, A. M. and Tye, B. K. (1993) 'Cell cycle-regulated nuclear localization of MCM2 and MCM3, which are required for the initiation of DNA synthesis at chromosomal replication origins in yeast', *Genes & development*, 7(11), pp. 2149-2160.
- Ye, T., Ip, J. P., Fu, A. K. and Ip, N. Y. (2014) 'Cdk5-mediated phosphorylation of RapGEF2 controls neuronal migration in the developing cerebral cortex', *Nature communications*, 5, pp. 4826.
- Yerkes, R. M. and Dodson, J. D. (1908) 'The relation of strength of stimulus to rapidity of habit-formation', *Journal of comparative neurology and psychology*.
- Yoshida, M., Suda, Y., Matsuo, I., Miyamoto, N., Takeda, N., Kuratani, S. and Aizawa, S. (1997) 'Emx1 and Emx2 functions in development of dorsal telencephalon', *Development (Cambridge, England)*, 124(1), pp. 101-111.
- You, H., Kim, Y. I., Im, S. Y., Suh-Kim, H., Paek, S. H., Park, S.-H. H., Kim, D. G. and Jung, H.-W. W. (2005) 'Immunohistochemical study of central neurocytoma, subependymoma, and subependymal giant cell astrocytoma', *Journal of neuro-oncology*, 74(1), pp. 1-8.
- Young, W. S., Li, J., Wersinger, S. R. and Palkovits, M. (2006) 'The vasopressin 1b receptor is prominent in the hippocampal area CA2 where it is unaffected by restraint stress or adrenalectomy', *Neuroscience*, 143(4), pp. 1031-1039.
- Yozu, M., Tabata, H. and Nakajima, K. (2005) 'The caudal migratory stream: a novel migratory stream of interneurons derived from the caudal ganglionic eminence in the developing mouse forebrain', *The Journal of neuroscience : the official journal of the Society for Neuroscience*, 25(31), pp. 7268-7277.

- Zamir, I., Harding, H. P., Atkins, G. B., Hörlein, A., Glass, C. K., Rosenfeld, M. G. and Lazar, M. A.** (1996) 'A nuclear hormone receptor corepressor mediates transcriptional silencing by receptors with distinct repression domains', *Molecular and cellular biology*, 16(10), pp. 5458-5465.
- Zappone, M. V., Galli, R., Catena, R., Meani, N., De Biasi, S., Mattei, E., Tiveron, C., Vescovi, A. L., Lovell-Badge, R., Ottolenghi, S. and Nicolis, S. K.** (2000) 'Sox2 regulatory sequences direct expression of a (beta)-geo transgene to telencephalic neural stem cells and precursors of the mouse embryo, revealing regionalization of gene expression in CNS stem cells', *Development (Cambridge, England)*, 127(11), pp. 2367-2382.
- Zembrzycki, A., Griesel, G., Stoykova, A. and Mansouri, A.** (2007) 'Genetic interplay between the transcription factors Sp8 and Emx2 in the patterning of the forebrain', *Neural development*, 2, pp. 8.
- Zhao, S., Chai, X., Bock, H. H., Brunne, B., Förster, E. and Frotscher, M.** (2006) 'Rescue of the reeler phenotype in the dentate gyrus by wild-type coculture is mediated by lipoprotein receptors for Reelin and Disabled 1', *The Journal of comparative neurology*, 495(1), pp. 1-9.
- Zhao, Y., Sheng, H. Z., Amini, R., Grinberg, A., Lee, E., Huang, S., Taira, M. and Westphal, H.** (1999) 'Control of hippocampal morphogenesis and neuronal differentiation by the LIM homeobox gene Lhx5', *Science (New York, N.Y.)*, 284(5417), pp. 1155-1158.
- Zheng, W., Xie, Y., Li, G., Kong, J., Feng, J. Q. and Li, Y. C.** (2004) 'Critical role of calbindin-D28k in calcium homeostasis revealed by mice lacking both vitamin D receptor and calbindin-D28k', *The Journal of biological chemistry*, 279(50), pp. 52406-52413.
- Zhou, C., Qiu, Y., Pereira, F. A., Crair, M. C., Tsai, S. Y. and Tsai, M. J.** (1999) 'The nuclear orphan receptor COUP-TFI is required for differentiation of subplate neurons and guidance of thalamocortical axons', *Neuron*, 24(4), pp. 847-859.
- Zhou, C., Tsai, S. Y. and Tsai, M. J.** (2001) 'COUP-TFI: an intrinsic factor for early regionalization of the neocortex', *Genes & development*, 15(16), pp. 2054-2059.
- Zhou, C.-J. J., Zhao, C. and Pleasure, S. J.** (2004) 'Wnt signaling mutants have decreased dentate granule cell production and radial glial scaffolding abnormalities', *The Journal of neuroscience : the official journal of the Society for Neuroscience*, 24(1), pp. 121-126.
- Zhuang, Y. and Gudas, L. J.** (2008) 'Overexpression of COUP-TFI in murine embryonic stem cells reduces retinoic acid-associated growth arrest and increases extraembryonic endoderm gene expression', *Differentiation; research in biological diversity*, 76(7), pp. 760-771.
- Zilles, K. and Wree, A.** (1995) 'Cortex: Areal and Laminar Structure. In The Rat Nervous System, 2nd ed., (ed. G. Paxinos)', *San Diego, CA: Academic Press*.
- Zou, Y. R., Kottmann, A. H., Kuroda, M., Taniuchi, I. and Littman, D. R.** (1998) 'Function of the chemokine receptor CXCR4 in haematopoiesis and in cerebellar development', *Nature*, 393(6685), pp. 595-599.

Résumé

L'hippocampe est un composant majeur du cerveau des mammifères. Il appartient à l'archicortex, la partie la plus ancienne du télencéphale, et joue d'importants rôles dans la mémoire, l'apprentissage et la navigation spatiale. L'hippocampe comprend deux régions distinctes : les champs ammoniens et le gyrus denté ou DG, composés de trois couches cellulaires. Le DG est la principale zone d'entrée d'informations dans l'hippocampe et son développement commence au jour embryonnaire 14 (E14.5) chez la souris. Pendant ma thèse, je me suis intéressée à un régulateur de transcription important, le récepteur nucléaire COUP-TFI, exprimé dans le neocortex et l'hippocampe, et décrit comme jouant des rôles clefs dans la spécification et la migration neocorticale. Cependant, peu de choses sont connues sur son implication dans l'hippocampe, et plus particulièrement dans le DG. COUP-TFI y est exprimé en gradient à la fois dans les progéniteurs proliférants et dans les neurones différenciés, et est fortement localisé dans le neuroépithélium du DG à E14.5. Le but majeur de ma thèse était ainsi de déchiffrer le rôle de COUP-TFI dans le développement de l'hippocampe, et spécifiquement au cours de la différenciation et migration des cellules granulaires, population principale du DG. À l'aide de deux lignées de souris mutantes, dans lesquelles COUP-TFI est soit inactivé dans les progéniteurs et leur descendance, soit seulement dans les cellules post-mitotiques, j'ai montré que l'absence de COUP-TFI induit différents degrés d'altérations de la croissance de l'hippocampe. En l'absence de COUP-TFI dans les progéniteurs, les précurseurs des cellules granulaires se différencient précocement et présentent une prolifération diminuée. De plus, la migration des granules est altérée conduisant à des localisations aberrantes et à la présence de clusters hétérotopiques dans le DG. Au stades postnataux, les afférences du cortex entorhinale n'innervent pas le DG septal et l'apoptose est accrue dans cette région. En conséquence, le gyrus denté en résulte fortement réduit à l'âge adulte, particulièrement dans la région septale, tandis que le pôle temporal est moins affecté. À l'inverse, la perte de COUP-TFI dans les cellules différenciées n'entraîne que des anomalies mineures et transitoires. Ensemble, mes résultats indiquent que COUP-TFI est impliqué dans la régulation d'aspects particuliers de la différenciation et migration des granules, principalement au niveau des progéniteurs, et propose COUP-TFI comme un nouveau régulateur de transcription requis dans le développement et le fonctionnement de l'hippocampe.